Advancing Precision Water Management in Smallholder Sugarcane Farming: Leveraging Unmanned Aerial Vehicle-Based Remote Sensing and Machine Learning for Evapotranspiration and Water Stress Assessment

by

AMEERA YACOOB

Submitted in fulfilment of the academic requirements of

Master of Science

Discipline of Hydrology

School of Agricultural, Earth and Environmental Sciences

College of Agriculture, Engineering and Science

University of KwaZulu-Natal

Pietermaritzburg

South Africa

December 2024

PREFACE

The candidate diligently undertook the research contained within this thesis while based at the Discipline of Hydrology, Centre for Water Resources Research (CWRR), School of Agricultural, Earth and Environmental Sciences of the College of Agriculture, Engineering, and Science, University of KwaZulu-Natal, Pietermaritzburg Campus, South Africa. This work constitutes an integral component of the comprehensive Water Research Commission (WRC) project entitled "Leveraging the Google Earth Engine to analyse very-high spatial resolution unmanned aerial vehicle data to guide and inform precision agriculture in smallholder farms," designated under Project Number C2021-2022-00800. The CWRR and the WRC financially supported the research and are gratefully acknowledged. The candidate has not disseminated the contents of this work with any other academic institution in any form. Furthermore, unless the text recognises the work of others, the findings delineated herein are the direct outcome of the candidate's investigations.

____

Signed: Ameera Yacoob

Date: December 2024

____

Signed: Dr Shaeden Gokool

Date: December 2024

____

Signed: Prof Alistair Clulow

Date: December 2024

DECLARATION 1: PLAGIARISM

I, Ameera Yacoob, declare that:

(i) the research reported in this dissertation, except where otherwise indicated or acknowledged, is my original work.

(ii) this dissertation has not been submitted in full or in part for any degree or examination to any other university.

(iii) this dissertation does not contain other persons' data, pictures, graphs or other information, unless specifically acknowledged as being sourced from other persons.

(iv) this dissertation does not contain other persons' writing unless specifically acknowledged as being sourced from other researchers. Where other written sources have been quoted, then:

   a) their words have been rewritten, but the general information attributed to them has been referenced.

   b) where their exact words have been used, their writing has been placed inside quotation marks and referenced.

(v) where I have used material for which publications followed, I have indicated my role in the work in detail.

(vi) this dissertation is primarily a collection of material, prepared by me, published as journal articles, or presented as a poster or oral presentation at conferences. In some cases, additional material has been included.

(vii) this dissertation does not contain text, graphics or tables copied and pasted from the Internet unless specifically acknowledged, and the source being detailed in the dissertation and the References sections.

Signed: Ameera Yacoob

Date: December 2024

DECLARATION 2: PUBLICATIONS

Details of contributions to publications that form part and/or include research presented in this thesis (include publications in preparation and published, giving details of the contributions of each author to the study and writing of each publication):

Publication 1 – Chapter 2 of this thesis:

Yacoob, A, Gokool, S, Clulow, A, Mahomed, M and Mabhaudhi, T. 2024. Leveraging unmanned aerial vehicle technologies to facilitate precision water management in smallholder farms: a scoping review and bibliometric analysis. *Drones* 8 (9): 476.

Author Contributions:

A. Yacoob conducted the research, data collection, and analysis for this publication, with writing and technical advice provided by S. Gokool, A.D. Clulow, M. Mahomed, and T. Mabhaudhi. A. Yacoob wrote the publication, and all figures, tables, and graphs were produced by A. Yacoob unless otherwise referenced in the text of the paper. S. Gokool, A.D. Clulow, M. Mahomed, and T. Mabhaudhi provided editing and advice on the structure and scientific content of the paper.

Publication 2 – Chapter 3 of this thesis:

In preparation for submission to Remote Sensing (MDPI):

Yacoob, A, Gokool, S, Clulow, A, Mahomed, M, Naiken, V and Mabhaudhi, T. 2024. Evaluating the potential of unmanned aerial vehicle-derived data for evapotranspiration estimation in smallholder farms.

Author Contributions:

A. Yacoob conducted the data collection, machine learning-based modelling, and analysis for this publication, with writing and technical advice provided by S. Gokool, A.D. Clulow, M. Mahomed, V. Naiken, and T. Mabhaudhi. A. Yacoob wrote the publication. All figures, tables, and graphs were produced by A. Yacoob unless otherwise referenced in the text of the paper. S. Gokool, A.D. Clulow, M. Mahomed, V. Naiken, and T. Mabhaudhi provided editing and advice on the structure and scientific content of the paper.

Publication 3 – Chapter 4 of this thesis:

In preparation for submission to Agricultural Water Management (Elsevier):

Yacoob, A, Gokool, S, Clulow, A, Mahomed, M, Naiken, V and Mabhaudhi, T. 2024. A machine learning approach for quantifying crop water stress in smallholder farms using unmanned aerial vehicle multispectral imagery.

Author Contributions:

The data collection, machine learning-based modelling, analysis, and interpretation of results for this publication were conducted by A. Yacoob, with writing, technical advice, and editing provided by S. Gokool, A.D. Clulow, M. Mahomed, V. Naiken, and T. Mabhaudhi. A. Yacoob wrote the publication. All figures, tables, and graphs were produced by A. Yacoob unless otherwise referenced in the text of the paper. S. Gokool, A.D. Clulow, M. Mahomed, V. Naiken, and T. Mabhaudhi provided editing and advice on the structure and scientific content of the paper.

Dissemination and Engagement Activities:

The * in each presentation indicates my role as the corresponding author.

Yacoob A*, Gokool S, Clulow AD, Mahomed M, Naiken V and Mabhaudhi T. 2023. Leveraging the Google Earth Engine to analyse UAV-derived data for precision agriculture. Agricultural Innovation Stakeholder Meeting, Mbava Community Hall, Swayimane, South Africa, 13 September 2023. (Chapter 3).

Yacoob A*, Gokool S, Clulow AD, Mahomed M, Naiken V and Mabhaudhi T. 2023. Estimating evapotranspiration from UAV-derived data for precision water management. 7th Fountainhill Research Foundation Symposium, Fountainhill Estate, Wartburg, South Africa, 18-19 October 2023. (Chapters 2 and 3).

Yacoob A*, Gokool S, Clulow AD, Mahomed M, Naiken V and Mabhaudhi T. 2023. Estimating evapotranspiration from UAV-derived data for precision water management. Postgraduate Research and Innovation Symposium 2023, Coastlands Musgrave Hotel, Durban, South Africa, 2-3 November 2023. Awarded second prize. (Chapter 3).

Yacoob A*, Gokool S, Clulow AD, Mahomed M, Naiken V and Mabhaudhi T. 2024. Assessing UAV-derived data for evapotranspiration estimation: a case study in Swayimane, KwaZulu-Natal, South Africa. Water Research Commission Online Presentation, 30 January 2024. (Chapters 2 and 3).

Yacoob A*, Gokool S, Clulow AD, Mahomed M, Naiken V and Mabhaudhi T. 2024. Assessing UAV-derived data for evapotranspiration estimation: a case study in Swayimane, KwaZulu-Natal, South Africa. Fulbright-Hays Group Project Delegation Visit, Council Chambers, University of KwaZulu-Natal, Pietermaritzburg, South Africa, 12 July 2024. (Chapter 3).

Yacoob A*, Gokool S, Clulow AD, Mahomed M, Naiken V and Mabhaudhi T. 2024. Assessing UAV-derived data for evapotranspiration estimation: a case study in Swayimane, KwaZulu-Natal, South Africa. South African Hydrological Society Conference 2024, Protea Breakwater Lodge, Cape Town, South Africa, 2-4 October 2024. Recognised among the top five student presentations. (Chapters 2 and 3).

Yacoob A*, Gokool S, Clulow AD, Mahomed M, Naiken V and Mabhaudhi T. 2024. Assessing UAV data for evapotranspiration estimation: a case study in Swayimane, KwaZulu-Natal, South Africa. Postgraduate Research and Innovation Symposium 2024, Coastlands Musgrave Hotel, Durban, South Africa, 29-30 October 2024. Awarded first prize. (Chapter 3).

Yacoob A*, Gokool S, Clulow AD, Mahomed M, Naiken V and Mabhaudhi T. 2024. Assessing UAV-derived data for evapotranspiration estimation: a case study in Swayimane, KwaZulu-Natal, South Africa. Water Research Commission Online Presentation, 21 January 2025. (Chapters 2 and 3).

Signed: Ameera Yacoob

Date: December 2024

EXTENDED ABSTRACT

This thesis addresses the imperative of optimising water resource management within smallholder sugarcane cultivation in Swayimane, KwaZulu-Natal, South Africa—a region contending with the dual pressures of escalating food demand and increasingly volatile climatic dynamics. Smallholder farmers are indispensable to advancing food security and socio-economic development, underpinning up to 80% of the region's agricultural output. Nevertheless, their capacity to mitigate food insecurity is hindered by restricted access to vital resources, including reliable water supplies and advanced tools. These limitations necessitate innovative and economically viable strategies to enhance productivity and optimise resource allocation. Precision agriculture (PA) methodologies, supported by cutting-edge technologies such as unmanned aerial vehicles (UAVs), hold promise for smallholder farmers. By enabling data-driven, resource-efficient cultivation practices, UAVs emerge as an instrument to foster sustainable agricultural systems tailored to the unique challenges of these communities.

Sugarcane, a high-value commodity crop, is integral to the socio-economic fabric of smallholder farming communities, substantially contributing to employment and subsequent regional economic advancement. However, the absence of irrigation infrastructure within smallholder systems and escalating water deficits driven by rising temperatures and prolonged dry spells present formidable challenges to sustainable production. This reliance emphasises the need for resource-efficient agronomic strategies that maximise water use while safeguarding yields. By harnessing the potential of PA methodologies, including UAVs equipped with advanced multispectral sensors, farmers can acquire high-resolution insights into crop water dynamics and evapotranspiration processes. To this end, this research pioneers integrating UAV technology with machine learning (ML) to refine water management practices, focusing on enhancing evapotranspiration (ET) estimation and monitoring crop water stress.

Chapter 2 undertakes a bibliometric analysis of UAV applications in precision water management, employing Biblioshiny and VOSviewer to identify key research trends and highlight potential strengths, limitations, and future opportunities. The findings reveal UAVs' potential to address the limitations of traditional ground-based and remote sensing (RS) methods, which are often labour-intensive, expensive, and lack sufficient spatial and temporal resolution for effective water management in smallholder farming systems. UAV technology, driven by advancements in high-resolution data acquisition and the proliferation of cost-

effective, open-source processing platforms, offers accessible, scalable solutions tailored to smallholders. While certain factors may moderate their adoption, continuous technological progress and decreasing costs present significant opportunities for UAV applications to enhance policy formulation, strategic planning, and operational decision-making, ultimately strengthening resilience in sustainable water management for smallholders.

Chapter 3 presents an empirical evaluation of vegetation index (VI)-based ET estimation methods. Using data from a smallholder sugarcane field equipped with an eddy covariance (EC) system for ground-truthing, the study assessed five actual ET (ETa) models—ET-NDVI, ET-NDVIscaled, ET-NDVIKc, ET-EVI, and ET-EVI2—alongside an ML-derived crop coefficient (Kc) prediction model correlating in-situ NDVI with Kc values. The EVI2 model demonstrated superior performance, achieving moderate to strong correlation ($R^2 = 0.63$) with lower Root Mean Square Error (RMSE = 0.67) and Mean Absolute Error (MAE = 0.52) compared to competing models. EVI2's resilience against NDVI saturation—a persistent challenge in mature sugarcane—translates to improved water use assessment, while reduced reliance on extensive in-situ data enhances its scalability for smallholder systems. Furthermore, high-resolution ETa maps derived from these models offer potential insights for optimising irrigation and improving productivity in resource-limited agricultural contexts.

Chapter 4 presents a novel ML-based predictive model for the Normalised Difference Water Index (NDWI), utilising correlations with structural VIs (SVIs) from UAV and Sentinel-2 data. The Random Forest (RF) ensemble model achieves exceptional accuracy ($R^2 = 0.95$, RMSE = 0.03, MAE = 0.02), offering a precise and efficient tool for monitoring sugarcane water stress. Validated against ETa and the Water Deficit Index (WDI), the model confirms NDWI's reliability as a proxy for assessing sugarcane water status. A Principal Component Analysis (PCA) reveals complex interactions between NDWI, SVIs, and physiological parameters, further enhancing insights into sugarcane water status. Additionally, temporal analysis highlights NDWI's responsiveness to rainfall, with marked fluctuations pinpointing critical stress periods. By minimising dependence on in-situ measurements, the model offers a scalable, cost-effective solution tailored to the needs of resource-constrained smallholder farmers.

In conclusion, this thesis advances PA by integrating UAV technology and ML to revolutionise water management in smallholder sugarcane farming. The VI-based ET estimation models and NDWI prediction framework deliver customised, high-resolution insights to optimise irrigation and enhance water efficiency during critical growth phases. Beyond showcasing these innovations, the study emphasises the necessity of capacity-building initiatives and user-friendly tools to enable farmer adoption, addressing climatic and socio-economic constraints. This work establishes a foundation for scalable, context-specific solutions despite its limited scope. Future research should prioritise decision support systems integrating UAV data and predictive models for real-time water stress monitoring and adaptive irrigation. By empowering smallholders, this study contributes to resilient agricultural systems, enhanced food security, and sustainable sugarcane production, laying the groundwork for global efforts against water scarcity and climate variability.

ACKNOWLEDGEMENTS

First and foremost, I praise ٱللَّٰه (*Allah*, the Arabic word for God) for allowing me to increase my knowledge through the pursuit of this project and for providing the wisdom, strength, and determination that has accompanied me on my academic path. His blessings have been the driving force behind my progress and achievements.

A collaborative community akin to the proverbial village that nurtures a child is essential for success in academic research. Therefore, I would like to extend my sincere gratitude to various institutions and individuals whose collective contributions were crucial in completing my Master of Science Degree.

- I am grateful to the Water Research Commission (WRC) for generously funding this research endeavour and allowing me to collaborate with their esteemed team under Project No. C2021-2022-00800. I acknowledge that all opinions expressed and conclusions drawn in this study solely reflect my perspective and do not necessarily represent the viewpoints of the WRC. Working alongside distinguished professionals and contributing to advancing knowledge within this domain is truly an honour. Furthermore, my involvement in exploring the Fourth Industrial Revolution and its alignment with the current global trajectory was an enriching experience. I am thankful for the opportunity to partake in this vital initiative.
- I extend special thanks to the University of KwaZulu-Natal for supporting my higher education since 2018, specifically the Centre for Water Resources Research, for providing the financial, administrative, and auxiliary resources used in this study.
- My thesis supervisor, Dr Shaeden Gokool, I have acquired a substantial amount of knowledge from you and wish to express my most profound appreciation for your consistent guidance, support, and encouragement throughout the process of writing this thesis. Your expertise and mentorship have significantly shaped my academic development, and I truly value being a part of your niche. I hope to continue my research journey with you. I also want to express my gratitude for your belief in my ability to carry out this study and for your sacrifices. The opportunities you have afforded me have undoubtedly strengthened my confidence in presenting my research to the scientific community and provided me with the necessary exposure.

- I want to express my sincerest appreciation to my co-supervisor, Prof Alistair Clulow, for your invaluable guidance, advice, and encouragement throughout my research project. Your extensive knowledge and expertise in the field have played a significant role in enhancing my research capabilities. I am deeply grateful for your unwavering support and for instilling the enthusiasm and motivation that led me to embark on this research endeavour. I am mindful of your sacrifices to offer valuable time and resources, and I acknowledge your trust and confidence in me. I look forward to learning from you in the future.
- Dr Maqsooda Mahomed, I am deeply grateful for your support and mentorship, which significantly influenced my journey. You consistently went the extra mile to provide advice, check my progress, and offer assistance whenever needed. Your kindness and encouragement during challenging times left a lasting impact on me. I am continually inspired by your research acumen and aspire to emulate your dedication and expertise. Thank you sincerely for all your contributions.
- I wish to express my appreciation to Vivek Naiken (Hydrology and Agrometeorology Senior Technician) for his unwavering support in fieldwork and laboratory tasks, which was crucial to the project's success. Your consistent guidance and aid were immensely valuable throughout the study.
- I acknowledge my esteemed colleagues, Gary Denton, Evania Chetty, Knowledge Muchonyerwa, and Thando Mthembu, for their invaluable assistance. I extend my best wishes to each of you for continued success in your future endeavours.
- Thank you to Brice Gijsbertsen for your research guidance and Trylee Matongera and Celuxolo Dlamini for assisting our team with drone flights. Moreover, special mention goes to Thulani Ncwane for accompanying me to the site and helping with field measurements.
- Additionally, I express my heartfelt gratitude to my family for their enduring motivation, love, and reassurance, which have been vital in completing this master's degree. Your steadfast encouragement has been critical in shaping my personal growth, and I am thankful for your constant push towards excellence.
- Furthermore, I thank the smallholder farming community of Swayimane for all their efforts throughout this project.

In conclusion, this thesis would not have been possible without the support and encouragement of all those mentioned above—each contribution, whether big or small, has played an essential role in shaping this research endeavour.

TABLE OF CONTENTS

Page

LIST OF TABLES

LIST OF FIGURES

LIST OF ABBREVIATIONS

AWS	Automatic Weather Station
BREB	Bowen Ratio Energy Balance
CART	Classification and Regression Trees
CC	Chlorophyll Content
CRP	Calibration Reflectance Panel
CWSI	Crop Water Stress Index
DE	Descriptive/Author Keywords
DLS	Downwelling Light Sensor
DSM	Digital Surface Model
EVI	Enhanced Vegetation Index
EVI2	Two-Band Enhanced Vegetation Index
ET-EC	Eddy Covariance-Based Evapotranspiration
ET-Predicted Kc	Evapotranspiration Predicted Using a Crop Coefficient
ET-VIs	Evapotranspiration Estimated Using Vegetation Indices
FAO	Food and Agriculture Organisation
GEE	Google Earth Engine
GIS	Geographic Information System
GLM	Generalised Linear Model
GNDVI	Green Normalised Difference Vegetation Index
GeoTIFF	Georeferenced Tagged Image File Format
GSD	Ground Sampling Distance
GTB	Gradient Tree Boosting
IPCC	Intergovernmental Panel on Climate Change
IQR	Interquartile Range
IRGA	Infrared Gas Analyser
kNN	k-Nearest Neighbours
LAI	Leaf Area Index
LST	Land Surface Temperature
MAE	Mean Absolute Error
MK	Mann-Kendall
ML	Machine Learning

MLAs	Machine Learning Algorithms
MLBMs	Machine Learning-Based Models
MLR	Multiple Linear Regression
NDVI	Normalised Difference Vegetation Index
NDVIre	Red Edge Normalised Difference Vegetation Index
NDWI	Normalised Difference Water Index
NIR	Near-Infrared
OSAVI	Optimised Soil-Adjusted Vegetation Index
PA	Precision Agriculture
PCA	Principal Component Analysis
PM	Penman-Monteith
PRISMA	Preferred Reporting Items for Systematic Reviews and Meta-Analyses
RFR	Random Forest Regression
RMSE	Root Mean Square Error
RPART	Recursive Partitioning and Regression Trees
RS	Remote Sensing
SAVI	Soil-Adjusted Vegetation Index
SCN	Stochastic Configuration Networks
ScR	Scoping Review
SEBAL	Surface Energy Balance Algorithm for Land
SEBS	Surface Energy Balance System
SEO	Satellite Earth Observation
SR	Surface Renewal
SVMRadial	Support Vector Machine with Radial Kernel
SVI	Structural Vegetation Index
SWIR	Shortwave Infrared
TIR	Thermal Infrared
TSEB	Two-Source Energy Balance
UAV	Unmanned Aerial Vehicle
VI	Vegetation Index
VTOL	Vertical Take-Off and Landing
WDI	Water Deficit Index
WUEc	Crop Water Use Efficiency

LIST OF SYMBOLS

Δ	Slope of the saturated vapour pressure curve (kPa $°C^{-1}$)
γ	Psychrometric constant (kPa $°C^{-1}$)
Chl	Total chlorophyll concentration per unit leaf area (µmol m^{-2})
ETo	Reference evapotranspiration (mm day^{-1})
ETa	Actual evapotranspiration (mm day^{-1})
ETp	Potential evapotranspiration (mm day^{-1})
G	Germination or Soil Heat Flux (depending on context) (-/ W m^{-2}/ MJ m^{-2} day^{-1})
H	Sensible heat flux (W m^{-2} or MJ m^{-2} day^{-1})
Kc	Crop coefficient (Dimensionless)
Ks	Soil water stress coefficient (Dimensionless)
LE	Latent heat flux (W m^{-2} or MJ m^{-2} day^{-1})
M	Maturation or SPAD value (depending on context) (Dimensionless)
RH	Relative Humidity (%)
Rn	Net radiation (W m^{-2} or MJ m^{-2} day^{-1})
T	Air temperature or Tillering (depending on context) (°C/ -)
u_2	Wind speed (m s^{-1})
w	Wind speed (used for LE covariance) (m s^{-1})
q	Specific humidity (kg kg^{-1})
e_s	Saturated vapour pressure (kPa)
e_a	Actual vapour pressure (kPa)
ρ	Spearman's rank correlation coefficient (Dimensionless)
τ	Kendall's Tau (trend or correlation coefficient) (Dimensionless)

GLOSSARY OF TERMS

1. **Chlorophyll Content (CC)**: a quantitative measure of the green pigment present in plants, indicating photosynthetic capacity and overall plant health.
2. **Crop Coefficient (Kc)**: a crucial parameter that establishes the relationship between reference evapotranspiration (ETo) and the actual evapotranspiration (ETa) of a specific crop variety.
3. **Crop Water Stress Index (CWSI)**: an analytical index utilised to assess the water stress levels experienced by crops based on temperature differentials.
4. **Eddy Covariance (EC)**: a sophisticated methodology for quantifying energy, water vapour, and gas exchanges between the terrestrial environment and the atmosphere.
5. **Enhanced Vegetation Index (EVI)**: a vegetation index specifically developed to improve sensitivity in regions with high biomass, effectively mitigating the influences of atmospheric and soil conditions.
6. **Enhanced Vegetation Index 2 (EVI2)**: a streamlined variant of the EVI that employs only two spectral bands, thereby enhancing computational efficiency while maintaining effectiveness.
7. **Evapotranspiration (ET)**: the cumulative processes of evaporation from soil surfaces and transpiration from plant systems integral to hydrological studies.
8. **Google Earth Engine (GEE)**: a cloud-based platform facilitating geospatial analysis and remote sensing data processing for various applications.
9. **Green Normalised Difference Vegetation Index (GNDVI)**: a vegetation index that exhibits heightened sensitivity to chlorophyll content, thus providing insights into plant health.
10. **Leaf Area Index (LAI)**: a dimensionless ratio representing the leaf area relative to a unit ground area, serving as a key metric for assessing vegetation density.
11. **Latent Heat Flux (LE)**: the measure of heat released or absorbed during the phase transitions of water, playing a pivotal role in calculations related to evapotranspiration.
12. **Machine Learning (ML)**: a branch of artificial intelligence that employs algorithms to analyse data, discern patterns, and derive informed decisions based on these insights.
13. **Net Radiation (Rn)**: the net balance of incoming and outgoing radiation at the Earth's surface, critical for understanding energy dynamics.

14. **Normalised Difference Vegetation Index (NDVI)**: a widely recognised vegetation index that quantifies plant health and density through remote sensing techniques.
15. **Normalised Difference Water Index (NDWI)**: A remote sensing index ranging from -1 to +1, used to assess vegetation water content, with higher values (closer to +1) indicating greater moisture and lower values (closer to 0 or negative) suggesting dryness or sparse vegetation.
16. **Optimised Soil-Adjusted Vegetation Index (OSAVI)**: a refined vegetation index that minimises the influence of soil brightness, providing a clearer assessment of vegetation health.
17. **Precision Agriculture (PA)**: an approach to farming management that integrates advanced technology to optimise resource inputs and enhance crop yields.
18. **Remote Sensing (RS)**: the process of acquiring information about the Earth's surface without direct physical contact, utilising aerial and satellite technologies.
19. **Soil Heat Flux (G)**: the rate at which heat is transferred through the soil, significantly affecting soil temperature and the overall energy balance.
20. **Soil-Adjusted Vegetation Index (SAVI)**: a vegetation index that accounts for soil reflectance effects, particularly effective in assessing sparse vegetation canopies.
21. **Unmanned Aerial Vehicle (UAV)**: a remotely piloted aircraft employed for data collection purposes within precision agriculture.
22. **Vegetation Index (VI)**: a numerical indicator extracted from remote sensing data that quantifies vegetation cover and health, serving as a vital tool in ecological assessments.
23. **Water Deficit Index (WDI)**: an index that quantifies crop water stress using vegetation and soil moisture assessment parameters.

1. CHAPTER 1: INTRODUCTION

South Africa, a region characterised by pronounced hydroclimatic variability, is classified as a semi-arid to arid nation grappling with markedly constrained freshwater reserves (WRC, 2015; Edokpayi, 2020). Despite its marginal contribution to global greenhouse gas emissions, this region is frequently challenged by the substantial repercussions of climate change (Tongwane and Moeletsi, 2018). The elevated susceptibility and low resilience of critical systems, notably water resources, render the region particularly vulnerable to adverse effects from environmental shifts (Ngcobo, 2023). Climate change inherently occurs, but anthropogenic activities, viz. industrialisation, urbanisation, and deforestation, inter alia, have notably expedited its adverse impacts (Muluneh, 2021).

Additionally, the escalating demand for water propelled by socio-economic advancement and rapid population growth has compounded the strain on South Africa's already scarce water reservoirs (du Plessis, 2023). A study by Kusangaya *et al.* (2013) highlights the country's heightened vulnerability to the negative impacts of climate change, citing its limited capacity for adaptation, widespread poverty, and inadequate utilisation of technological advancements (Kusangaya *et al.*, 2013; Hosea and Khalema, 2020). Foreseen climate changes, which notably amplify precipitation and temperature variability, pose distinctive challenges for agriculture due to shifting weather patterns influenced by climate change (Ngcobo *et al.*, 2023). These changes are projected to heighten inter and intra-annual precipitation variability, elevate drought risks, diminish water availability, and raise concerns about reduced crop yields (IPCC, 2019).

Furthermore, South Africa faces substantial agricultural challenges due to inherent water scarcity (WRC, 2015; Mabhaudhi *et al.*, 2021). With over three-quarters of the nation receiving less than 500 mm of rainfall annually (Johnson and Smithers, 2020), this scarcity exacerbates drought conditions and severely limits water availability for irrigation (Meza *et al.*, 2021). Consequently, insufficient moisture for optimal crop development results (Bodner *et al.*, 2015). This reduction in agricultural output has significant economic implications for rural communities, including diminished earnings, increased poverty, and heightened vulnerability to food and nutrition insecurity (Gokool *et al.*, 2023; Sibanda *et al.*, 2023). Therefore, proactive measures, such as implementing water-efficient farming techniques, are essential to enhance water resilience and ensure sustainable agricultural productivity.

According to the Food and Agriculture Organisation of the United Nations (FAO), acute food insecurity in Southern Africa increased by 1.5% between 2021 and 2022, as reported in 2023 (FAO *et al.*, 2023). The region's dependence on rainfed agriculture for food production renders it particularly vulnerable to the impacts of climate change due to erratic rainfall patterns (Mpandeli *et al.*, 2018). Additionally, average crop yields are frequently low due to the unpredictable climate and other stress-related factors such as soil fertility, weeds, pests, diseases, and improper crop management practices, including incorrect fertiliser application and poor weed control (DAFF, 2010; Reddy, 2020). These factors further exacerbate rainfed agriculture's challenges, as water availability for plant growth is limited and unreliable (Reddy, 2020). Hence, the region's agricultural productivity is at risk without dependable irrigation systems or alternative water sources.

Given the low water availability, effective water management strategies are crucial for maximising agricultural productivity (Gheewala *et al.*, 2011; Rosegrant *et al.*, 2013). Precision agriculture (PA) can potentially optimise using fertilisers, energy, water, herbicides, and pesticides, thereby enhancing agricultural output (Awais *et al.*, 2023). Kamara *et al.* (2019) report that 80% of the food consumed in Sub-Saharan Africa (SSA) is produced by smallholder farmers operating at a subsistence level (Kamara *et al.*, 2019). Smallholder farmers encompass previously disadvantaged subsistence and emerging farmers (Reddy, 2020). Several factors, including underdevelopment, inadequate policies for smallholder farmers, reliance on unpredictable precipitation, severe soil degradation, population growth, and natural disasters, exacerbate food demands while reducing the likelihood of achieving food and nutrition security (Sibanda *et al.*, 2023).

Smallholder farmers constitute 50% of the population reliant on agriculture as their primary source of income in Sub-Saharan Africa (SSA), representing 70% of the nation's population (Sibanda *et al.*, 2023). Moreover, a significant portion of the region's 1.2 billion inhabitants live below the poverty line of one dollar per day, impeding their ability to access the resources necessary for larger-scale commercial farming (Blair *et al.*, 2018; Brewer *et al.*, 2022). This limited resource availability adversely affects the productivity and potential of smallholder farms, as many agricultural decisions are based on indigenous knowledge (Brewer *et al.*, 2022). Consequently, smallholder farmers in rural areas face numerous challenges requiring cost-effective, objective, and innovative approaches to improve their agricultural output (Nhamo *et al.*, 2020; Brewer *et al.*, 2022).

As such, this study addresses precision water management in agriculture, specifically focusing on sugarcane cultivation. Sugarcane production is markedly sensitive to climate variability, particularly temperature and precipitation changes (Zhao *et al.*, 2015). Regions dependent on rainfed agriculture and lacking irrigation infrastructure face heightened susceptibility to these challenges (Shiferaw *et al.*, 2014). Research by Hennessy *et al.* (2022) highlights the growing threats to sugarcane sustainability from the increasing frequency of extreme hydrological events, such as prolonged droughts and severe floods (Hennessy *et al.*, 2022; Ngcobo, 2023). The attention to small-scale farmers is crucial due to their pivotal role in sugarcane production and susceptibility to climatic variations (Ngcobo, 2023), emphasising the importance of this investigation.

Sugarcane is a highly consequential cash crop akin to maize, cassava, sorghum, and sweet potatoes, ensuring the sustenance of numerous communities within the region (German *et al.*, 2020; Ngcobo *et al.*, 2023). During the 2018/2019 agricultural season, the sugar industry in southern Africa facilitated the exportation of nearly 1.2 million tonnes of refined sugar, yielding revenue exceeding $2.15 billion (Ngcobo, 2023). On average, sugarcane cultivation necessitates an annual precipitation of 1,800 mm to achieve optimal yields (Ngcobo *et al.*, 2023). Nonetheless, sugarcane cultivation in watersheds is responsible for consuming more than 40% of the available water resources (Knox *et al.*, 2010; Singels *et al.*, 2013; Jones *et al.*, 2015). Given the heavy dependence of thousands of farmers on sugarcane as their primary income source, it is imperative to explore advanced technological methods to enhance crop yields (Narimoto and Camarotto, 2018).

Furthermore, water use in the region has increased despite stagnant sugarcane production, as rising temperatures and total evaporation intensify water deficits (Carr and Knox, 2011; Watson, 2011; Ngcobo, 2023). Consequently, smallholder farmers face challenges from reduced crop yields that fall short of the land's potential due to climatic extremes (Adisa *et al.*, 2018; Walker *et al.*, 2018). This necessitates adjustments in crop management practices, potentially jeopardising the sugar industry's long-term viability in the region (Biggs *et al.*, 2013; Ngcobo, 2023). According to Ngcobo *et al.* (2023), declines in agricultural productivity in South Africa are linked to soil management techniques, pest infestations, and disease (Ngcobo *et al.*, 2023). Thus, the economic feasibility of sugarcane production hinges on resource conservation measures to maintain international competitiveness.

Small-scale farmers operating under rainfed conditions typically achieve low average crop yields, resulting in suboptimal crop water use efficiency (WUEc) (Reddy, 2020). Crop water use, primarily through evapotranspiration (ET), is critical for various physiological functions (Shukla and Kot, 2015). Therefore, understanding crop water consumption patterns is essential for improving WUEc on smallholder farms. According to Allen *et al.* (1998), ET encompasses the combined water flux from soil, plant, and water surface evaporation and plant transpiration (Allen *et al.*, 1988; Awada *et al.*, 2024). Accurate ET estimation is crucial for precision agricultural water management, as it informs strategies for evaluating soil moisture, monitoring drought conditions, and assessing crop water stress levels, ultimately enhancing crop productivity, yield, and quality (Niu *et al.*, 2022).

In addition, monitoring ET allows farmers to proactively detect and respond to meteorological changes, enabling them to adjust their cultivation and water management practices accordingly (Sabir *et al.*, 2024). This is particularly vital in regions prone to drought or erratic precipitation, as it helps subsistence farmers enhance the long-term sustainability of their agricultural systems (Yacoob *et al.*, 2024). Fundamentally, accurate ET estimation is paramount for smallholder farmers, providing indispensable data to optimise crop yields, preserve water resources, and alleviate the repercussions of climate variability (Yacoob *et al.*, 2024). Additionally, enhancing and expanding our understanding of accurate ET measurement at appropriate temporal and spatial scales is crucial for assessing water stress in small-scale agricultural operations (Yacoob *et al.*, 2024). ET can be measured locally with specialised instruments and at larger spatial scales using remote sensing (RS) techniques (Ellsäßer *et al.*, 2020).

In terms of specialised instruments, various micrometeorological methods exist, including eddy covariance (EC), surface renewal (SR), the Bowen ratio energy balance (BREB) method, large weighing lysimeters, and scintillometry that can be employed to estimate ET at the field scale (Kunz *et al.*, 2015; Chimonyo *et al.*, 2016; Mbangiwa *et al.*, 2019) (refer to Table 1.1). However, these methods are characterised by limited measurement scales, typically less than 150 metres, which limits their applicability for capturing spatial variability in agricultural contexts (Wang and Liang, 2008; Bachour, 2013; Tian *et al.*, 2017). Additionally, the high costs of advanced equipment and the lack of skilled technicians to install and operate such instruments often limit their use in economically disadvantaged areas, such as small-scale agricultural enterprises (Yacoob *et al.*, 2024).

Table 1.1 Micrometeorological methods for ET estimation.

Method/Approach	Description	Strengths	Limitations	References
Eddy covariance	Computes latent heat flux (Le) as the covariance between turbulent fluctuations; also uses the shortened energy balance approach to calculate Le indirectly.	There are few theoretical assumptions and a broad application scope. Considered the standard for determining energy flux.	High cost, ongoing maintenance, complex operation, limited use in small experimental plots, and sensitivity of sensors.	(Aubinet *et al.*, 2012; Rosa and Tanny, 2015; Aldworth *et al.*, 2023)
Surface Renewal	Estimation of H using high-frequency air temperature measurements and structure-function theory; calculates LE as a residual of the shortened energy balance.	Applicable to homogeneous and heterogeneous canopies. Suitable for long-term monitoring of ET in regions with limited data.	Limited spatial coverage in measurements requires a calibration period with independent H measurement for SR1.	(Mengistu and Savage, 2010; Suvočarev *et al.*, 2019; Gray *et al.*, 2022)
Bowen ratio energy balance	An indirect method for determining latent heat flux using micrometeorological parameters.	Inexpensive, simple calculation, accurate results for meteorological variables.	Relatively large errors compared to EC.	(Spittlehouse and Black, 1980; Todd *et al.*, 2000; Mukherjee *et al.*, 2021)
Large weighing lysimeters	Measures change in mass of isolated soil volume to estimate crop water use.	Provides the most accurate ET estimates.	Costly, it requires high operational and data processing expertise for accurate measurements.	(Perez-Priego *et al.*, 2017; Moorhead *et al.*, 2019; Chávez *et al.*, 2020)
Scintillometry	A transmitter and receiver measure flux contributions over a fixed path length.	Accounts for variation in the measurement area. Provides some level of representativeness.	High cost, signal saturation, signal dependence on inner-scale, tower vibrations.	(George and Savage, 2009; Savage, 2009; Moorhead *et al.*, 2017)

In recent decades, advancements in satellite earth observation (SEO) systems have enabled the acquisition of hydro-meteorological data on expansive geographic scales and remote territories (Sorooshian *et al.*, 2011; Dasgupta *et al.*, 2023). However, among the SEO systems, the primary drawback of satellite imagery is its often insufficient spatial resolution to accurately depict the spatial heterogeneity of small-scale farms (Sandbrook, 2015; Aliabad *et al.*, 2022). Moreover, the frequency of data collection is limited by satellite revisit times and atmospheric disturbances, such as cloud cover (Nhamo *et al.*, 2020). While specific satellite-based datasets, viz. WorldView (Mandanici *et al.*, 2019), GeoEye (Caturegli *et al.*, 2015), and PlanetScope (Planet Labs, 2021), as well as manned aerial vehicles (Rejeb *et al.*, 2022) can address spatiotemporal resolution challenges, they are often too costly for smallholder agricultural applications (Cucho-Padin *et al.*, 2019).

Subsequently, as an alternative, the adoption of unmanned aerial vehicles (UAVs) for PA is on the rise (Messina and Modica, 2020). UAVs are particularly promising for small-scale farming due to their ability to collect data at low altitudes (Yadav *et al.*, 2024), providing intricate spatial details with centimetre-level precision (Zhang and Zhu, 2023). The spectral resolution of the data depends on the camera used (Nhamo *et al.*, 2020). Additionally, data acquisition can occur at customisable time intervals and ground sampling distances (Brewer *et al.*, 2022). This technological advancement facilitates the identification and mapping of variations in plant growth over time, known as phenological growth variations (Cucho-Padin *et al.*, 2019). Consequently, UAVs can provide farmers with precise and timely agrometeorological information, allowing them to effectively monitor crop conditions during phenotyping (Brewer *et al.*, 2022).

Presently, two primary frameworks are used for estimating ET with UAV-derived data: thermal band-based energy balance methods and empirical models based on vegetation indices (VIs) (Tang *et al.*, 2019; Ellsäßer *et al.*, 2020). Surface energy balance models that utilise thermal-infrared imagery to map land surface temperature (LST) have been developed to overcome the limitations of in-situ techniques (Molaei *et al.*, 2023). In contrast, VI-based methods estimate ET or the crop coefficient (Kc) by establishing relationships between these parameters and predictor variables, such as VIs (Ihuoma *et al.*, 2021). Traditionally, energy balance methods relied on satellite data, requiring adjustments for UAV integration (Molaei *et al.*, 2023). Thus, further exploration of practical ET estimation approaches could significantly benefit smallholder farmers, addressing existing research gaps.

In crop health evaluations, a crop's productivity is gauged by critical indicators, including heightened photosynthesis rates, increased chlorophyll concentrations, lower leaf temperatures, and enhanced stomatal conductance (Brewer *et al.*, 2022). The vibrant green pigmentation of the leaves serves as a marker for chlorophyll content, providing valuable insights into the biochemical processes and overall health of the crops (Brewer *et al.*, 2022). Moreover, the photosynthetic efficacy of the crop is intricately intertwined with the fluctuating rates of stomatal conductance, which are influenced by the crop's moisture content and the ET rate (Jackson, 1982; Saseendran *et al.*, 2015; Xiong *et al.*, 2022). Consequently, optimal levels of stomatal conductance and augmented chlorophyll concentrations result in reduced temperatures within the crop, indicating robust health and productivity with minimal water stress (Brewer *et al.*, 2022).

Advanced multispectral and thermal infrared data acquired from UAVs facilitate the analysis of crop image data and the objective assessment of crop characteristics (Jones *et al.*, 2009; Niu *et al.*, 2020; Brewer *et al.*, 2022). Moreover, scholarly studies have demonstrated the utility of vegetation indices (VIs) derived from various parts of the electromagnetic (EM) spectrum in capturing information on plant health and water status, accounting for atmospheric effects, soil background reflectance, and sun angle (Tahir *et al.*, 2018; Brewer *et al.*, 2022). For example, the Normalised Difference Vegetation Index (NDVI) stands out as a widely utilised tool in vegetation monitoring, serving diverse purposes such as estimating ET (Niu *et al.*, 2020; Abbasi *et al.*, 2021; Niu *et al.*, 2022), detecting water stress (Zhao *et al.*, 2015; Zhao *et al.*, 2017), and evaluating crop yield (Zhao *et al.*, 2017).

Water indices, such as the Normalised Difference Water Index (NDWI), are crucial for assessing vegetation water content, helping to identify and address crop water stress (Virnodkar *et al.*, 2020). By leveraging Near Infrared (NIR) and Short-Wave Infrared (SWIR) bands, NDWI enhances precision in water content assessment, which is essential for optimising irrigation in water-limited settings (Ihuoma and Madramootoo, 2017). Its strong correlations with other indices, such as NDVI, further highlight its versatility in monitoring crop health across growth stages (Gao, 1996; Strashok *et al.*, 2022). While satellite-based methods often lack the spatial resolution to capture the variability of smallholder farms (Gokool *et al.*, 2023), UAV-based approaches offer a promising solution for applying NDWI to improve water stress monitoring in these contexts.

Furthermore, machine learning (ML) regression models such as Support Vector Regression (SVR), Random Forest Regression (RFR), and Gradient Tree Boosting (GTB) are utilised for predicting agricultural parameters such as crop yield (Sakamoto, 2020) and ET (Fan *et al.*, 2021). These models also analyse various crop attributes, including water content and health status across different crop species (Guo *et al.*, 2020). Studies consistently show that the RF ensemble outperforms other algorithms by utilising meteorological data and VIs for accurate predictions (Yao *et al.*, 2013). By integrating data from UAVs, especially spectral and thermal infrared bands for calculating VIs, with advanced ML algorithms, precise assessments of crop health and water stress on smallholder farms can be achieved (Hassanijalilian *et al.*, 2020). This integration holds promise for enhancing agricultural decision-making and productivity in farming (Teshome *et al.*, 2023).

Given the above, the primary objective of this research is to evaluate the efficacy of UAVs and ML algorithms for estimating ET and detecting crop water status in small-scale agriculture. While UAV-based RS techniques have proven useful for monitoring crop water status (Brewer *et al.*, 2022), research concerning reliable ET estimation using UAV-derived data remains limited (Yacoob *et al.*, 2024). Subsequently, this study aims to validate ET estimates from UAVs and apply ML techniques with structural and water indices to assess crop water status. Given the limitations of conventional ET estimation methods, UAV technology presents a practical solution for smallholder farmers (Yacoob *et al.*, 2024). Subsequently, this study emphasises the need for scalable, accessible methods to enhance ET estimation and crop water stress monitoring in resource-limited agricultural systems.

Furthermore, conventional ET estimation methods are often costly, necessitating the exploration of UAV-based approaches, especially for smallholder farmers with limited technical resources (Gokool *et al.*, 2023). However, UAV-based methods present challenges, such as the high computational demands for processing data, which require specialised software and expertise (Gokool *et al.*, 2023). Cloud-based platforms like Google Earth Engine (GEE) are increasingly recommended to address these challenges (Gokool *et al.*, 2023). Despite the interest in UAV-derived ET estimation, practical implementation strategies remain scarce (Yacoob *et al.*, 2024). This study seeks to fill this gap by improving the accuracy and reliability of ET estimation. While UAVs offer a viable alternative, reliance on in-situ data poses limitations (Yacoob *et al.*, 2024). Thus, this research prioritises less data-dependent techniques to assess accuracy loss and enhance feasibility for smallholder farmers.

1.1 Aim

Given the limited scholarly discourse on pragmatic approaches for implementing precision water management strategies in small-scale agricultural holdings, this study aims to evaluate the potential of UAV-based remote sensing methodologies for estimating actual ET (ETa) and monitoring crop water stress. The research is structured to develop and assess methodologies that provide smallholder farmers with reliable, actionable data to guide decision-making and optimise water use. This study seeks to enhance productivity and resource efficiency in water-scarce agricultural landscapes by refining water management strategies.

1.2 Objectives

In alignment with the overarching aim of this study, the thesis is structured into three distinct sections, each progressively addressing established and novel methodologies designed to achieve the following specific objectives:

i. Conduct a scoping review and bibliometric analysis of the literature concerning the practical application of UAVs for estimating ETa or detecting crop water stress, providing current, precise insights to guide and enhance PA practices (**Chapter 2**).
ii. Apply and evaluate RS methodologies for estimating ETa using UAV-acquired data, incorporating VI-based (ET-VI) models, ML techniques for Kc prediction, and validation against EC measurements (**Chapter 3**).
iii. Assess the potential of integrating UAV-acquired multispectral data with Sentinel-2 satellite imagery to enhance crop water stress monitoring and optimise water management strategies through ML-based predictive modelling (**Chapter 4**).

Building adaptive capacity and empowering smallholder farmers to enhance their livelihoods amidst a changing climate and increasing extreme weather events necessitates exploring advanced technologies like UAVs. As mentioned, these technologies offer cost-effective solutions for assessing crop water status and guiding irrigation management. While ground-based systems and SEO technologies can provide such information, they often lack the spatial and temporal resolutions required for small-scale farms, limiting timely interventions. Furthermore, research gaps persist regarding how UAV sensors and computational techniques can support site-specific applications and improve irrigation precision by accounting for within-field variability in subsistence agriculture. The research questions guiding this investigation are outlined below and were tested in **Chapter 3**.

RQ1: How can in-situ NDVI be utilised to predict Kc for smallholder farms?

RQ2: What is the accuracy of UAV-based VIs in estimating ETa compared to ground-based EC flux tower measurements?

RQ3: Which VI-based methodology is most suitable for estimating ETa in small-scale agricultural systems?

Building on the establishment of an effective technique for estimating ETa using UAV-derived data, **Chapter 4** focuses on developing a methodology to determine crop water stress. The following research questions frame this investigation:

RQ4: How do UAV-acquired structural VIs (SVIs) correlate with satellite-derived NDWI for monitoring crop water stress?

RQ5: Can UAV-based data be used to develop a predictive model for satellite-derived NDWI that is applicable to smallholder farming systems?

RQ6: How do UAV-based NDWI estimates compare with in-situ ETa measurements and the Water Deficit Index (WDI) for monitoring crop water stress?

1.3 Overview of thesis structure

The thesis comprises five chapters, with three crafted as "publishable" articles and submitted adhering to the guidelines stipulated by the College of Agriculture, Engineering, and Science at the University of KwaZulu-Natal. Despite this approach, each antecedent chapter laid the groundwork for subsequent sections (Figures 1.1 and 1.2), all unified by a central theme: the evaluation of data obtained from UAVs to enhance precision water management in smallholder agricultural settings. It should be noted that, due to the paper-like structure adopted in this thesis, a degree of redundancy may be apparent across the chapters, notably within the three independent articles. This deliberate repetition is intentional, as these articles were written for submission to different local and international academic journals for publication.

Chapter One serves as the foundational element of this study, offering a comprehensive rationale for the research while highlighting the local research landscape on critical subjects such as smallholder farming, ETa, crop water stress, and precision water management.

Chapter Two presents a scoping review employing advanced bibliometric techniques to discern key journals, seminal publications, leading authors, and influential countries that have significantly contributed to the application of UAVs in ETa estimation and crop water stress detection to inform irrigation management decisions. The principal objective of this chapter is to provide a precise and detailed assessment of the current state of research in this domain.

Chapter Three investigates innovative and robust methods to enhance the sustainability and productivity of small-scale sugarcane farms in water-scarce regions such as South Africa, with a particular emphasis on RS technology, specifically UAVs. The study addresses the limitations of traditional ETa estimation techniques by assessing potential UAV-based ETa estimation approaches through comparisons against ground-based measurements.

Chapter Four presents a novel methodology which identifies and exploits the synergies between satellite- and UAV-acquired data to predict crop water stress by leveraging the computational and predictive power of geospatial cloud computing and ML, respectively. This approach provides insights into crop water status, validating its potential to optimise irrigation strategies and improve water resource management in smallholder farming.

Chapter Five synthesises the insights from Chapters One to Four, emphasising the key findings from the research results and outlining the primary contributions to new knowledge derived from this investigation. Additionally, it provides recommendations for future studies.

Advancing Precision Water Management in Smallholder Sugarcane Farming: Leveraging Unmanned Aerial Vehicle-Based Remote Sensing and Machine Learning for Evapotranspiration and Water Stress Assessment

Chapter 2: Leveraging Unmanned Aerial Vehicle Technologies to Facilitate Precision Water Management in Smallholder Farms: A Scoping Review and Bibliometric Analysis

i. Conduct a scoping literature review on UAV-based RS techniques to facilitate precision water management within smallholder farms.

ii. Identify significant journals, publications, authors, and nations that have made notable contributions using UAVs in ETa estimation and crop water stress detection.

iii. Describe UAV-based approaches to monitor crop water use and aid PA.

iv. Use co-citation analysis to group publications according to their semantic similarity, identify thematic areas, and map studies' main "intellectual structure."

v. Identify data analytic methods used to support the estimation of ETa and detection of crop water stress and analyse these results within the context of smallholder farming.

Chapter 3: Evaluating the Potential of Unmanned Aerial Vehicle-Derived Data for Evapotranspiration Estimation in Smallholder Farms

i. Develop a predictive model to establish the correlation between in-situ Kc measurements and NDVI values through applying advanced ML methodologies.

ii. Evaluate RS-derived ET-VI techniques by conducting a comparative assessment of five VIs: NDVI, NDVIscaled, NDVIKc, EVI and EVI2 for estimating ETa vis-à-vis measurements from a ground-based EC flux tower.

iii. Conduct a comprehensive assessment of the previously mentioned VI-based methodologies (objectives i and ii) to determine the most suitable approach for implementation in smallholder agriculture.

Chapter 4: A Machine Learning Approach for Quantifying Crop Water Stress in Smallholder Farms Using Unmanned Aerial Vehicle Multispectral Imagery

i. Determine the relationships between satellite-derived NDWI and SVIs.

ii. Derive a predictive model for satellite-derived NDWI based on the identified UAV-acquired SVIs.

iii. Correlate the predicted UAV-based NDWI estimates with in-situ derived ETa measurements and the WDI.

Chapter 5: Synthesis of Aims and Objectives, Key Findings, and Recommendations for Future Research

Figure 1.1 Conceptual framework of the study.

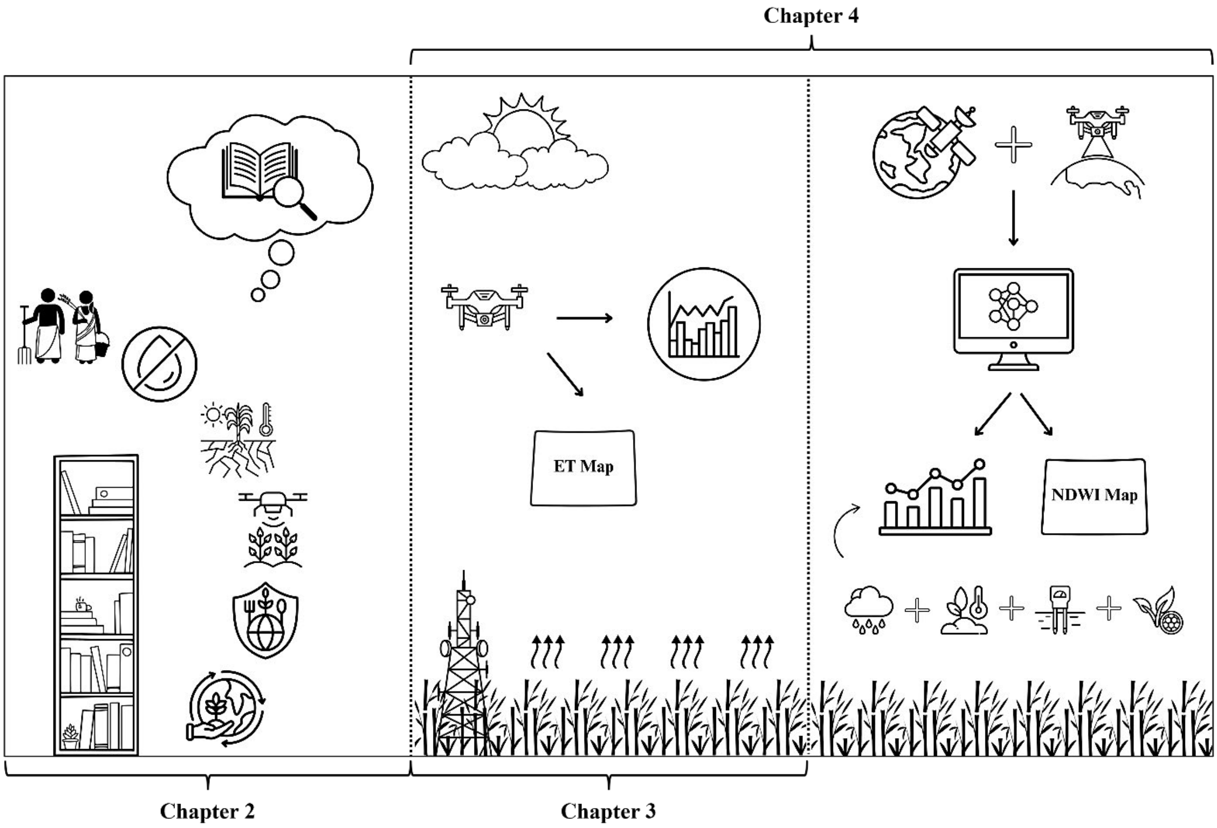

Figure 1.2 Focus areas and methodologies in Chapters 2 to 4, illustrating their integration to achieve the overarching research objectives.

1.4 References

Abbasi, N, Nouri, H, Didan, K, Barreto-Muñoz, A, Chavoshi Borujeni, S, Opp, C, Nagler, P, Thenkabail, PS and Siebert, S. 2023. Mapping vegetation index-derived actual evapotranspiration across croplands using the Google Earth Engine platform. *Remote Sensing* 15 (4): 1017.

Abbasi, N, Nouri, H, Didan, K, Barreto-Muñoz, A, Chavoshi Borujeni, S, Salemi, H, Opp, C, Siebert, S and Nagler, P. 2021. Estimating actual evapotranspiration over croplands using vegetation index methods and dynamic harvested area. *Remote Sensing* 13 (24): 5167.

Adisa, O, Botai, CM, Botai, JO, Hassen, A, Darkey, D, Tesfamariam, EH, Adisa, AF, Adeola, AM and Ncongwane, KP. 2018. Analysis of agro-climatic parameters and their influence on maize production in South Africa. *Theoretical and Applied Climatology* 134 (1): 991-1004.

Aldworth, TA, Toucher, MLW, Clulow, AD and Swemmer, AM. 2023. The effect of woody encroachment on evapotranspiration in a semi-arid savanna. *Hydrology* 10 (1): 9.

Aliabad, FA, Shojaei, S, Mortaz, M, Ferreira, CSS and Kalantari, Z. 2022. Use of Landsat 8 and UAV images to assess changes in temperature and evapotranspiration by economic trees following foliar spraying with light-reflecting compounds. *Remote Sensing* 14 (23): 6153.

Allen, R, Pereira, L, Raes, D and Smith, M. 1998. *Crop Evapotranspiration: Guidelines for Computing Crop Water Requirements.* FAO Irrigation and Drainage Paper No. 56. Food and Agriculture Organization of the United Nations, Rome, Italy.

Aubinet, M, Vesala, T and Papale, D. 2012. *Eddy Covariance: A Practical Guide to Measurement and Data Analysis.* Springer Science & Business Media, Dordrecht, Netherlands.

Awada, H, Sirca, C, Marras, S, Castellini, M, Spano, D and Pirastru, M. 2024. Modelling soil moisture and daily actual evapotranspiration: integrating remote sensing surface energy balance and 1D Richards equation. *International Journal of Applied Earth Observation and Geoinformation* 128 (1): 103744.

Awais, M, Li, W, Cheema, M, Zaman, Q, Shaheen, A, Aslam, B, Zhu, W, Ajmal, M and Faheem, M. 2023. UAV-based remote sensing in plant stress imaging using high-resolution thermal sensor for digital agriculture practices: a meta-review. *International Journal of Environmental Science and Technology* 20 (1): 1135-1152

Bachour, R. 2013. Evapotranspiration modelling and forecasting for efficient management of irrigation command areas. Unpublished thesis, Department of Civil and Environmental Engineering, Utah State University, Logan, Utah, United States.

Biggs, JS, Thorburn, PJ, Crimp, S, Masters, B and Attard, SJ. 2013. Interactions between climate change and sugarcane management systems for improving water quality leaving farms in the Mackay Whitsunday region, Australia. *Agriculture, Ecosystems & Environment* 180 (1): 79-89.

Blair, D, Shackleton, CM and Mograbi, PJ. 2018. Cropland abandonment in South African smallholder communal lands: land cover change (1950-2010) and farmer perceptions of contributing factors. *Land* 7 (4): 121.

Bodner, G, Nakhforoosh, A and Kaul, H-P. 2015. Management of crop water under drought: a review. *Agronomy for Sustainable Development* 35 (2): 401-442.

Brewer, K, Clulow, A, Sibanda, M, Gokool, S, Odindi, J, Mutanga, O, Naiken, V, Chimonyo, VGP and Mabhaudhi, T. 2022. Estimation of maize foliar temperature and stomatal conductance as indicators of water stress based on optical and thermal imagery acquired using an unmanned aerial vehicle (UAV) platform. *Drones* 6 (7): 169.

Carr, M and Knox, J. 2011. The water relations and irrigation requirements of sugar cane (Saccharum officinarum): a review. *Experimental Agriculture* 47 (1): 1-25.

Caturegli, L, Casucci, M, Lulli, F, Grossi, N, Gaetani, M, Magni, S, Bonari, E and Volterrani, M. 2015. GeoEye-1 satellite versus ground-based multispectral data for estimating nitrogen status of turfgrasses. *International Journal of Remote Sensing* 36 (8): 2238-2251.

Chávez, R, Grönwall, J, Kwast, J, Danert, K and Foppen, J. 2020. Estimating domestic self-supply groundwater use in urban continental Africa. *Environmental Research Letters* 15 (10): 1040b2.

Chimonyo, V, Modi, A and Mabhaudhi, T. 2016. Assessment of sorghum-cowpea intercrop system under water-limited conditions using a decision support tool. *Water SA* 42 (2): 316-327.

Cucho-Padin, G, Loayza, H, Palacios, S, Balcazar, M, Carbajal, M and Roberto, Q. 2019. Development of low-cost remote sensing tools and methods for supporting smallholder agriculture. *Applied Geomatics* 12 (1): 247-263.

DAFF. 2010. *Soya beans production guideline*. Department of Agriculture, Forestry and Fisheries, Pretoria, South Africa.

Dasgupta, A, Arnal, L, Emerton, R, Harrigan, S, Matthews, G, Muhammad, A, O'Regan, K, Pérez-Ciria, T, Valdez, E, van Osnabrugge, B, Werner, M, Buontempo, C, Cloke, H, Pappenberger, F, Pechlivanidis, IG, Prudhomme, C, Ramos, M-H and Salamon, P. 2023. Connecting hydrological modelling and forecasting from global to local scales: perspectives from an international joint virtual workshop. *Journal of Flood Risk Management* 1 (1): e12880.

du Plessis, A. 2023. *South Africa's water predicament*. Springer Cham.

Edokpayi, J, Makungo, R, Mathivha, F, Nkuna, TR, Volenzo, T and Odiyo, J. 2020. Influence of global climate change on water resources in South Africa: toward an adaptive management approach. In: *Water Conservation and Wastewater Treatment in BRICS Nations.*

Ellsäßer, F, Röll, A, Stiegler, C, Hendrayanto and Hölscher, D. 2020. Introducing QWaterModel, a QGIS plugin for predicting evapotranspiration from land surface temperatures. *Environmental Modelling & Software* 130 (1): 104739.

Fan, J, Zheng, J, Wu, L and Zhang, F. 2021. Estimation of daily maize transpiration using support vector machines, extreme gradient boosting, artificial and deep neural networks models. *Agricultural Water Management* 245 (1): 106547.

FAO, IFAD, UNICEF, WFP and WHO. 2023. *The State of Food Security and Nutrition in the World 2023. Urbanisation, agrifood systems transformation and healthy diets across the rural-urban continuum*. FAO, Rome, Italy.

Gao, B-c. 1996. NDWI—A normalised difference water index for remote sensing of vegetation liquid water from space. *Remote Sensing of Environment* 58 (3): 257-266.

George, O and Savage, M. 2009. Surface layer scintillometry for estimating the sensible heat flux component of the surface energy balance. *South African Journal of Science* 105 (1): 108-116.

German, LA, Hepinstall-Cymerman, J, Biggs, T, Parker, L and Salinas, M. 2020. The environmental effects of sugarcane expansion: a case study of changes in land and water use in southern Africa. *Applied Geography* 121 (1): 102240.

Gheewala, S, Berndes, G and Jewitt, G. 2011. The bioenergy and water nexus. *Biofuels, Bioproducts and Biorefining* 5 (4): 353-360.

Gokool, S, Mahomed, M, Kunz, R, Clulow, A, Sibanda, M, Naiken, V, Chetty, K and Mabhaudhi, T. 2023. Crop monitoring in smallholder farms using unmanned aerial vehicles to facilitate precision agriculture practices: a scoping review and bibliometric analysis. *Sustainability* 15 (4): 3557.

Gray, BA, Toucher, ML, Savage, MJ and Clulow, AD. 2022. Seasonal evapotranspiration over an invader vegetation (Pteridium aquilinum) in a degraded montane grassland using surface renewal. *Journal of Hydrology: Regional Studies* 40 (1): 101012.

Guo, Y, Yin, G, Sun, H, Wang, H, Chen, S, Senthilnath, J, Wang, J and Fu, Y. 2020. Scaling effects on chlorophyll content estimations with RGB camera mounted on a UAV platform using machine-learning methods. *Sensors* 20 (18): 5130.

Hassanijalilian, O, Igathinathane, C, Doetkott, C, Bajwa, SG, Nowatzki, J and Esmaeili, SAH. 2020. Chlorophyll estimation in soybean leaves infield with smartphone digital imaging and machine learning. *Computers and Electronics in Agriculture* 174 (1): 105433.

Hennessy, K, Lawrence, J and Mackey, B. 2022. *IPCC Sixth Assessment Report (AR6): climate change 2022 - impacts, adaptation and vulnerability: regional factsheet Australasia*.

Hosea, P and Khalema, E. 2020. Scoping the nexus between climate change and water-security realities in rural South Africa. *Town and Regional Planning* 77 (1): 18-30.

Ihuoma, SO and Madramootoo, CA. 2017. Recent advances in crop water stress detection. *Computers and Electronics in Agriculture* 141 (1): 267-275.

IPCC. 2019. *Climate Change and Land: an IPCC special report on climate change, desertification, land degradation, sustainable land management, food security, and*

greenhouse gas fluxes in terrestrial ecosystems. Cambridge University Press, Cambridge, UK and New York, USA.
Jackson, RD. 1982. Canopy temperature and crop water stress. In: ed. Hillel, D, *Advances in Irrigation*. Elsevier.
Johnson, KA and Smithers, JC. 2020. Updating the estimation of 1-day probable maximum precipitation in South Africa. *Journal of Hydrology: Regional Studies* 32 (1): 100736.
Jones, HG, Serraj, R, Loveys, BR, Xiong, L, Wheaton, A and Price, AH. 2009. Thermal infrared imaging of crop canopies for the remote diagnosis and quantification of plant responses to water stress in the field. *Functional Plant Biology* 36 (1): 978-989.
Jones, MR, Singels, A and Ruane, AC. 2015. Simulated impacts of climate change on water use and yield of irrigated sugarcane in South Africa. *Agricultural Systems* 139 (1): 260-270.
Kamara, A, Conteh, AR, Rhodes, E and Cooke, R. 2019. The relevance of smallholder farming to African agricultural growth and development. *African Journal of Food, Agriculture, Nutrition and Development* 19 (1): 14043-14065.
Knox, JW, Rodríguez Díaz, JA, Nixon, DJ and Mkhwanazi, M. 2010. A preliminary assessment of climate change impacts on sugarcane in Swaziland. *Agricultural Systems* 103 (2): 63-72.
Kunz, R, Mengistu, M, Steyn, J, Doidge, I, Gush, M, du Toit, E, Davis, N, Jewitt, G and Everson, C. 2015. *Assessment of Biofuel Feedstock Production in South Africa: Synthesis Report on Estimating Water Use Efficiency of Biofuel Crops*. 1874/1/15. Water Research Commission, Pretoria, South Africa.
Kusangaya, S, Warburton Toucher, M, Archer, E and Jewitt, G. 2013. Impacts of climate change on water resources in southern Africa: a review. *Physics and Chemistry of the Earth Parts A/B/C* 67-69: 47-54
Mabhaudhi, T, Nhamo, L and Mpandeli, S. 2021. Enhancing crop water productivity under increasing water scarcity in South Africa. In: eds. Ting, DSK and Stagner, JA, *Climate Change Science*. Elsevier.
Mandanici, E, Girelli, VA and Poluzzi, L. 2019. Metric accuracy of digital elevation models from WorldView-3 stereo-pairs in urban areas. *Remote Sensing* 11 (7): 878.
Mbangiwa, NC, Savage, MJ and Mabhaudhi, T. 2019. Modelling and measurement of water productivity and total evaporation in a dryland soybean crop. *Agricultural and Forest Meteorology* 266-267 (1): 65-72.
Mengistu, M and Savage, M. 2010. Surface renewal method for estimating sensible heat flux. *Water SA* 36 (1).
Messina, G and Modica, G. 2020. Applications of UAV thermal imagery in precision agriculture: state of the art and future research outlook. *Remote Sensing* 12 (1): 1491.
Meza, I, Eyshi Rezaei, E, Siebert, S, Ghazaryan, G, Nouri, H, Dubovyk, O, Gerdener, H, Herbert, C, Kusche, J, Popat, E, Rhyner, J, Jordaan, A, Walz, Y and Hagenlocher, M. 2021. Drought risk for agricultural systems in South Africa: drivers, spatial patterns, and implications for drought risk management. *Science of The Total Environment* 799 (1): 149505.
Moorhead, J, Marek, G, Gowda, P, Lin, X, Colaizzi, P, Evett, S and Kutikoff, S. 2019. Evaluation of evapotranspiration from eddy covariance using large weighing lysimeters. *Agronomy* 9 (1): 99.
Moorhead, JE, Marek, GW, Colaizzi, PD, Gowda, PH, Evett, SR, Brauer, DK, Marek, TH and Porter, DO. 2017. Evaluation of sensible heat flux and evapotranspiration estimates using a surface layer scintillometer and a large weighing lysimeter. *Sensors* 17 (10): 2350.

Mpandeli, S, Naidoo, D, Mabhaudhi, T, Nhemachena, C, Nhamo, L, Liphadzi, S, Hlahla, S and Modi, AT. 2018. Climate change adaptation through the water-energy-food nexus in southern Africa. *International Journal of Environmental Research and Public Health* 15 (10): 2306.

Mukherjee, J, Sharma, A, Dhakar, R, Sehgal, VK, Chakraborty, D and Das, DK. 2021. Estimation and validation of actual evapotranspiration (ETa) of maize wheat cropping system using SSEBop model over IARI research farm, New Delhi, India. *Journal of the Indian Society of Remote Sensing* 49 (8): 1823-1837.

Muluneh, MG. 2021. Impact of climate change on biodiversity and food security: a global perspective—a review article. *Agriculture & Food Security* 10 (1): 36.

Narimoto, L and Camarotto, J. 2018. Technology transfer and anthropotechnology: an analysis of the sugarcane harvesting in Australia and Brazil. *African Journal of Agricultural Research* 13 (1): 1564-1576.

Ngcobo, SI. 2023. An assessment of the potential impacts of climate variability on sugarcane production across Southern Africa. Unpublished thesis, Discipline of Hydrology, University of KwaZulu-Natal, Pietermaritzburg, South Africa.

Ngcobo, SI, Hill, TR, Jewitt, G and Archer, E. 2023. A yield gap analysis to assess vulnerability of commercial sugarcane to climatic extremes in southern Africa. *Journal of Agriculture and Food Research* 14 (1): 100734.

Nhamo, L, Magidi, J, Nyamugama, A, Clulow, AD, Sibanda, M, Chimonyo, VGP and Mabhaudhi, T. 2020. Prospects of improving agricultural and water productivity through unmanned aerial vehicles. *Agriculture* 10 (7): 256.

Niu, H, Zhao, T, Wang, D and Chen, Y. 2022. Estimating evapotranspiration of pomegranate trees using stochastic configuration networks (SCN) and UAV multispectral imagery. *Journal of Intelligent & Robotic Systems* 104 (66).

Perez-Priego, O, El-Madany, TS, Migliavacca, M, Kowalski, AS, Jung, M, Carrara, A, Kolle, O, Martín, MP, Pacheco-Labrador, J, Moreno, G and Reichstein, M. 2017. Evaluation of eddy covariance latent heat fluxes with independent lysimeter and sapflow estimates in a Mediterranean savannah ecosystem. *Agricultural and Forest Meteorology* 236 (1): 87-99.

Planet Labs. 2021. *PlanetScope product specifications*. Lake Mead, United States.

Reddy, KTC. 2020. Estimation of water use efficiency of soybean (Glycine max) for biodiesel production in KwaZulu-Natal. Unpublished thesis, Discipline of Hydrology, University of KwaZulu-Natal, Pietermaritzburg, South Africa.

Rejeb, A, Abdollahi, A, Rejeb, K and Treiblmaier, H. 2022. Drones in agriculture: a review and bibliometric analysis. *Computers and Electronics in Agriculture* 198 (1): 107017.

Rosa, R and Tanny, J. 2015. Surface renewal and eddy covariance measurements of sensible and latent heat fluxes of cotton during two growing seasons. *Biosystems Engineering* 136 (1): 149-161

Rosegrant, MW, Ringler, C, Zhu, T, Tokgoz, S and Bhandary, P. 2013. Water and food in the bioeconomy: challenges and opportunities for development. *Agricultural Economics* 44 (1): 139-150.

Sabir, RM, Sarwar, A, Shoaib, M, Saleem, A, Alhousain, MH, Wajid, SA, Rasul, F, Adnan Shahid, M, Anjum, L, Safdar, M, Muhammad, NE, Waqas, RM, Zafar, U and Raza, A. 2024. Managing water resources for sustainable agricultural production. In: eds. Kanga, S, Singh, SK, Shevkani, K, Pathak, V and Sajan, B, *Transforming agricultural management for a sustainable future: climate change and machine learning perspectives*. Springer Nature Switzerland.

Sakamoto, T. 2020. Incorporating environmental variables into a MODIS-based crop yield estimation method for United States corn and soybeans through the use of a Random Forest Regression algorithm. *ISPRS Journal of Photogrammetry and Remote Sensing* 160 (1): 208-228.

Sandbrook, C. 2015. The social implications of using drones for biodiversity conservation. *Ambio* 44 (4): 636-647.

Saseendran, SA, Trout, TJ, Ahuja, LR, Ma, L, McMaster, GS, Nielsen, DC, Andales, AA, Chávez, JL and Ham, JM. 2015. Quantifying crop water stress factors from soil water measurements in a limited irrigation experiment. *Agricultural Systems* 137 (1): 191-205.

Savage, M. 2009. Estimation of evaporation using a dual-beam surface layer scintillometer and component energy balance measurements. *Agricultural and Forest Meteorology* 149 (1): 501-517.

Shiferaw, B, Tesfaye, K, Kassie, M, Abate, T, Prasanna, BM and Menkir, A. 2014. Managing vulnerability to drought and enhancing livelihood resilience in sub-Saharan Africa: technological, institutional and policy options. *Weather and Climate Extremes* 3 (1): 67-79.

Shukla, A and Kot, R. 2015. Significance of remotely sensed evapotranspiration in plant life: a review. *2015 Fourth International Conference on Agro-Geoinformatics (Agro-geoinformatics)*, 266-270.

Sibanda, M, Ndlovu, HS, Brewer, K, Buthelezi, S, Matongera, TN, Mutanga, O, Odidndi, J, Clulow, AD, Chimonyo, VGP and Mabhaudhi, T. 2023. Remote sensing hail damage on maize crops in smallholder farms using data acquired by remotely piloted aircraft system. *Smart Agricultural Technology* 6 (1): 100325.

Singels, A, Jones, M, Marin, F, Ruane, A and Thorburn, P. 2013. Predicting climate change impacts on sugarcane production at sites in Australia, Brazil and South Africa using the Canegro model. *Sugar Tech* 16 (1): 1-9.

Sorooshian, S, Aghakouchak, A, Arkin, P, Eylander, J, Foufoula-Georgiou, E, Harmon, R, Hendrickx, J, Imam, B, Kuligowski, R, Skahill, B and Jackson, G. 2011. Advanced concepts on remote sensing of precipitation at multiple scales. *Bulletin of the American Meteorological Society* 92 (1): 1353-1357.

Spittlehouse, D and Black, A. 1980. Evaluation of the Bowen ratio/energy balance method for determining forest evapotranspiration. *Atmosphere-Ocean* 18 (1): 98-116.

Strashok, O, Ziemiańska, M and Strashok, V. 2022. Evaluation and correlation of Sentinel-2 NDVI and NDMI in Kyiv (2017–2021). *Journal of Ecological Engineering* 23 (9): 212-218.

Suvočarev, K, Castellví, F, Reba, ML and Runkle, BRK. 2019. Surface renewal measurements of H, λE and CO_2 fluxes over two different agricultural systems. *Agricultural and Forest Meteorology* 279 (1): 107763.

Tahir, N, Naqvi, SM, Lan, Y, Zhang, Y, Wang, Y, Afzal, M and Cheema, MJ. 2018. Real time monitoring chlorophyll content based on vegetation indices derived from multispectral UAVs in the kinnow orchard. *International Journal of Precision Agricultural Aviation* 1 (1): 24-31.

Teshome, FT, Bayabil, HK, Hoogenboom, G, Schaffer, B, Singh, A and Ampatzidis, Y. 2023. Unmanned aerial vehicle (UAV) imaging and machine learning applications for plant phenotyping. *Computers and Electronics in Agriculture* 212 (1): 108064.

Tian, X, Yan, M, Tol, C, Li, Z, Su, B, Erxue, C, Li, L, Wang, X, Pan, X, Gao, L and Han, Z. 2017. Modeling forest above-ground biomass dynamics using multi-source data and incorporated models: a case study over the qilian mountains. *Agricultural and Forest Meteorology* 246 (1): 1-14.

Todd, R, Evett, S and Howell, T. 2000. The Bowen ratio-energy balance method for estimating latent heat flux of irrigated alfalfa evaluated in a semi-arid, advective environment. *Agricultural and Forest Meteorology* 103 (1): 335-348.

Tongwane, MI and Moeletsi, ME. 2018. A review of greenhouse gas emissions from the agriculture sector in Africa. *Agricultural Systems* 166 (1): 124-134.

Virnodkar, S, Pachghare, V, Patil, VC and Jha, S. 2020. Remote sensing and machine learning for crop water stress determination in various crops: a critical review. *Precision Agriculture* 21 (13): 1121-1155.

Walker, BJ, Drewry, DT, Slattery, RA, VanLoocke, A, Cho, YB and Ort, DR. 2018. Chlorophyll can be reduced in crop canopies with little penalty to photosynthesis. *Plant Physiology* 176 (2): 1215-1232.

Wang, K and Liang, S. 2008. An improved method for estimating global evapotranspiration based on satellite determination of surface net radiation, vegetation index, temperature, and soil moisture. *Journal of Hydrometeorology* 9 (1): 712-727.

Watson, HK. 2011. Potential to expand sustainable bioenergy from sugarcane in southern Africa. *Energy Policy* 39 (10): 5746-5750.

WRC. 2015. *WRC Drought Factsheet 1: background to the current drought situation in South Africa*. Water Research Commission, Pretoria, South Africa.

Xiong, Z, Dun, Z, Wang, Y, Yang, D, Xiong, D, Cui, K, Peng, S and Huang, J. 2022. Effect of stomatal morphology on leaf photosynthetic induction under fluctuating light in rice. *Frontiers in Plant Science* 12 (1): 754790

Yacoob, A, Gokool, S, Clulow, A, Mahomed, M and Mabhaudhi, T. 2024. Leveraging unmanned aerial vehicle technologies to facilitate precision water management in smallholder farms: a scoping review and bibliometric analysis. *Drones* 8 (9): 476.

Yadav, M, Vashisht, BB, Vullaganti, N, Kumar, P, Jalota, SK, Kumar, A and Kaushik, P. 2024. UAV-enabled approaches for irrigation scheduling and water body characterisation. *Agricultural Water Management* 304 (1): 109091.

Yao, D, Yang, J and Zhan, X. 2013. An improved Random Forest algorithm for class-imbalanced data classification and its application in PAD risk factors analysis. *The Open Electrical & Electronic Engineering Journal* 7 (1): 62-70.

Zhao, T, Doll, D and Chen, Y. 2017. *Better Almond Water Stress Monitoring Using Fractional-order Moments of Non-normalised Difference Vegetation Index*.

Zhao, T, Stark, B, Chen, Y, Ray, A and Doll, D. 2015. A detailed field study of direct correlations between ground truth crop water stress and normalised difference vegetation index (NDVI) from small unmanned aerial system (sUAS). *2015 International Conference on Unmanned Aircraft Systems, ICUAS 2015* 520-525.

*****

Lead-In to Chapter 2:

In the face of escalating water scarcity and the adverse impacts of climate change, Chapter 1 emphasised the urgent need for enhanced water management strategies in South Africa's agricultural sector, particularly for smallholder farmers. These farmers, vital to food production, encounter increased vulnerability due to hydroclimatic variability and limited water resources. Precision agriculture (PA) and efficient water use are essential for improving crop yields and ensuring sustainable livelihoods. Moreover, accurate evapotranspiration (ET) estimation is critical for optimising water use and identifying crop stress. Chapter 2 builds on the framework established in Chapter 1, providing a scoping review and bibliometric analysis of unmanned aerial vehicle (UAV) applications for ET estimation and crop water stress monitoring. It analyses relevant research, revealing key trends, influential journals, leading researchers, and technological advancements. The chapter evaluates the practical applications and limitations of UAV technologies in smallholder farming contexts, identifying significant research gaps that inform the methodologies of subsequent chapters. It concludes with a discussion of methodological limitations, justifying the chosen approaches for this thesis and laying a foundation for the empirical investigations presented in Chapters 3 and 4.

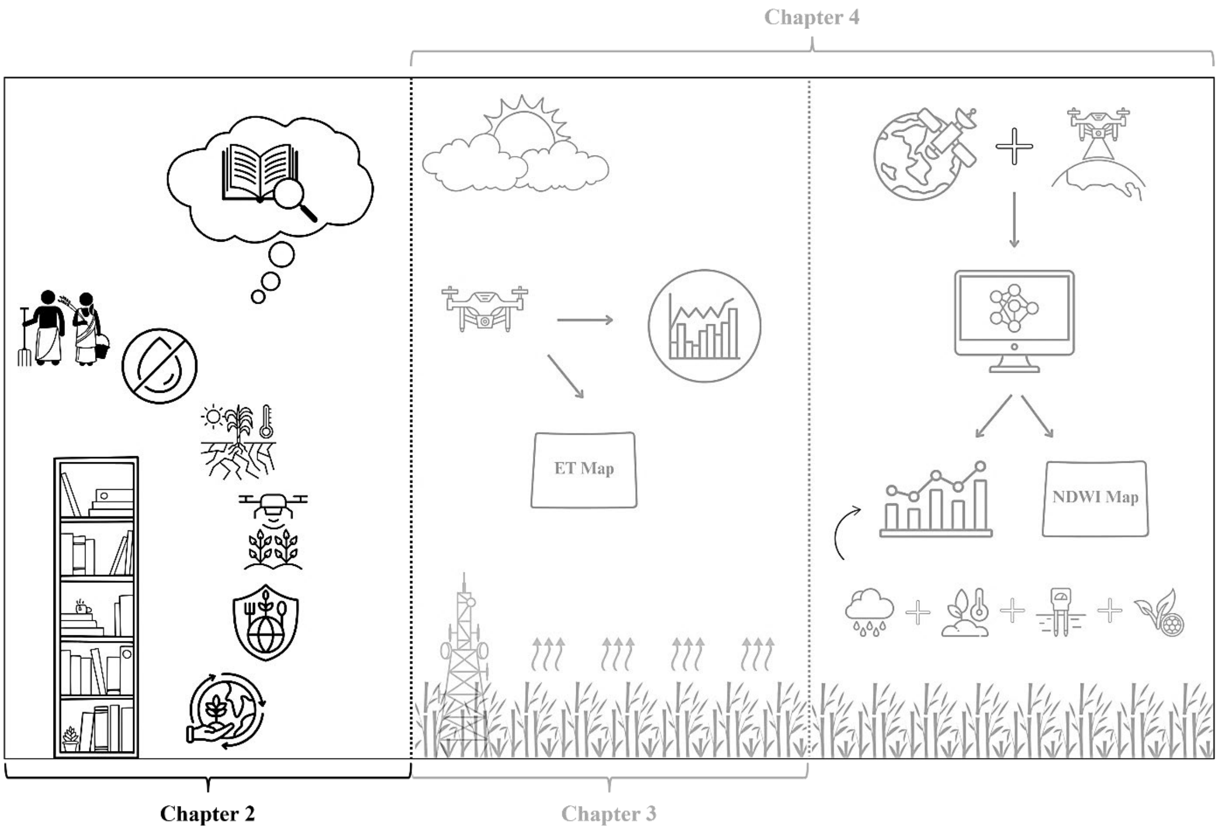

2. CHAPTER 2: LEVERAGING UNMANNED AERIAL VEHICLE TECHNOLOGIES TO FACILITATE PRECISION WATER MANAGEMENT IN SMALLHOLDER FARMS: A SCOPING REVIEW AND BIBLIOMETRIC ANALYSIS (PAPER 1)

Ameera Yacoob [1*], Shaeden Gokool [1], Alistair Clulow [1,2], Maqsooda Mahomed [1] and Tafadzwanashe Mabhaudhi [3,4]

[1] *Centre for Water Resources Research, School of Agricultural, Earth & Environmental Sciences, University of KwaZulu-Natal, P/Bag X01, Pietermaritzburg 3209, South Africa; gokools@ukzn.ac.za; clulowa@ukzn.ac.za; mahomedm@ukzn.ac.za*

[2] *Discipline of Agrometeorology, School of Agricultural, Earth and Environmental Sciences, University of KwaZulu-Natal, P/Bag X01, Pietermaritzburg 3209, South Africa*

[3] *Centre for Transformative Agricultural and Food Systems, School of Agricultural, Earth & Environmental Sciences, University of KwaZulu-Natal, P/Bag X01, Pietermaritzburg 3209, South Africa; tafadzwanashe.mabhaudhi@lshtm.ac.uk*

[4] *Centre of Climate Change and Planetary Health, London School of Hygiene and Tropical Medicine, London, United Kingdom*

[*] *Correspondence: 218023873@stu.ukzn.ac.za; Tel.: +2*[redacted]

Abstract:

While there is immense potential in using unmanned aerial vehicles (UAVs) to facilitate precision water management, there is currently no consensus on practical strategies to operationally implement these technologies to guide water resources management decisions, particularly within smallholder farming contexts. To address this gap, this study employs bibliometric techniques to assess the current state of UAV applications for evapotranspiration (ET) estimation in agricultural settings. The analysis of 49 peer-reviewed papers from Scopus was conducted using Biblioshiny and VOSviewer to enhance comprehension of this expanding

---

Published as: Yacoob, A.; Gokool, S.; Clulow, A.; Mahomed, M.; Mabhaudhi, T. Leveraging unmanned aerial vehicle technologies to facilitate precision water management in smallholder farms: a scoping review and bibliometric analysis. *Drones* **2024**, 8, 476, doi:10.3390/drones8090476.

References in this chapter adhere to the format specified by the Drones journal (MDPI).

research field. The study highlights a significant increase in scholarly research on utilising UAVs for precision water management over the past decade. The investigations indicate that UAVs in agriculture are gaining prominence and exhibit substantial potential for various precision agriculture (PA) applications. Significant cost reductions for UAV technology and remote sensing (RS) are anticipated soon, primarily driven by the availability of open-source platforms for processing tasks, such as Google Earth Engine (GEE). This research aims to inform smallholder farmers about the benefits of integrating UAVs into their farming practices, enhancing operational efficiency and productivity. Policymakers can use these findings to develop regulatory frameworks and incentive schemes that facilitate UAV adoption among smallholder farmers. Additionally, technology developers can leverage insights from this study to identify areas needing innovation and optimisation tailored to small-scale agriculture. Hence, this study seeks to bridge the gap between technological advancements and practical agricultural applications, promoting sustainable farming practices and enhancing the socioeconomic welfare of smallholder farmers.

Keywords: Biblioshiny; evapotranspiration; food security; precision agriculture; smallholder farming; UAV; water stress

2.1 Introduction

In numerous developing nations globally, smallholder farms, defined as those encompassing less than two hectares, constitute significant contributors to agricultural output and stand as primary drivers of socioeconomic development [1]. Given their substantial yield output vis-à-vis land occupancy, these entities possess the capacity to serve as pivotal agents in addressing concerns regarding food security [1–3]. Despite their relative significance, the precarious circumstances prevailing among many such smallholder farmers often hinder realising their agricultural productivity potential and render them ill-equipped to cope with climatic adversities [1,4].

From a South African perspective, many smallholder farmers, particularly those dependent on rainfed agriculture, persistently encounter food and nutritional insecurity challenges attributable to water shortages, erratic weather patterns, and prolonged dry spells [5]. South Africa, on average, receives approximately half of the global mean annual precipitation (MAP), with pronounced precipitation variability and climatic extremities exacerbating these conditions; consequently, diminished water availability frequently compromises the optimal cultivation of crops, notably within dryland agricultural systems [6,7]. Given these circumstances and the distinctive challenges these farmers face, implementing innovative, evidence-based, and cost-effective interventions tailored to bolster productivity and fortify resilience against adversities holds promise for their improvement [4,8].

Precision Agriculture (PA) is pivotal in mitigating the global challenge of food security by implementing tailored strategies and management interventions. The PA process comprises data collection, analysis and communication technologies, decision-making, and practice management [9]. Central to these endeavours is minimising the unnecessary depletion of critical resources, such as nutrients and water, while increasing crop yields and mitigating potential adverse environmental repercussions [10,11]. PA technologies serve as instrumental decision-support tools aimed at optimising agricultural operations, facilitating interventions in mitigating plant water stress, diagnosing plant diseases, assessing crop yields, and undertaking plant phenotyping, among other functions [9,12,13].

Accurate evapotranspiration (ET) spatiotemporal estimation and assessment of crop water status constitute fundamental aspects of precision water management, which is a vital component of the PA paradigm [14,15]. Several methodologies have been devised for ET monitoring, with two primary categories prevalent in scientific inquiry: ground-based/in-situ and remote sensing (RS) approaches. ET estimation through field-based methods typically entails the application of water balance principles. Moreover, micrometeorological techniques based on the principles of the shortened energy balance, such as the Bowen ratio [16,17], eddy covariance [18], scintillometry [19,20], and surface renewal [21] methods have garnered extensive utilisation in ET estimation endeavours.

Nonetheless, these measurements often exhibit limitations, being confined to specific points or weighted by area, posing challenges in extrapolating findings to broader scales owing to the intrinsic heterogeneity of land surfaces. Furthermore, there has been a notable interest in utilising RS and, more specifically, UAVs for PA applications in the past decade [15,22,23]. Given their distinctive attributes, UAVs offer advantages conducive to smallholder farms, enabling circumvention of limitations associated with in-situ and satellite-based techniques.

2.1.1 Drone applications in precision agriculture

UAVs are equipped with lightweight sensors capable of capturing high spatial-resolution images. This capability contrasts with many freely available satellite-based datasets, which often lack the spatial resolution to accurately represent smallholder farms' spatial heterogeneity [24,25]. Moreover, satellite-based RS is more susceptible to cloud cover, whereas UAVs can be flown at lower altitudes, making them less prone to their impacts. UAVs can also be flown at user-defined intervals. In contrast, the satellite's flight path is fixed, and revisit and repeat cycles are restricted [26–28].

Despite their advantages, UAVs possess inherent limitations that warrant consideration. These include limited flight durations due to battery constraints, data processing and analysis challenges, and regulatory restrictions that may complicate operations. Moreover, the initial capital investment may create significant financial barriers for smallholder farmers, potentially hindering the widespread adoption of this technology [8,29,30].

Several essential factors emerge when comparing costs between UAVs and other RS platforms, such as satellites or manned aerial vehicles (MAVs). UAVs typically require a lower initial investment, being more affordable than high-resolution satellite data and devoid of recurring subscription fees for data access [8]. Although operational training for UAVs is necessary, it often proves more straightforward and accessible than the specialised qualifications required for traditional RS methods, making UAVs more user-friendly for smallholder farmers.

Additionally, UAVs facilitate user-defined flight plans for immediate data acquisition, eliminating delays associated with satellite revisit times [4,5,28]. This combination of accessibility and cost-effectiveness positions UAVs as a viable option for smallholder farmers, allowing them to obtain timely, high-resolution data to enhance their agricultural practices without the financial constraints imposed by satellite-based RS services.

As research on UAV applications in agriculture has increased, it is necessary to synthesise the existing literature and explain the intellectual framework of this domain. Moreover, few reviews discuss UAV applications in the PA sector, focusing on ET estimation. For example, Rejeb *et al.* (2022) undertook a bibliometric analysis to summarise drone research in agriculture [13]. Similarly, Gokool *et al.* (2023) assessed using UAV technology in facilitating PA techniques, specifically emphasising small-scale farming operations [8].

Singh *et al.* (2022) conducted a scholarly investigation similar to Rejeb *et al.* (2022), focusing mainly on viticulture [31]. In contrast, Awais *et al.* (2022) detailed crop water status estimation using UAV-based methods [32]. Nhamo *et al.* (2020) examined the significance of UAVs in agricultural water management and crop health, highlighting their potential as an alternative approach to enhance productivity in smallholder farms [4]. In addition, Raparelli and Bajocco (2019) analysed the use of UAVs in agriculture and forestry research over the last twenty years. However, their investigation is limited to academic studies published only between 1995 and 2017, failing to capture the constantly evolving nature of this rapidly advancing field [33].

While the aforementioned studies offer a comprehensive analysis and generate novel and valuable insights, their primary focus has generally been on the capabilities of UAVs, particularly in the context of crop mapping and monitoring. Therefore, this study aims to fill the existing knowledge gap by conducting a comprehensive scoping review and bibliometric analysis of the literature on the practical use of UAVs for estimating ET or detecting crop water stress. The objective is to give current, concise insights that may guide and enhance PA practices.

Moreover, this research may serve as a vital resource for gaining a more profound understanding of using UAVs to enhance precision water management practices. With the increasing volume of scholarly output in scientific disciplines, it has become imperative for researchers to use quantitative review methodologies to comprehend the structure of knowledge [34]. Furthermore, as the complexity of research fields increases, it is essential to analyse the information created within these disciplines [35]. This analysis serves several purposes, including uncovering new contributions, documenting research traditions and trends, identifying the themes that have been investigated, and exploring prospective avenues for future research.

Consequently, the study endeavours to attain the objectives below:

i. Conduct a scoping literature review on UAV-based RS techniques to facilitate precision water management within smallholder farms.
ii. Identify significant journals, publications, authors, and nations that have made notable contributions using UAVs in ET estimation and crop water stress detection.
iii. Describe UAV-based approaches to monitor crop water use and aid PA.
iv. Use co-citation analysis to group publications according to their semantic similarity, identify thematic areas, and map studies' main "intellectual structure."
v. Identify data analytic methods used to support the estimation of ET and detection of crop water stress and analyse these results within the context of smallholder farming.

2.2 Methodology

2.2.1 Literature search

An initial literature search was conducted using academic search engines, such as Elsevier, Scopus, and Science Direct, to identify prominent keywords in published papers from high-impact-factor journals that addressed three main areas of interest: precision water management (S1), unmanned aerial vehicles (S2), and crop water status (S3). An iterative procedure facilitated the identification of a definitive keyword string that most accurately described the objective of the investigation.

After this, Scopus was selected as the sole abstract and citation database for the bibliometric analysis due to its comprehensive and trustworthy standardised results. The meta-data of publications were retrieved using the following query string: "("precision agriculture" OR "precision farm*" OR "precision irrigation" OR "precision water management" OR "site-specific irrigation management" OR "site-specific management") AND ("unmanned aerial vehicle" OR "UAV" OR "unmanned aerial system" OR "UAS" OR "unmanned aerial systems imagery" OR "drone") AND ("evapotranspiration" OR "transpiration" OR "crop water use" OR "crop water requirement" OR "water requirement" OR "water stress" OR "stomatal conductance")" on 7 August 2023.

Despite recognising smallholder farms as a significant area of interest in this study, they were excluded from the search query due to the limited number of studies assessing the relevance of UAV applications in these settings. Consequently, the search query was broadened to enable a more comprehensive review of applicable techniques and to facilitate the contextualisation of the main findings. However, the ensuing discussion portion of this review will undertake a more comprehensive analysis of the findings to ascertain the cost-effectiveness of the platforms and methodologies used in the final selection of studies. The search was conducted without applying any constraints on the timespan; however, articles that were not published in accredited peer-reviewed journals and not written in English were excluded. The search results returned 69 references. The Preferred Reporting Items for Systematic Reviews and Meta-Analyses extension for scoping reviews (PRISMA-ScR) framework was used to avoid biased reporting by guiding decisions regarding selecting articles to be included or excluded from the review (see Figure 2.1).

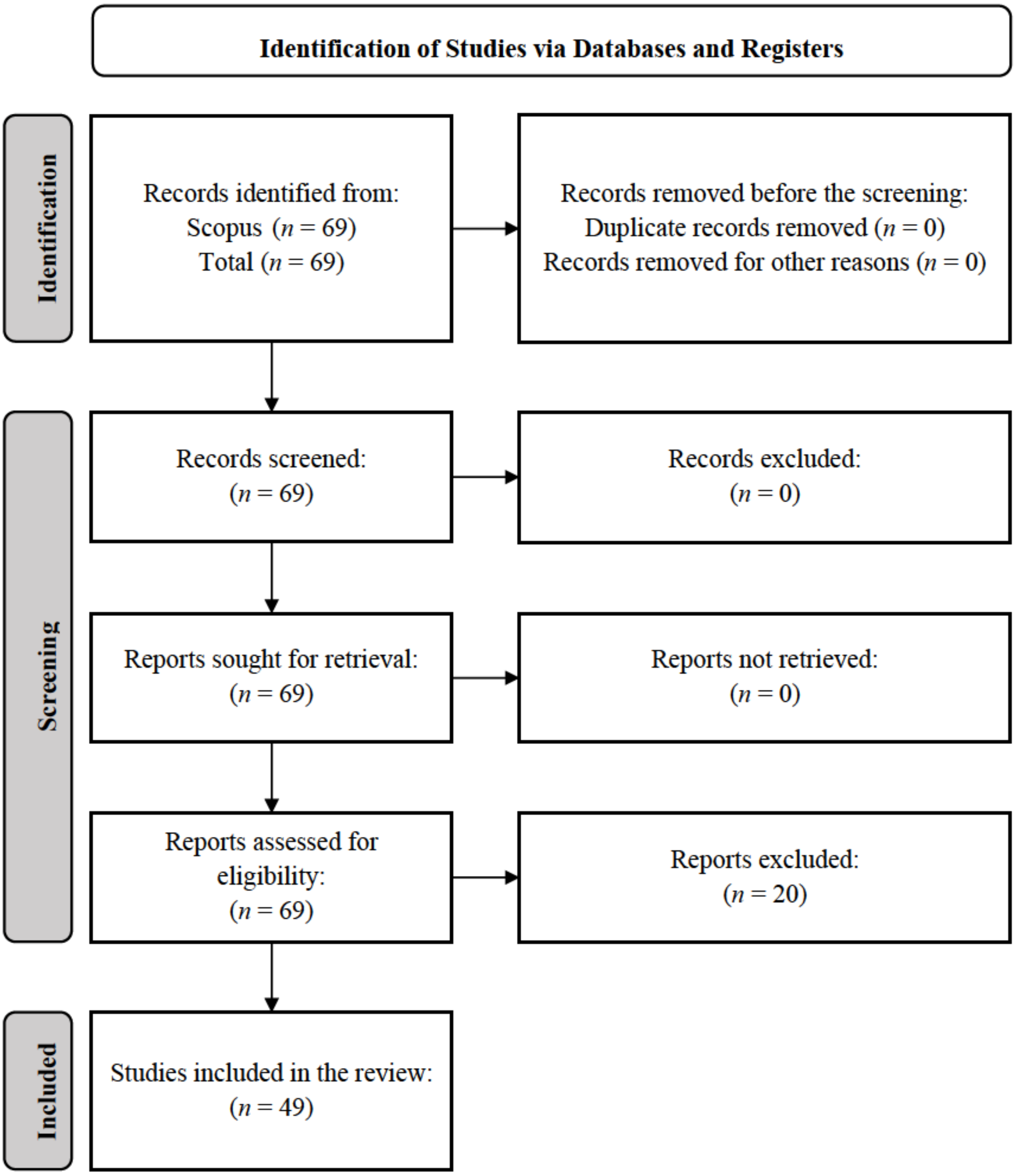

Figure 2.1 The flow diagram for article selection according to the PRISMA-ScR framework.

Eligibility criteria for the review were established as follows:

i. The full-length article must be peer-reviewed, published in English, easily accessible, and readily available.
ii. The study or review should specifically address the use of UAV technology for estimating ET or detecting crop water stress within the context of PA.

Two reviewers screened the title, abstract, and full-length article. Subsequently, a third-party independent reviewer resolved disputes to ascertain that all the papers included in the study adhered to the predetermined eligibility criteria. After screening these articles' titles and abstracts, 49 full-length articles were identified as eligible and were sought for downloading. No additional articles were sought following this process.

2.2.2 Data analysis

Once the final database (n = 49) had been compiled, a citation analysis was executed using the Biblioshiny App version 4.3.0 (accessed using the R environment: Bibliometrix-R package) to explore the connection between authors and peer-reviewed articles, underlying citation patterns and the most influential authors and publications. Biblioshiny is a standard citation and co-citation analysis tool. This tool offers simple interaction with other software and significant data handling and analysis freedom. Moreover, a co-citation analysis was conducted using VOSviewer (version 1.6.19) software to visualise the findings and generate the bibliometric networks. VOSviewer offers a range of intuitive visualisations, particularly for analysing bibliometric maps [36]. Finally, the connections and linkages between countries, institutions, and journals were analysed to depict the collaboration network.

2.3 Results

The initial analysis focused on the temporal distribution of scholarly research on agricultural UAVs in precision water management, as shown in Figure 2.2. There has been a notable surge in publications since 2019, with six recorded publications. Hence, the period from 2013 to 2018 may be characterised as the first phase, during which an average of one article was published yearly. The surge in publications after 2019 indicates a notable rise in research activity, signifying the widespread use of UAVs in RS and PA [9]. Specifically, there was an increase in the number of publications from 6 in 2019 to 12 in 2022, reaching its highest point at 13 in 2021.

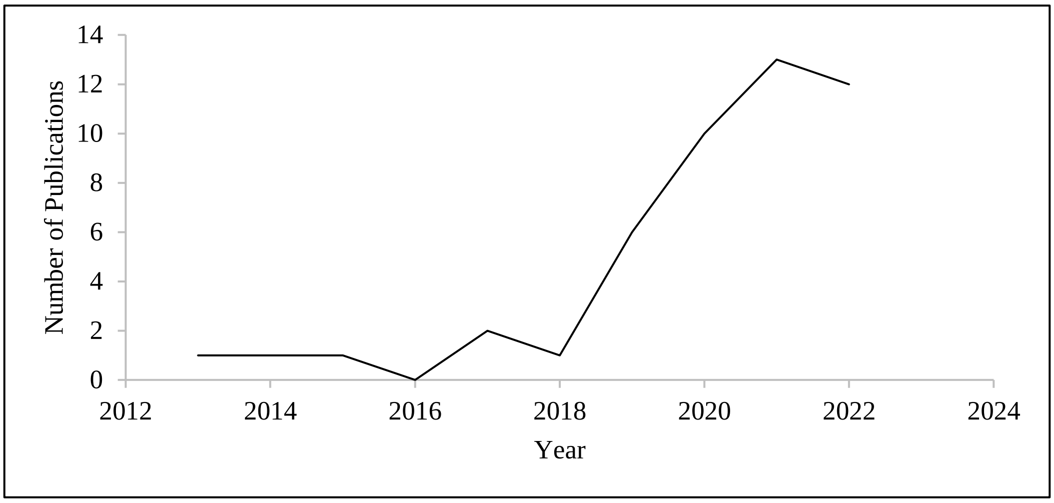

Figure 2.2 Annual distribution of publications.

2.3.1 Fundamental statistical data

Table 2.1 presents a comprehensive overview of the essential statistical information on the overall literature dataset. Studies on using UAVs to enhance precision water management were first documented in 2013. Since then, this field of research has shown an upward trajectory, with a compound annual growth rate of about 7.18%. In 2015, there was a notable increase in the average total citations (TCs) per publication, reaching its highest point at 372. Similarly, it is worth noting that 2015 had the highest average total citations (TCs) per year, amounting to 41.33 (Figure 2.3).

Table 2.1 Essential bibliographic details contained in the completed literature dataset.

Description	**Result**	**Description**	**Result**
Timespan	2013-2023	References	3040
Number of journals	21	Author's keywords (DE)	185
Number of publications	49	Authors	243
Annual growth rate (%)	7.18	Single-authored documents	0
Document average age	2.78	Co-authors per document	5.94
Average citations per document	41.29	International co-authorships (%)	36.73

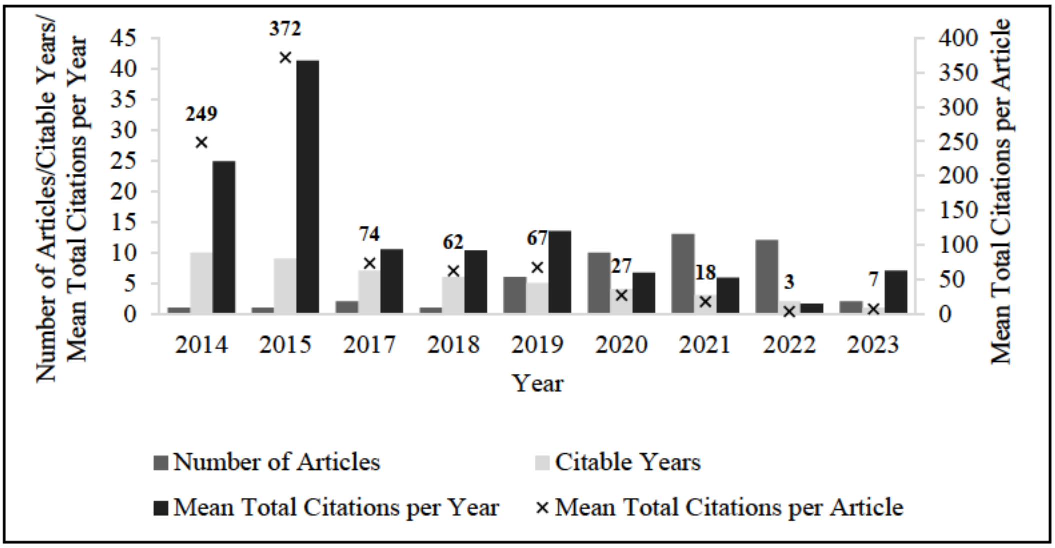

Figure 2.3 The dissemination of mean annual citations and publications.

2.3.2 Distribution characteristics of leading research countries

The distribution parameters of significant research nations indicate the respective countries' impact on the UAV applications for ET estimation within the PA domain. The dataset used in this scholarly research was disseminated throughout 22 distinct nations. The published papers have been circulated across different continents, including eight European countries (Spain, Italy, Greece, Denmark, France, Sweden, Portugal, Germany), seven Asian countries (China, Israel, South Korea, Pakistan, Saudi Arabia, Egypt, Iran), four American countries (USA, Brazil, Canada, Chile), two African countries (South Africa and Zimbabwe), and one Oceania country (Australia). As seen in Figure 2.4, most publications were published in the United States and China. The United States of America is first in terms of paper volume, with 15 articles. Nevertheless, the average number of article citations for the nation under review was comparatively lower than that of countries such as Spain and China.

China emerged as the only developing nation in the top three regarding scholarly output, surpassing other countries significantly. China's research contributions constituted almost 22% of the overall production, demonstrating its substantial presence in the academic landscape. Furthermore, the average citation for each paper was 34.6, surpassing that of the United States (26.5). Additionally, its paper volume attained the second-highest position on a worldwide scale. Spain ranked second in total citations, with a cumulative count of 361; however, it achieved the highest average citations per article at 120.3. Furthermore, Spain positioned itself as the third highest publication volume, indicating its substantial impact on academic literature.

Another significant contributor is South Africa, which is sixth in publication volume. This developing nation ranks fifth in total citations, with a total of 53. Additionally, South Africa had an average citation score of 26.5 per article.

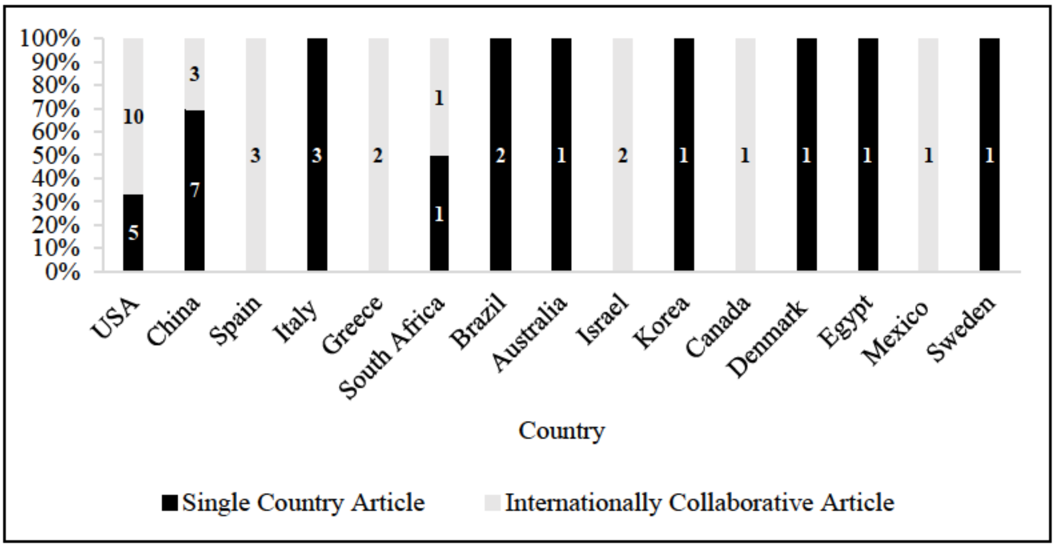

Figure 2.4 The nationalities of corresponding authors in the top 15 nations with the highest productivity in UAV applications in precision water management.

2.3.3 Influential authors and citation analysis

This section provides an overview of prominent authors and explores the use of author citation networks to represent and structure the existing body of literature visually. A collective of 243 authors contributed to the 49 articles on using UAVs to enhance precision water management. A total of 207 researchers contributed to the publication of a single paper, while 28 authors published two articles. Additionally, four authors had three articles published, and another four authors had four articles published. Figure 2.5 displays the author-level performance data for the 15 authors with the most publications (in chronological order). The authors showing the most activity in this study's emphasis area are Wenting Han, Lav Khot, Huihui Zhan, and Liyuan Zhang. Moreover, Wenting Han and Liyuan Zhang have garnered the most citations.

The publications' global citation score (GCS), average TCs per year, and normalised citation score were all examined (Table 2.2). The GCS, which also contains citations from works in other fields, accurately represents the TCs a publication received in the abstract and citation database (Scopus) that was utilised. Gago *et al.* (2015) had the publication with the highest rank in terms of TCs and average TC per year [37]. The researchers comprehensively reviewed the capability of UAVs to analyse the water use of plants at a crop scale to enhance crop water stress management. This was accomplished by exploring the various RS-based indices obtained from UAV technology and their capacity to ascertain plant physiological properties.

According to the normalised citation performance measure, the work authored by Messina *et al.* (2020) had the highest normalised TC score. This study comprehensively analyses the current advancements in UAV thermal RS in the agricultural sector. It provides a detailed description of the most recent applications and offers insights into potential areas for future research. The authors highlight that the crucial task of detecting water stress based on plant temperature data has significant value. In addition, Messina *et al.* (2020) explain that temperature-based indicators provide a rapid and efficient approach to evaluating and estimating the water status of crops. One widely used indicator for monitoring plant water status and managing irrigation resources is the crop water stress index (CWSI).

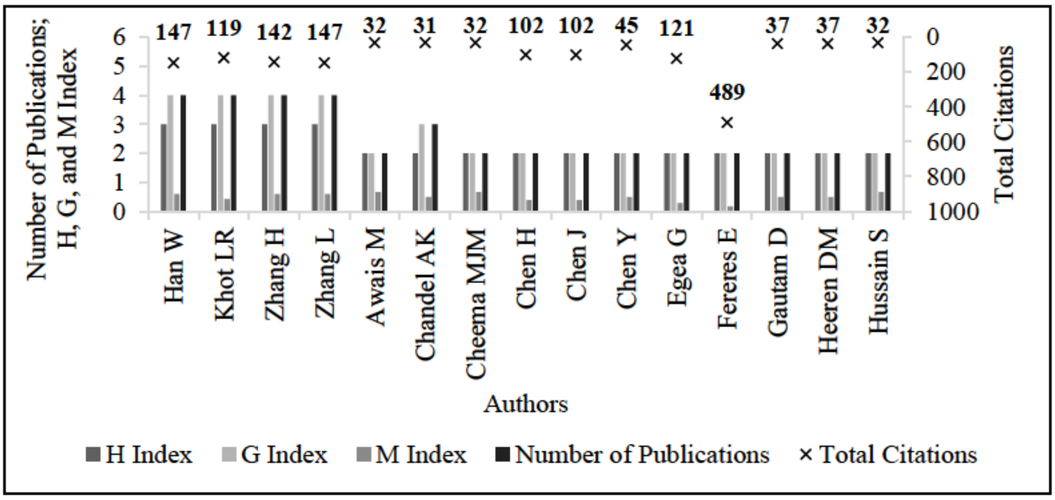

Figure 2.5 Key author-level citation metrics for authors with several publications.

Another vital article in Table 2.2, which features a prominent author in the field, was the publication by Zhang *et al.* (2019). This study used high-resolution multispectral images obtained from a UAV to assess the suitability of the data for mapping the water stress condition of maize under different levels of deficit irrigation. Nine VIs associated explicitly with agricultural water stress were calculated from the multispectral imagery. They were then used to develop inversion models for the CWSI. According to Zhang *et al.* (2019), "the ratio of the Transformed Chlorophyll Absorption in Reflectance Index (TCARI) and the Renormalised Difference Vegetation Index (RDVI), and TCARI and the Soil Adjusted Vegetation Index

(SAVI) had the best correlations with CWSI." The VI-CWSI regression models were compared to an empirical CWSI model developed using on-site canopy temperature, air temperature, and relative humidity measurements. In assessing crop and soil variability, the VI-CWSI regression models devised in this investigation were more effective than on-site measurements.

Furthermore, Sagan *et al.* (2019) ranked among the top five publications with the highest citation counts. The researchers assessed three commercially accessible thermal cameras for UAVs: the ICI 8640 P-series, FLIR Vue Pro R 640, and thermoMap. The study's findings indicate that the three thermal cameras yielded valuable temperature data that may be effectively used in PA and plant phenotyping. The ICI 8640 P-series had the most favourable outcomes among the three systems [38]. However, given its affordability and acceptable performance, the FLIR Vue Pro R 640 is a cost-effective alternative. Farmers and researchers may acquire crucial discernment on crop water conditions by using sophisticated analytics and integrating thermal data with other pertinent information, enabling them to implement prompt and precise irrigation management. This balance between cost and efficacy is essential for addressing agricultural challenges, particularly for smallholder farmers, by providing practical and affordable UAV-based thermal imaging solutions.

Table 2.2 The global citation score of the ten highest-ranking publications.

Journal	TC	TC per Year	Normalised TC
Agricultural Water Management	372	41.33	1.00
Precision Agriculture	249	24.90	1.00
Precision Agriculture	240	21.82	1.00
Remote Sensing	146	29.20	2.17
Remote Sensing	108	27.00	4.03
Remote Sensing	97	19.40	1.44
Remote Sensing	88	12.57	1.20
Remote Sensing	82	16.40	1.22
Biosystems Engineering	62	10.33	1.00
Computers and Electronics in Agriculture	61	20.33	3.48

2.3.4 Influential academic journals

The completed literature database included 21 scholarly journals with a total of 49 papers that explore the use of UAVs for identifying crop water stress to facilitate PA. *Remote Sensing* and

Agricultural Water Management exhibit the highest volume of papers, comprising around 53% of the overall publications. *Remote sensing* maintains its position at the forefront of the rankings for TCs, with a score of 660. Hence, this journal is prominent in the field of study focus. Figure 2.6 presents a visual representation of the critical journals categorised based on Bradford's law, a method used to determine the correlation between published articles and the journals in which they are published.

Bradford's law proposes separating the pool of journal citations for a particular study emphasis area into three distinct zones based on their frequency. Zone 1 signifies the journals of utmost significance since they obtain the highest frequency of citations within their respective topic areas and hence receive the most scholarly attention. Zones 2 and 3 correspond to the journals with the average and least number of citations, respectively. According to Bradford's law, eighteen papers were published in a single journal under Zone 1. Additionally, fifteen articles were published across four journals under Zone 2, while five were published across five journals under Zone 3. According to the findings shown in Table 2.3, *Remote Sensing* emerges as one of the most influential journals, as it attains a high ranking in terms of output, TCs, and citation.

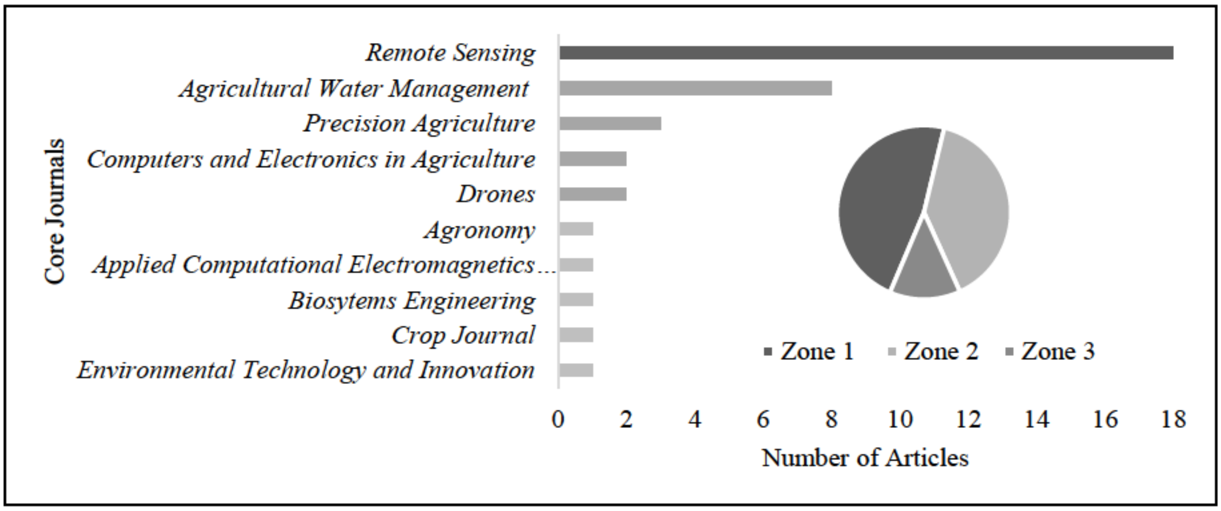

Figure 2.6 The categorisation of academic journals based on Bradford's law, fostering the dissemination of scholarly investigations.

Table 2.3 Evaluation of publishing sources based on the number of articles published.

Journal	Publication Start Year	Number of Publications	h-Index	TCs
Remote Sensing	2017	18	11	660
Agricultural Water Management	2015	8	6	504
Precision Agriculture	2013	3	3	548
Computers and Electronics in Agriculture	2021	2	2	65
Drones	2020	2	2	26
International Journal of Environmental Science and Technology	2023	1	1	14
Crop Journal	2022	1	1	2
Journal of Intelligent and Robotic Systems: Theory and Applications	2022	1	1	2
Journal of ASABE	2022	1	1	2
Journal of Universal Computer Science	2022	1	1	4
Remote Sensing Applications: Society and Environment	2022	1	1	1
Environmental Technology and Innovation	2021	1	1	18
Hydrology	2021	1	1	12
Information Sciences Letters	2021	1	1	13
International Journal of Applied Earth Observation and Geoinformation	2021	1	1	11
Journal of Sensors	2021	1	1	6
Agronomy	2020	1	1	27
Applied Computational Electromagnetics Society Journal	2020	1	1	11
Sensors (Switzerland)	2020	1	1	25
Water (Switzerland)	2020	1	1	10
Biosystems Engineering	2018	1	1	62

2.3.5 The frequency, growth, and co-occurrence of keywords

The selection of keywords by authors for a publication has a pivotal role in shaping the communication of the article within scientific communities [39]. Keyword analysis is a method to uncover overarching research patterns by aggregating the terms found in relevant papers within a particular field [40]. The Bibliometrix and Biblioshiny installation packages in R Studio were used to quantify the top twenty authors and supplementary keywords inside this domain (Tables 2.4 and 2.5). To ensure consistency, semantically equivalent terms were merged, such as the consolidation of "drone" and "drones," as well as "Crop Water Stress Index" and "CWSI."

According to Table 2.4, it is evident from the respective frequencies of 14% and 4% that authors prefer the term UAVs over the colloquial phrase "drones." Additionally, "evapotranspiration" and "precision agriculture" are highly ranked. Despite being ranked sixth, the CWSI is the first term that offers valuable information concerning an index used to quantify crop water stress. As a result, it is considered one of the most widely utilised indices whose values range from 0 to 1 and positively correlate with the water stress level of many plant species. The CWSI integrates canopy temperature and environmental variables such as humidity and solar radiation to comprehensively measure plant water stress. Awais *et al.* (2023) revealed that the CWSI obtained via thermal sensors on UAVs might be deemed suitable for real-time irrigation management. Additionally, this index has been used in the detection of ET, as shown by previous studies conducted by Bellvert *et al.* (2016), Santesteban *et al.* (2017), and Awais *et al.* (2023).

Stomatal conductance (4%) and canopy temperature (3%) are also valuable indicators of water stress [5,41]. However, in terms of their frequency of occurrence, stomatal conductance was shown to be more prevalent. The widespread use of "deep learning" and "machine learning" suggests that much of the literature has been dedicated to exploring Artificial Intelligence (AI) techniques for UAV-based agriculture. Machine Learning (ML) methods are well-suited for analysing data supplied by UAVs and other remote-sensing and ground-based systems due to their adaptability and capacity to process large quantities of nonlinear data [42,43]. Another notable term that garnered attention was thermal imaging, accounting for 3% of the data. Thermal imaging serves to detect variations in the temperature of the leaf surface caused by physiological changes resulting from water stress. Moreover, leaf stomata closure decreases transpiration and evaporative cooling, resulting in a noticeable elevation in leaf temperature detected by thermal sensors [9].

Table 2.4 Frequency of the top 20 author's keywords.

Author Keyword	Frequency (%)	Author Keyword	Frequency (%)
remote sensing	14.00	canopy temperature	3.00
unmanned aerial vehicles	14.00	land surface temperature	3.00
evapotranspiration	10.00	thermal imagery	3.00
precision agriculture	9.00	deep learning	3.00
cwsi	7.00	irrigation	3.00
water stress	6.00	grapevines	2.00
precision irrigation	4.00	image processing	2.00
stomatal conductance	4.00	irrigation scheduling	2.00
vegetation index	4.00	landsat 8	2.00
drone	4.00	machine learning	2.00

Antennas (8%) transmit high-frequency radio signals between a smart controller and a UAV. Several studies have referenced the use of antennas in the context of georeferencing, namely the Global Navigation Satellite System (GNSS) [44,45] and telemetry antennas [46,47]. Furthermore, soil moisture (4%) is crucial to crop water management, affecting ET and crop growth [48]. InfraRed-imaging (3%) has emerged as a valuable technique for identifying and measuring crop water stress [49]. Moreover, methodologies for estimating ET with the use of UAVs mostly employ VI-based modelling (3%) [50] or energy balance (2%) techniques [51]. Another crucial term is land surface temperature (2%). This variable is often included as a principal input in energy balance models like the Surface Energy Balance Algorithm for Land (SEBAL) for estimating ET [52] (Table 2.5).

Table 2.5 Frequency of the top 20 keywords plus.

Keyword Plus	Frequency (%)	Keyword Plus	Frequency (%)
remote sensing	13.00	water stress	3.00
unmanned aerial vehicle	11.00	infrared-imaging	3.00
antennas	8.00	crop water stress indices	3.00
crops	8.00	vegetation index	3.00
evapotranspiration	8.00	agricultural robots	2.00
irrigation	7.00	energy balance	2.00
precision agriculture	7.00	satellite imagery	2.00
water management	4.00	land surface temperature	2.00
soil moisture	4.00	plants (botany)	2.00
vegetation	3.00	water supply	2.00

2.3.6 Visualising thematic clusters in keyword co-occurrence networks

Keyword co-occurrence networks allow researchers to identify fundamental themes within a particular domain of study [13]. Furthermore, these networks serve as a powerful scientometric instrument that enables the visualisation and demonstration of shared characteristics among co-occurring phrases or themes in scholarly literature. Using this methodology, researchers can comprehensively understand a publication's content and crucial details on the procedures, theoretical frameworks, and perspectives. Thirty nodes are distributed between three distinct clusters. In addition, nodes in Figure 2.7 represent keywords that appeared at least six times in the literature.

One cluster involves precision irrigation, which relates to water management. Other keywords within this cluster include crop water stress indices such as 'stomatal conductance' and 'canopy temperature.' Information on these indicators can aid in providing insight into the water status of crops, thereby optimising water use concerning irrigation management. The second cluster relates to ET. 'Crops' and 'soil moisture' are integral to the ET process since they influence the amount of water lost from the land surface to the atmosphere. Moreover, RS-based approaches are widespread in ET estimation. The two leading RS platforms include 'UAVs' and 'satellite imagery.'

RS-based ET estimation often employs the 'energy balance' method, which considers the energy exchanges at the land surface. 'Land surface temperature' (LST) is a vital component of this method and is measured using thermal infrared sensors on RS platforms (e.g., satellites or drones). The third cluster relates to 'vegetation' involving 'VIs.' The Normalised Difference Vegetation Index (NDVI) has been widely used in vegetation monitoring, specifically in ET estimation and crop water stress detection. Moreover, vegetation, including trees, shrubs, crops, and grasses, plays a central role in transpiration. Nevertheless, the transpiration rate depends on factors such as the type of vegetation, its growth stage, and environmental conditions.

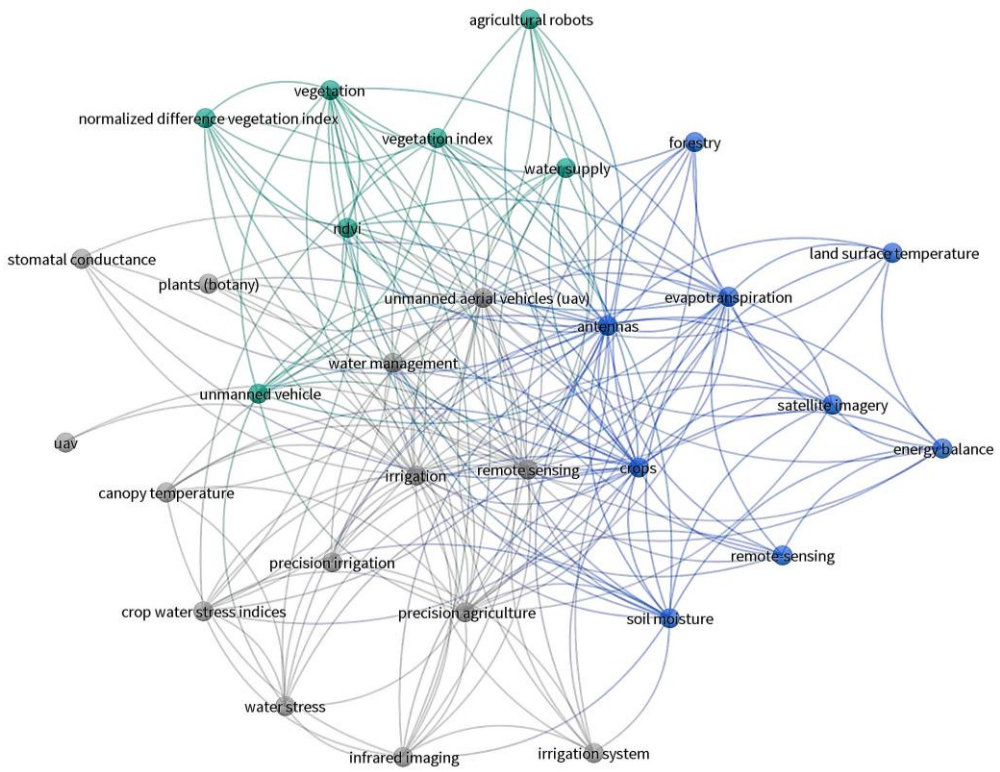

Figure 2.7 Co-occurrence network of keywords that appeared at least six times in the literature database. The various colours represent distinct thematic clusters, indicating groups of related keywords.

2.4 Discussion

Currently, there is no established method for selecting a practical UAV-based approach to determine crop water status and subsequently guide irrigation management decisions for small-scale agriculture. This is crucial since these farmers' challenges and limitations are primarily due to the prevalent resource constraints in their environments. Therefore, in this study, clustering techniques were employed to facilitate the identification of overarching themes on case study applications involving UAVs to estimate ET or detect crop water stress in PA. The results section consolidates data from 49 publications across various journals. Hence, these themes were examined and will be further discussed concerning the smallholder farmer context.

2.4.1 Advances in thermal remote sensing

Thermal RS has gained prominence in the literature due to advancements in sensor technology and a subsequent reduction in costs. This technology utilises thermal and near-infrared (NIR) imagery to compute the crop coefficient (Kc) and ET, as the transpiration rate is closely related to canopy temperature. Kc has been shown to correlate with canopy reflectance; however, the accuracy of these measurements can be influenced by various factors, including the properties of the thermal camera, prevailing weather conditions, and the multiple sources of emitted and reflected thermal radiation. Consequently, meticulous calibration of ground data collection and reference panels for temperature measurement and data processing is essential to ensure accurate temperature retrieval [9,53].

In water stress conditions, the closure of leaf stomata leads to reduced transpiration and evaporative cooling, resulting in a significant increase in leaf temperature, which thermal sensors can detect. Using thermal images obtained from UAVs and establishing correlations between foliar temperature and stomatal conductance, valuable insights can be gained into how plants respond to water stress [5,24,41,54,55]. Monitoring these variables during crop growth enables small-scale farmers to implement effective strategies to minimise losses and maximise crop production.

It is noteworthy, however, that leaf or canopy temperature alone does not comprehensively characterise crop water status; an equally stressed canopy can exhibit temperatures of 25 °C or 35 °C, depending on the ambient temperature (Ta). To address this limitation, the canopy-to-air temperature difference (Tc−Ta) has been proposed as a more informative metric, demonstrating a strong correlation with stem water potential, leaf water potential, and stomatal conductance in horticultural crops [45]. While these in-situ measurements provide a viable means for detecting crop water stress, relying solely on UAV-based measurements can present challenges.

2.4.2 Practical UAV solutions for small-scale farmers

Using an RGB sensor on a cost-effective UAV may be the most practical option for small-scale farmers concerned with irrigation applications. For example, Messina and Modica (2022) suggest enhancing RGB sensors to capture images in spectral bands such as Red Edge and NIR, thereby circumventing the need to invest in a more expensive multispectral camera. Furthermore, Gautam *et al.* (2021) used an RGB camera mounted on an autonomous UAV to compute the canopy area as a proxy of Kc. Thus, with the enhanced autonomy of UAVs and the improved efficiency of data processing techniques, it may be feasible for farmers to estimate irrigation needs at various stages throughout the season by using a UAV-based RGB camera. Furthermore, images captured by these sensors require less processing, eliminating the need for additional processing software. As a result, operational expenses are reduced [56].

2.4.3 Energy balance models for evapotranspiration estimation

Two primary models that facilitated ET estimation emerged in the database: thermal band-based energy-balance techniques and empirical VI models [57]. UAV-based energy balance methods are generally modified versions of satellite-based energy balance models, such as SEBAL, Surface Energy Balance System (SEBS), Mapping Evapotranspiration at High Resolution with Internalised Calibration (METRIC), One Source Energy Balance (OSEB), Two Source Energy Balance (TSEB), Dual-Temperature-Difference (DTD), and High-Resolution Mapping of Evapotranspiration (HRMET), leveraging UAV datasets for accurate ET estimation [30,58]. Moreover, energy balance approaches are subdivided into various approaches whereby UAV inputs are used directly, or a coarser satellite resolution image is downscaled.

Adopting RS-based ET estimation models in smallholder settings is often hindered by their complexity and data requirements. Smallholder farmers frequently lack access to comprehensive in-situ datasets, such as meteorological data, land surface temperature, and canopy structure data, which are essential for many ET models. The acquisition of these datasets is often costly and necessitates specialised equipment, placing an additional burden on limited resources. Furthermore, the technical expertise required to operate these models frequently exceeds the capabilities of smallholder farmers. Moreover, utilising these models necessitates a thorough understanding of the underlying principles and advanced data processing and analysis skills, which are typically unavailable within this demographic.

The data requirements inherent in many energy balance models, such as SEBS and SEBAL, pose significant challenges for their application in smallholder farming contexts. Models like SEBS, demanding extensive data inputs including thermal infrared imagery, meteorological data, and land cover information, often prove too intricate and data-intensive for resource-constrained smallholder settings [59]. Furthermore, these models frequently lack direct measurement validation and are best suited for larger spatial scales, limiting their practical applicability for smaller, more fragmented farmlands. Models like SEBAL require calibration against ground-based measurements or other independent ET data sources [52,60,61], which may be scarce in smallholder settings. Additionally, the specialised expertise in remote sensing, meteorology, and data analysis needed to implement these models may not be readily available to farmers in these contexts.

Addressing the limitations of complex ET models in smallholder settings requires a shift towards simplified approaches and tailored solutions. OSEB and HRMET, with minimal input data requirements, offer alternative approaches worth further investigation [30]. Developing adapted methods designed to align with the resource constraints and expertise levels of smallholder farmers is crucial. Collaborative efforts involving researchers, extension services, and farmers are essential to develop and implement practical ET estimation methods that are locally relevant and sustainable. Additionally, models like METRIC-EEFLUX and the QWaterModel, known for their low data requirements, free accessibility, and user-friendliness [62-64], provide promising alternatives. However, further testing of these models in diverse smallholder farming environments is necessary to validate their accuracy and reliability.

The versatility and practicality of UAVs, coupled with using less data-intensive energy balance models, make them particularly well-suited for smallholder agriculture. Future research should prioritise the development of user-friendly ET estimation methods tailored for smallholder settings, focusing on accessible data collection methods and straightforward analysis techniques. Empowering farmers through training programmes that foster an understanding of ET, utilise readily available sensors, and interpret data for informed decision-making is crucial. By prioritising accessibility and practicality, researchers can better support smallholder farmers in adopting sustainable water management practices and enhancing agricultural productivity.

2.4.4 Vegetation index methods for evapotranspiration estimation

To this end, the use of VI-based ET estimation methods may prove to be most appropriate. Methods utilising VIs to estimate ET often involve establishing a relationship between a VI and Kc [65]. Past studies have employed diverse spectral and thermal indicators like NDVI and CWSI to predict Kc [45]. The association between NDVI and Kc can be ascertained through basic linear regression or advanced approaches involving ML techniques. Subsequently, by using NDVI as a proxy for Kc, the computation of ET becomes more accessible. NDVI is often the preferred indicator of choice as it is versatile and can be easily computed using the data acquired from most multi-spectral sensors onboard various RS platforms. Subsequently, it has frequently been used as a primary indicator for vegetation assessment in agricultural studies [66].

2.4.5 The role of Crop Water Stress Index in water management

Tang *et al.* (2019) confirmed that the CWSI may be a more effective indicator when included in maize ET calculations under rainfed conditions. The researchers used the index to ascertain the stress coefficient (Ks = 1 – CWSI). Their findings indicated that ET calculated using the Ks-CWSI approach had a stronger association with the modified FAO-56 Kc technique, as shown by a coefficient of determination (R^2) value of 0.81. Notably, numerous small-scale farms in sub-Saharan Africa rely on rainfall for irrigation, leading to significant water scarcity issues. As a result, most agricultural development in these settings occurs under water-stress conditions [4].

2.4.6 Utilisation of the Water Deficit Index for crop stress assessment

The Water Deficit Index (WDI) is another valuable indicator for assessing crop water stress by depicting the relationship between actual ET (ETa) and potential ET (ETp), defined as WDI = 1 − (ETa/ETp) [67]. In a study by Antoniuk *et al.* (2021), the authors utilised a UAS equipped with multispectral and thermal sensors to detect and quantify drought stress in winter wheat using WDI. The results concluded that the significant correlation of the WDI to stomatal conductance and leaf water potential indicates the possibility of detecting early drought signals [68].

2.4.7 The role of machine learning in water stress assessment

The literature database has extensively employed ML techniques to estimate ET and water stress. These approaches offer several advantages in dealing with complex and high-dimensional data and capturing nonlinear relationships, making them well-suited for modelling and forecasting hydrological variables. Moreover, numerous studies have demonstrated that ML can accurately capture complex relationships between VIs, environmental factors, and ET, enabling more precise mapping of ET across different land covers and weather conditions [69-72].

In addition, ML algorithms, such as Random Forest Regression (RFR), Support Vector Machines (SVM), and Multiple Linear Regression (MLR), have proven effective in analysing crop characteristics such as water and health status [73-75]. However, among these algorithms, the RF ensemble has consistently outperformed the other two mentioned algorithms. This was demonstrated in various studies [50,76]. In addition, deep learning, a branch of ML, has been extensively used in agricultural water status research and has consistently achieved better outcomes than conventional ML methods [56]. Although these models may provide accurate results that require little user involvement, their complexity, demanding computational and data-intensive requirements may restrict their practicality for broad usage in facilitating precision water management in smallholder farms. For example, Niu *et al.* (2022) compared a stochastic configuration networks (SCN) model to a linear regression model. The authors established a relationship between NDVI and Kc for estimating the ET of pomegranate trees. The findings showed that the SCN model achieved an R^2 value of 0.995, while the linear regression model achieved 0.975. While the SCN model achieved superior performance, the linear regression model demonstrated exemplary performance and may be the preferred method of choice in many instances due to its simplicity, interpretability, and computing efficiency.

2.4.8 Future directions and research gaps

In addition to the various approaches that have been identified from the literature database for the estimation of ET and crop water stress, most research has been focused on orchards, including pistachio [52], olive [77], almond [24,78], pomegranate [46], pecan [79], and vineyards, including grapevine [45,80,81] and pinot noir [82,83]. Fewer studies have been conducted on staple crops like maize [9,57,84] or winter wheat [49,68], and no studies on neglected and underutilised crops. Therefore, it would be advantageous to prioritise research on these and other climate-resilient and nutrient-rich crops since many smallholder farmers grow these staple crops. Improving the productivity of these farms can not only aid in enhancing food and nutrition security but also improve the socioeconomic conditions of these often marginalised smallholder communities.

2.4.9 Challenges and opportunities

The previous discussion emphasised the many themes of using UAVs to facilitate precision water management in smallholder farms. Nevertheless, despite the global recognition and demonstration of the immense potential of these advanced technologies, their adoption in resource-constrained nations has significantly lagged. The innovation gap in the context of smallholder farms within these regions might be ascribed to many factors.

- Cost and affordability: the price of UAV technology might be a considerable obstacle, particularly for small-scale farms or enterprises, due to the initial outlay costs and infrastructure requirements involved in obtaining and maintaining the equipment. Fortunately, as UAV technology advances, new camera designs are being introduced, costs are decreasing, image processing techniques are improving, and more experiments are being conducted on UAV-based RS for agricultural purposes. In addition, the initial outlay is also offset by the potential for repeat flights, resulting in more frequent datasets and reduced labour and resource expenses.
- Technical literacy and information accessibility: insufficient technical literacy among smallholder farmers may hinder their comprehension, operation, and maintenance of drone technology. Moreover, inequities in accessing information and extension services might lead to unequal dissemination of knowledge on the advantages and uses of UAV technology. Therefore, smallholder farmers may exhibit risk aversion and be reluctant to invest in new technology without compelling information about their benefits, hindering the pace at which it is adopted. Nevertheless, collaboration between the public and private sectors can be established through partnerships with non-governmental organisations with a local presence, such as agricultural extension workers. These partnerships can provide practical training to farmers and enhance their technological skills.
- Limited infrastructure: inadequate infrastructure might impede the implementation and use of UAVs in rural regions where many smallholder farms are situated. These factors include substandard road networks, insufficient electrical supply, and no charging

facilities. Subsequently, governmental organisations should ensure capacity development by equipping the relevant farmers with the necessary tools to operate these technologies.

- Data-intensive methods: in small-scale farming, it is anticipated that the UAV will collect most of the data. Nevertheless, several techniques outlined in the literature rely on high-quality in-situ measurements to develop and verify the models for predicting crucial variables. Hence, more research is necessary regarding UAV-based methodologies, including all the required data acquisition to provide the desired outcome.
- Research into practical alternatives: the most frequently used VIs rely on multispectral cameras to detect crop water stress. Furthermore, the thermal sensor attachment is widespread in several investigations. However, as previously stated, an RGB sensor on an affordable UAV might be the most feasible choice for small-scale farmers interested in irrigation applications. Nevertheless, a few investigations have shown the sensor's capacity in this aspect. Hence, further research using the RBG sensor and cutting-edge methodologies is necessary to decrease operating expenses.
- Computational resources: processing, disseminating, and displaying UAV data require considerable computational capacity. Potential users may need supplementary resources or new skills to manage the substantial amounts of data associated with UAVs effectively. However, geospatial cloud computing platforms, such as GEE, have significantly transformed how geospatial data is handled and processed. These systems offer several advantages over conventional approaches by integrating ML techniques. Furthermore, this platform provides access to sophisticated computational capabilities for handling large volumes of geographical data and warrants further investigation.

2.5 Conclusion

Smallholder farmers primarily rely on indigenous knowledge for their agricultural practices; however, these practices can be enhanced by integrating modern farming techniques to improve productivity and resilience in the face of climate change. Consequently, further efforts are needed to improve accessibility to and utilisation of technological advancements for small-scale and developing farmers. The agricultural industry is increasingly recognising the significance of this research area and is supporting the development of practical approaches that benefit all agrarian stakeholders. UAVs are gaining traction for various precision agriculture applications, with anticipated cost reductions due to open-source processing platforms like Google Earth Engine. This review highlights various methods, challenges, and opportunities for using UAV technologies to estimate crop water use, identify water stress, and understand the contextual conditions in which smallholder farmers operate. UAVs equipped with multispectral or hyperspectral cameras can effectively map crop water stress, enabling precise irrigation and reducing water waste. High-resolution UAV imagery provides insights into crop health indicators, such as chlorophyll levels and VIs, facilitating early interventions and improved yields. Furthermore, deploying RGB sensors on cost-effective UAVs offers a practical solution for small-scale farmers focused on irrigation, especially as these sensors can be adapted to capture images in spectral bands such as Red Edge and NIR, thereby eliminating the need for more expensive equipment. A multi-pronged approach is essential for implementing drone technology in small-scale agriculture; this approach should include user-friendly UAV applications, farmer training programmes, and collaborative efforts among researchers, extension services, and farmers. Such initiatives will bridge the gap between cutting-edge technology and the practical needs of smallholders, promoting sustainable and productive agricultural practices. While this review contributes to the growing body of knowledge in the field, it acknowledges limitations stemming from the subjective selection of studies included. Nonetheless, the findings offer a foundation for developing effective precision water management practices by applying UAV technologies in agriculture.

2.6 References

1. Kamara, A.; Conteh, A.R.; Rhodes, E.; Cooke, R. The relevance of smallholder farming to African agricultural growth and development. *African Journal of Food, Agriculture, Nutrition and Development* **2019**, *19*, 14043-14065, doi:10.18697/ajfand.84.BLFB1010.
2. Lowder, S.; Skoet, J.; Singh, S. What do we really know about the number and distribution of farms and family farms in the world? Background paper for the State of Food and Agriculture 2014. *ESA Working Paper No. 14-02* **2014**.
3. Kpienbaareh, D.; Sun, X.; Wang, J.; Luginaah, I.; Bezner Kerr, R.; Lupafya, E.; Dakishoni, L. Crop type and land cover mapping in northern Malawi using the integration of Sentinel-1, Sentinel-2, and PlanetScope satellite data. *Remote Sensing* **2021**, *13*, 700, doi:10.3390/rs13040700.
4. Nhamo, L.; Magidi, J.; Nyamugama, A.; Clulow, A.D.; Sibanda, M.; Chimonyo, V.G.P.; Mabhaudhi, T. Prospects of improving agricultural and water productivity through unmanned aerial vehicles. *Agriculture* **2020**, *10*, 256, doi:10.3390/agriculture10070256.
5. Brewer, K.; Clulow, A.; Sibanda, M.; Gokool, S.; Odindi, J.; Mutanga, O.; Naiken, V.; Chimonyo, V.G.P.; Mabhaudhi, T. Estimation of maize foliar temperature and stomatal conductance as indicators of water stress based on optical and thermal imagery acquired

using an unmanned aerial vehicle (UAV) platform. *Drones* **2022**, *6*, doi:10.3390/drones6070169.
6. Pitman, W. Overview of water resource assessment in South Africa: current state and future challenges. *Water SA* **2011**, *37*, doi:10.4314/wsa.v37i5.3.
7. Haarhoff, S.J.; Kotzé, T.; Swanepoel, P. A. Prospectus for sustainability of rainfed maize production systems in South Africa. *Crop Science* **2020**, *60*, 14-28, doi:10.1002/csc2.20103.
8. Gokool, S.; Mahomed, M.; Kunz, R.; Clulow, A.; Sibanda, M.; Naiken, V.; Chetty, K.; Mabhaudhi, T. Crop monitoring in smallholder farms using unmanned aerial vehicles to facilitate precision agriculture practices: a scoping review and bibliometric analysis. *Sustainability* **2023**, *15*, doi:10.3390/su15043557.
9. Messina, G.; Modica, G. Applications of UAV thermal imagery in precision agriculture: state of the art and future research outlook. *Remote Sensing* **2020**, *12*, 1491, doi:10.3390/rs12091491.
10. Sishodia, R.P.; Ray, R.L.; Singh, S.K. Applications of remote sensing in precision agriculture: a review. *Remote Sensing* **2020**, *12*, 3136, doi:10.3390/rs12193136.
11. Boursianis, A.D.; Papadopoulou, M.S.; Diamantoulakis, P.; Liopa-Tsakalidi, A.; Barouchas, P.; Salahas, G.; Karagiannidis, G.; Wan, S.; Goudos, S.K. Internet of Things (IoT) and agricultural Unmanned Aerial Vehicles (UAVs) in smart farming: a comprehensive review. *Internet of Things* **2022**, *18*, 100187, doi:10.1016/j.iot.2020.100187.
12. Bukowiecki, J.; Rose, T.; Kage, H. Sentinel-2 data for precision agriculture?—A UAV-based assessment. *Sensors* **2021**, *21*, doi:10.3390/s21082861.
13. Rejeb, A.; Abdollahi, A.; Rejeb, K.; Treiblmaier, H. Drones in agriculture: a review and bibliometric analysis. *Computers and Electronics in Agriculture* **2022**, *198*, 107017, doi:10.1016/j.compag.2022.107017.
14. Verstraeten, W.W.; Veroustraete, F.; Feyen, J. Assessment of evapotranspiration and soil moisture content across different scales of observation. *Sensors* **2008**, *8*, 70-117, doi:10.3390/s8010070.
15. Niu, H.; Wang, D.; Chen, Y. Estimating actual crop evapotranspiration using deep stochastic configuration networks model and UAV-based crop coefficients in a pomegranate orchard. *Journal of Intelligent & Robotic Systems* **2020**, *104*, doi:10.1117/12.2558221.
16. Fritschen, L.J. Accuracy of evapotranspiration determinations by the Bowen ratio method *Hydrological Sciences Journal* **1965**, *10*, 38-48, doi:10.1080/02626666509493388.
17. Angus, D.E.; Watts, P.J. Evapotranspiration - how good is the Bowen ratio method? In Developments in Agricultural and Managed Forest Ecology, Sharma, M.L., Ed.; Elsevier: **1984**; Volume 13, pp. 133-150.
18. Nagler, P.L.; Scott, R.L.; Westenburg, C.; Cleverly, J.R.; Glenn, E.P.; Huete, A.R. Evapotranspiration on western U.S. rivers estimated using the Enhanced Vegetation Index from MODIS and data from eddy covariance and Bowen ratio flux towers. *Remote Sensing of Environment* **2005**, 97, 337-351, doi:10.1016/j.rse.2005.05.011.
19. de Bruin, H.; Meijninger, W.; Smedman, A.-S.; Magnusson, M. Displaced-beam small aperture scintillometer test. Part I: the Wintex dataset. *Boundary-Layer Meteorology* **2002**, *105*, 129-148, doi:10.1023/A:1019639631711.
20. Beyrich, F.; Bange, J.; Hartogensis, O.K.; Raasch, S.; Braam, M.; van Dinther, D.; Gräf, D.; van Kesteren, B.; van den Kroonenberg, A.C.; Maronga, B. Towards a validation of

scintillometer measurements: the LITFASS-2009 experiment. *Boundary-Layer Meteorology* **2012**, *144*, 83-112, doi:10.1007/s10546-012-9715-8.
21. Paw U, K.T.; Qiu, J.; Su, H.-B.; Watanabe, T.; Brunet, Y. Surface renewal analysis: a new method to obtain scalar fluxes. *Agricultural and Forest Meteorology* **1995**, *74*, 119-137, doi:10.1016/0168-1923(94)02182-j.
22. Díaz-Varela, R.A.; De la Rosa, R.; León, L.; Zarco-Tejada, P.J. High-resolution airborne UAV imagery to assess olive tree crown parameters using 3D photo reconstruction: application in breeding trials. *Remote Sensing* **2015**, *7*, 4213-4232, doi:10.3390/rs70404213.
23. Abbasi, N.; Nouri, H.; Didan, K.; Barreto-Muñoz, A.; Chavoshi Borujeni, S.; Opp, C.; Nagler, P.; Thenkabail, P.S.; Siebert, S. Mapping vegetation index-derived actual evapotranspiration across croplands using the Google Earth Engine platform. *Remote Sensing* **2023**, *15*, 1017, doi:10.3390/rs15041017.
24. Gonzalez-Dugoa, V.; Zarco-Tejadaa, P.; Fereres, E. Applicability and limitations of using the Crop Water Stress Index as an indicator of water deficits in citrus orchards. *Agricultural and Forest Meteorology* **2014**, *198-199*, 94–104, doi:10.1016/j.agrformet.2014.08.003.
25. Santesteban, L.G.; Di Gennaro, S.F.; Herrero-Langreo, A.; Miranda, C.; Royo, J.B.; Matese, A. High-resolution UAV-based thermal imaging to estimate the instantaneous and seasonal variability of plant water status within a vineyard. *Agricultural Water Management* **2017**, *183*, 49-59, doi:10.1016/j.agwat.2016.08.026.
26. Torres-Sánchez, J.; Peña, J.M.; de Castro, A.I.; López-Granados, F. Multi-temporal mapping of the vegetation fraction in early-season wheat fields using images from UAV. *Computers and Electronics in Agriculture* **2014**, *103*, 104-113, doi:10.1016/j.compag.2014.02.009.
27. Bennett, M.K.; Younes, N.; Joyce, K. Automating drone image processing to map coral reef substrates using Google Earth Engine. *Drones* **2020**, *4*, doi:10.3390/drones4030050.
28. Cucho-Padin, G.; Loayza, H.; Palacios, S.; Balcazar, M.; Carbajal, M.; Roberto, Q. Development of low-cost remote sensing tools and methods for supporting smallholder agriculture. *Applied Geomatics* **2019**, *12*, 247-263, doi:10.1007/s12518-019-00292-5.
29. Zhang, C.; Kovacs, J.M. The application of small unmanned aerial systems for precision agriculture: a review. *Precision Agriculture* **2012**, *13*, 693-712, doi:10.1007/s11119-012-9274-5.
30. Niu, H.; Hollenbeck, D.; Zhao, T.; Wang, D.; Chen, Y. Evapotranspiration estimation with small UAVs in precision agriculture. *Sensors* **2020**, *20*, 6427, doi:10.3390/s20226427.
31. Singh, A.P.; Yerudkar, A.; Mariani, V.; Iannelli, L.; Glielmo, L. A bibliometric review of the use of unmanned aerial vehicles in precision agriculture and precision viticulture for sensing applications. *Remote Sensing* **2022**, *14*, 1604, doi:10.3390/rs14071604.
32. Awais, M.; Li, W.; Cheema, M.; Zaman, Q.; Shaheen, A.; Aslam, B.; Zhu, W.; Ajmal, M.; Faheem, M. UAV-based remote sensing in plant stress imagine using high-resolution thermal sensor for digital agriculture practices: a meta-review. *International Journal of Environmental Science and Technology* **2023**, *20*, 1135-1152, doi:10.1007/s13762-021-03801-5.
33. Raparelli, E.; Bajocco, S. A bibliometric analysis on the use of unmanned aerial vehicles in agricultural and forestry studies. *International Journal of Remote Sensing* **2019**, *40*, 9070-9083, doi:10.1080/01431161.2019.1569793.

34. Rivera, M.; Pizam, A. Advances in hospitality research: from Rodney Dangerfield to Aretha Franklin. *International Journal of Contemporary Hospitality Management* **2015**, *27*, 362-378, doi:10.1108/IJCHM-03-2014-0146.
35. Ferreira, M.A.; Pinto, C.; Serra, F. The transaction costs theory in international business research: A bibliometric study over three decades. *Scientometrics* **2014**, *98*, 1899-1922, doi:10.1007/s11192-013-1172-8.
36. Geng, D.; Feng, Y.; Zhu, Q. Sustainable design for users: a literature review and bibliometric analysis. *Environmental Science and Pollution Research* **2020**, *27*, 29824-29836, doi:10.1007/s11356-020-09283-1.
37. Gago, J.; Douthe, C.; Coopman, R.E.; Gallego, P.P.; Ribas-Carbo, M.; Flexas, J.; Escalona, J.; Medrano, H. UAVs challenge to assess water stress for sustainable agriculture. *Agricultural Water Management* **2015**, *153*, 9-19, doi:10.1016/j.agwat.2015.01.020.
38. Sagan, V.; Maimaitijiang, M.; Sidike, P.; Eblimit, K.; Peterson, K.; Hartling, S.; Esposito, F.; Khanal, K.; Newcomb, M.; Pauli, D. UAV-based high-resolution thermal imaging for vegetation monitoring and plant phenotyping using ICI 8640 P, FLIR Vue Pro R 640, and thermoMap cameras. *Remote Sensing* **2019**, *11*, 330, doi:10.3390/rs11030330.
39. Kim, W.; Khan, G.; Wood, J.; Mahmood, M. Employee engagement for sustainable organisations: keyword analysis using social network analysis and burst detection approach. *Sustainability* **2016**, *8*, 631, doi:10.3390/su8070631.
40. Dixit, A.; Jakhar, S. Airport capacity management: a review and bibliometric analysis. *Journal of Air Transport Management* **2021**, *91*, 102010, doi:10.1016/j.jairtraman.2020.102010.
41. Han, Y.; Tarakey, B.A.; Hong, S.-J.; Kim, S.-Y.; Kim, E.; Lee, C.-H.; Kim, G. Calibration and image processing of aerial thermal image for UAV application in crop water stress estimation. *Journal of Sensors* **2021**, *2021*, 5537795, doi:10.1155/2021/5537795.
42. Inoue, Y. Satellite- and drone-based remote sensing of crops and soils for smart farming–a review. *Soil Science and Plant Nutrition* **2020**, *66*, 798-810, doi:10.1080/00380768.2020.1738899.
43. Ali, I.; Greifeneder, F.; Stamenkovic, J.; Neumann, M.; Notarnicola, C. Review of machine learning approaches for biomass and soil moisture retrievals from remote sensing data. *Remote Sensing* **2015**, *7*, 16398-16421, doi:10.3390/rs71215841.
44. Gautam, D.; Pagay, V. A review of current and potential applications of remote sensing to study the water status of horticultural crops. *Agronomy* **2020**, *10*, 140, doi:10.3390/agronomy10010140.
45. Gautam, D.; Ostendorf, B.; Pagay, V. Estimation of grapevine crop coefficient using a multispectral camera on an unmanned aerial vehicle. *Remote Sensing* **2021**, *13*, 2639, doi:10.3390/rs13132639.
46. Niu, H.; Zhao, T.; Wang, D.; Chen, Y. Estimating evapotranspiration of pomegranate trees using stochastic configuration networks (SCN) and UAV multispectral imagery. *Journal of Intelligent & Robotic Systems* **2022**, *104*, doi:10.1007/s10846-022-01588-2.
47. Chávez, R.; Grönwall, J.; Kwast, J.; Danert, K.; Foppen, J. Estimating domestic self-supply groundwater use in urban continental Africa. *Environmental Research Letters* **2020**, *15*, doi:10.1088/1748-9326/ab9af9.
48. Said Mohamed, E.; Belal, A.A.; Kotb Abd-Elmabod, S.; El-Shirbeny, M.A.; Gad, A.; Zahran, M.B. Smart farming for improving agricultural management. *The Egyptian*

Journal of Remote Sensing and Space Science **2021**, *24*, 971-981, doi:10.1016/j.ejrs.2021.08.007.
49. Zhou, Z.; Majeed, Y.; Naranjo, G.; Gambacorta, E. Assessment for crop water stress with infrared thermal imagery in precision agriculture: a review and future prospects for deep learning applications *Computers and Electronics in Agriculture* **2021**, *182*, 106019, doi:10.1016/j.compag.2021.106019.
50. Shao, G.; Han, W.; Zhang, H.; Wang, Y.; Zhang, L.; Niu, Y.; Zhang, Y.; Cao, P. Estimation of transpiration coefficient and aboveground biomass in maize using time-series UAV multispectral imagery. *The Crop Journal* **2022**, *10*, 1376-1385, doi:10.1016/j.cj.2022.08.001.
51. Ortega-Farías, S.; Ortega-Salazar, S.; Poblete, T.; Kilic, A.; Allen, R.; Poblete-Echeverría, C.; Ahumada-Orellana, L.; Zuñiga, M.; Sepúlveda, D. Estimation of energy balance components over a drip-irrigated olive orchard using thermal and multispectral cameras placed on a helicopter-based Unmanned Aerial Vehicle (UAV). *Remote Sensing* **2016**, *8*, doi:10.3390/rs8080638.
52. Aliabad, F.A.; Shojaei, S.; Mortaz, M.; Ferreira, C.S.S.; Kalantari, Z. Use of Landsat 8 and UAV images to assess changes in temperature and evapotranspiration by economic trees following foliar spraying with light-reflecting compounds. *Remote Sensing* **2022**, *14*, 6153, doi:10.3390/rs14236153.
53. Masina, M.; Lambertini, A.; Daprà, I.; Mandanici, E.; Lamberti, A. Remote sensing analysis of surface temperature from heterogeneous data in a maize field and related water stress. *Remote Sensing* **2020**, *12*, 2506, doi:10.3390/rs12152506.
54. Gerhards, M.; Schlerf, M.; Mallick, K.; Udelhoven, T. Challenges and future perspectives of multi-/hyperspectral thermal infrared remote sensing for crop water-stress detection: a review. *Remote Sensing* **2019**, *11*, doi:10.3390/rs11101240.
55. Jackson, R.D. Canopy temperature and crop water stress. In *Advances in Irrigation*, Hillel, D., Ed.; Elsevier: 1982; Volume 1, pp. 43-85.
56. Rosle, R.; Che'Ya, N.N.; Ang, Y.; Rahmat, F.; Wayayok, A.; Berahim, Z.; Fazlil Ilahi, W.F.; Ismail, M.R.; Omar, M.H. Weed detection in rice fields using remote sensing technique: a review. *Applied Sciences* **2021**, *11*, doi:10.3390/app112210701.
57. Tang, J.; Han, W.; Zhang, L. UAV multispectral imagery combined with the FAO-56 dual approach for maize evapotranspiration mapping in the North China Plain. *Remote Sensing* **2019**, *11*, 2519, doi:10.3390/rs11212519.
58. Molaei, B.; Chandel, A.K.; Peters, R.T.; Khot, L.R.; Khan, A.; Maureira, F.; Stockle, C. Investigating the application of artificial hot and cold reference surfaces for improved ETc estimation using the UAS-METRIC energy balance model. *Agricultural Water Management* **2023**, *284*, 108346, doi:10.1016/j.agwat.2023.108346
59. Gibson, L.A.; Münch, Z.; Engelbrecht, J. Particular uncertainties encountered in using a pre-packaged SEBS model to derive evapotranspiration in a heterogeneous study area in South Africa. *Hydrology and Earth Systems Sciences* **2011**, *15*, 295-310, doi:10.5194/hess-15-295-2011.
60. Bastiaanssen, W.G.M.; Cheema, M.J.M.; Immerzeel, W.W.; Miltenburg, I.J.; Pelgrum, H. Surface energy balance and actual evapotranspiration of the transboundary Indus Basin estimated from satellite measurements and the ETLook model. *Water Resources Research* **2012**, *48*, doi:10.1029/2011WR010482.
61. Guzinski, R.; Nieto, H.; Jensen, R.; Mendiguren, G. Remotely sensed land-surface energy fluxes at sub-field scale in heterogeneous agricultural landscape and coniferous plantation. *Biogeosciences* **2014**, *11*, 5021-5046, doi:10.5194/bg-11-5021-2014.

62. Timmermans, W.; Kustas, W.; Andreu, A. Utility of an automated thermal-based approach for monitoring evapotranspiration. *Acta Geophysica* **2015**, *63*, 1571-1608, doi:10.1515/acgeo-2015-0016.
63. Filgueiras, R.; Mantovani, E.; Althoff, D.; Balieiro Ribeiro, R.; Venancio, L.; Argolo dos Santos, R. Dynamics of actual crop evapotranspiration based in the comparative analysis of SEBAL and METRIC-EEFLUX. *IRRIGA* **2019**, *1*, 72-80, doi:10.15809/irriga.2019v1n1p72-80.
64. Ellsäßer, F.; Röll, A.; Stiegler, C.; Hendrayanto; Hölscher, D. Introducing QWaterModel, a QGIS plugin for predicting evapotranspiration from land surface temperatures. *Environmental Modelling & Software* **2020**, *130*, 104739, doi:10.1016/j.envsoft.2020.104739.
65. Ihuoma, S.O.; Madramootoo, C.A.; Kalacska, M. Integration of satellite imagery and in situ soil moisture data for estimating irrigation water requirements. *International Journal of Applied Earth Observation and Geoinformation* **2021**, *102*, 102396, doi:10.1016/j.jag.2021.102396.
66. Venancio, L.P.; Eugenio, F.C.; Filgueiras, R.; França da Cunha, F.; Argolo dos Santos, R.; Ribeiro, W.R.; Mantovani, E.C. Mapping within-field variability of soybean evapotranspiration and crop coefficient using the Earth Engine Evaporation Flux (EEFlux) application. *PLoS ONE* **2020**, *15*, e0235620, doi:10.1371/journal.pone.0235620.
67. Moran, M.S.; Clarke, T.R.; Inoue, Y.; Vidal, A. Estimating crop water deficit using the relation between surface-air temperature and spectral vegetation index. *Remote Sensing of Environment* **1994**, *49*, 246-263, doi:10.1016/0034-4257(94)90020-5.
68. Antoniuk, V.; Manevski, K.; Kørup, K.; Larsen, R.; Sandholt, I.; Zhang, X.; Andersen, M.N. Diurnal and seasonal mapping of Water Deficit Index and evapotranspiration by an unmanned aerial system: a case study for winter wheat in Denmark. *Remote Sensing* **2021**, *13*, 2998, doi:10.3390/rs13152998.
69. Tabari, H.; Martinez, C.; Ezani, A.; Hosseinzadeh Talaee, P. Applicability of support vector machines and adaptive neurofuzzy inference system for modelling potato crop evapotranspiration. *Irrigation Science* **2013**, *31*, 575-588, doi:10.1007/s00271-012-0332-6.
70. Gocic, M.; Petković, D.; Shamshirband, S.; Kamsin, A. Comparative analysis of reference evapotranspiration equations modelling by extreme learning machine. *Computers and Electronics in Agriculture* **2016**, *127*, 56-63, doi:10.1016/j.compag.2016.05.017.
71. Kisi, O.; Sanikhani, H.; Zounemat-Kermani, M.; Niazi, F. Long-term monthly evapotranspiration modelling by several data-driven methods without climatic data. *Computers and Electronics in Agriculture* **2015**, *115*, 66-77, doi:10.1016/j.compag.2015.04.015.
72. Petković, D.; Gocic, M.; Shamshirband, S.; Qasem, S.N.; Trajkovic, S. Particle swarm optimization-based radial basis function network for estimation of reference evapotranspiration. *Theoretical and Applied Climatology* **2016**, *125*, 555-563, doi:10.1007/s00704-015-1522-y.
73. Han, L.; Yang, G.; Dai, H.; Xu, B.; Yang, H.; Feng, H.; Li, Z.; Yang, X. Modelling maize above-ground biomass based on machine learning approaches using UAV remote-sensing data. *Plant Methods* **2019**, *15*, 10, doi:10.1186/s13007-019-0394-z.
74. Hassanijalilian, O.; Igathinathane, C.; Doetkott, C.; Bajwa, S.G.; Bajwa, S.G.; Nowatzki, J.; Esmaeili, S.A.H.; Esmaeili, S.A.H. Chlorophyll estimation in soybean

leaves infield with smartphone digital imaging and machine learning. *Computers and Electronics in Agriculture* **2020**, *174*, 105433, doi:10.1016/j.compag.2020.105433.

75. Guo, Y.; Yin, G.; Sun, H.; Wang, H.; Chen, S.; Senthilnath, J.; Wang, J.; Fu, Y. Scaling effects on chlorophyll content estimations with RGB camera mounted on a UAV platform using machine-learning methods. *Sensors* **2020**, *20*, doi:10.3390/s20185130
76. Marques Ramos, A.P., Osco, L. P., Garcia Furuya, D. E., Nunes Gonçalves, W., Cordeiro Santana, D., Ribeiro Teodoro, L. P., da Silva Junior, C. A., Capristo-Silva, G. F., Li, J., Rojo Baio, F. H., Marcato Junior, J., Teodoro, P. E., Pistori, H. A Random Forest ranking approach to predict yield in maize with UAV-based vegetation spectral indices. *Computers and Electronics in Agriculture* **2020**, *178*, 105791, doi:10.1016/j.compag.2020.105791.
77. Messina, G.; Modica, G. Twenty years of remote sensing applications targeting landscape analysis and environmental issues in olive growing: a review. *Remote Sensing* **2022**, *14*, 5430, doi:10.3390/rs14215430.
78. Peddinti, S.R.; Kisekka, I. Estimation of turbulent fluxes over almond orchards using high-resolution aerial imagery with one and two-source energy balance models. *Agricultural Water Management* **2022**, *269*, 107671, doi:10.1016/j.agwat.2022.107671.
79. Mokari, E.; Samani, Z.; Heerema, R.; Dehghan-Niri, E.; DuBois, D.; Ward, F.; Pierce, C. Development of a new UAV-thermal imaging based model for estimating pecan evapotranspiration. *Computers and Electronics in Agriculture* **2022**, *194*, 106752, doi:10.1016/j.compag.2022.106752.
80. Chandel, A.K.; Molaei, B.; Khot, L.R.; Peters, R.T.; Stöckle, C.O. High-resolution geospatial evapotranspiration mapping of irrigated field crops using multispectral and thermal infrared imagery with METRIC energy balance model. *Drones* **2020**, *4*, 52, doi:10.3390/drones4030052.
81. Espinoza, C.Z.; Khot, L.R.; Sankaran, S.; Jacoby, P.W. High resolution multispectral and thermal remote sensing-based water stress assessment in subsurface irrigated grapevines. *Remote Sensing* **2017**, *9*, doi:10.3390/rs9090961.
82. Lu, S.; Xuan, J.; Zhang, T.; Bai, X.; Tian, F.; Ortega-Farias, S. Effect of the shadow pixels on evapotranspiration inversion of vineyard: a high-resolution UAV-based and ground-based remote sensing measurements. *Remote Sensing* **2022**, *14*, 2259, doi:10.3390/rs14092259.
83. Bellvert, J.; Zarco-Tejada, P.; Girona, J.; Fereres, E. Mapping Crop Water Stress Index in a Pinot-noir vineyard: comparing ground measurements with thermal remote sensing imagery from an unmanned aerial vehicle. *Precision Agriculture* **2014**, *15*, 361-376, doi:10.1007/s11119-013-9334-5.
84. Zhang, L.; Niu, Y.; Zhang, H.; Han, W.; Li, G.; Tang, J.; Peng, X. Maize canopy temperature extracted from UAV thermal and RGB imagery and its application in water stress monitoring. *Frontiers in Plant Science* **2019**, *10*, 1270, doi:10.3389/fpls.2019.01270.

*****

Lead-In to Chapter 3:

Building upon the theoretical and methodological foundations established in Chapter 2—a comprehensive scoping review and bibliometric analysis of unmanned aerial vehicle (UAV) applications in precision water management—Chapter 3 presents an empirical investigation into the accuracy and practicality of UAV-based remote sensing (RS) for evapotranspiration (ET) estimation within a smallholder sugarcane farm in Swayimane, KwaZulu-Natal, South Africa. This study examines the premise that UAV-based RS can accurately quantify the spatiotemporal dynamics of crop water use in fragmented smallholder farming systems. This involved acquiring high-resolution multispectral imagery using a DJI Matrice 300 platform with a MicaSense Altum camera and processing using Pix4Dfields and Google Earth Engine (GEE). Two distinct actual ET (ETa) estimation approaches—vegetation index (VI)-based methods (Normalised Difference VI [NDVI], NDVIscaled, NDVIKc, Enhanced VI [EVI], and EVI2) and an independent Random Forest Regression (RFR) ensemble model trained on in-situ data—were employed and compared against measurements from a gold-standard eddy covariance (EC) flux tower. Results, shown as spatially explicit ETa maps (ArcGIS Pro), are presented in Chapter 3, including a detailed discussion and interpretation of these findings.

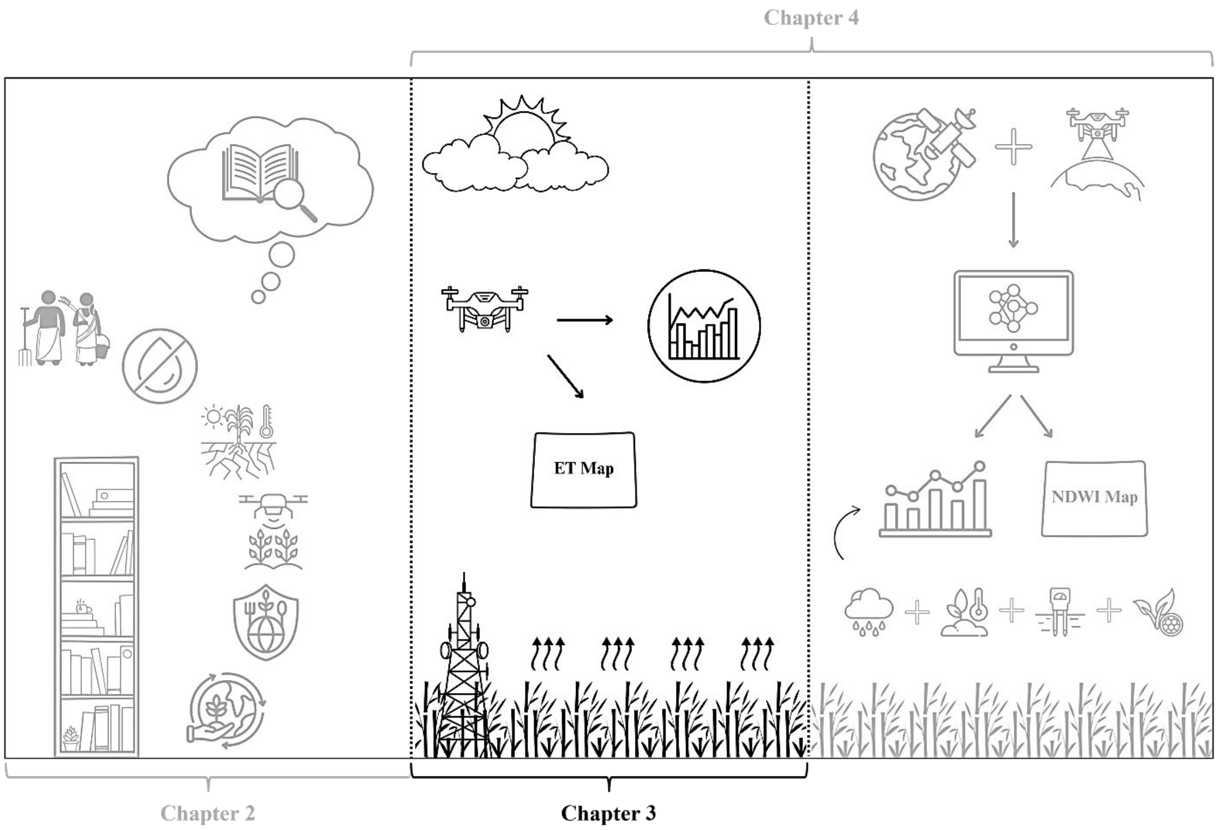

3. CHAPTER 3: EVALUATING THE POTENTIAL OF UNMANNED AERIAL VEHICLE-DERIVED DATA FOR EVAPOTRANSPIRATION ESTIMATION IN SMALLHOLDER FARMS (PAPER 2)

Ameera Yacoob [1*], Shaeden Gokool [1], Alistair Clulow [1,2], Maqsooda Mahomed [1], Vivek Naiken [1,2] and Tafadzwanashe Mabhaudhi [3,4]

[1] *Centre for Water Resources Research, School of Agricultural, Earth & Environmental Sciences, University of KwaZulu-Natal, P/Bag X01, Scottsville, Pietermaritzburg 3209, South Africa; gokools@ukzn.ac.za; clulowa@ukzn.ac.za; mahomedm@ukzn.ac.za; naikenv@ukzn.ac.za*

[2] *Discipline of Agrometeorology, School of Agricultural, Earth and Environmental Sciences, University of KwaZulu-Natal, P/Bag X01, Scottsville, Pietermaritzburg 3209, South Africa*

[3] *Centre for Transformative Agricultural and Food Systems, School of Agricultural, Earth & Environmental Sciences, University of KwaZulu-Natal, P/Bag X01, Pietermaritzburg 3209, South Africa; tafadzwanashe.mabhaudhi@lshtm.ac.uk*

[4] *Centre of Climate Change and Planetary Health, London School of Hygiene and Tropical Medicine, London, United Kingdom*

[*] *Correspondence: 218023873@stu.ukzn.ac.za; Tel.: +27-792913882*

Abstract:

The rising global population has heightened food demand, placing immense pressure on agricultural systems, particularly in water-scarce regions such as South Africa. Smallholder farmers, essential to the farming sector, encounter considerable challenges from climatic variability and resource limitations, necessitating innovative solutions to enhance farm sustainability and productivity. To this end, this study demonstrates and evaluates the application of unmanned aerial vehicles (UAVs) to generate spatially explicit evapotranspiration (ET) estimates for a small-scale sugarcane field, facilitating precision water

This chapter is a working draft for submission to the *Remote Sensing* journal (MDPI). It includes additional sections and details tailored to the comprehensiveness required for this master's thesis. The chapter will be revised and condensed to comply with the journal's submission requirements.

References in this chapter follow the 2019 Bioresources Engineering style from the Centre for Water Resources Research, University of KwaZulu-Natal.

management in these farming operations. Various vegetation indices (VIs) derived from UAV-based multispectral imagery are evaluated to predict actual ET (ETa) and validated against ground-based eddy covariance (EC) measurements. The findings present three ETa models based on the Normalised Difference Vegetation Index (NDVI)—ET-NDVI, ET-NDVIscaled, and ET-NDVIKc—and two models based on the Enhanced Vegetation Index (EVI)—ET-EVI and ET-EVI2. Additionally, machine learning (ML) techniques are employed to correlate ground-based crop coefficients (Kc) with NDVI values, facilitating the development of a Kc prediction model. The EVI2 model, integrating in-situ and UAV-derived data, yields the most accurate ETa estimates for sugarcane, with a coefficient of determination (R^2) of 0.63, Root Mean Square Error (RMSE) of 0.67, and Mean Absolute Error (MAE) of 0.52. Furthermore, the ET-VI approaches, especially EVI2, are well-suited for smallholder farms due to their lower technological complexity and reduced data requirements. Although the results of this research are promising, further investigation into minimising the reliance on in-situ data is crucial for enhancing the accessibility of advanced agricultural monitoring techniques for smallholder farmers.

Keywords: evapotranspiration estimation; food security; Google Earth Engine; Kc prediction model; machine learning; remote sensing; smallholder farmers; sugarcane cultivation; UAV technology; vegetation indices

3.1 Introduction

The burgeoning global population has increased the demand for sustenance, thereby placing substantial pressure on agricultural systems to enhance production efficiency (Gokool *et al.*, 2023). In South Africa, this demand strains resources and infrastructure, impacting water reservoirs crucial for agriculture, which use up to 70% of available resources (Wagner *et al.*, 2022). Concurrent demands from agricultural, industrial, and domestic sectors further stress finite water supplies (du Plessis, 2017). Water scarcity poses an additional acute challenge nationwide (Mabhaudhi *et al.*, 2021). Regrettably, the compounding effects of climate change exacerbate this issue through shifts in precipitation patterns and a proliferation of extreme weather phenomena (Hosea and Khalema, 2020), while higher temperatures increase evapotranspiration (ET), reducing soil moisture and reservoir volumes (Lawal *et al.*, 2019).

The abovementioned challenges threaten crop growth and yield, undermining efforts to eradicate hunger and malnutrition by 2030—a task further complicated by the COVID-19 pandemic (Panday *et al.*, 2020). With the anticipation of the exacerbation of several issues in the foreseeable future, the resilience and efficacy of contemporary agricultural food production systems face significant jeopardy (Segarra *et al.*, 2020). Hence, there is a paramount imperative to improve the sustainability and productivity of farming systems, given that many are presently incapable of meeting the rising food demand (Pawlak and Kołodziejczak, 2020). This necessity is particularly pronounced for smallholder farms, which, despite their modest scale, typically less than two hectares, constitute the bedrock of our agricultural frameworks (Brewer *et al.*, 2022; Gokool *et al.*, 2023).

Smallholder farms are essential in achieving food security objectives by significantly strengthening agricultural productivity, supporting livelihoods, and fostering socio-economic advancement, particularly within developing regions (Kamara *et al.*, 2019; Gokool *et al.*, 2023). Nonetheless, persistent climatic variability and limited access to critical resources pose formidable challenges to smallholder farming practices in sub-Saharan Africa, leading to diminished productivity and profitability (Adisa *et al.*, 2018; Brewer *et al.*, 2022). The sugarcane industry is crucial in South Africa's agricultural sector, providing substantial employment opportunities and promoting rural development and food security (Hess *et al.*, 2016; Ngcobo, 2023).

Numerous small-scale farmers cultivate sugarcane using rainfed agriculture due to limited access to irrigation resources, impacting their capacity to maximise production and achieve competitive yields (Adisa *et al.*, 2018; Madamombe *et al.*, 2024). However, their reliance on precipitation entails a substantial threat to agricultural yields, as reduced seasonal rainfall and occurrences of extreme weather can detrimentally impact crop vitality, biochemical functions, and physical development (Walker and Schulze, 2006; Okonya *et al.*, 2013; Lawal *et al.*, 2019). Therefore, investigating inventive and economically viable approaches to improve smallholder farmers' efficacy and adaptability is vital. Shi *et al.* (2016) and Nhamo *et al.* (2020) propose that the implementation of such strategies can reinforce their capacity to confront adversities (Shi *et al.*, 2016; Nhamo *et al.*, 2020).

Furthermore, erratic precipitation may increase reliance on irrigation to sustain agricultural yields in forthcoming years (Shiferaw *et al.*, 2014; Meza *et al.*, 2021). Thus, efficient and environmentally sound irrigation techniques are crucial to adapt to changing climates. As such, precise estimates of crop water needs are vital for managing irrigation systems (Lakhiar *et al.*, 2024). A significant portion of crop water use is due to ET, which includes water released through soil evaporation and plant transpiration (Reddy, 2020; Wagner *et al.*, 2022). Consequently, accurate ET estimates are essential for rigorous water management (Niu *et al.*, 2020a). Over time, various in-situ methodologies have been devised and implemented to ascertain ET levels with precision (Gray *et al.*, 2022). The ensuing section explores several such techniques.

3.1.1 In-situ techniques for actual evapotranspiration estimation

Three principal classifications for estimating actual ET (ETa) are i) water balance or hydrological methods, ii) micrometeorological methods, and iii) empirical methods (Tanner, 1967; Shaomin and Xu, 2018). The former two categories are founded rationally on established scientific principles and theoretical frameworks, providing a systematic approach to understanding and estimating ETa. In contrast, empirical methods involve calibrating models to develop relationships between empirical ET indices and ETa measurements, typically achieved with a reasonable confidence level. These methods often rely on observational data and may lack a robust theoretical basis compared to the first two classifications (Tanner, 1967; Shaomin and Xu, 2018).

Micrometeorological methodologies are extensively employed to determine ETa due to their advantages over alternative techniques (Shaomin and Xu, 2018). These methods leverage atmospheric observations to estimate the water vapour flux from the land surface, affording precise ETa estimates (Drexler *et al.*, 2004; Savage *et al.*, 2017). Notably, the eminent eddy covariance (EC) technique yields real-time, height-independent sensible heat flux estimates (Savage *et al.*, 2017). Additionally, the latent heat flux (LE) can be determined by directly measuring the covariance between wind speed w (m s^{-1}) and specific humidity q (kg kg^{-1}) (Savage *et al.*, 2017). Alternatively, the simplified energy balance equation computes LE as a residual (Savage *et al.*, 2017).

The residual estimation of latent heat flux at the land-air interface is:

$$\mathrm{LE} = \mathrm{Rn} - \mathrm{H} - \mathrm{G} \tag{3.1}$$

where LE is latent energy flux density, Rn is net irradiance, H is sensible heat flux density, and G is soil heat flux, all in W m^{-2} (Savage *et al.*, 2017).

Micrometeorological techniques provide continuous, high-frequency datasets essential for analysing temporal fluctuations in ETa (Savage *et al.*, 2017). Such capabilities are crucial for informing irrigation management strategies (Lakhiar *et al.*, 2024). Alternative methods for estimating ETa through ground-based measurements encompass the weighing lysimeter, the Bowen Ratio, surface renewal pan evaporation, sap flow, and the scintillometer (Minacapilli *et al.*, 2016; Tian *et al.*, 2017). However, these systems require sophisticated instrumentation and skilled technicians to install and operate them, limiting their use in smallholder farms (Yacoob *et al.*, 2024). Additionally, EC towers offer point measurements, restricting spatial coverage and complicating broader extrapolation (Hu *et al.*, 2015; Tian *et al.*, 2017).

Given the limitations of the techniques, which are primarily applicable at local scales and lack scalability for broader coverage, remote sensing (RS) methodologies can be considered a suitable alternative. RS approaches provide extensive data coverage across large geographical extents, including remote and data-scarce regions (Bachour, 2013; Ali *et al.*, 2023). Particularly noteworthy is the increasing prominence of RS within precision agriculture (PA) and the integration of technologies associated with the fourth industrial revolution in agricultural practices (Brewer *et al.*, 2022). Subsequent sections will delve into prominent RS technologies and the related techniques facilitating the estimation of ETa through these approaches.

3.1.2 Actual evapotranspiration estimation using remote sensing approaches

The scholarly discourse identifies three principal technologies encompassed within the expansive domain of RS: Satellite Earth Observation (SEO) technologies, manned aerial vehicles, and unmanned aerial vehicles (UAVs) (Rejeb *et al.*, 2022). These technologies afford farmers diverse options for monitoring and managing their agricultural endeavours (Rejeb *et al.*, 2022). However, each technique possesses distinctive advantages and is tailored to suit different operational scales, spanning from comprehensive crop surveillance facilitated by satellites to precise and localised assessments enabled by UAVs (Brewer *et al.*, 2022; Gokool *et al.*, 2023).

Satellite-based RS leverages Earth-orbiting satellites with sensors designed to capture data across various spectral bands (Omia *et al.*, 2023). This capability facilitates monitoring crop health (Omia *et al.*, 2023), land cover alterations (Mashala *et al.*, 2023), and soil conditions (Emery and Camps, 2017) across expansive agricultural landscapes (Ali *et al.*, 2023; Dasgupta *et al.*, 2023). Nonetheless, intrinsic fragmentation and diversity in smallholder farming systems present a considerable obstacle to efficiently utilising freely available SEO datasets (Gokool *et al.*, 2023; Yacoob *et al.*, 2024).

The constraints of these datasets predominantly stem from their spatial, spectral, and temporal attributes (Brewer *et al.*, 2022; McCarthy *et al.*, 2023). Hence, there is a pressing need for alternative methods to accommodate the distinct characteristics of smallholder agricultural systems and to ensure that the datasets utilised are customised to suit the requirements of these contexts. Moreover, the substantial financial ramifications of adopting more sophisticated satellite and manned aerial systems render these alternatives unfeasible for many farming communities (Huang *et al.*, 2017; Mohidem *et al.*, 2021).

3.1.3 UAV-based remote sensing for smallholder agriculture

UAVs offer distinctive advantages in PA, serving as a cost-effective tool that provides spatially representative data at user-defined intervals, thus enhancing PA outcomes and reducing atmospheric disturbances like cloud cover (Cucho-Padin *et al.*, 2019; Brewer *et al.*, 2022). Their potential deployment in smallholder contexts emphasises their significance (Hoffmann *et al.*, 2016; Messina and Modica, 2020). Moreover, integrating Very High-Resolution (VHR) cameras on UAVs improves crop image analytics, overcoming the limitations of satellite imagery (Maes and Steppe, 2019; Nhamo *et al.*, 2020). This high-resolution imagery enables the prompt acquisition of spectral data crucial for analysing crop phenology, foliar temperature, and moisture content (Park *et al.*, 2017; Zhang *et al.*, 2019).

In summary, conventional approaches to ETa estimation entail significant costs and technical complexities related to data processing and analysis. This highlights the need for further investigation into UAV-based methodologies. Such research is vital for smallholder farmers requiring enhanced technical resources to effectively utilise these innovations (Yacoob *et al.*, 2024). Moreover, extracting relevant insights from UAV data may present challenges due to the computational intensity of the processing involved, necessitating specialised software and expertise that may not be readily accessible (Yacoob *et al.*, 2024). Addressing these constraints is essential to ensure the successful integration of UAV technologies into the agricultural practices of smallholder farmers.

Despite increasing interest in ETa estimation using UAV-derived data, there remains a notable lack of consensus on the most practical and suitable implementation strategies (Yacoob *et al.*, 2024). Moreover, most UAV-based RS techniques documented in the literature rely heavily on extensive in-situ data records, making their practical application dependent on the availability of such data (Yacoob *et al.*, 2024). However, these comprehensive datasets are often unavailable in the context of smallholder agriculture (Yacoob *et al.*, 2024). Consequently, there is a pressing need to identify and evaluate techniques that minimise reliance on in-situ data.

3.1.4 Vegetation index-based models for actual evapotranspiration estimation

Two primary models estimate ETa using UAV data: thermal band-based energy-balance approaches and empirical vegetation index (VI) models (Tang *et al.*, 2019). VI models use the relationship between the crop coefficient (Kc) and reference ET (ETo) to forecast crop water needs (Ihuoma *et al.*, 2021). The ET-VI method employs VIs as proxies for Kc, as outlined in the Food and Agriculture Organisation (FAO56) method (Allen *et al.*, 1998). This method applies the Penman-Monteith equation (Monteith, 1965) to calculate ETo, which is then adjusted by Kc to estimate potential ET (ETp) under ideal conditions (Abbasi *et al.*, 2023). ETp is further adjusted using the stress coefficient (Ks) to account for water deficits, resulting in the ETa (Abbasi *et al.*, 2023).

The Ks delineates the reduction in ETa attributed to water deficit (Abbasi *et al.*, 2021). Under conditions of sufficient irrigation, the Ks is conventionally assigned a value of 1 (Abbasi *et al.*, 2021). Correspondingly, a VI approximates the combined impact of Kc and the Ks within the ET-VI methodology (Abbasi *et al.*, 2021). The FAO56 framework encompasses two distinct methodologies for determining Kc: the single Kc method, which integrates crop transpiration and soil evaporation into a unified coefficient, and the dual Kc method, which treats crop transpiration and soil evaporation as separate components (Tang *et al.*, 2019). However, the single Kc approach predominates in the literature (Akdim *et al.*, 2014; Abbasi *et al.*, 2023).

Frequently utilised VIs include the Normalised Difference Vegetation Index (NDVI), Enhanced Vegetation Index (EVI), and the two-band variant of the EVI (EVI2) (Abbasi *et al.*, 2023). These indices have undergone extensive evaluation to estimate ETa across diverse landscape settings (Hunsaker *et al.*, 2003; Murray *et al.*, 2009; Nouri *et al.*, 2014; Khand *et al.*, 2017; French *et al.*, 2018; Nagler *et al.*, 2022). Among these VIs, NDVI has gained significant traction as a surrogate for Kc at the field level across various crop types (Filgueiras *et al.*, 2019; Abbasi *et al.*, 2021). This was achieved by investigating the relationship between Kc and NDVI (Shao *et al.*, 2021; Niu *et al.*, 2022).

Researchers initially used in-situ measurements to explore VI-Kc relationships (Bausch and Neale, 1987). Advances in satellite technology later enabled the widespread use of satellite-derived VIs as proxies for ground-based assessments (Nouri *et al.*, 2020). UAVs further revolutionised this field, introducing UAV-based NDVI for analysing NDVI-Kc dynamics (Shao *et al.*, 2023). Bausch and Neale (1987) demonstrated that radiometric NDVI could effectively estimate Kc from lysimeter data. Nouri *et al.* (2020) evaluated temporal ETa variations using WorldView2, Landsat, and MODIS with VIs like NDVI, EVI, and EVI2, identifying ET-MODIS (EVI2) as the most accurate, with a coefficient of determination (R^2) of 0.95.

Ihuoma *et al.* (2021) evaluated UAV multispectral imaging (MSI) and data from PlanetScope and Sentinel-2 for ETa prediction in southeastern Canada, reporting strong correlations between Kc and NDVI ($R^2 = 0.98$ for Sentinel-2; $R^2 = 0.78$ for PlanetScope). Similarly, Niu *et al.* (2022) demonstrated a significant correlation between UAV-derived NDVI and lysimeter-measured Kc in a pomegranate orchard, achieving $R^2 = 0.975$ (Root Mean Square Error [RMSE] = 0.05) with linear regression and a superior $R^2 = 0.995$ (RMSE = 0.046) with a Stochastic Configuration Network model, highlighting UAVs' potential for precise water management.

3.1.5 Research objectives and methodological framework

This research assesses RS-based ET-VI methodologies over a sugarcane field in the Swayimane smallholder farming area in the eastern coastal region of rural South Africa. While most studies establish a regression relationship between Kc and VIs to estimate ETa (Wright, 1982; Hunsaker *et al.*, 2003; Gontia and Tiwari, 2009; Er-Raki *et al.*, 2013; Niu *et al.*, 2020b), this study advances these methods by developing a machine learning (ML) model that correlates in-situ Kc with NDVI values for improved ETa estimation. In addition, five of the six approaches employed in this study substitute VIs for Kc, reducing reliance on in-situ ETa measurements. Following the methodology by Abbasi *et al.* (2023), the comparative evaluation focuses on NDVI, scaled NDVI (NDVIscaled), Kc-adjusted NDVI (NDVIKc), EVI, and EVI2. To the best of available knowledge, this methodology has been applied only twice (Abbasi *et al.*, 2023; Woldemariam *et al.*, 2024), and neither study examined smallholder farms or exclusively utilised UAV data. By leveraging UAV-derived data, this research enriches the limited knowledge of these methodologies and demonstrates their potential for enhancing ETa estimation in smallholder farming systems.

Consequently, the study endeavours to attain the objectives below:

i. Develop a predictive model to establish the correlation between in-situ Kc measurements and NDVI values by applying advanced ML methodologies.

ii. Evaluate RS-derived ET-VI techniques by conducting a comparative assessment of five VIs: NDVI, NDVIscaled, NDVIKc, EVI and EVI2 for estimating ETa vis-à-vis measurements from a ground-based EC flux tower.
iii. Conduct a comprehensive assessment of the previously mentioned VI-based methodologies (objectives i and ii) to determine the most suitable approach for implementation in smallholder agriculture.

3.2 Methodology

3.2.1 Study site description

Data collection for this study was conducted on a sugarcane field within the communal area of Swayimane, located in KwaZulu-Natal, South Africa (29°31′24″ S; 30°41′37″ E), spanning from July 2023 to May 2024 (Figures 3.1 and 3.2). This geographic region falls under the jurisdiction of the uMshwathi Local Municipality and encompasses an approximate area of 36 km^2 (Basdew *et al.*, 2017). The residents of Swayimane predominantly engage in semi-subsistence agricultural practices, which constitute a vital source of sustenance, livelihood, and food security (Brewer *et al.*, 2022). The prevalent crop varieties in this locale encompass white and yellow maize, sugarcane, tomatoes, taro (amadumbe), and sweet potatoes (Brewer *et al.*, 2022; Kapari *et al.*, 2024). Agricultural plots are typically managed using manual methods, such as hand-weeding and applying herbicides via knapsack sprayers, while the harvesting process commonly entails manual, labour-intensive techniques (Brewer *et al.*, 2022). Presently, most smallholder farmers in this region rely on rainfed agriculture (Kapari *et al.*, 2024). Given the projected increase in droughts and intermittent flooding, threatening food security and livelihoods (Adaptation Fund, 2014; Mahomed *et al.*, 2021), farmers may need to adopt irrigation practices to maintain crop productivity.

Figure 3.1 Photographs depicting the smallholder sugarcane field: (a) ground-level perspective, (b) aerial viewpoint, and (c) bird's-eye view of EC flux tower.

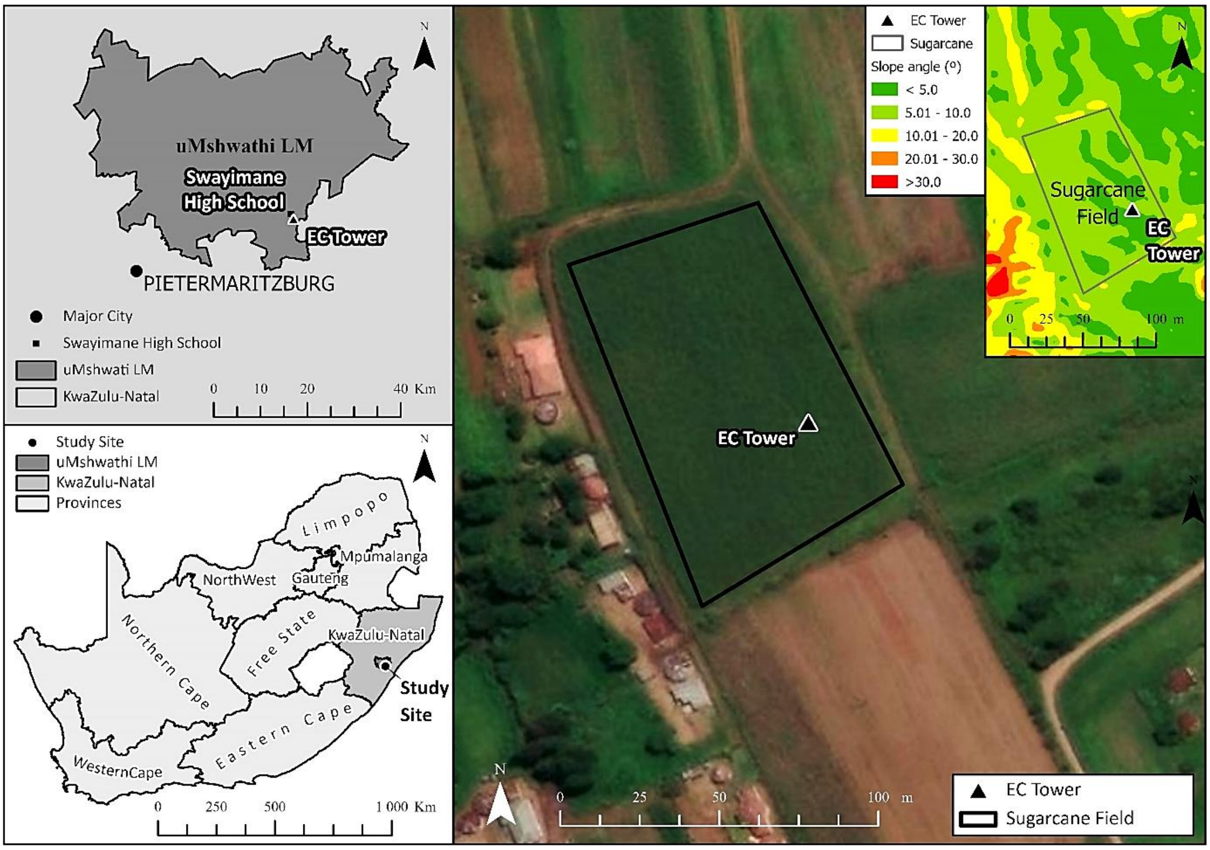

Figure 3.2 Study area map of the smallholder sugarcane field in Swayimane, KwaZulu-Natal, South Africa.

An Automatic Weather Station (AWS) (Climavue 50, Campbell Scientific, Logan, UT, USA) that continuously records weather conditions was situated at a high school near the study site. Due to the proximity of the AWS to the smallholder farm (approximately 1.05 km), it was deemed suitable for recording meteorological conditions at the study site. During data collection, Swayimane had an average daily air temperature of 17.85 °C and a total rainfall of 1190.46 mm. In addition, the average wind speed, relative humidity, and solar irradiance were measured at 1.86 m s^{-1}, 80.45%, and 13.69 MJ m^{-2}, respectively. The study site had also been instrumented with a meteorological flux tower equipped with sensors for measuring the various components of the shortened energy balance equation as well as meteorological variables, including precipitation (mm), wind speed (m s^{-1}), solar irradiance (MJ m^{-2}), and air temperature (˚C) inter alia. Moreover, these measurements were conducted over a small-scale sugarcane field characterised by sloping terrain, with elevations ranging from 843.24 to 850.95 m and encompassing an area of 7253.74 m^2 (ESRI, 2024).

3.2.2 Sugarcane growth stages

This study reviewed existing literature to substantiate the rationale behind delineating periods assigned to individual stages within the sugarcane growth cycle, a necessity arising from the absence of specific cultivar information (Table 3.1). The sugarcane ratoon crop underwent successive harvests, commencing on November 30, 2022, and concluding on May 29, 2024, covering a total growth cycle spanning 18 months (547 days). The crop traversed developmental phases throughout this cycle, including germination (G), tillering (T), stalk elongation (SE), and maturation (M). The ETa estimation measurements concentrated on the SE and M stages as the canopy became well-developed and conducive for RS studies starting on July 1, 2023. Nonetheless, a description of the entire growth cycle provides contextual understanding.

3.2.2.1 Germination

In ratoon cropping, new shoots emerge from the buds at the nodes of the residual underground stalk following harvest (Meyer *et al.*, 2011; Stoller, 2024). The G phase begins with harvest activities and ends with the shoots' emergence above the soil surface, typically lasting up to 30 days, depending on environmental conditions (Stoller, 2024).

3.2.2.2 Tillering

During the T phase, buds from the primary shoot generate 6-8 secondary shoots, known as tillers, which may produce additional tertiary shoots until the maximum tiller count is achieved (Stoller, 2024). This phase lasts from primary shoot emergence to the attainment of peak tiller population, occurring approximately 90 to 120 days post-planting, and is influenced by cultivar variation and ambient temperature (Inman-Bamber, 1994; Smit and Singels, 2006).

3.2.2.3 Stalk elongation and maturation

As some tillers undergo senescence due to resource competition, others develop into harvestable stalks, reaching a stable stalk count characteristic of the cultivar (Martins *et al.*, 2016). Stalk elongation, observed after the emergence of seven or eight leaves, occurs over approximately 270-300 days (Zhou *et al.*, 2003; Srivastava and Rai, 2012). Towards the end of the SE phase, a decline in growth rate leads to sucrose accumulation in the stalks (Meyer *et al.*, 2011). The M period coincides with SE and is influenced by factors such as crop flowering, ripening agent application, and water stress induction (drying-off) (Gosnell and Lonsdale, 1974; Rostron, 1985; Inman-Bamber, 2004; Carr and Knox, 2011; Rossler, 2013).

Table 3.1 Key phenological stages of sugarcane growth.

Growth stage	Crop cycle (days)	Corresponding dates (D/M/Y)	Crop height (m)	Figure
Germination	0 – 30	01/12/2022 – 30/12/2022	0 – 0.2	
Tillering	30 – 120	31/12/2022 – 30/03/2023	0.2 – 1.6	
Stalk Elongation	120 – 390	31/03/2023 – 25/12/2023	1.6 – 2.5	
Maturation	390 – 547	26/12/2023 – 29/05/2024	2.5 – 4.0	

3.2.3 Crop water use

This section outlines critical variables related to crop water use: ETa, ETo, and Kc. Understanding these variables is essential for developing methodologies to assess water consumption in small-scale sugarcane cultivation. A firm grasp of ETa, ETo, and Kc enables researchers and practitioners to implement effective ground-based and RS techniques for quantifying and managing water requirements, contributing to sustainable agricultural practices and efficient water resource management.

3.2.3.1 Reference evapotranspiration

Determining water use coefficients throughout a crop's growth cycle relies significantly on ETo (Allen *et al.*, 1998). Reference ET represents the rate at which water evaporates from a hypothetical reference surface (Paredes *et al.*, 2018). This surface consists of a theoretical grass cover uniformly measuring 0.12 m in height, with a fixed daily canopy resistance $r_s = 70$ s m^{-1} and an albedo of 0.23 (Paredes *et al.*, 2018). Notably, the reference surface is assumed to maintain optimal moisture levels (i.e., not lacking water) and to be well-managed (Allen *et al.*, 1998). The Penman-Monteith equation (Monteith, 1965) is the preeminent method advocated for computing ETo (in mm day^{-1}) (Chimonyo *et al.*, 2016; Roby *et al.*, 2017).

$$\mathrm{ETo} = \frac{0.408\Delta(R_n - G) + \gamma \frac{900}{T + 273} u_2(e_s - e_a)}{\Delta + \gamma(1 + 0.34u_2)} \tag{3.2}$$

Where Δ represents the slope of the saturated vapour pressure curve in units of kPa ºC^{-1}, Rn represents the net radiation in (MJ m^{-2} day^{-1}), G represents the soil heat flux in (MJ m^{-2} day^{-1}), γ represents the psychrometric constant in (kPa ºC^{-1}), T represents the air temperature in (ºC), u_2 represents the wind speed in units of m s^{-1}, e_s represents the saturated vapour pressure in (kPa), and e_a represents the actual vapour pressure in (kPa). ETo was calculated for the crop analysis period from July 1, 2023, to May 15, 2024, using the Penman-Monteith equation (Equation 3.2) (Allen *et al.*, 1998). Data were collected half-hourly from instruments on the meteorological flux tower at the study site in Swayimane and aggregated into hourly and daily time steps to facilitate Kc computation and enable comparative analysis with daily ET-EC (ET calculated using the EC system).

3.2.3.2 Actual evapotranspiration

Due to the underlying processes' intricate interplay, the individual assessment of crop transpiration, soil water evaporation, and interception loss remains challenging. Collectively, these processes contribute to the combined entity known as ETa. Consequently, ETa is quantified as an integrated measure that is fundamental in determining Kc across various crop types. The predominant methodologies for estimating ETa, as advocated by authoritative sources, entail using micrometeorological techniques such as surface renewal, EC, and surface layer scintillometry (Kunz *et al.*, 2015; Chimonyo *et al.*, 2016; Mbangiwa *et al.*, 2019).

In this study, the estimation of ETa was carried out utilising the EC method, which stands as the predominant and reliable technique for quantifying ETa in the scientific literature (Snyder *et al.*, 2008; Castellví and Snyder, 2009; Kelley and Higgins, 2018; Cui and Chui, 2019; Morán *et al.*, 2020; Gray *et al.*, 2022; Lu *et al.*, 2022; Peddinti and Kisekka, 2022; Wagner *et al.*, 2022). The EC system comprises two integral components: an anemometer for measuring wind speed and direction and an Infrared Gas Analyser (IRGA) for analysing gas concentrations, notably water vapour, in the atmosphere (Savage *et al.*, 2017). The concurrent measurement of vertical air velocity and water vapour concentration enables the computation of ETa as the vertical flux of water vapour (Ghiat *et al.*, 2021). For detailed information regarding the instrumentation and experimental setup, readers are referred to section 3.2.4.1.

3.2.3.3 Crop coefficients

The crop coefficient (Kc) serves as a metric in evaluating the water requirements of crops across diverse developmental stages. It is defined as the ratio of the ETp to the ETo (Allen *et al.*, 1998), as delineated in Equation 3.3. Furthermore, Kunz *et al.* (2015) assert that Kc values acquired from international literature may not adequately capture the nuanced growing conditions specific to a given locality (Ortega-Farias *et al.*, 2009; Kunz *et al.*, 2015). Consequently, an investigation was undertaken to ascertain Kc values tailored specifically for sugarcane cultivation. These coefficients were derived using hourly ETo and ET-EC data to calculate hourly Kc values, spanning 1 July 2023 to 15 May 2024. Subsequently, an arithmetic mean was employed to derive the daily temporal resolution of Kc for rainfed sugarcane. Nevertheless, it is essential to acknowledge that Kc values were established under atypical (i.e., non-irrigated) circumstances (Gokool *et al.*, 2017; Drechsler *et al.*, 2022; Ippolito *et al.*, 2022; Mukiibi *et al.*, 2023; Pereira *et al.*, 2023; Nagy *et al.*, 2024) since the crop may have encountered water stress during its growth period.

$$\mathrm{Kc} = \frac{\mathrm{ETc}}{\mathrm{ETo}} \tag{3.3}$$

3.2.4 Field preparation and management

In late November 2022, following the ratoon crop's harvest, debris clearance and weed control were achieved through controlled burning. Although the new crop emerged from the existing root system, soil amelioration was necessary to create an optimal growth milieu. This involved shallow tillage using manual implements such as hand hoes to reduce soil compaction and incorporate organic amendments, with local indigenous labourers from the Swayimane community engaged in these preparatory activities. Applying a balanced NPK fertiliser from Omnia Nutriology enhanced crop vigour and productivity (Omnia Nutriology, 2022). This formulation contained 6.7% nitrogen, 10% phosphorus, and 13.3% potassium, ensuring the crops received essential nutrients for robust development and improved yield potential.

Effective weed management was essential to minimise competition with emerging sugarcane shoots. Mechanised approaches, particularly herbicide application, were employed in the early growth to control weed proliferation. The herbicide 'Gramazone,' produced by Syngenta (Syngenta, 2024), was used to suppress annual grasses and broadleaf weeds in the field. Following these land preparation and management practices, systematic monitoring of meteorological parameters and ETa dynamics was initiated, covering the sugarcane growth cycle. Data collection began seven months post-planting, from July 1, 2023, to May 15, 2024. The subsequent discussion will present a detailed account of the field data collection methodologies and measurement procedures.

3.2.4.1 In-situ data

Sugarcane water use was measured using the EC approach. A 4-metre meteorological flux tower was installed within the sugarcane field, with instrumentation oriented to the prevailing wind direction (Figure 3.3a). These instruments, outlined in Appendix A, enabled the calculation of the shortened energy balance equation. The installation of the meteorological flux tower adhered to stringent eligibility criteria to ensure methodological rigour, including (a) representativeness in terms of spatial variability, topography, and land use; (b) homogeneity regarding land cover; (c) fetch distance; and (d) sensor heights.

The EC system comprised an integrated open-path infrared gas analyser and 3D sonic anemometer (IRGASON, Campbell Scientific, Logan, UT, USA) mounted at a height of approximately 2.00 m above the plant canopy and capturing data at a 10 Hz observation rate, enabling direct measurement of latent heat flux (LE). Sensible heat flux (H) was calculated using a 3D sonic anemometer (CSAT3A, Campbell Scientific, Logan, UT, USA). A net radiometer (CNR4-L, Campbell Scientific, Logan, UT, USA) was incorporated to compute net radiation (Rn). At the same time, soil heat flux (G) was measured in row and interrow locations using two soil heat flux plates (HFPs) at a depth of 0.06 m (HFP01-L, Hukseflux, Delft, The Netherlands) (Figure 3.3b). Each location also included four soil averaging thermocouples (TCAV, Campbell Scientific, Logan, UT, USA) for monitoring soil temperature at depths of 0.04 and 0.08 m, as well as a water content reflectometer (CS616, Campbell Scientific, Logan, UT, USA) for measuring volumetric water content in the top 0.08 m of soil. Additional measurements at 0.30, 0.60, and 0.90 m depths were obtained using the CS616.

Air temperature and relative humidity were recorded using two integrated probes (H2CS3, Campbell Scientific, Logan, UT, USA) positioned near the IRGASON, supplemented by fine-wire thermocouples for additional temperature data. A rain gauge (TE525MM-L, Campbell Scientific, Logan, UT, USA) was mounted on the structure, and an infrared radiometer (IRR, Apogee SI-111, Apogee Instruments Inc., Logan, UT, USA) was installed to monitor canopy temperature. All instruments underwent calibration before deployment to ensure accuracy. Data loggers (CR3000 and CR1000, Campbell Scientific, Logan, UT, USA) collected measurements at 30-minute intervals (Figure 3.3c). The Easy Flux™ DL software facilitated the acquisition of fully corrected fluxes from the EC system, including CO_2, LE, H, G, and momentum, integrating optional energy balance sensors.

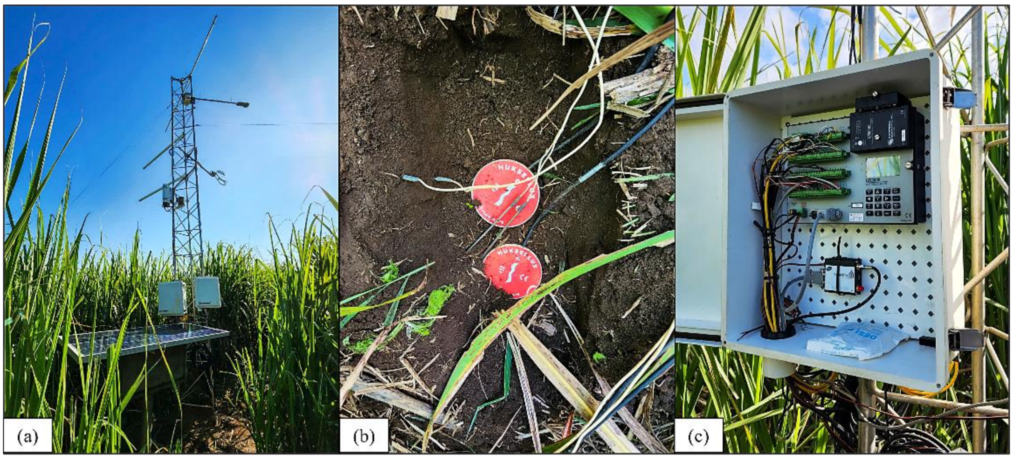

Figure 3.3 (a) EC system, (b) installation of the soil HFPs, and (c) CR3000 datalogger.

Data processing procedures were performed using Microsoft Excel, following a structured approach. A time-based filter was applied to the flux data, including only measurements taken between 6:00 AM and 6:00 PM (SAST), as daytime solar radiation is essential for the energy balance equation. Negative values for Rn and G were excluded, particularly in instances where G exceeded Rn. Additionally, a correction factor for G was applied from September 16 to October 26, 2023, due to missing data, determined by the mean ratio of G to Rn calculated between July 1 and September 15, 2023, which yielded a value of 6.64%. Data corresponding to quality assurance grades 6-9 were excluded (Savage *et al.*, 2017).

NDVI measurements were obtained from sensors installed on the tower at a height of approximately 2.00 m above the plant canopy, beginning February 3, 2024, and averaged at 10- and 30-minute intervals (Figures 3.4a and 3.4b). Data were downloaded from the measurement site using a 3G cellular network and published online to monitor system status. Email alerts were configured to address low battery voltages and communication failures, thereby minimising data loss. Two 100 Ah batteries connected in parallel powered the measurement systems via a solar panel. Precipitation (mm), wind speed (m s^{-1}), solar irradiance (MJ m^{-2}), and air temperature (°C) were recorded at the nearby AWS (Climavue 50, Campbell Scientific, Logan, UT, USA) located at a local high school for backup purposes (Figure 3.4c).

Figure 3.4 (a) The NDVI sensor setup in the laboratory, (b) its installation at the study site, and (c) the AWS at the high school in Swayimane.

3.2.5 UAV: DJI Matrice 300 and MicaSense Altum camera

The DJI Matrice 300 (M-300) platform, equipped with a MicaSense Altum camera and a downwelling light sensor (DLS-2), enabled the capture of very high spatial resolution imagery of the smallholder cropland (Figures 3.5a and 3.5b) (Vélez *et al.*, 2023; Khormizi *et al.*, 2024). The four-rotor M-300, featuring vertical take-off and landing (VTOL) capabilities, is well-suited for aerial operations in rural areas adjacent to populated regions (Brewer *et al.*, 2022). Notable features include a transmission range of up to 15 kilometres, a maximum operational altitude of 7,000 m, obstacle detection and avoidance systems, flight path planning functions, and an integrated GPS tracker. With the Altum camera, the M-300 achieves a maximum flight duration of approximately 42 minutes and reaches speeds of up to 27 m s^{-1} (Brewer *et al.*, 2022).

The MicaSense Altum camera integrates optical and thermal infrared functionalities (Zarzar *et al.*, 2020). It encompasses five high-resolution narrow spectral bands: blue, green, red, red-edge, and near-infrared, along with a radiometric longwave infrared thermal sensor (Table 3.2) (Seiche *et al.*, 2024). It features a global shutter mechanism that ensures high spatial resolution and alignment at a capture rate of up to one image per second (Hutton *et al.*, 2020). The optical bands deliver a sensor resolution of 2064 × 1544 pixels. The corresponding ground sample distance (GSD) at a flying height of 120 m measures 0.052 m per pixel (Brewer *et al.*, 2022). Furthermore, the thermal infrared camera exhibits a sensor resolution of 160 × 120 pixels, with a GSD of 0.81 m per pixel at 120 metres (Brewer *et al.*, 2022).

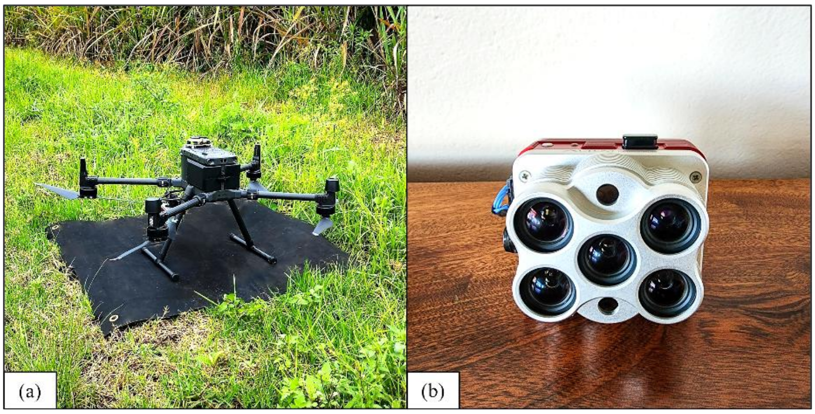

Figure 3.5 (a) DJI-M300 series platform, (b) MicaSense Altum camera.

Table 3.2 Specifications of the MicaSense Altum camera (after Brewer *et al.*, 2022).

Band	Spectral colour	Band centre/range (nm)	GSD at a flying height of 120 m (m pixel^{-1})
1	Blue	475	0.052
2	Green	560	0.052
3	Red	668	0.052
4	Red Edge	717	0.052
5	Near-infrared (NIR)	842	0.052
6	LWIR thermal infrared	8000 - 14000	0.81

3.2.5.1 UAV: image acquisition and processing

The flight area was delineated on the UAV console to define the geographical boundaries of the Swayimane study area (Figure 3.6a), enabling semi-autonomous flight operations (refer to Table 3.3). UAV flights were scheduled on days with minimal cloud cover to optimise data acquisition conditions. A calibrated reflectance panel (CRP) was employed to calibrate the MicaSense Altum camera pre- and post-flight (Figure 3.6b) (Brewer *et al.*, 2022). The CRP, functioning as a radiometric calibration target, is designed to provide consistent reflectance properties across the light spectrum captured by the Altum device (Sibanda *et al.*, 2023). Additionally, it facilitated the acquisition of absolute reflectance values, allowing for comparative data analysis across multiple flights (Kapari *et al.*, 2024). Following each flight, the acquired aerial imagery was processed using Pix4Dfields photogrammetry software (version 1.8.0, Pix4D Inc., San Francisco, California, USA). This workflow involved radiometric corrections and the generation of mosaics, resulting in the creation of an orthomosaic image exported in GeoTIFF format.

Table 3.3 Flight specifications for the DJI-M300.

Parameters	Specifications
Altitude	100 m
GSD	0.07 m pixel^{-1}
Speed	10 m s^{-1}
Flight duration	36 m 32 s
Image overlap	80%
Camera system	MicaSense Altum

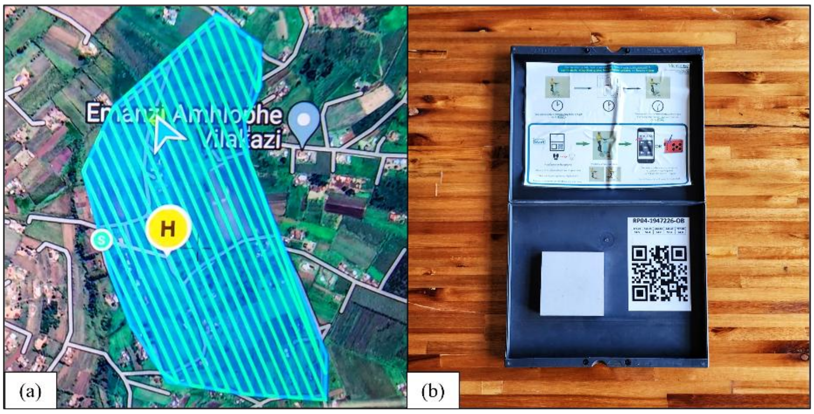

Figure 3.6 (a) DJI-M300 flight plan, (b) MicaSense Altum CRP.

3.2.6 Google Earth Engine

Google Earth Engine (GEE) is a cloud-based platform characterised by its user-friendly interface and extensive computational resources, designed for processing large volumes of geospatial data (Senay *et al.*, 2022). Importantly, GEE enables users to generate systematic data products or develop interactive applications utilising their algorithms without requiring expertise in application development or web programming (Gorelick *et al.*, 2017). This investigation evaluates the effectiveness of GEE's advanced image processing capabilities for analysing high-resolution multispectral imagery obtained from UAVs in small-scale agricultural operations. A data visualisation and processing tool was developed and utilised within GEE to compute spatially explicit NDVI, EVI, and EVI2 across the study site, using a

UAV image collection uploaded to the platform. Furthermore, time-series data were extracted with this tool for subsequent analysis; comprehensive details are provided in Section 3.2.8.

3.2.7 The empirical relationship between in-situ crop coefficients and Normalised Difference Vegetation Index

The utility of NDVI in assessing plant health, along with its ease of computation and non-destructive application, has facilitated its adoption as a viable surrogate for Kc within agricultural settings (Tucker and Sellers, 1986; Sellers *et al.*, 1992). The NDVI measurements were collected from February 3 to May 15, 2023, utilising an NDVI sensor (Apogee Instruments, Inc., Logan, UT, USA) mounted on the meteorological flux tower at 10- and 30-minute intervals (see Section 3.2.4.1). This index is calculated by comparing the reflectance measurements of the vegetation canopy in the near-infrared (NIR) and red (R) spectral bands (Rouse *et al.*, 1973; Kamble *et al.*, 2013). The mathematical formulation for this VI is as follows:

$$\mathrm{NDVI} = \frac{\mathrm{NIR} - \mathrm{R}}{\mathrm{NIR} + \mathrm{R}} \tag{3.4}$$

Establishing an empirical correlation requires ground-truth data that provide measured Kc values to relate NDVI and Kc. Therefore, daily Kc measurements were acquired via sensors on the meteorological flux tower, concurrently paired with corresponding daily NDVI values.

3.2.7.1 In-situ crop coefficients and Normalised Difference Vegetation Index with machine learning

This study aimed to evaluate the efficacy of ML algorithms (MLAs) in predicting the Kc from the NDVI. To support this objective, a comprehensive literature review was conducted to identify prevalent MLAs (Gangat *et al.*, 2020; Yamaç and Todorovic, 2020; Han *et al.*, 2021; Chaudhary *et al.*, 2022; Kibirige *et al.*, 2023). Methodologically, in-situ Kc and corresponding NDVI data were imported into RStudio from a Microsoft Excel file. The classification and regression training (Caret) package and its extension caretEnsemble (Mayer, 2013) were utilised to establish the ML-based models (MLBMs) (Figure 3.7). The MLAs included in the analysis were Random Forest (RF), Recursive Partitioning (RPART), Generalised Linear Models (GLM), k-Nearest Neighbours (kNN), and Support Vector Machines with a radial kernel (SVMRadial).

The R programming environment facilitated the assessment of individual model performance through a rigorous ten-fold cross-validation procedure, repeated ten times. Resampling results were synthesised after validation, and performance metrics were visually depicted. The outputs of individual models were subsequently combined to leverage their unique strengths and enhance predictive accuracy, resulting in an ensemble model that utilised NDVI values to predict Kc. The correlation between predicted and actual Kc values was assessed, with evaluation metrics including R^2, RMSE and MAE. Monthly averages of Kc were computed from predicted values and subsequently multiplied by daily ETo to derive daily ETa. Finally, predicted daily ETa values were compared against ET-EC using the aforementioned performance metrics.

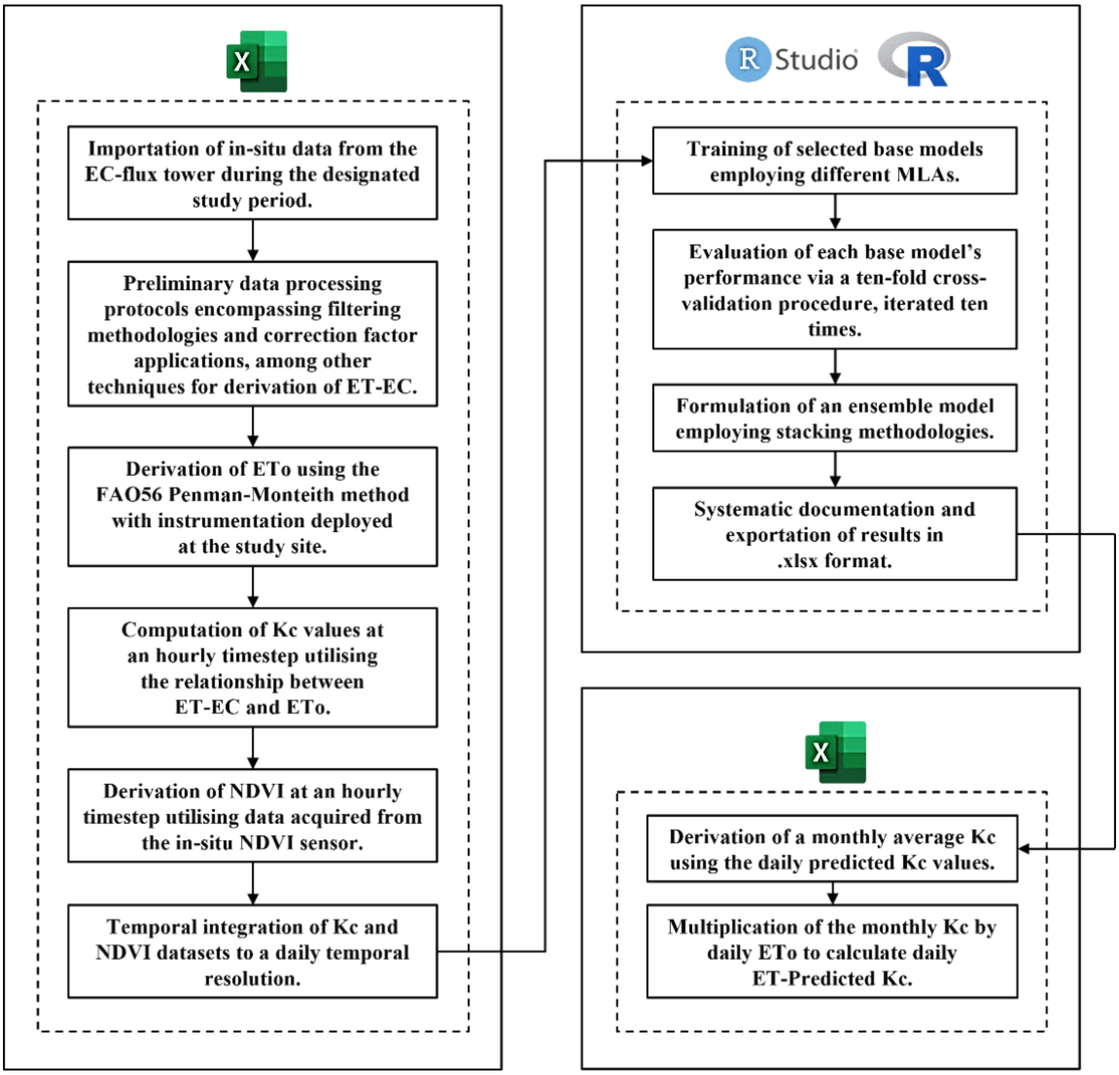

Figure 3.7 Conceptual flow diagram of the methodology for data acquisition, processing, and ML-based NDVI-Kc modelling.

3.2.8 Vegetation index-based actual evapotranspiration estimation from UAV imagery and GEE processing

UAV imagery was processed using Pix4Dfields photogrammetry software (version 1.8.0, Pix4D Inc., San Francisco, California, USA). In total, 15 orthomosaic GeoTIFF files (representing UAV flights conducted between July 2023 and March 2024) were created and resampled to a spatial resolution of 0.07 m for further processing. To facilitate quick and easy analysis, a data processing and visualisation app was developed in GEE to visualise and extract the data necessary for ETa estimation. The UAV-derived data and the visualisation app can be accessed at: https://shaedengokool.users.earthengine.app/view/swayimane-smallholder-farm-crop-monitoring-app-beta-version.

This investigation employed three distinct NDVI-based proxies—NDVI, NDVIscaled, and NDVIKc—as well as two EVI-based proxies, ET-EVI and ET-EVI2, to derive Kc values for estimating ET-NDVIs and ET-EVIs. According to the FAO56 methodology, the computation of ETa involves multiplying the Ks, Kc, and ETo (Allen *et al.*, 1998). Consequently, the VIs serve as proxies for the product of Ks and Kc (Equation 3.5) (Abbasi *et al.*, 2023):

$$\mathrm{ETa} = \mathrm{Kc} \times \mathrm{Ks} \times \mathrm{ETo} \text{ or} \tag{3.5}$$

$$\mathrm{ETa} = \mathrm{VI} \times \mathrm{ETo}$$

Under sufficient moisture conditions and the absence of stress, the maximum Kc may approach 1.2, whereas NDVI is limited to a maximum of 1 (Abbasi *et al.*, 2023). Therefore, adjustments to the NDVI values are necessary to align them with the Kc range (Equation 3.6). Furthermore, numerous studies have documented a generalisable association between NDVI and Kc across various crops (Equation 3.7) (Belmonte *et al.*, 2005; D'Urso, 2010; Akdim *et al.*, 2014).

$$\mathrm{NDVIscaled} = 1.2 \times \mathrm{NDVI} \tag{3.6}$$

$$\mathrm{NDVIKc} = (1.25 \times \mathrm{NDVI}) + 0.2 \tag{3.7}$$

The subsequent step involved retrieving VI values from the GEE Application. However, it was observed that the mean NDVI values from two drone flights conducted on September 28 and October 26, 2023, were anomalously low at 0.31 and 0.26, respectively. Additionally, RGB images from these flights exhibited visible abnormalities. Consequently, these flights were excluded from further analysis, resulting in a final collection of 13 images.

Due to the bi-weekly collection of UAV images, the UAV-derived VI values were aggregated into monthly averages based on the respective VI values obtained each month. These monthly UAV-derived VIs served as inputs for the various VI-based models to estimate monthly Kc. In line with the methodology outlined by Gokool *et al.* (2024), the monthly Kc estimates were utilised alongside daily ETo to calculate daily ETa using each of the five models.

The EVI and EVI2 were calculated using the following equations:

$$\mathrm{EVI} = 2.5 \times \left(\frac{\mathrm{NIR} - \mathrm{RED}}{\mathrm{NIR} + 6\mathrm{RED} - 7.5\mathrm{BLUE} + 1}\right) \tag{3.8}$$

$$\mathrm{EVI2} = 2.5 \times \left(\frac{\mathrm{NIR} - \mathrm{RED}}{\mathrm{NIR} + \mathrm{RED} + 1}\right) \tag{3.9}$$

Subsequently, five iterations of ETa were computed by multiplying pixel-specific estimates of Kc values (NDVI, NDVIscaled, NDVIKc, EVI, and EVI2) with the corresponding ETo values, as specified in Equations (3.10) through (3.14) (see Figure 3.8).

$$\mathrm{ET} - \mathrm{NDVI} = \mathrm{ETo} \times \mathrm{NDVI} \tag{3.10}$$

$$\mathrm{ET} - \mathrm{NDVIscaled} = \mathrm{ETo} \times \mathrm{NDVIscaled} \tag{3.11}$$

$$\mathrm{ET} - \mathrm{NDVIKc} = \mathrm{ETo} \times \mathrm{NDVIKc} \tag{3.12}$$

$$\mathrm{ET} - \mathrm{EVI} = \mathrm{ETo} \times \mathrm{EVI} \tag{3.13}$$

$$\mathrm{ET} - \mathrm{EVI2} = \mathrm{ETo} \times \mathrm{EVI2} \tag{3.14}$$

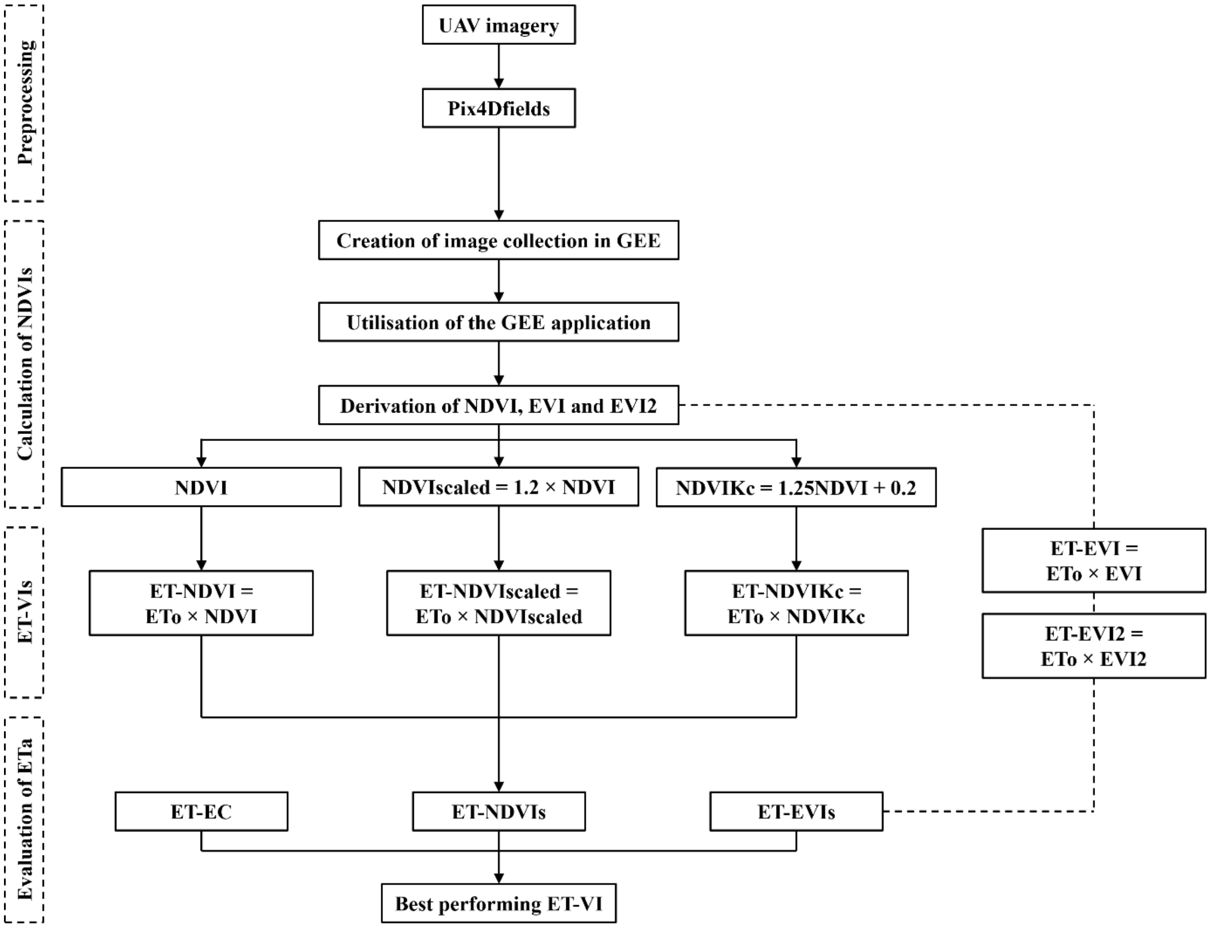

Figure 3.8 Conceptual flow diagram delineating the sequential processes involved in deriving ET-VIs.

3.2.9 Evaluation of actual evapotranspiration models based on predicted crop coefficients and vegetation index products

Before evaluating the accuracy of the VI-based ET estimates, the uncertainty in the in-situ ET-EC measurements was established through an assessment of energy balance closure (EBC) (Section 3.3.1). Subsequently, a comparative analysis was conducted to assess daily ETa estimates from ET-Predicted Kc and ET-VIs. Due to differences in data collection periods, results are presented separately: ET-Predicted Kc versus ET-EC (Section 3.3.2) and ET-VIs versus ET-EC (Section 3.3.3). Time series evaluations were employed to assess the efficacy of ET-Predicted Kc and ET-VIs in replicating ET-EC trends. Additionally, cumulative ET-EC values were compared to cumulative ET-Predicted Kc and ET-VIs across the respective periods, highlighting the models' ability to replicate ET-EC dynamics and supporting their predictive robustness.

Performance metrics, including R², RMSE, and MAE, were used to evaluate the accuracy of the VI-based ET estimation models. A Shapiro-Wilk normality test was performed to select appropriate statistical tests. Subsequently, Spearman's correlation and Mann-Kendall (MK) nonparametric tests were utilised to detect monotonic trends across the datasets, as supported by prior literature (Hamed and Ramachandra Rao, 1998; Espadafor *et al.*, 2011; Shadmani *et al.*, 2012). Additionally, statistical analysis and visualisation of the ET-VIs were conducted using software packages such as R (Allaire, 2024), SPSS (IBM Corp, 2021), and ArcGIS Pro (ESRI, 2024). These analyses were integral in examining relationships and trends within the datasets, thereby enhancing the understanding of the underlying dynamics of ET processes.

3.3 Results

3.3.1 Assessment of in-situ data quality

The average air temperature within the sugarcane field ranged from 7.3 to 27.9 °C (Figure 3.9). Mean wind velocity was recorded at 2.0 m s^{-1} (Figure 3.9), while the saturated vapour pressure was measured at 2.19 kPa (Figure 3.10). Relative humidity (RH) exhibited notable seasonal variation. Higher RH values were observed during summer months, ranging from 69% to 99%, whereas winter RH values ranged from 38% to 96% (Figure 3.10). Measurements of mean Rn and G yielded values of 6.75 MJ m^{-2} and 0.35 MJ m^{-2}, respectively (Figure 3.11). Cumulative precipitation over the 10-month measurement period totalled 1228 mm, with seasonal variability. Summer months recorded higher precipitation, peaking at 331 mm in December, compared to a maximum monthly accumulation of 11 mm in July during winter (Figure 3.11).

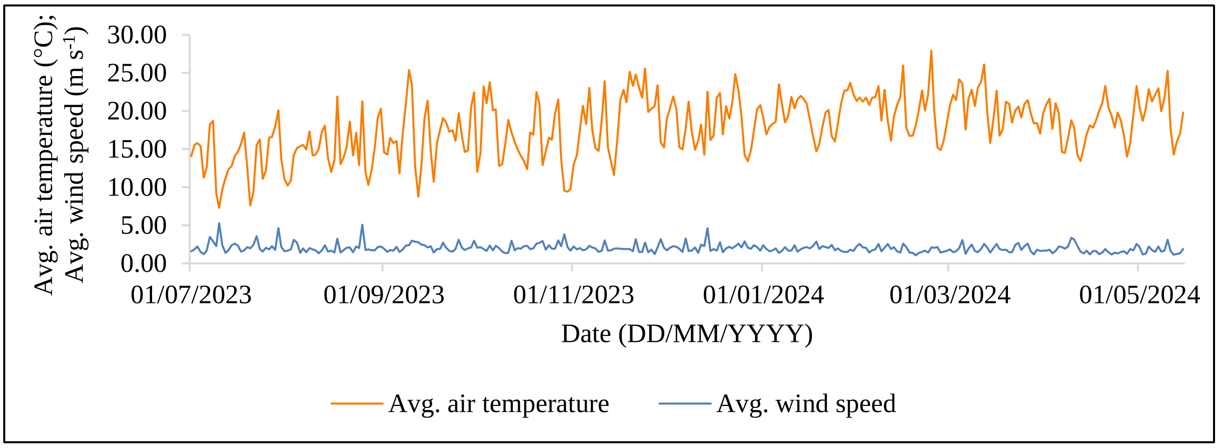

Figure 3.9 Average daily air temperature (°C) and wind speed (m s^{-1}) measured from July 1, 2023, to May 15, 2024.

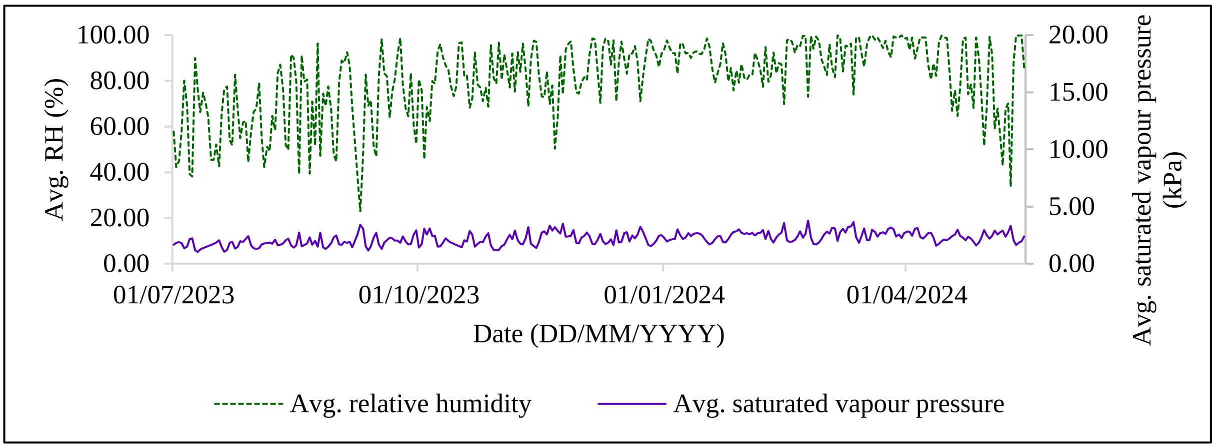

Figure 3.10 Daily averages of RH (%) and saturated vapour pressure (kPa) from July 1, 2023, to May 15, 2024.

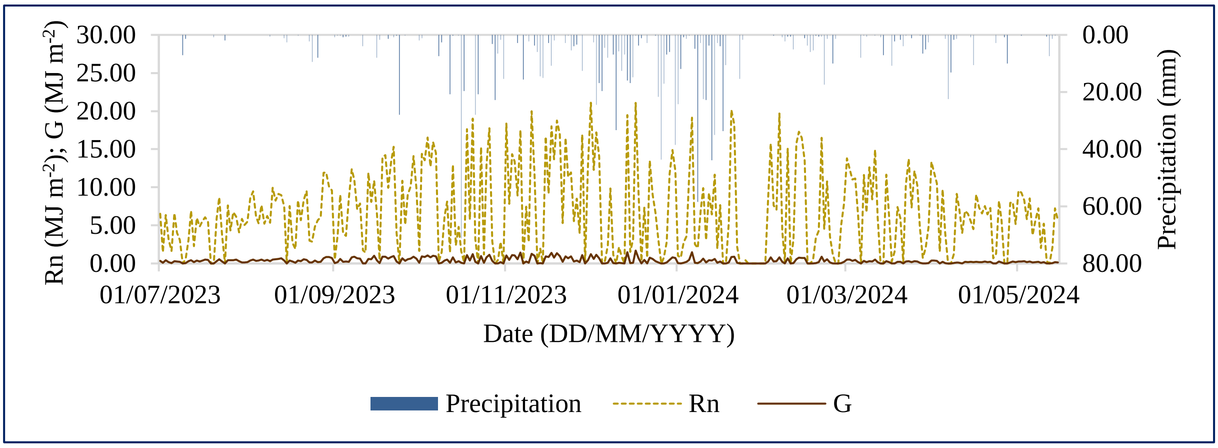

Figure 3.11 Daily mean values of Rn (MJ m^{-2}), G (MJ m^{-2}), and precipitation (mm) from July 1, 2023, to May 15, 2024.

The series analysis reveals a pronounced seasonal trend in ETo and ET-EC (Figure 3.12). ETo consistently surpasses ET-EC across the observation period, with both metrics exhibiting evident seasonal variations. Daily values reach their lowest in June, peak in December, and gradually decrease through May. This cyclical pattern is consistent with expected seasonal climate changes, where warmer temperatures, increased rainfall, and higher solar radiation during summer promote elevated ET rates, while cooler and drier winter conditions suppress them. The persistent difference between ETo and ET-EC, with ETo consistently higher, corresponds to a Kc ranging from 0.39 to 0.52 over the monitoring period (Figure 3.13). This Kc variation indicates changes in crop water requirements and physiological responses to environmental conditions across the SE and M growth stages.

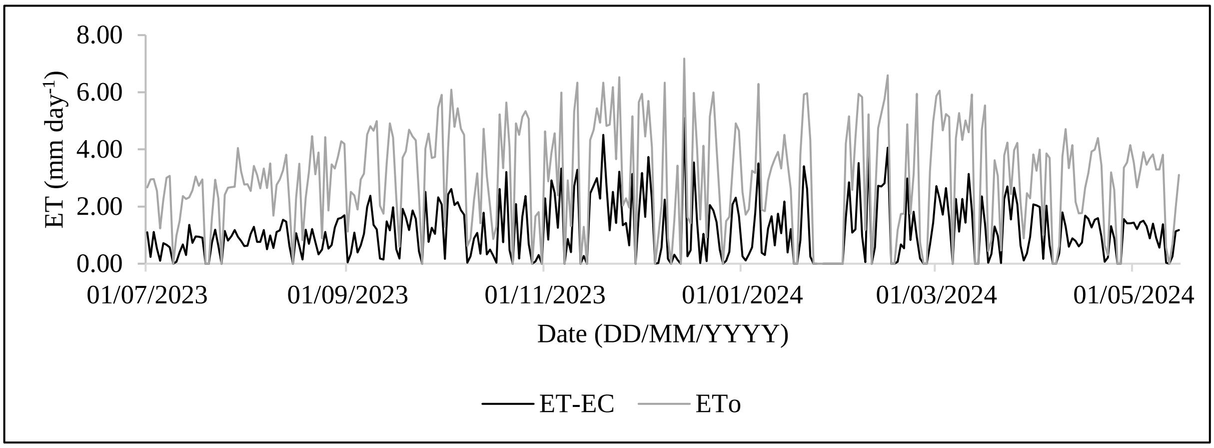

Figure 3.12 Daily ET-EC (mm day^{-1}) with ETo (mm day^{-1}) during the sugarcane growing season.

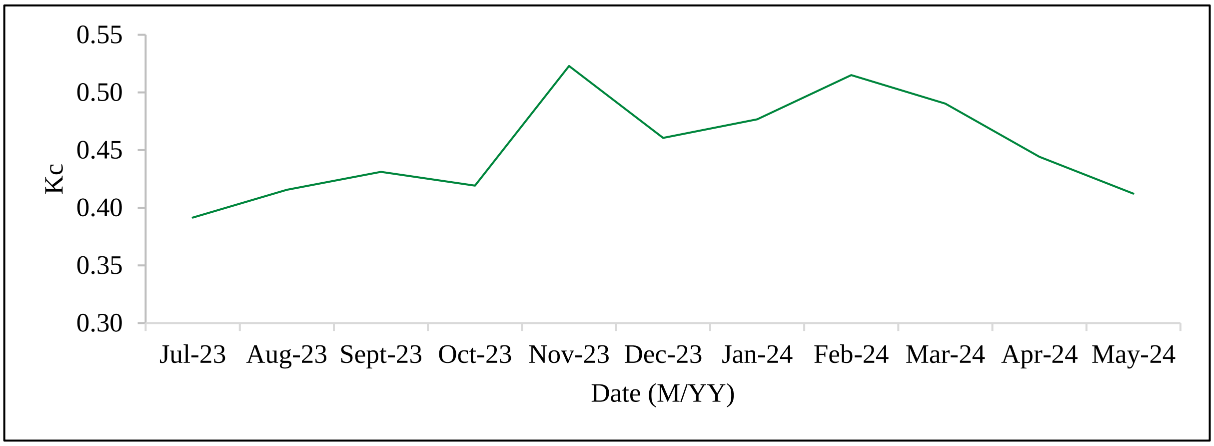

Figure 3.13 Monthly distribution of observed mean Kc values from July 2023 to May 2024.

Hydrological variables of ET-EC and ETo exhibit significant statistical attributes. ET-EC is approximately 588 mm lower than ETo across the entire data collection period and, on average, approximately 2.12 mm day^{-1} lower than ETo. Furthermore, the standard deviation of 0.95 mm day^{-1} for ET-EC reflects moderate variability influenced by environmental factors, vegetation composition, soil moisture content, and potential measurement inaccuracies. In contrast, the standard deviation of 1.51 mm day^{-1} for ETo suggests greater variability in ETo rates throughout the observation period (Table 3.4).

Table 3.4 Summary of daily ET-EC (mm day^{-1}) and ETo (mm day^{-1}) measured during the 2023-2024 growing season at the study site in Swayimane.

	ET-EC	**ETo**
Minimum (mm day^{-1})	0.02	0.31
Maximum (mm day^{-1})	5.09	7.18
Mean (mm day^{-1})	1.30	3.42
Median (mm day^{-1})	1.16	3.35
Std dev (mm day^{-1})	0.95	1.51
Sum (mm)	361.75	949.38

The precision of the EC system in quantifying turbulent fluxes was assessed through energy balance closure (EBC) analysis. Energy balance closure involves a linear regression between turbulent energy fluxes (H + LE) and available energy (Rn - G) (Baldocchi *et al.*, 2000; Twine *et al.*, 2000; Wilson *et al.*, 2002). Jin *et al.* (2022) state that perfect energy balance closure requires the slope of the regression line to equal one and the intercept to be zero. Accordingly, the analyses constrained the intercept to zero (Jin *et al.*, 2022). The findings revealed that turbulent fluxes were approximately 27% and 24% lower than available energy for the 30-minute and daily intervals, respectively (Figure 3.14). These results indicate satisfactory EBC, consistent with previous studies reporting deficits ranging from 10% to 30% (Baldocchi *et al.*, 2000; Twine *et al.*, 2000; Testi *et al.*, 2003; Poblete-Echeverría and Ortega-Farias, 2013). Additionally, R^2 values were 0.98 for the 30-minute timestep and 0.99 for the daily timestep, further supporting the reliability of the measurements.

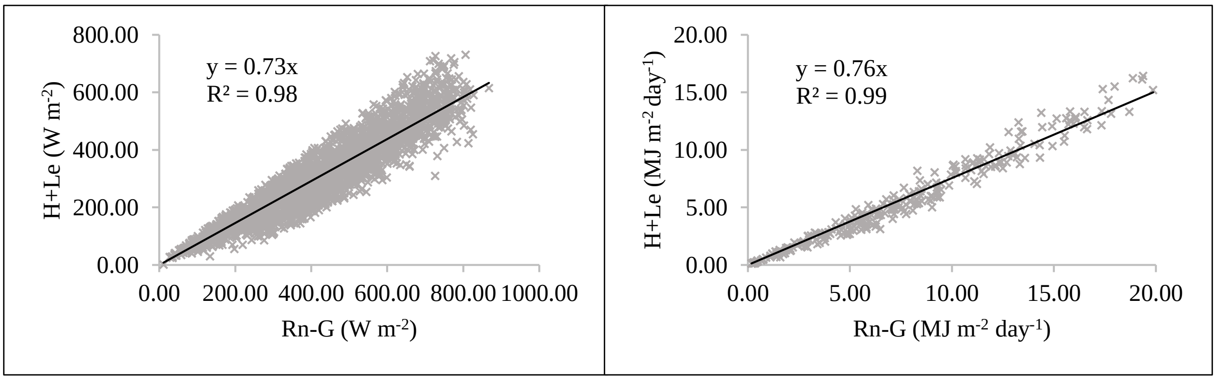

Figure 3.14 Scatter plots of Rn–G vs H+LE from the Swayimane flux tower, showing EBC gradients at 30-minute (left, W m^{-2}) and daily (right, MJ m^{-2} day^{-1}) temporal resolutions.

During the 10.5-month observational period, discernible seasonal variability in ETa was evident, as delineated by fluctuations in the monthly cumulative ET-EC (Figure 3.15). The zenith of monthly observed total ET-EC, amounting to 55 mm, transpired in November 2023. After this, the December and February summer months exhibited levels akin to the November monthly total ET-EC. However, January presented a diminished ET-EC attributable to data loss from 23 January to 2 February 2024. It is postulated that including data from these nine days would render the monthly ET-EC comparable with the other summer months.

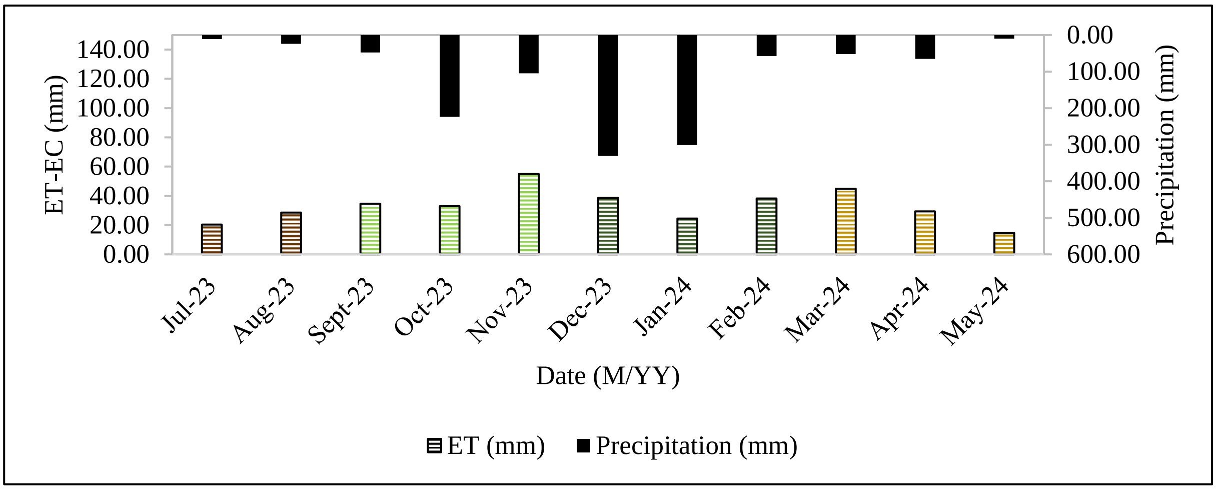

Figure 3.15 Monthly cumulative ET-EC (mm) above the sugarcane canopy and total rainfall, with seasons indicated by colours: dark green (summer), light green (spring), light brown (autumn), and dark brown (winter).

Estimates of energy balance components for sugarcane under rainfed conditions demonstrate variability influenced by several factors, including local climatic conditions, soil type, crop developmental stage, and agronomic practices. Specifically, Rn shows a significant range affected by solar irradiance, cloud cover, and surface reflectance properties, with typical values between 10 and 20 MJ m^{-2} day^{-1} and potentially exceeding these limits. Soil heat flux, which denotes the exchange of thermal energy between the soil and its environment, is influenced by soil moisture content, soil type, and vegetative cover, with expected values ranging from 0.5 to 2 MJ m^{-2} day^{-1} (Figure 3.16).

Latent heat flux, representing the energy expended during ET, typically ranges from 5 to 15 MJ m^{-2} day^{-1}. In contrast, H, which characterises heat transfer through conduction and convection, varies from 1 to 5 MJ m^{-2} day^{-1}. As illustrated in Figure 3.16, the observed fluxes generally align with established acceptable ranges; however, a slight deviation was noted for H, particularly during the summer. As mentioned, a data acquisition interruption occurred from January 23 to February 2, 2024, due to disturbances from avian interference, which resulted in soil accumulation on the 3-D sonic anemometer co-located with the CO_2/H_2O open-path gas analyser (see Appendix B, Figure 7.2).

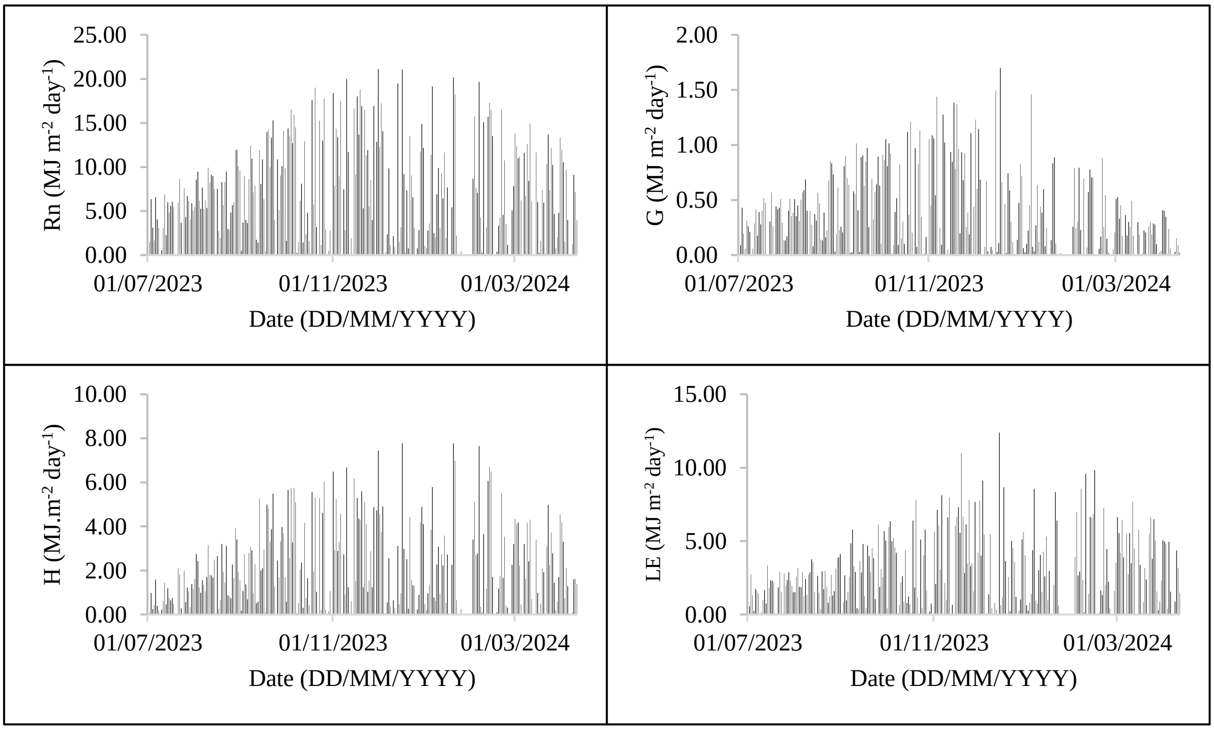

Figure 3.16 (Top left) Rn, (Top right) G, (Bottom left) H, and (Bottom right) LE, all in MJ m^{-2} day^{-1}, showing typical ranges and the temporal dynamics for each energy flux over the SE and M portion of the sugarcane phenological cycle.

3.3.2 Comparative analysis of eddy covariance observed evapotranspiration and crop coefficient model predictions

The ensemble model, utilising the RF algorithm as the meta-model, demonstrated robust predictive performance for ET-Predicted Kc values, as indicated by the performance metrics. The model achieved an RMSE of 0.11, suggesting that, on average, predictions deviate from observed values by this amount. This low RMSE reflects high predictive accuracy with minimal errors. The R^2 was 0.68, indicating that the model explains 68% of the variability in observed ET-Predicted Kc values, signifying a good correlation between the predictors and the target variable. Additionally, the MAE of 0.07 further emphasises the model's precision, representing the average absolute error in predictions.

Figure 3.17 illustrates the daily variations in NDVI recorded in-situ during the specified period. NDVI values ranged from 0.76 to 0.82, with a mean of 0.79. During the M phase of sugarcane, NDVI typically decreases as the crop approaches harvest (Gunnula *et al.*, 2012), reflecting reductions in green biomass and leaf area. However, the values indicate that the sugarcane maintained substantial green biomass and leaf area throughout M. This scenario is typical of well-managed crops with adequate water and nutrient supply, which minimises water stress and promotes sustained photosynthetic activity.

The monthly observed Kc values varied from 0.48 to 0.80 (Table 3.5). The highest observed Kc of 0.80 was recorded in February, indicating elevated water use. Conversely, observed Kc values declined to 0.48 by May, reflecting reduced water use as the growing season progressed. Predicted Kc values ranged from 0.56 to 0.62, with the highest in February. The lower variability of predicted Kc compared to observed values suggests the prediction model may provide a conservative water use estimate. In March, the predicted Kc value closely matched the observed value (0.57 predicted vs 0.58 observed), while the lowest predicted Kc of 0.56 aligned well with observed Kc values in April and May.

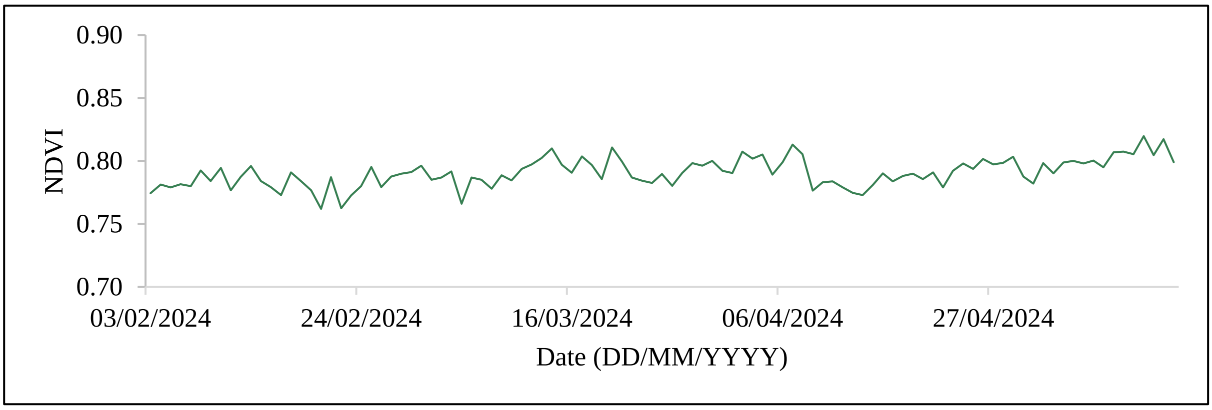

Figure 3.17 The observed daily NDVI variation from 3 February to 15 May 2024.

Table 3.5 Monthly mean observed and predicted Kc during the 2023-2024 growing season.

	February	March	April	May
Observed Kc	0.8	0.58	0.51	0.48
Predicted Kc	0.62	0.57	0.56	0.56

The temporal distribution of observed and predicted ETa values reveals a consistent over-simulation by the prediction model throughout the data collection period (Figure 3.18). Descriptive statistics highlight this trend, with the mean predicted ETa at 1.99 mm day^{-1} compared to the observed mean of 1.40 mm day^{-1} (Table 3.6). The median predicted ETa of 2.05 mm day^{-1} similarly exceeds the observed median of 1.32 mm day^{-1}, indicating a persistent bias in the model's estimation of ETa. Variability around the mean is comparable between datasets, with predicted ETa values displaying a slightly higher standard deviation (0.94) than observed values (0.91). However, the cumulative effect of this overestimation is evident, with the total predicted ETa reaching 181.35 mm, significantly surpassing the total observed ETa of 127.12 mm over the study period.

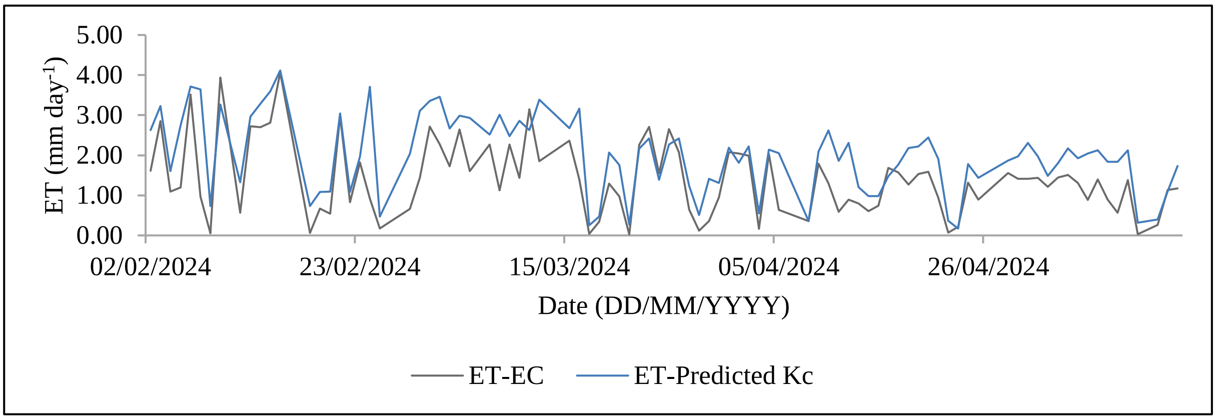

Figure 3.18 Comparison of ET-EC (mm day^{-1}) with ET-Predicted Kc (mm day^{-1}) at a daily temporal resolution derived using average monthly Kc values from the ensemble model output.

Table 3.6 Descriptive statistics for daily ET-EC and ET-Predicted Kc.

	ET-EC	**ET-Predicted Kc**
Minimum (mm day^{-1})	0.02	0.17
Maximum (mm day^{-1})	4.06	4.12
Mean (mm day^{-1})	1.40	1.99
Median (mm day^{-1})	1.32	2.05
Std dev (mm day^{-1})	0.91	0.94
Sum (mm)	127.12	181.35

The percentile analysis (95% CI) corroborates these findings, indicating overestimation across all percentiles and suggesting a systematic bias in the prediction algorithm (Table 3.7). Figure 3.19 offers a visual summary via violin plots, which display a generally higher distribution for predicted ETa values with a notable upward skew, aligning with the trends observed in the descriptive statistics and percentile analysis. These results highlight the model's tendency to overestimate ETa and the need for model adjustments to align closely with observed data.

Table 3.7 Percentiles of daily measured ET-EC and ET-Predicted Kc (mm day^{-1}).

	Percentiles (PC)						
ET-variant	5	10	25	50	75	90	95
ET-EC	0.06	0.18	0.67	1.31	1.89	2.71	2.91
ET-Predicted Kc	0.36	0.51	1.33	2.04	2.63	3.26	3.52

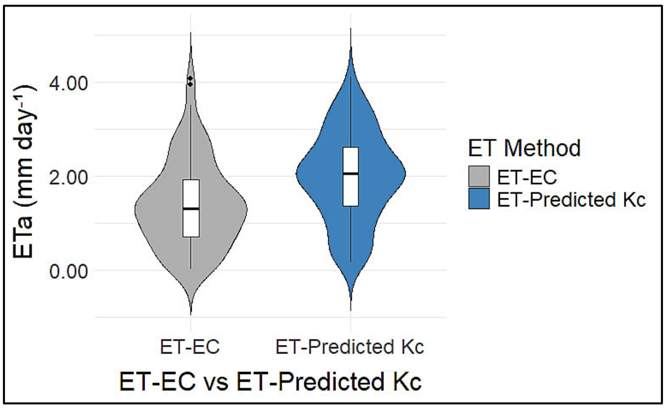

Figure 3.19 Violin plots of daily ET-EC (mm day^{-1}) and ET-Predicted Kc (mm day^{-1}) during the M growth phase of sugarcane.

The regression analysis between ET-Predicted Kc and ET-EC yielded an R^2 of 0.61, indicating that the model explains 61% of the variability in observed ET-EC, suggesting moderate predictive strength (Figure 3.20). However, the RMSE of 0.86 mm day^{-1} and MAE of 0.66 mm day^{-1} further highlight the model's average deviations from observed values, indicating room for improvement in predictive precision.

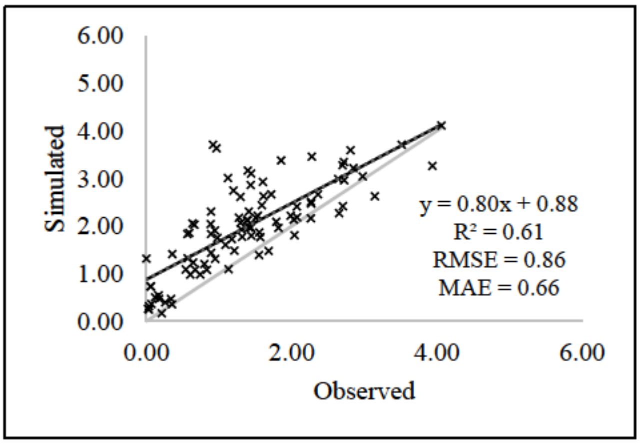

Figure 3.20 Regression analysis examining the concordance between daily ET-EC (observed) and ET-Predicted Kc (simulated). The solid black line represents the regression line, while the grey line indicates perfect agreement between observed and simulated ETa (mm day^{-1}).

The Shapiro-Wilk test assessed the normality of the ET-EC and ET-Predicted Kc datasets. Results indicated that the observed ET-EC values deviated significantly from a normal distribution ($W = 0.958$, $p = 0.005$), while the predicted ET-Kc values did not show significant deviation ($W = 0.979$, $p = 0.151$). Given the non-normality of the observed data, non-parametric tests were deemed appropriate for trend and correlation analysis, justifying the MK test and Spearman's correlation.

The MK test yielded a tau (τ) of 0.607 ($p < 2.22E-16$), indicating a significant positive trend in ET-Predicted Kc relative to ET-EC, thus supporting the model's reliability in capturing temporal trends. Spearman's correlation further confirmed this relationship, with a rho (ρ) of 0.783 ($p < 2.2E-16$), demonstrating a strong positive correlation between ET-Predicted Kc and ET-EC. These results validate that the model's predictions closely follow the variations in observed ET-EC values, validating its accuracy in reflecting observed trends (Table 3.8).

Table 3.8 Trend analysis of ET-Predicted Kc depicting MK's tau (τ) and Spearman's rho (ρ) with associated p-values at a daily resolution.

Mann-Kendall test		**Spearman's correlation**	
tau (τ)	p-value	rho (ρ)	p-value
0.607	< 2.22E-16	0.783	< 2.2E-16

3.3.3 Comparative analysis of evapotranspiration-vegetation index products against eddy covariance measurements

To assess the accuracy of the ET-VI products, ET-VI estimates were juxtaposed with reported ET-EC values (see Figures 3.21 and 3.22). The findings reveal that all ET-VIs surpassed the ET-EC values, with ET-EVI2 demonstrating the closest approximation to ET-EC. Notably, ET-NDVIKc exhibited the most significant deviation from ET-EC, with a disparity of 639 mm. Conversely, ET-EVI2 exhibited the slightest deviation from reported ET-EC values (71 mm), followed by ET-EVI, ET-NDVI, and ET-NDVIscaled (94 mm, 441 mm, and 315 mm, respectively). As depicted in Figure 3.21, the ET-NDVI estimates bear a closer resemblance to ET-EVI and EVI2 than ET-NDVIscaled and ET-NDVIKc. The lowest and highest ETa values were attributed to ET-EVI2 and ET-NDVIKc, respectively.

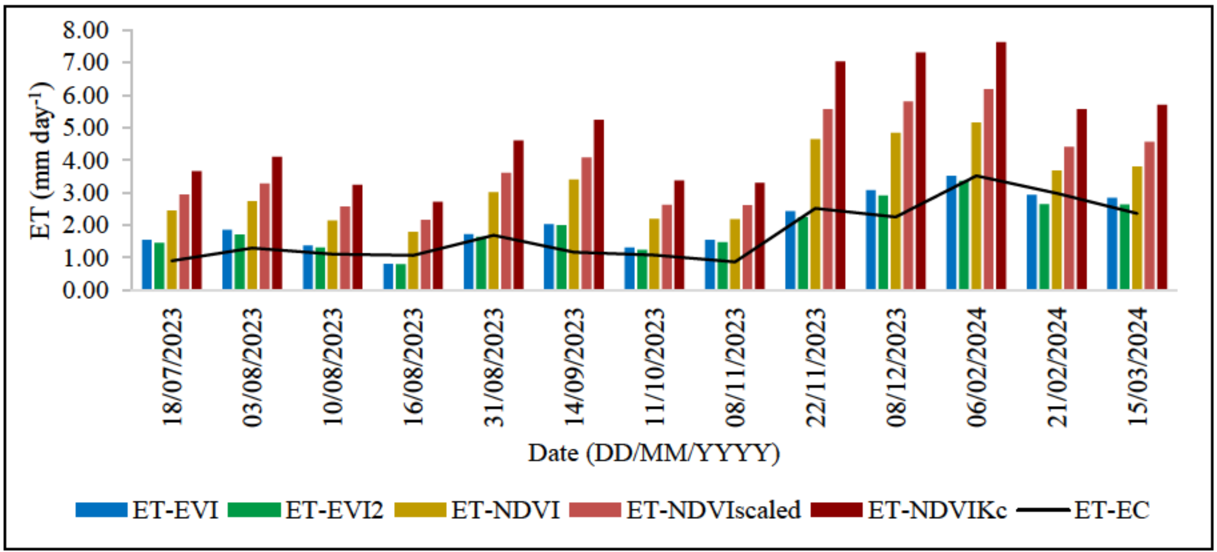

Figure 3.21 Comparison of daily ET-VIs (mm day^{-1}) with daily ET-EC (mm day^{-1}) for individual drone flights.

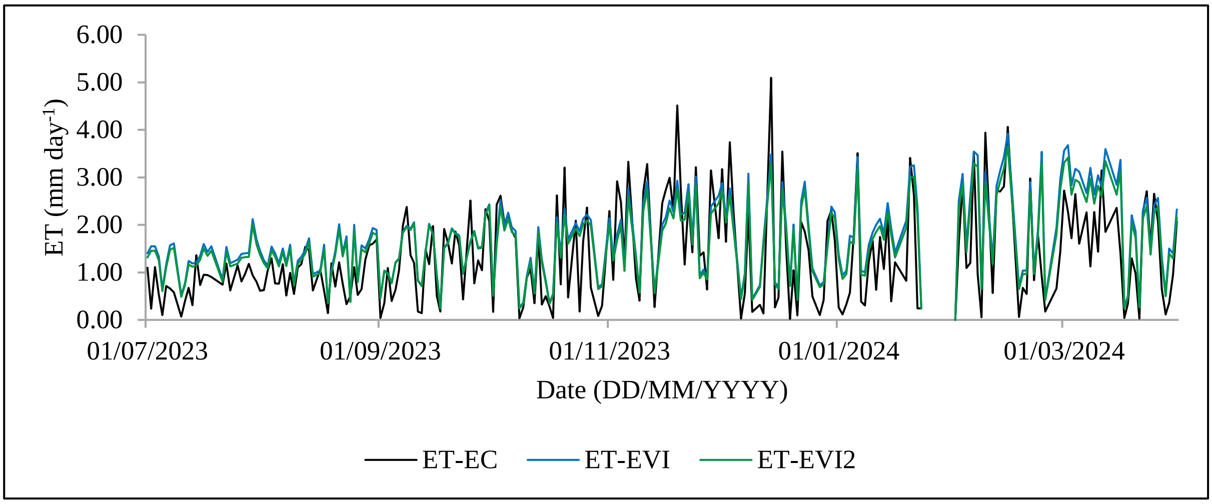

Figure 3.22 Comparison of daily ET-EVIs (mm day^{-1}) with ET-EC (mm day^{-1}).

Table 3.9 highlights notable differences between observed ET-EC and predicted ET-VI values. The ET-EC shows a narrow range (5.07 mm day^{-1}) and lower median (1.12 mm day^{-1}), indicating stable ETa patterns with minimal extremes. In contrast, ET-NDVIKc has the broadest range (7.75 mm day^{-1}) and highest interquartile range (IQR) (2.69 mm day^{-1}), reflecting greater variability. Mean and median values for ET-VIs consistently exceed ET-EC, suggesting a general overestimation. Among the indices, ET-EVI2 aligns most closely with ET-EC, with a mean (1.63 mm day^{-1}) and median (1.55 mm day^{-1}) comparable to ET-EC's mean (1.34 mm day^{-1}) and median (1.12 mm day^{-1}). The ET-EVI2's low standard deviation (0.78 mm day^{-1}) further supports its consistency and suitability for capturing typical ETa patterns, making it the most favourable index in matching ET-EC distribution.

Table 3.9 Descriptive statistics for daily ET-EC and ET-VI variants.

	EC	**NDVI**	**NDVIscaled**	**NDVIKc**	**EVI**	**EVI2**
Minimum (mm day^{-1})	0.02	0.36	0.43	0.53	0.25	0.24
Maximum (mm day^{-1})	5.09	5.48	6.57	8.28	3.92	3.65
Mean (mm day^{-1})	1.34	2.66	3.19	4.02	1.73	1.63
Median (mm day^{-1})	1.12	2.58	3.09	3.95	1.62	1.55
Std dev (mm day^{-1})	1.00	1.19	1.43	1.79	0.83	0.78
Sum (mm)	317.73	632.64	759.17	956.97	412.39	388.53

Table 3.10 shows that the ET-EC data generally exhibits lower values than ET-VIs across all percentiles. For instance, at the 50th percentile, ET-EC is 1.14 mm day^{-1} (95% CI: [1.00, 1.28]), while ET-VIs range from 1.14 to 3.95 mm day^{-1}, with corresponding 95% confidence intervals of [1.40, 1.78] for the lower end and [3.80, 4.10] for the upper end. Percentile trends indicate a general increase in ETa values across all variables, reflecting similar distribution patterns. However, ET-EC has a narrower IQR of 1.49 mm day^{-1} compared to the broader IQRs of ET-VIs, suggesting lower variability. At higher percentiles (e.g., 90th and 95th), ET-EC also shows lower values than ET-VIs, indicating potential differences in extreme ETa values. Figure 3.23's violin plots reinforce these findings, showing generally higher distributions and an upward skew for ET-VIs relative to ET-EC. The EVI-based methods align more closely with the ET-EC distribution, indicating their potential for more accurate ETa estimation.

Table 3.10 Percentiles of daily measured ET-EC and ET-VI variants (mm day^{-1}).

	Percentiles (PC)						
ET-variant	5	10	25	50	75	90	95
ET-EC	0.09	0.18	0.54	1.14	2.03	2.73	3.24
ET-NDVI	0.70	1.04	1.73	2.60	3.52	4.33	4.74
ET-NDVIscaled	0.84	1.25	2.08	3.12	4.23	5.20	5.69
ET-NDVIKc	1.05	1.56	2.63	3.95	5.33	6.55	7.16
ET-EVI	0.46	0.69	1.06	1.64	2.25	2.95	3.29
ET-EVI2	0.43	0.65	1.02	1.58	2.13	2.75	3.05

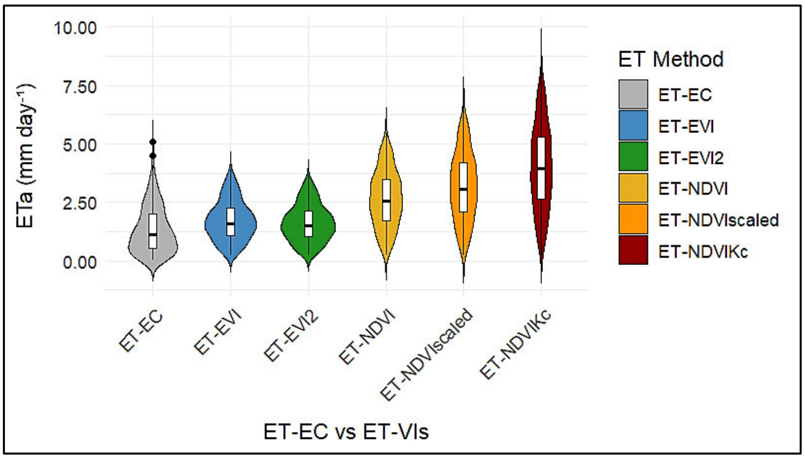

Figure 3.23 Violin plots illustrating the distribution of daily ET-EC (mm day^{-1}) and ET-VIs (mm day^{-1}) during the SE and M growth phases of sugarcane.

The findings indicate that ET-NDVI, ET-NDVIscaled, and ET-NDVIKc have identical R^2 values (0.67) (Table 3.11), indicating that approximately 67% of the observed variability in ETa can be attributed to these methods. Similarly, ET-EVI and ET-EVI2 show an R^2 of 0.63, accounting for 63% of the variability. This suggests that the NDVI variants possess superior explanatory power over the EVI methods. Notably, ET-NDVI, ET-NDVIscaled, and ET-NDVIKc tend to overestimate ETa, with ET-NDVIKc exhibiting the most pronounced overestimation, followed by ET-NDVI and ET-NDVIscaled. Conversely, ET-EVI and ET-EVI2 tend to under-simulate lower ETa values while overestimating at higher ranges.

Regarding error metrics, ET-EVI2 shows the lowest RMSE (0.67 mm day^{-1}) and MAE (0.52 mm day^{-1}), indicating more minimal discrepancies. ET-EVI closely follows with an RMSE of 0.73 mm day^{-1} and MAE of 0.56 mm day^{-1}. In contrast, ET-NDVI presents higher RMSE (1.49 mm day^{-1}) and MAE (1.32 mm day^{-1}), while ET-NDVIscaled and ET-NDVIKc reveal greater discrepancies, with ET-NDVIKc exhibiting the highest mean difference (201%), followed by ET-NDVIscaled (139%) and ET-NDVI (99%). In comparison, ET-EVI (30%) and ET-EVI2 (22%) demonstrate smaller mean differences, reflecting closer alignment with ET-EC values.

Table 3.11 Model evaluation metrics of ET-VI variants.

Method	R^2	RMSE	MAE	Mean Difference (%)
ET-NDVI	0.67	1.49	1.32	99
ET-NDVIscaled	0.67	2.03	1.85	139
ET-NDVIKc	0.67	2.91	2.69	201
ET-EVI	0.63	0.73	0.56	30
ET-EVI2	0.63	0.67	0.52	22

The Shapiro-Wilk test was conducted to assess the normality of the datasets for ET-EC and various VIs. The results indicate that the ET-EC dataset significantly deviates from a normal distribution ($W = 0.932$, $p < 0.001$). In contrast, while NDVI, NDVIscaled, and NDVIKc exhibit statistics exceeding 0.98, the corresponding p-values (<0.01) still lead to the rejection of the null hypothesis of normality. Similarly, EVI and EVI2 show statistics of 0.976 and 0.979, respectively, with p-values indicating a significant departure from normality. Consequently, the reliance on non-parametric methods, such as the MK test and Spearman's correlation, is advocated for trend analysis.

The MK test results indicate strong positive associations for NDVI, NDVIscaled, and NDVIKc, all exhibiting τ values of 0.652 and p-values of 2.22E-16, suggesting significant upward trends (Table 3.12). ET-EVI and ET-EVI2 also demonstrate substantial upward trends with τ values of 0.638 and 0.643, respectively, maintaining the same significance level. Spearman's correlation analysis further corroborates these findings, with correlation coefficients (ρ) for all indices ranging from 0.822 to 0.835, indicating strong positive monotonic relationships with ET-EC. The associated p-values (<0.001) confirm the statistical significance of these relationships, providing robust evidence against the null hypothesis of no correlation.

Table 3.12 Trend analysis of ET-VIs depicting MK's tau and Spearman's rho with associated p-values at a daily resolution.

	Mann-Kendall test		**Spearman's correlation**	
ET-VI	tau (τ)	p-value	rho (ρ)	p-value
NDVI	0.652	2.22E-16	0.835	<0.001
NDVIscaled	0.652	2.22E-16	0.835	<0.001
NDVIKc	0.652	2.22E-16	0.835	<0.001
EVI	0.638	2.22E-16	0.822	<0.001
EVI2	0.643	2.22E-16	0.827	<0.001

3.3.4 Actual evapotranspiration maps

Spatially explicit ETa maps (Figures 3.24 and 3.25) for the sugarcane cropland were generated for select dates during the cooler and drier winter (18 July 2023) and the warmer and wetter summer (6 February 2024), utilising the ET-VI approaches. For the winter ETa maps, the mean ETa ranged from 1.45 mm day^{-1} (ET-EVI2 method) to 3.65 mm day^{-1} (NDVIKc method) (Table 3.13). The summer ETa maps show noticeably higher ETa values, with mean ETa values ranging from 3.29 mm day^{-1} (ET-EVI2) to 7.21 mm day^{-1} (ET NDVIKc) (Table 3.14). The standard deviations and minimum ETa values also increased in the summer, indicating greater variability and a higher baseline ETa (Tables 3.13 and 3.14). Across both seasons, the ET-NDVIKc method consistently yielded the highest ETa values. These findings demonstrate a significant rise in ETa from winter to summer, corresponding to increased water usage during the warmer season.

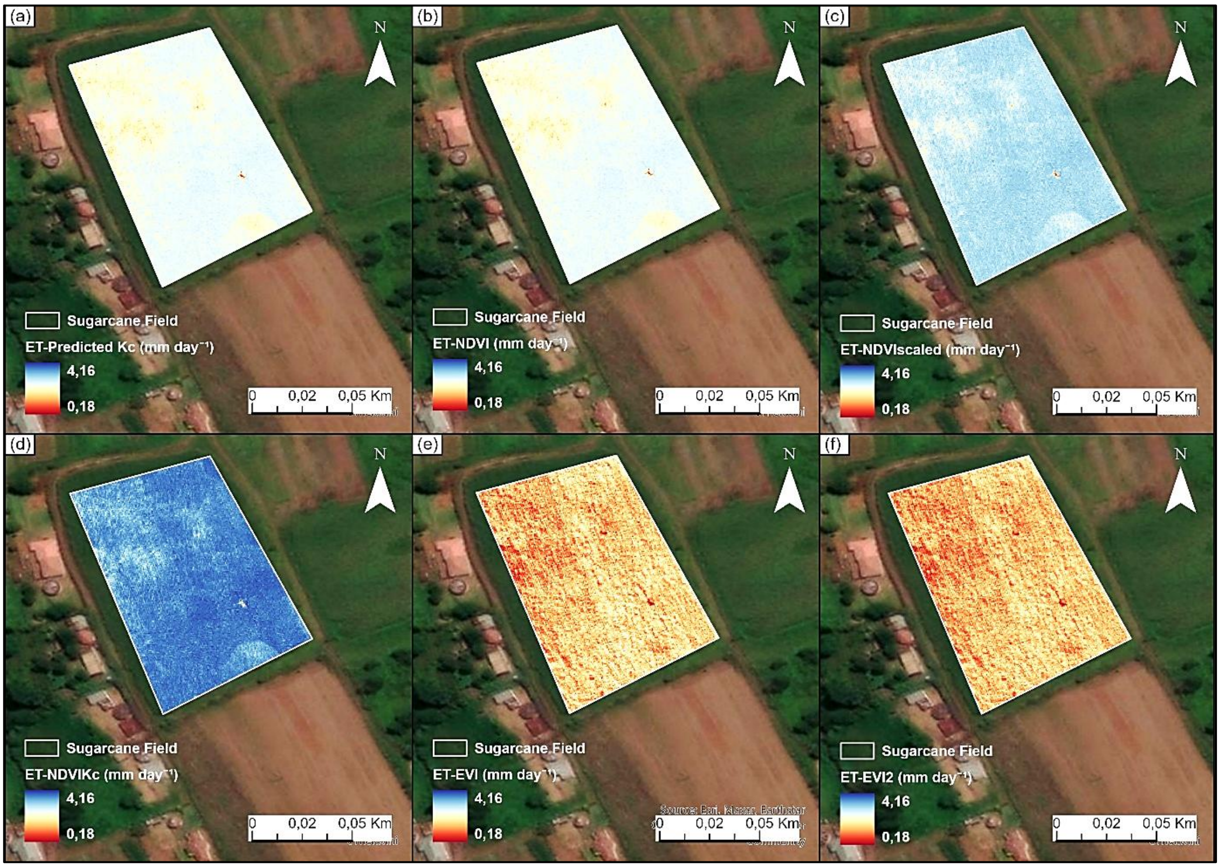

Figure 3.24 Modelled ETa maps (mm day^{-1}) for (a) ET-Predicted Kc, (b) ET-NDVI, (c) ET-NDVIscaled, (d) ET-NDVIKc, (e) ET-EVI, and (f) ET-EVI2 on July 18, 2023.

Table 3.13 Descriptive statistics for the six ETa maps on 18 July 2023.

	Predicted Kc	**NDVI**	**NDVI scaled**	**NDVIKc**	**EVI**	**EVI2**
Mean (mm day^{-1})	2.47	2.45	2.94	3.65	1.55	1.45
Maximum (mm day^{-1})	2.86	2.86	3.43	4.16	2.89	2.62
Minimum (mm day^{-1})	0.41	0.41	0.50	1.11	0.25	0.18
Std dev (mm day^{-1})	0.17	0.17	0.21	0.21	0.38	0.35

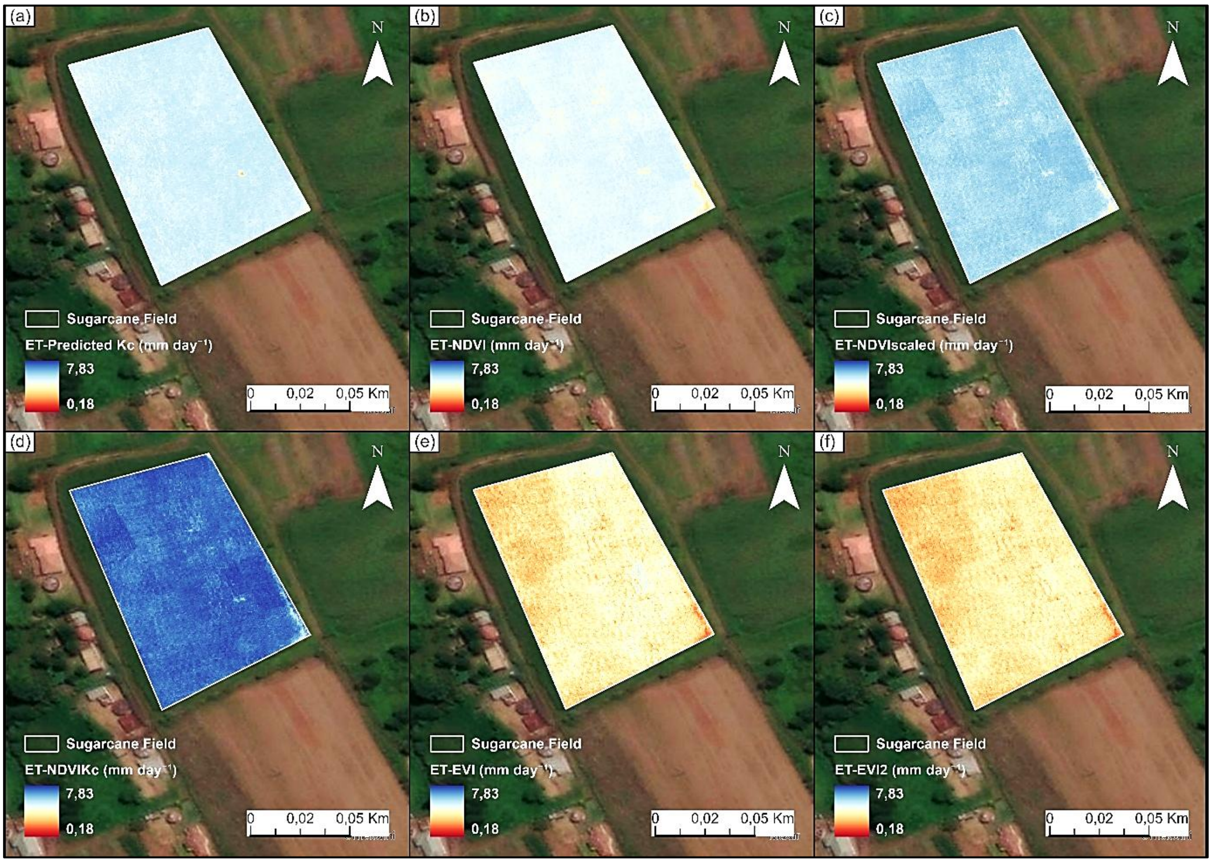

Figure 3.25 Modelled ETa maps (mm day^{-1}) depicting (a) ET-Predicted Kc, (b) ET-NDVI, (c) ET-NDVIscaled, (d) ET-NDVIKc, (e) ET-EVI, and (f) ET-EVI2, observed on February 6, 2024.

Table 3.14 Descriptive statistics for the six ETa maps on 6 February 2024.

	Predicted Kc	**NDVI**	**NDVI scaled**	**NDVIKc**	**EVI**	**EVI2**
Mean (mm day^{-1})	5.15	4.82	5.78	7.21	3.54	3.29
Maximum (mm day^{-1})	5.63	5.31	6.37	7.83	5.34	4.87
Minimum (mm day^{-1})	2.50	1.26	1.52	2.77	1.01	0.93
Std dev (mm day^{-1})	0.18	0.21	0.25	0.26	0.53	0.47

3.4 Discussion

Smallholder farmers increasingly grapple with the challenges posed by climate change, particularly regarding post-harvest losses that threaten food security and health. In this context, UAV-based ETa estimation presents a promising mitigation strategy. Ground truth data was crucial for validating the accuracy and performance of this study's RS-based VI approaches. The EC system, recognised as the gold standard, was utilised for this assessment. The following subsection discusses the implementation and performance of the EC system.

3.4.1 Assessment of in-situ data quality

Before the instrumentation setup at the research site, sensor accuracy, stability, and response time were verified. Calibration procedures ensured data quality and reliability (Appendix B). The spatial representativeness of EC measurements was prioritised by analysing the flux footprint and considering surface heterogeneity for accurate characterisation of fluxes over the sugarcane field (Campbell Scientific, 2013). Terrain factors like slopes and wind directions were evaluated to optimise the EC system's coverage, enhancing data reliability. Despite inherent challenges in achieving complete EBC, such as sensor footprint mismatches and large-scale turbulence, the daily EBC ratio of 76% is satisfactory, supporting ET-EC data use as a validation metric against UAV-derived methodologies. Non-closure factors include landscape homogeneity violations, measurement errors, and advection influences (Reed *et al.*, 2018; Mauder *et al.*, 2020). However, EBC improves with longer time steps, as daily averaging mitigates atmospheric fluctuations (Reed *et al.*, 2018).

Seasonal ETa variations align with phenological and environmental changes, with vigorous growth in winter SE leading to higher ETa values and summer conditions maintaining significant ETa rates despite M. Environmental drivers like temperature and solar radiation significantly affect ETa, with summer rainfall ensuring soil moisture for robust growth. Winter's lower rainfall restricts transpiration rates despite the SE growth phase. Observed ETa patterns align with expected seasonal dynamics, validating the EC-derived ET dataset for VI-based estimation methods. However, a data gap in January 2024 suggests possible monthly ETa alignment issues, pending future data recovery. Measurement limitations include potential errors and weather disturbances, such as rainfall affecting Rn and sensor accuracy (Zhao *et al.*, 2023). Moreover, water droplets on sensors can alter radiation measurements, impacting precision.

3.4.2 Performance evaluation of crop coefficient prediction models using machine learning approaches

A relationship between in-situ NDVI and Kc was assessed using linear regression (LR) during a portion of the mature sugarcane growing phase (February 3 to May 15, 2024), yielding a low R^2 value of 0.04. A sixth-order polynomial regression (PR) also produced a similarly low R^2 of 0.11. Consequently, ML techniques, including RF, RPART, GLM, kNN, and SVMRadial, were implemented to capture this complex relationship better. While individual ML algorithms exhibited poor performance metrics for R^2, RMSE, and MAE, the RF ensemble model demonstrated robust predictive capacity with an R^2 of 0.68, an RMSE of 0.11, and an MAE of 0.07.

The initial weak association observed with the LR and PR models can be attributed to capturing data solely from the late season of sugarcane cultivation. As Hunsaker *et al.* (2003) noted, NDVI values exceeding 0.8 may deviate from linearity due to saturation effects, particularly when full vegetative cover is achieved (Hunsaker *et al.*, 2003). This saturation limits NDVI's sensitivity to variations in crop water stress and Kc. Although polynomial models provide increased flexibility, they may still fall short in representing the non-linear relationships between NDVI and Kc under full canopy cover. Thus, ML techniques are justified, as they can more effectively model these complex interactions.

The RF algorithm recorded the highest R^2 value of 0.19 among the individual ML models. Although its RMSE (0.19) and MAE (0.15) were not the most optimal compared to other models, the differences were minimal, suggesting that RFR estimates Kc more accurately than the different algorithms. The subsequent derivation of performance metrics using the RFR ensemble model (R^2 = 0.68, RMSE = 0.11, MAE = 0.07) are consistent with those reported in previous studies. For instance, Shao *et al.* (2021) found R^2 values ranging from 0.48 to 0.77 and RMSE values between 0.11 and 0.17 when estimating Kc for maize crops using UAV-based VIs and ground-based leaf area index (LAI) with the RFR algorithm (Shao *et al.*, 2021).

Shao *et al.* (2023) also utilised UAV-based VIs and ML techniques to predict maize Kc, identifying RFR as the most accurate (R^2 = 0.69, RMSE = 0.10). Their integration of multispectral, thermal, and texture indices enhanced Kc estimation, with strong predictive performance for cumulative ETa (R^2 = 0.89) and soil water content (R^2 = 0.85). However, maize's canopy structure and growth dynamics differ from sugarcane, impacting model transferability. Unlike Shao *et al.* (2023), who incorporated thermal and textural features, this study relied on an NDVI-based approach, potentially explaining performance differences. Moreover, their validation used FAO-56 and soil water balance-derived ETa, whereas this study employed EC data, which directly captures local energy balance complexities.

Er-Raki *et al.* (2013) established an NDVI-Kc relationship for table grapes (R^2 = 0.63) using EC-derived ETa but found NDVI saturation led to Kc underestimation at peak growth. Similarly, NDVI's reduced sensitivity at high biomass limits Kc predictions in sugarcane. Unlike this study, which applies ML-based approaches (R^2 = 0.61 for RFR) to mitigate these effects, Er-Raki *et al.* (2013) relied solely on empirical correlations. Their FAO-56-based Kc values overestimated ETc by 46%, highlighting the need for site-specific adjustments. The higher R^2 in this study suggests crop-specific factors and dataset variability influence ML performance in sugarcane Kc estimation.

Alam *et al.* (2018) established an NDVI-Kc relationship for irrigated pasture (R^2 = 0.84) using portable chamber ETa measurements and FAO-56-derived ETo. While their study confirms NDVI's viability for Kc estimation under well-irrigated conditions, it highlights the need for site-specific calibrations, as Kc varied with the pasture growth stage. Unlike this rainfed study, which applies ML-based techniques (R^2 = 0.61 for RFR) to mitigate NDVI saturation, Alam *et al.* (2018) relied on empirical regression models, limiting transferability. Their small-scale approach (<1 m^2) contrasts with the UAV-based framework used here, reinforcing the need for spatiotemporal adaptability in heterogeneous cropping systems like sugarcane.

Alavi *et al.* (2024) reported RFR as the most accurate model for sugarcane ETa estimation (R^2 = 0.92–0.99), exceeding this study's 0.68. This discrepancy likely stems from differences in data inputs, seasonal coverage, and validation methods. While Alavi *et al.* (2024) incorporated LAI and sugarcane height to refine Kc estimates, this study relied primarily on NDVI, which saturates at high biomass, reducing sensitivity to Kc variability. Their validation used FAO-56 Penman-Monteith ETo and ground-based Kc measurements, whereas this study employed EC data, which better captures spatiotemporal ET variability. These distinctions highlight the context-dependent performance of RFR in ETa prediction.

The limited research on NDVI-Kc relationships for sugarcane highlights this study's significance. While Kc estimation is well-documented for maize, grapes, and pasture, ML-based NDVI-Kc modelling for rainfed sugarcane remains scarce. This study addresses this gap by evaluating RFR for Kc estimation, demonstrating its applicability despite NDVI saturation.

With Alavi *et al.* (2024) as the only direct comparison, further research is needed to refine ML-driven sugarcane Kc models, integrating alternative spectral indices and multi-source datasets to enhance accuracy and adaptability across varying growth conditions.

3.4.3 Comparative analysis of evapotranspiration-vegetation index products against eddy covariance measurements

The VI methodology integrates crop transpiration and soil evaporation into a single Kc value, often estimated using NDVI. While a Kc of 1.2 (NDVI ≈ 0.8) is typical for peak vegetative vigour under minimal water stress and 0.4 (NDVI ≈ 0.16) for early growth stages, the VI methodology primarily accounts for transpiration, potentially underestimating soil evaporation (Abbasi *et al.*, 2023). Data collection, however, commenced seven months into the growing season. Therefore, this extensive pre-existing vegetation cover mitigated potential Kc underestimation from a lack of early-growth-stage data (French *et al.*, 2020). Nevertheless, rainfed cultivation suggests the possibility of water stress if precipitation is insufficient for optimal growth, potentially leading to an overestimation of the Kc value (1.2) used in empirical relationships, especially considering available in-situ Kc data derived from instrumentation on the meteorological flux tower.

Acknowledging these inherent limitations, the study assessed three NDVI-based ETa models (ET-NDVI, ET-NDVIscaled, ET-NDVIKc) and two EVI-based models (ET-EVI, ET-EVI2) against EC system-derived ET (ET-EC) over nine months (July 2023–March 2024). Results indicated consistently higher ETa estimates from all VI-based approaches compared to ET-EC. However, EVI-based models (ET-EVI, ET-EVI2) demonstrated superior performance, likely due to their greater resilience to canopy saturation and soil variability (Woldemariam *et al.*, 2024). The observed overestimation of VI-based ET models relative to ET-EC may partially reflect an underrepresentation of ETa in the EC data caused by a lack of EBC. Additionally, the non-parametric nature of the data (Shapiro-Wilk test) dictated the use of Mann-Kendall and Spearman rank correlation tests to assess monotonic trends and relationships between ET-VIs and ET-EC, respectively.

Although ET-EVI and ET-EVI2 displayed similarities to ET-EC, the Mann-Kendall test indicated a stronger association between ET-NDVI and ET-EC. Spearman's rho showed stronger positive monotonic relationships for ET-NDVI ($\rho = 0.835$) compared to ET-EVI ($\rho = 0.822$) and ET-EVI2 ($\rho = 0.827$). Despite this, ET-EVI2 and ET-EVI exhibited superior RMSE and MAE performance. Conversely, ET-NDVIKc and ET-NDVIscaled displayed poorer performance, highlighting the limitations of NDVI at high biomass, where saturation reduces sensitivity to vegetation changes (Abbasi *et al.*, 2023). EVI's inclusion of a blue band and its coefficients mitigate atmospheric and soil background effects, improving its robustness (Jiang *et al.*, 2008). Consistent with Woldemariam *et al.* (2024), EVI-based models outperformed NDVI-based models, emphasising EVI's superior sensitivity to biophysical changes crucial for monitoring sugarcane growth (Woldemariam *et al.*, 2024). This aligns with previous research highlighting EVI's and EVI2's superiority in estimating ETa in semi-arid regions (Nouri *et al.*, 2020; Abbasi *et al.*, 2023). These findings underline the ET-VI approach's potential for sustainable water and resource management in small-scale agriculture.

3.4.4 Optimal methods and considerations for the smallholder farmer context

Among the developed ET-VI products—ET-NDVI, ET-NDVIscaled, ET-NDVIKc, ET-EVI, and ET-EVI2—the ET-EVI2 method emerged as the most reliable based on comprehensive performance metrics and statistical analyses. A subsequent comparison between the ET-EVI2 dataset and ET-Predicted Kc data from the RFR ensemble model with ET-EC data is warranted, acknowledging the limitation related to differences in data collection periods: ET-EVI2 spans from July 1, 2023, to March 31, 2024, while ET-Predicted Kc covers February 3, 2023, to May 15, 2024.

Evaluation metrics reveal that EVI2 consistently outperforms the RFR ensemble model, achieving a higher R^2 value (0.63 vs 0.61), lower RMSE (0.67 vs 0.86), and reduced MAE (0.52 vs 0.66). Additionally, EVI2 displays a mean percentage difference of 21.64%, significantly less than the RFR's 29.65%. Statistical analyses further confirm EVI2's superiority, with a higher Tau (0.643 vs 0.607) and significant p-values in the Mann-Kendall test, indicating a more reliable trend. Additionally, a higher Spearman's rho (0.827 vs 0.783) shows the increased correlation between predicted and observed values, with significant p-values.

These findings support the reliability and robustness of the EVI2 approach, making it the preferred method for estimating ETa in this analysis. Furthermore, adopting ML to develop Kc prediction models is significantly data-intensive and technically demanding (Elbasi *et al.*, 2023). This requirement for extensive in-situ data poses challenges for smallholder farmers, who may lack the resources for such detailed data-collection practices (Gokool *et al.*, 2023). Moreover, the reliance on accurate in-situ NDVI values emphasises the complexity of correlating variables across diverse agronomic conditions.

While the RFR ensemble model was developed from a limited dataset of 86 points, leveraging a larger dataset throughout the growing season could yield enhanced performance metrics and more robust statistical results. In contrast, empirical correlations offer notable advantages by reducing dependence on in-situ data, exemplified by the consistent performance of the EVI2 approach. Such considerations are vital for developing accessible methodologies that align with the needs of smallholder farmers, where resource constraints can limit data collection and analysis capabilities (Gokool *et al.*, 2023; Yacoob *et al.*, 2024).

3.4.5 Limitations and recommendations for future research

Local EC data were employed to validate the Kc prediction model and ET-VI methodologies, enhancing reliability and highlighting their dependability. However, to strengthen the credibility of these methods, it is essential to utilise a larger and more representative dataset encompassing the entire sugarcane growth cycle beyond the 10-month period of this study. This dataset should incorporate a broader spectrum of soil moisture levels and diverse sugarcane genotypes across various regions to better capture the variability in crop responses and environmental interactions, ultimately improving the models' robustness and applicability across different scenarios.

Sugarcane Kc estimates were rapidly and accurately derived using UAV-based VIs and ground-based ETo. This methodology, applied to ET-VI products, relied on some empirical relationships. In addition, including ground-based Kc and NDVI data for developing an ML ensemble model further enhanced its reliability. However, the need for on-site measurements limits the scalability and convenience of these models. Thus, future research should prioritise techniques that are less reliant on in-situ data to enhance applicability for smallholder farmers facing challenges in accessing advanced measurement tools and ensuring consistent data collection.

This research utilised a UAV with a multispectral camera capturing images across five spectral bands, including visible and infrared regions, to obtain VIs. However, the costs associated with UAVs and the expertise and software required for processing add constraints, making this technology primarily viable as a research tool at present. To improve accessibility for smallholder farmers, future studies should examine the feasibility of incorporating more affordable RGB sensors alongside VI-based approaches for estimating ETa (Yacoob *et al.*, 2024).

In light of the pressing challenges posed by climate change and population growth, efficient water management and increased crop yields are critical for local farmers. The findings of this research could significantly enhance sugarcane and crop production by improving water use efficiency and effectively managing crop-water stress. Decision support systems that integrate these results could equip farmers with valuable insights to optimise irrigation practices, ultimately improving crop yields, livelihoods, and food security while positively impacting local economies. Such tools could provide real-time data on crop stress indicators, enabling informed decision-making for effective resource management.

Despite their perceived simplicity (Glenn *et al.*, 2010), VI-based methodologies are prone to inaccuracies and biases. The near-infrared (NIR) and red (R)-reflectance from the visible band typically yield higher resolution than thermal bands (Nagler *et al.*, 2005; Nagler *et al.*, 2013; French *et al.*, 2020). However, these spectral bands are insufficient for capturing soil evaporation following irrigation and precipitation events, complicating drought and water stress assessments. Though immediate effects of water scarcity on plant characteristics are generally minimal (Moran *et al.*, 1994), NDVI saturation in densely vegetated regions limits its reliability as an indicator of short-term variations in plant water stress.

EVI proves more effective in alleviating NDVI saturation, particularly in dense vegetation, by mitigating atmospheric influences and demonstrating reduced sensitivity to background noise (Huete *et al.*, 2002). However, EVI's dependence on a blue band may lead to low signal-to-noise ratios and potential instability (Abbasi *et al.*, 2023). Consequently, EVI2 was introduced as a supplementary metric, circumventing the need for a blue band and offering greater noise resilience, thus enhancing its reliability as an index (Jiang *et al.*, 2007; Jiang *et al.*, 2008).

In summary, to maximise these techniques' benefits for broader communities, future research should emphasise increasing the accessibility of technologies and tools that assist smallholder farmers in managing water resources and improving crop productivity amid climate change and population growth challenges.

3.5 Conclusion

This study introduces innovative and robust methodologies for monitoring ETa in sugarcane on smallholder farms, utilising ground-based and UAV-based VIs. Integrating these advanced techniques could enhance precision water management and lay a foundation for future advancements in agricultural water management. Among the various RS-based VI approaches employed, EVI2 proved to be the most effective for ETa estimation, demonstrating superior predictive accuracy over alternative ET-VI products. Several studies have documented this finding, emphasising EVI2's potential as a viable UAV-based crop water use estimation approach. Additionally, this research addresses the technical complexities and data requirements of ML techniques that may limit their practicality in smallholder contexts. The necessity for extensive ground truth data to accurately determine VIs and Kc emphasises essential implementation challenges. Nevertheless, integrating ET-VI products with computational tools, such as crop simulation models, could establish a clear link between water productivity and irrigation decisions. For instance, real-time ETa data can optimise irrigation schedules, improving crop yields and conserving water resources. This research offers valuable insights for policymakers, agronomists, and irrigation planners who require reliable ETa data. It emphasises the need for comprehensive datasets encompassing the entire sugarcane growth cycle and accommodating diverse irrigation practices and genotypes, thereby strengthening the applicability of ET-VI models in real-world conditions. Addressing current limitations in VI methodologies—such as NDVI saturation and the need for high temporal resolution data—will enhance the accuracy and relevance of advanced agricultural monitoring techniques. While the uptake of these technologies for smallholder farm applications remains limited due to capacity constraints, it is envisaged that these challenges will diminish in the future, increasing the accessibility and viability of UAV-based approaches to guide agricultural management decisions.

3.6 References

Abbasi, N, Nouri, H, Didan, K, Barreto-Muñoz, A, Chavoshi Borujeni, S, Opp, C, Nagler, P, Thenkabail, PS and Siebert, S. 2023. Mapping vegetation index-derived actual evapotranspiration across croplands using the Google Earth Engine platform. *Remote Sensing* 15 (4): 1017.

Abbasi, N, Nouri, H, Didan, K, Barreto-Muñoz, A, Chavoshi Borujeni, S, Salemi, H, Opp, C, Siebert, S and Nagler, P. 2021. Estimating actual evapotranspiration over croplands using vegetation index methods and dynamic harvested area. *Remote Sensing* 13 (24): 5167.

Adaptation Fund. 2014. Building resilience in the greater uMngeni catchment, South Africa. [Internet]. Available from: https://www.adaptation-fund.org/project/building-resilience-in-the-greater-umngeni-catchment/. [Accessed: 31 January 2024].

Adisa, O, Botai, CM, Botai, JO, Hassen, A, Darkey, D, Tesfamariam, EH, Adisa, AF, Adeola, AM and Ncongwane, KP. 2018. Analysis of agro-climatic parameters and their influence on maize production in South Africa. *Theoretical and Applied Climatology* 134 (1): 991-1004.

Alavi, M, Albaji, M, Golabi, M, Naseri, AA and Homayouni, S. 2024. Estimation of sugarcane evapotranspiration from remote sensing and limited meteorological variables using machine learning models. *Journal of Hydrology* 629: 130605.

Akdim, N, Alfieri, SM, Habib, A, Choukri, A, Cheruiyot, EK, Labbassi, K and Menenti, M. 2014. Monitoring of irrigation schemes by remote sensing: phenology versus retrieval of biophysical variables. *Remote Sensing* 6 (1): 5815-5851.

Alam, M, Lamb, D and Rahman, M. 2018. A refined method for rapidly determining the relationship between canopy NDVI and the pasture evapotranspiration coefficient. *Computers and Electronics in Agriculture* 147 (1): 12-17.

Ali, MH, Popescu, I, Jonoski, A and Solomatine, DP. 2023. Remote sensed and/or global datasets for distributed hydrological modelling: a review. *Remote Sensing* 15 (6): 1642.

Allen, R, Pereira, L, Raes, D and Smith, M. 1998. *Crop Evapotranspiration: Guidelines for Computing Crop Water Requirements.* FAO Irrigation and Drainage Paper No. 56. Food and Agriculture Organization of the United Nations, Rome, Italy.

Bachour, R. 2013. Evapotranspiration modelling and forecasting for efficient management of irrigation command areas. Unpublished thesis, Department of Civil and Environmental Engineering, Utah State University, Logan, Utah, United States.

Baldocchi, DD, Law, BE and Anthoni, PM. 2000. On measuring and modelling energy fluxes above the floor of a homogeneous and heterogeneous conifer forest. *Agricultural and Forest Meteorology* 102 (2): 187-206.

Basdew, M, Jiri, O and Mafongoya, PL. 2017. Integration of indigenous and scientific knowledge in climate adaptation in KwaZulu- Natal, South Africa. *Change and Adaptation in Socio-Ecological Systems* 3 (1): 56-67.

Bausch, WC and Neale, CM. 1987. Crop coefficients derived from reflected canopy radiation: a concept. *Transactions of the ASAE* 30 (3): 703-709.

Belmonte, AC, Jochum, AM, GarcÍa, AC, Rodríguez, AM and Fuster, PL. 2005. Irrigation management from space: towards user-friendly products. *Irrigation and Drainage Systems* 19 (3): 337-353.

Brewer, K, Clulow, A, Sibanda, M, Gokool, S, Odindi, J, Mutanga, O, Naiken, V, Chimonyo, VGP and Mabhaudhi, T. 2022. Estimation of maize foliar temperature and stomatal conductance as indicators of water stress based on optical and thermal imagery acquired using an unmanned aerial vehicle (UAV) platform. *Drones* 6 (7): 169.

Campbell Scientific. 2013. *Open-Path Eddy-Covariance System Operator's Manual* Campbell Scientific, Inc., Logan, Utah, United States.

Campbell Scientific. 2025. [Internet]. Campbell Scientific, Inc. Available from: https://www.campbellsci.com/. [Accessed: 30 October 2024].

Carr, M and Knox, J. 2011. The water relations and irrigation requirements of sugar cane (Saccharum officinarum): a review. *Experimental Agriculture* 47 (1): 1-25.

Castellví, F and Snyder, RL. 2009. On the performance of surface renewal analysis to estimate sensible heat flux over two growing rice fields under the influence of regional advection. *Journal of Hydrology* 375 (3): 546-553.

Chaudhary, SK, Srivastava, PK, Gupta, DK, Kumar, P, Prasad, R, Pandey, DK, Das, AK and Gupta, M. 2022. Machine learning algorithms for soil moisture estimation using Sentinel-1: model development and implementation. *Advances in Space Research* 69 (4): 1799-1812.

Chimonyo, V, Modi, A and Mabhaudhi, T. 2016. Assessment of sorghum-cowpea intercrop system under water-limited conditions using a decision support tool. *Water SA* 42 (2): 316-327.

Cucho-Padin, G, Loayza, H, Palacios, S, Balcazar, M, Carbajal, M and Roberto, Q. 2019. Development of low-cost remote sensing tools and methods for supporting smallholder agriculture. *Applied Geomatics* 12 (1): 247-263.

Cui, W and Chui, TFM. 2019. Temporal and spatial variations of energy balance closure across FLUXNET research sites. *Agricultural and Forest Meteorology* 271 (1): 12-21.

D'Urso, G. 2010. Current status and perspectives for the estimation of crop water requirements from Earth observation. *Italian Journal of Agronomy* 5 (1): 107-120

Dasgupta, A, Arnal, L, Emerton, R, Harrigan, S, Matthews, G, Muhammad, A, O'Regan, K, Pérez-Ciria, T, Valdez, E, van Osnabrugge, B, Werner, M, Buontempo, C, Cloke, H, Pappenberger, F, Pechlivanidis, IG, Prudhomme, C, Ramos, M-H and Salamon, P. 2023. Connecting hydrological modelling and forecasting from global to local scales: perspectives from an international joint virtual workshop. *Journal of Flood Risk Management* 1 (1): e12880.

Drechsler, K, Fulton, A and Kisekka, I. 2022. Crop coefficients and water use of young almond orchards. *Irrigation Science* 40 (1): 379-395.

Drexler, J, Snyder, R, Spano, D and U, K. 2004. A review of models and micrometeorological methods used to estimate wetland evapotranspiration. *Hydrological Processes* 18 (11): 2071-2101.

du Plessis, A. 2017. Water scarcity and other significant challenges for South Africa. In: *Freshwater Challenges of South Africa and Its Upper Vaal River*. Springer Water. Cham, Switzerland: Springer Nature.

Elbasi, E, Zaki, C, Topcu, AE, Abdelbaki, W, Zreikat, AI, Cina, E, Shdefat, A and Saker, L. 2023. Crop prediction model using machine learning algorithms. *Applied Sciences* 13 (16): 9288.

Emery, WJ and Camps, A. 2017. *Introduction to Satellite Remote Sensing: Atmosphere, Ocean, Land, and Cryosphere Applications.* Amsterdam, Netherlands: Elsevier.

Er-Raki, S, Rodriguez, JC, Garatuza-Payan, J, Watts, CJ and Chehbouni, A. 2013. Determination of crop evapotranspiration of table grapes in a semi-arid region of Northwest Mexico using multi-spectral vegetation index. *Agricultural Water Management* 122 (1): 12-19.

Espadafor, M, Lorite, IJ, Gavilán, P and Berengena, J. 2011. An analysis of the tendency of reference evapotranspiration estimates and other climate variables during the last 45 years in Southern Spain. *Agricultural Water Management* 98 (6): 1045-1061.

Filgueiras, R, Mantovani, E, Althoff, D, Balieiro Ribeiro, R, Venancio, L and Argolo dos Santos, R. 2019. Dynamics of actual crop evapotranspiration based in the comparative analysis of SEBAL and METRIC-EEFLUX. *Irriga* 1 (1): 72-80.

French, A, Hunsaker, D, Sanchez, C, Saber, M, Gonzalez, J and Anderson, R. 2020. Satellite-based NDVI crop coefficients and evapotranspiration with eddy covariance validation for multiple durum wheat fields in the US Southwest. *Agricultural Water Management* 239 (1): 106266.

French, AN, Hunsaker, DJ, Bounoua, L, Karnieli, A, Luckett, WE and Strand, RJ. 2018. Remote Sensing of Evapotranspiration over the Central Arizona Irrigation and Drainage District, USA. *Agronomy* 8 (12): 278.

Gangat, R, van Deventer, H, Naidoo, L and Adam, E. 2020. Estimating soil moisture using Sentinel-1 and Sentinel-2 sensors for dryland and palustrine wetland areasa. *South African Journal of Science* 116 (7/8).

Glenn, E, Nagler, P and Huete, A. 2010. Vegetation index methods for estimating evapotranspiration by remote sensing. *Surveys in Geophysics* 31 (1): 531-555.

Gokool, S, Jarmain, C, Riddell, E, Swemmer, A, Lerm, R and Chetty, KT. 2017. Quantifying riparian total evaporation along the Groot Letaba River: A comparison between infilled and spatially downscaled satellite derived total evaporation estimates. *Journal of Arid Environments* 147 (1): 114-124.

Gokool, S, Mahomed, M, Kunz, R, Clulow, A, Sibanda, M, Naiken, V, Chetty, K and Mabhaudhi, T. 2023. Crop monitoring in smallholder farms using unmanned aerial vehicles to facilitate precision agriculture practices: a scoping review and bibliometric analysis. *Sustainability* 15 (4): 3557.

Gokool, S, Mahomed, M, Clulow, A, Sibanda, M, Kunz, R, Naiken, V and Mabhaudhi, T. 2024. Exploring the potential of remote sensing to facilitate integrated weed management in smallholder farms: a scoping review. *Drones* 8 (3): 81.

Gontia, N and Tiwari, K. 2009. Estimation of crop coefficient and evapotranspiration of wheat (Triticum aestivum) in an irrigation command using remote sensing and GIS. *Water Resources Management* 24 (1): 1399-1414.

Gorelick, N, Hancher, M, Dixon, M, Ilyushchenko, S, Thau, D and Moore, R. 2017. Google Earth Engine: planetary-scale geospatial analysis for everyone. *Remote Sensing of Environment* 202 (1): 18-27.

Gosnell, JM and Lonsdale, JE. 1974. Some effects of drying-off before harvest on cane yield and quality. *Proceedings XV Congress, International Society of Sugar Cane Technologists* 15 (1): 701-712.

Gray, BA, Toucher, ML, Savage, MJ and Clulow, AD. 2022. Seasonal evapotranspiration over an invader vegetation (Pteridium aquilinum) in a degraded montane grassland using surface renewal. *Journal of Hydrology: Regional Studies* 40 (1): 101012.

Gunnula, W, Kosittrakun, M, Weerathaworn, P and Prabpan, M. 2012. Evaluating Sugarcane Growth and Maturity Using Ground-Based Measurements and Remote Sensing Data. *Thai Journal of Agricultural Science* 45 (1): 17-28.

Hamed, KH and Ramachandra Rao, A. 1998. A modified Mann-Kendall trend test for autocorrelated data. *Journal of Hydrology* 204 (1): 182-196.

Han, Y, Tarakey, BA, Hong, S-J, Kim, S-Y, Kim, E, Lee, C-H and Kim, G. 2021. Calibration and image processing of aerial thermal image for UAV application in crop water stress estimation. *Journal of Sensors* 2021 (1): 5537795.

Hess, TM, Sumberg, J, Biggs, T, Georgescu, M, Haro-Monteagudo, D, Jewitt, G, Ozdogan, M, Marshall, M, Thenkabail, P, Daccache, A, Marin, F and Knox, JW. 2016. A sweet deal? Sugarcane, water and agricultural transformation in Sub-Saharan Africa. *Global Environmental Change* 39 (1): 181-194.

Hoffmann, H, Nieto, H, Jensen, R, Guzinski, R, Zarco-Tejada, P and Friborg, T. 2016. Estimating evaporation with thermal UAV data and two-source energy balance models. *Hydrology and Earth System Science* 20 (2): 697-713.

Hu, G, Jia, L and Menenti, M. 2015. Comparison of MOD16 and LSA-SAF MSG evapotranspiration products over Europe for 2011. *Remote Sensing of Environment* 156 (1): 510-526.

Huang, Y, Reddy, K, Fletcher, R and Pennington, D. 2017. UAV low-altitude remote sensing for precision weed management. *Weed Technology* 32 (1): 1-5.

Huete, A, Didan, K, Miura, T, Rodriguez, E, Gao, X and Ferreira, LG. 2002. Overview of the radiometric and biophysical performance of the MODIS vegetation indices. *Remote Sensing of Environment* 83 (1): 195-213.

Hunsaker, DJ, Pinter, P, Barnes, EM and Kimball, BA. 2003. Estimating cotton evapotranspiration crop coefficients with a multispectral vegetation index. *Irrigation Science* 22 (1): 95-104.

Hutton, JJS, Lipa, G, Baustian, D, Sulik, JJ and Bruce, RW. 2020. High accuracy direct georeferencing of the altum multi-spectral UAV camera and its application to high throughput plant phenotyping. *International Archives of the Photogrammetry, Remote Sensing and Spatial Information Sciences* 2020 (1): 451-456.

Ihuoma, SO, Madramootoo, CA and Kalacska, M. 2021. Integration of satellite imagery and in situ soil moisture data for estimating irrigation water requirements. *International Journal of Applied Earth Observation and Geoinformation* 102 (1): 102396.

Inman-Bamber, NG. 1994. Temperature and seasonal effects on canopy development and light interception of sugarcane. *Field Crops Research* 36 (1): 41-51.

Inman-Bamber, NG. 2004. Sugarcane water stress criteria for irrigation and drying off. *Field Crops Research* 89 (1): 107-122.

Ippolito, M, De Caro, D, Ciraolo, G, Minacapilli, M and Provenzano, G. 2022. Estimating crop coefficients and actual evapotranspiration in citrus orchards with sporadic cover weeds based on ground and remote sensing data. *Irrigation Science* 41 (1): 1-18.

Jiang, Z, Huete, A, Kim, Y and Didan, K. 2007. Two-Band enhanced vegetation index without a blue band and its application to AVHRR data. *Proceedings of SPIE - The International Society for Optical Engineering* 6679.

Jiang, Z, Huete, AR, Didan, K and Miura, T. 2008. Development of a two-band enhanced vegetation index without a blue band. *Remote Sensing of Environment* 112 (10): 3833-3845.

Jin, Y, Liu, Y, Liu, J and Zhang, X. 2022. Energy balance closure problem over a tropical seasonal rainforest in Xishuangbanna, Southwest China: role of latent heat flux. *Water* 14 (3): 395.

Kamara, A, Conteh, AR, Rhodes, E and Cooke, R. 2019. The relevance of smallholder farming to African agricultural growth and development. *African Journal of Food, Agriculture, Nutrition and Development* 19 (1): 14043-14065.

Kamble, B, Kilic, A and Hubbard, K. 2013. Estimating crop coefficients using remote sensing-based vegetation index. *Remote Sensing* 5 (4): 1588-1602.

Kapari, M, Sibanda, M, Magidi, J, Mabhaudhi, T, Nhamo, L and Mpandeli, S. 2024. Comparing machine learning algorithms for estimating the maize crop water stress index using UAV-acquired remotely sensed data in smallholder croplands. *Drones* 8 (2): 16.

Kelley, J and Higgins, C. 2018. Computational efficiency for the surface renewal method. *Atmospheric Measurement Techniques* 11 (4): 2151-2158.

Khand, K, Taghvaeian, S and Hassan-Esfahani, L. 2017. Mapping annual riparian water use based on the single-satellite-scene approach. *Remote Sensing* 9 (8): 832.

Khormizi, HZ, Malamiri, HRG and Ferreira, CSS. 2024. Estimation of evaporation and drought stress of pistachio plant using UAV multispectral images and a surface energy balance approach. *Horticulturae* 10 (5): 515.

Kibirige, D, Gokool, S and Mkhize, Z. 2023. Estimation of soil moisture using environmental covariates and machine learning algorithms in Cathedral Peak Catchment, South Africa. *Vadose Zone Journal* 23 (3): e20289.

Kunz, R, Mengistu, M, Steyn, J, Doidge, I, Gush, M, du Toit, E, Davis, N, Jewitt, G and Everson, C. 2015. *Assessment of Biofuel Feedstock Production in South Africa: Synthesis Report on Estimating Water Use Efficiency of Biofuel Crops*. 1874/1/15. Water Research Commission, Pretoria, South Africa.

Lakhiar, IA, Yan, H, Zhang, C, Wang, G, He, B, Hao, B, Han, Y, Wang, B, Bao, R, Syed, TN, Chauhdary, JN and Rakibuzzaman, M. 2024. A review of precision irrigation water-saving technology under changing climate for enhancing water use efficiency, crop yield, and environmental footprints. *Agriculture* 14 (7): 1141.

Lawal, S, Lennard, C and Hewitson, B. 2019. Response of southern African vegetation to climate change at 1.5 and 2.0° global warming above the pre-industrial level. *Climate Services* 16 (1): 100134.

Lu, S, Xuan, J, Zhang, T, Bai, X, Tian, F and Ortega-Farias, S. 2022. Effect of the shadow pixels on evapotranspiration inversion of vineyard: a high-resolution UAV-based and ground-based remote sensing measurements. *Remote Sensing* 14 (9): 2259.

Mabhaudhi, T, Nhamo, L and Mpandeli, S. 2021. Enhancing crop water productivity under increasing water scarcity in South Africa. In: eds. Ting, DSK and Stagner, JA, *Climate Change Science*. Elsevier.

Madamombe, S, Karanja, S, Oborn, I, George, N, Chirinda, N, Kihara, J and Libère, N. 2024. Climate change awareness and adaptation strategies by smallholder farmers in semi-arid areas of Zimbabwe. *International Journal of Agricultural Sustainability* 22 (1).

Maes, WH and Steppe, K. 2019. Perspectives for remote sensing with unmanned aerial vehicles in precision agriculture. *Trends in Plant Science* 24 (2): 152-164.

Mahomed, M, Clulow, AD, Strydom, S, Mabhaudhi, T and Savage, MJ. 2021. Assessment of a ground-based lightning detection and near-real-time warning system in the rural community of Swayimane, Kwazulu-Natal, South Africa. *Weather, Climate, and Society* 13 (3): 605-621.

Martins, MTB, de Souza, WR, da Cunha, BADB, Basso, MF, de Oliveira, NG, Vinecky, F, Martins, PK, de Oliveira, PA, Arenque-Musa, BC, de Souza, AP, Buckeridge, MS, Kobayashi, AK, Quirino, BF and Molinari, HBC. 2016. Characterisation of sugarcane (Saccharum spp.) leaf senescence: implications for biofuel production. *Biotechnology for Biofuels* 9 (1): 153.

Mashala, MJ, Dube, T, Mudereri, BT, Ayisi, KK and Ramudzuli, MR. 2023. A systematic review on advancements in remote sensing for assessing and monitoring land use and land cover changes impacts on surface water resources in semi-arid tropical environments. *Remote Sensing* 15 (16): 3926.

Mauder, M, Foken, T and Cuxart, J. 2020. Surface-energy-balance closure over land: a review. *Boundary-Layer Meteorology* 177 (2): 395-426.

Mayer, Z. 2014. CaretEnsemble: framework for combining caret models into ensembles (Version 1.0).

Mbangiwa, NC, Savage, MJ and Mabhaudhi, T. 2019. Modelling and measurement of water productivity and total evaporation in a dryland soybean crop. *Agricultural and Forest Meteorology* 266-267 (1): 65-72.

Messina, G and Modica, G. 2020. Applications of UAV thermal imagery in precision agriculture: state of the art and future research outlook. *Remote Sensing* 12 (1): 1491.

Meyer, J, Rein, P, Turner, P and Mathias, K. 2011. *Good Management Practices Manual for the Cane Sugar Industry.* PGBI Sugar and Bio Energy Pty Ltd, Johannesburg, South Africa.

Meza, I, Eyshi Rezaei, E, Siebert, S, Ghazaryan, G, Nouri, H, Dubovyk, O, Gerdener, H, Herbert, C, Kusche, J, Popat, E, Rhyner, J, Jordaan, A, Walz, Y and Hagenlocher, M. 2021. Drought risk for agricultural systems in South Africa: drivers, spatial patterns, and implications for drought risk management. *Science of The Total Environment* 799 (1): 149505.

Minacapilli, M, Consoli, S, Vanella, D, Ciraolo, G and Motisi, A. 2016. A time domain triangle method approach to estimate actual evapotranspiration: application in a Mediterranean region using MODIS and MSG-SEVIRI products. *Remote Sensing of Environment* 174 (1): 10-23.

Monteith, JL. 1965. Evaporation and environment. *Symposia of the Society for Experimental Biology* 19 (1): 205-234.

Moran, MS, Clarke, TR, Inoue, Y and Vidal, A. 1994. Estimating crop water deficit using the relation between surface-air temperature and spectral vegetation index. *Remote Sensing of Environment* 49 (3): 246-263.

Mukiibi, A, Franke, AC and Steyn, JM. 2023. Determination of crop coefficients and evapotranspiration of potato in a semi-arid climate using canopy state variables and satellite-based NDVI. *Remote Sensing* 15 (18): 4579.

Murray, RS, Nagler, PL, Morino, K and Glenn, EP. 2009. An empirical algorithm for estimating agricultural and riparian evapotranspiration using MODIS Enhanced Vegetation Index and ground measurements of ET. II. Application to the Lower Colorado River, U.S. *Remote Sensing* 1 (4): 1125-1138.

Nagler, PL, Scott, RL, Westenburg, C, Cleverly, JR, Glenn, EP and Huete, AR. 2005. Evapotranspiration on western U.S. rivers estimated using the Enhanced Vegetation Index from MODIS and data from eddy covariance and Bowen ratio flux towers. *Remote Sensing of Environment* 97 (3): 337-351.

Nagler, PL, Glenn, EP, Nguyen, U, Scott, RL and Doody, T. 2013. Estimating riparian and agricultural actual evapotranspiration by reference evapotranspiration and MODIS Enhanced Vegetation Index. *Remote Sensing* 5 (8): 3849-3871.

Nagler, P, Sall, I, Barreto-Muñoz, A, Gómez-Sapiens, M, Nouri, H, Chavoshi Borujeni, S and Didan, K. 2022. Effect of restoration on plant greenness and water use in relation to drought in the riparian corridor of the Colorado River Delta. *JAWRA Journal of the American Water Resources Association* 58 (5): 746-784.

Nagy, A, Kiss, NÉ, Buday-Bódi, E, Magyar, T, Cavazza, F, Gentile, SL, Abdullah, H, Tamás, J and Fehér, ZZ. 2024. Precision estimation of crop coefficient for maize cultivation using high-resolution satellite imagery to enhance evapotranspiration assessment in agriculture. *Plants* 13 (9): 1212.

Ngcobo, SI. 2023. An assessment of the potential impacts of climate variability on sugarcane production across Southern Africa. Unpublished thesis, Discipline of Hydrology, University of KwaZulu-Natal, Pietermaritzburg, South Africa.

Nhamo, L, Magidi, J, Nyamugama, A, Clulow, AD, Sibanda, M, Chimonyo, VGP and Mabhaudhi, T. 2020. Prospects of improving agricultural and water productivity through unmanned aerial vehicles. *Agriculture* 10 (7): 256.

Niu, H, Hollenbeck, D, Zhao, T, Wang, D and Chen, Y. 2020a. Evapotranspiration estimation with small UAVs in precision agriculture. *Sensors* 20 (22): 6427.

Niu, H, Wang, D and Chen, Y. 2020b. Estimating actual crop evapotranspiration using deep stochastic configuration networks model and UAV-based crop coefficients in a pomegranate orchard. *Journal of Intelligent & Robotic Systems* 104 (66).

Niu, H, Zhao, T, Wang, D and Chen, Y. 2022. Estimating evapotranspiration of pomegranate trees using stochastic configuration networks (SCN) and UAV multispectral imagery. *Journal of Intelligent & Robotic Systems* 104 (4).

Nouri, H, Beecham, S, Anderson, S and Nagler, P. 2014. High spatial resolution WorldView-2 imagery for mapping NDVI and its relationship to temporal urban landscape evapotranspiration factors. *Remote Sensing* 6 (1): 580-602.

Nouri, H, Nagler, P, Chavoshi Borujeni, S, Barreto Munez, A, Alaghmand, S, Noori, B, Galindo, A and Didan, K. 2020. Effect of spatial resolution of satellite images on estimating the greenness and evapotranspiration of urban green spaces. *Hydrological Processes* 34 (15): 3183-3199.

Okonya, J, Syndikus, K and Kroschel, J. 2013. Farmers' Perception of and Coping Strategies to Climate Change: Evidence from Six Agro-Ecological Zones of Uganda. *Journal of Agricultural Science* 5 (1): 252-262.

Omia, E, Bae, H, Park, E, Kim, MS, Baek, I, Kabenge, I and Cho, B-K. 2023. Remote sensing in field crop monitoring: a comprehensive review of sensor systems, data analyses and recent advances. *Remote Sensing* 15 (2): 354.

Omnia Nutriology. 2022. Granular Fertilizer. [Internet]. Available from: https://nutriology.co.za/nutriology/products/granular-fertiliser/. [Accessed: 30 September 2024].

Ortega-Farias, S, Irmak, S and Cuenca, RH. 2009. Special issue on evapotranspiration measurement and modelling. *Irrigation Science* 28 (1): 1-3.

Panday, US, Pratihast, AK, Aryal, J and Kayastha, RB. 2020. A review on drone-based data solutions for cereal crops. *Drones* 4 (3): 41.

Paredes, P, Martins, DS, Pereira, LS, Cadima, J and Pires, C. 2018. Accuracy of daily estimation of grass reference evapotranspiration using ERA-Interim reanalysis products with assessment of alternative bias correction schemes. *Agricultural Water Management* 210 (1): 340-353.

Pawlak, K and Kołodziejczak, M. 2020. The role of agriculture in ensuring food security in developing countries: considerations in the context of the problem of sustainable food production. *Sustainability* 12 (13): 5488.

Peddinti, SR and Kisekka, I. 2022. Estimation of turbulent fluxes over almond orchards using high-resolution aerial imagery with one and two-source energy balance models. *Agricultural Water Management* 269 (1): 107671.

Pereira, L, Paredes, P, Espírito-Santo, M and Salman, M. 2023. Actual and standard crop coefficients for semi-natural and planted grasslands and grasses: a review aimed at supporting water management to improve production and ecosystem services. *Irrigation Science* 2 (1): 1139-1170

Poblete-Echeverría, C and Ortega-Farias, S. 2013. Evaluation of single and dual crop coefficients over a drip-irrigated Merlot vineyard (Vitis viniferaL.) using combined measurements of sap flow sensors and an eddy covariance system. *Australian Journal of Grape and Wine Research* 19 (1): 249-260.

Reddy, KTC. 2020. Estimation of water use efficiency of soybean (Glycine max) for biodiesel production in KwaZulu-Natal. Unpublished thesis, Discipline of Hydrology, University of KwaZulu-Natal, Pietermaritzburg, South Africa.

Reed, DE, Frank, JM, Ewers, BE and Desai, AR. 2018. Time dependency of eddy covariance site energy balance. *Agricultural and Forest Meteorology* 249 (1): 467-478.

Rejeb, A, Abdollahi, A, Rejeb, K and Treiblmaier, H. 2022. Drones in agriculture: a review and bibliometric analysis. *Computers and Electronics in Agriculture* 198 (1): 107017.

Robertson, MJ and Donaldson, RA. 1998. Changes in the components of cane and sucrose yield in response to drying-off of sugarcane before harvest. *Field Crops Research* 55 (3): 201-208.

Roby, MC, Salas Fernandez, MG, Heaton, EA, Miguez, FE and VanLoocke, A. 2017. Biomass sorghum and maize have similar water-use-efficiency under non-drought conditions in the rain-fed Midwest U.S. *Agricultural and Forest Meteorology* 247 (1): 434-444.

Rossler, R. 2013. Water stress effects on the growth, development, and yield of sugarcane. Unpublished thesis, Department of Plant Production and Soil Science, University of Pretoria, Pretoria, South Africa.

Rostron, H. 1985. Chemical ripening of sugarcane with Fusilade Super. *Proceedings of The South African Sugar Technologists' Association.* Farmers' Organisation (Natal) (Pty)

Rouse, J.W., Haas, R.H., Schell, J.A., and Deering, D.W. 1973. Monitoring vegetation systems in the Great Plains with ERTS. *3rd ERTS Symposium*, NASA SP-351, Washington, DC, 309-317.

Savage, M, Pasi, J, Myeni, L and Clulow, A. 2017. *Open water evaporation measurement using micrometeorological methods*. Water Research Commission, Pretoria, South Africa.
Seiche, AT, Wittstruck, L and Jarmer, T. 2024. Weed detection from unmanned aerial vehicle imagery using deep learning—a comparison between high-end and low-cost multispectral sensors. *Sensors* 24 (5): 1544.
Sellers, PJ, Berry, JA, Collatz, GJ, Field, CB and Hall, FG. 1992. Canopy reflectance, photosynthesis, and transpiration. A reanalysis using improved leaf models and a new canopy integration scheme. *Remote Sensing of Environment* 42 (3): 187-216.
Segarra, J, Buchaillot, ML, Araus, JL and Kefauver, SC. 2020. Remote sensing for precision agriculture: Sentinel-2 improved features and applications. *Agronomy* 10 (5): 641.
Senay, G, Friedrichs, M, Morton, C, Parrish, G, Schauer, M, Khand, K, Kagone, S, Boiko, O and Huntington, J. 2022. Mapping actual evapotranspiration using Landsat for the conterminous United States: Google Earth Engine implementation and assessment of the SSEBop model. *Remote Sensing of Environment* 275 (1): 113011.
Shadmani, M, Marofi, S and Roknian, M. 2012. Trend analysis in reference evapotranspiration using Mann-Kendall and Spearman's Rho tests in arid regions of Iran. *Water Resources Management* 26 (1): 211-224.
Shao, G, Han, W, Zhang, H, Liu, S, Wang, Y, Zhang, L and Cui, X. 2021. Mapping maize crop coefficient Kc using Random Forest algorithm based on leaf area index and UAV-based multispectral vegetation indices. *Agricultural Water Management* 252 (1): 106906.
Shao, G, Han, W, Zhang, H, Zhang, L, Wang, Y and Zhang, Y. 2023. Prediction of maize crop coefficient from UAV multisensor remote sensing using machine learning methods. *Agricultural Water Management* 276 (1): 108064.
Shaomin, L., and Xu, Z. 2018. Micrometeorological methods to determine evapotranspiration. In: eds. Li, X and Vereecken, H, *Observation and Measurement of Ecohydrological Processes.* Springer Nature, Germany, 1-39.
Shi, Y, Thomasson, JA, Murray, SC, Pugh, NA, Rooney, WL, Shafian, S, Rajan, N, Rouze, G, Morgan, CL, Neely, HL, Rana, A, Bagavathiannan, MV, Henrickson, J, Bowden, E, Valasek, J, Olsenholler, J, Bishop, MP, Sheridan, R, Putman, EB, Popescu, S, Burks, T, Cope, D, Ibrahim, A, McCutchen, BF, Baltensperger, DD, Avant, RV, Jr., Vidrine, M and Yang, C. 2016. Unmanned aerial vehicles for high-throughput phenotyping and agronomic research. *PLoS One* 11 (7): e0159781.
Shiferaw, B, Tesfaye, K, Kassie, M, Abate, T, Prasanna, BM and Menkir, A. 2014. Managing vulnerability to drought and enhancing livelihood resilience in sub-Saharan Africa: technological, institutional and policy options. *Weather and Climate Extremes* 3 (1): 67-79.
Sibanda, M, Ndlovu, HS, Brewer, K, Buthelezi, S, Matongera, TN, Mutanga, O, Odidndi, J, Clulow, AD, Chimonyo, VGP and Mabhaudhi, T. 2023. Remote sensing hail damage on maize crops in smallholder farms using data acquired by remotely piloted aircraft system. *Smart Agricultural Technology* 6 (1): 100325.
Smit, MA and Singels, A. 2006. The response of sugarcane canopy development to water stress. *Field Crops Research* 98 (2): 91-97.
Snyder, RL, Spano, D, Duce, P, Paw U, KT and Rivera, M. 2008. Surface renewal estimation of pasture evapotranspiration. *Journal of Irrigation and Drainage Engineering* 134 (6): 716-721.
Srivastava, AK and Rai, M. 2012. Review: Sugarcane production: Impact of climate change and its mitigation. *Biodiversitas* 13 (1): 214-227.
Stoller. 2024. Sugarcane [Internet]. Corteva Agriscience. Available from: https://stollersouthafrica.co.za/sugarcane/. [Accessed: 14 October 2024].

Syngenta. 2024. Gramoxone SL 2.0 Herbicide. [Internet]. Available from: https://www.syngenta-us.com/herbicides/gramoxone-sl-2.0. [Accessed: 30 September 2024].

Tang, J, Han, W and Zhang, L. 2019. UAV multispectral imagery combined with the FAO-56 dual approach for maize evapotranspiration mapping in the North China Plain. *Remote Sensing* 11 (21): 2519.

Tanner, C.B. 1967. Measurement of evapotranspiration. In: eds. Hagan, RM, Haise, HR and Edminster, TW, *Irrigation of Agricultural Lands*. American Society of Agronomy, Inc., Madison, 11 (1): 534-574.

Testi, L, Villalobos, F and Orgaz, F. 2003. Evapotranspiration of a young irrigated olive orchard in southern Spain. *Agricultural and Forest Meteorology* 121 (1): 1-18.

Tian, X, Yan, M, Tol, C, Li, Z, Su, B, Erxue, C, Li, L, Wang, X, Pan, X, Gao, L and Han, Z. 2017. Modelling forest above-ground biomass dynamics using multi-source data and incorporated models: A case study over the qilian mountains. *Agricultural and Forest Meteorology* 246 (1): 1-14.

Tucker, CJ and Sellers, PJ. 1986. Satellite remote sensing of primary production. *International Journal of Remote Sensing* 7 (11): 1395-1416.

Twine, T, Kustas, WP, Norman, J, Cook, D, Houser, P, Teyers, TP, Prueger, J, Starks, P and Wesely, M. 2000. Correcting eddy-covariance flux underestimates over a grassland. *Agricultural and Forest Meteorology* 103 (2000) 279-300.

Vélez, S, Ariza-Sentís, M and Valente, J. 2023. VineLiDAR: high-resolution UAV-LiDAR vineyard dataset acquired over two years in northern Spain. *Data in Brief* 51 (1): 109686.

Wagner, W, Francisco, JP, Flumignan, DL, Marin, FR and Folegatti, MV. 2022. Optimised algorithm for evapotranspiration retrieval via remote sensing. *Agricultural Water Management* 262 (1): 107390.

Walker, NJ and Schulze, RE. 2006. An assessment of sustainable maize production under different management and climate scenarios for smallholder agroecosystems in KwaZulu-Natal, South Africa. *Physics and Chemistry of the Earth, Parts A/B/C* 31 (15): 995-1002.

Wilson, K, Goldstein, A, Falge, E, Aubinet, M, Baldocchi, D, Berbigier, P, Bernhofer, C, Ceulemans, R, Dolman, H, Field, C, Grelle, A, Ibrom, A, Law, BE, Kowalski, A, Meyers, T, Moncrieff, J, Monson, R, Oechel, W, Tenhunen, J, Valentini, R and Verma, S. 2002. Energy balance closure at FLUXNET sites. *Agricultural and Forest Meteorology* 113 (1): 223-243.

Woldemariam, G, Awoke, BG and Maretto, RV. 2024. Remote sensing vegetation indices-driven models for sugarcane evapotranspiration estimation in the semiarid Ethiopian Rift Valley. *Journal of Photogrammetry and Remote Sensing* 215 (1): 136-156.

Wright, JL. 1982. New evapotranspiration crop coefficients. *Journal of the Irrigation and Drainage Division* 108 (1): 57-74.

Yacoob, A, Gokool, S, Clulow, A, Mahomed, M and Mabhaudhi, T. 2024. Leveraging unmanned aerial vehicle technologies to facilitate precision water management in smallholder farms: a scoping review and bibliometric analysis. *Drones* 8 (9): 476.

Yamaç, SS and Todorovic, M. 2020. Estimation of daily potato crop evapotranspiration using three different machine learning algorithms and four scenarios of available meteorological data. *Agricultural Water Management* 228 (1): 105875.

Zarzar, CM, Dash, P, Dyer, JL, Moorhead, R and Hathcock, L. 2020. Development of a simplified radiometric calibration framework for water-based and rapid deployment unmanned aerial system operations. *Drones* 4 (2): 17.

Zhang, L, Zhang, H, Niu, Y and Han, W. 2019. Mapping maize water stress based on UAV multispectral remote sensing. *Remote Sensing* 11 (1): 605.

Zhao, Y, Wu, J, Guo, C, Wu, H, Wang, J, Zhang, Q, Xiao, Y and Qiu, R. 2023. Comparing the eddy covariance and gradient methods for measuring water and heat fluxes in paddy fields. *Agricultural Water Management* 284 (1): 108340.

Zhou, MM, Singels, A and Savage, MJ. 2003. Physiological parameters for modelling differences in canopy development between sugarcane cultivars. *Agricultural and Food Sciences* 7 (1): 610-621.

*****

Lead-In to Chapter 4:

Building upon the empirical findings of Chapter 3, which evaluated unmanned aerial vehicle (UAV)-based remote sensing (RS) for evapotranspiration (ET) estimation, Chapter 4 presents the development of a UAV-based Normalised Difference Water Index (NDWI) predictive model. Correlation analyses, integrating UAV- and in-situ-derived data, will explore the relationships between predicted NDWI, other structural vegetation indices (SVIs) (Normalised Difference VI [NDVI], Green NDVI [GNDVI], Optimised Soil-Adjusted VI [OSAVI], etc.), and in-situ measurements (chlorophyll content [CC], leaf area index [LAI], crop height, etc.) to understand the biophysical mechanisms influencing sugarcane water status. Temporal NDWI dynamics are analysed using critical environmental factors to assess the impact of climate variability. Finally, the chapter discusses the model's practical implications for smallholder farmers in South Africa—its potential as a user-friendly, cost-effective tool for water stress monitoring and improved irrigation management—concluding with recommendations for future research. This chapter integrates the empirical results with the theoretical framework and literature review of Chapters 1 and 2 to offer a comprehensive interpretation and discussion of the findings within the context of sustainable sugarcane production in water-scarce regions.

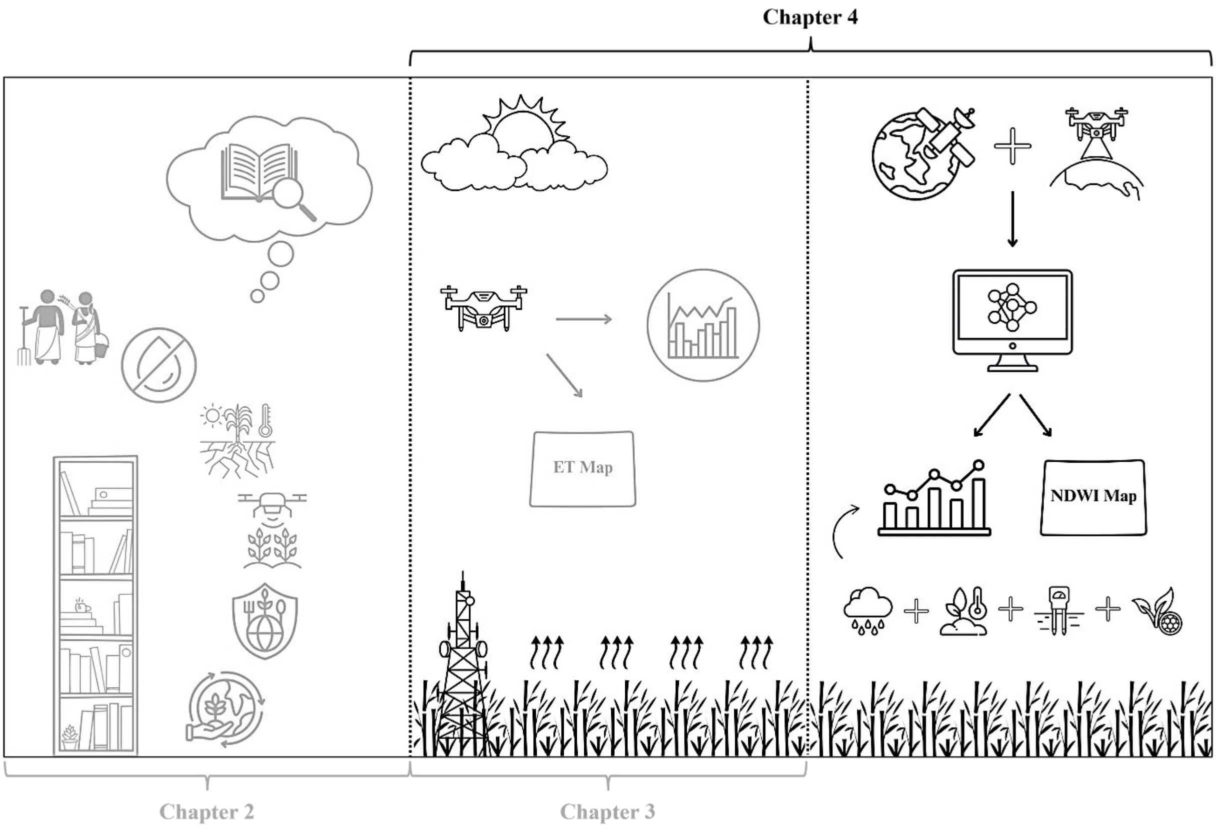

4. CHAPTER 4: A MACHINE LEARNING APPROACH FOR QUANTIFYING CROP WATER STRESS IN SMALLHOLDER FARMS USING UNMANNED AERIAL VEHICLE MULTISPECTRAL IMAGERY (PAPER 3)

Ameera Yacoob [1*], Shaeden Gokool [1], Alistair Clulow [1,2], Maqsooda Mahomed [1], Vivek Naiken [1,2] and Tafadzwanashe Mabhaudhi [3,4]

[1] *Centre for Water Resources Research, School of Agricultural, Earth & Environmental Sciences, University of KwaZulu-Natal, P/Bag X01, Scottsville, Pietermaritzburg 3209, South Africa; gokools@ukzn.ac.za; clulowa@ukzn.ac.za; mahomedm@ukzn.ac.za; naikenv@ukzn.ac.za*

[2] *Discipline of Agrometeorology, School of Agricultural, Earth and Environmental Sciences, University of KwaZulu-Natal, P/Bag X01, Scottsville, Pietermaritzburg 3209, South Africa*

[3] *Centre for Transformative Agricultural and Food Systems, School of Agricultural, Earth & Environmental Sciences, University of KwaZulu-Natal, P/Bag X01, Pietermaritzburg 3209, South Africa; tafadzwanashe.mabhaudhi@lshtm.ac.uk*

[4] *Centre of Climate Change and Planetary Health, London School of Hygiene and Tropical Medicine, London, United Kingdom*

[*] *Correspondence: 218023873@stu.ukzn.ac.za; Tel.: +27-792913882*

Abstract:

This study investigates the critical challenge of water stress impacting sugarcane production among smallholder farmers in Swayimane, KwaZulu-Natal, South Africa. The Normalised Difference Water Index (NDWI) is a vital indicator of vegetation water content and stress, which is essential for understanding agricultural water dynamics. Subsequently, this research presents a novel machine-learning (ML) model to predict NDWI using Sentinel-2 satellite data and unmanned aerial vehicle (UAV)-acquired multispectral imagery. The model demonstrates

---

This chapter is a working draft for submission to the *Agricultural Water Management* journal (Elsevier). It includes additional sections and details tailored to the comprehensiveness required for this master's thesis. The chapter will be revised to comply with the journal's submission requirements.

References in this chapter follow the 2019 Bioresources Engineering style from the Centre for Water Resources Research, University of KwaZulu-Natal.

high predictive accuracy, achieving a coefficient of determination (R^2) of 0.95, with Root Mean Square Error (RMSE) and Mean Absolute Error (MAE) of 0.03 and 0.02, respectively, effectively capturing spatiotemporal water stress during stalk elongation (SE) and early maturation (M) phases. Strong correlations between predicted NDWI and parameters—such as Normalised Difference Vegetation Index (NDVI), Green NDVI (GNDVI), and Optimised Soil Adjusted Vegetation Index (OSAVI)—enhance the model's robustness. Additionally, a positive correlation (R^2 = 0.60) with evapotranspiration (ET) highlights NDWI's role as a proxy for sugarcane water status. In contrast, a negative correlation (R^2 = 0.62) with the Water Deficit Index (WDI) emphasises its sensitivity to water deficits. Although further research is needed to address limitations related to data availability and model generalisability, particularly the reliance on a single study site and a limited training dataset, this study represents a significant advancement in data provision for precision water management to facilitate sustainable sugarcane cultivation, improve crop yields and enhance regional food security efforts in South Africa.

Keywords: irrigation strategies; NDWI prediction; precision farming; smallholder agriculture; sugarcane; UAV-based monitoring; water stress

4.1 Introduction

Widespread water scarcity, erratic weather patterns, and arid conditions increasingly compromise agricultural productivity in South Africa (Lickley and Solomon, 2018). This crisis disproportionately affects many smallholder farmers across the region, who cultivate less than two hectares of land and predominantly practice dryland agriculture, leading to significant water-related challenges due to unpredictable precipitation (Rockstrom, 2000; Adisa *et al.*, 2018). Consequently, livelihoods and food security remain acutely threatened. The absence of comprehensive, spatially explicit tools for assessing water stress in small-scale agricultural settings, particularly sugarcane cultivation, significantly hinders effective mitigation strategies (Andersson *et al.*, 2009; Lu *et al.*, 2017). South Africa, a key player in the Southern African Development Community (SADC), which collectively contributes nearly 58% of Africa's sugar production and exports over 1.2 million tonnes annually, faces increasing pressure to sustain its agricultural output amid environmental challenges (Ngcobo, 2023).

Limited access to financial resources, technology, and appropriate irrigation systems causes substantial socio-economic hardships among these smallholder farmers (Gokool *et al.*, 2023).

This situation is severely exacerbated by sugarcane's high water demand (approximately 850 mm per growth cycle for sustainable rainfed production) (Carr and Knox, 2011; Jones *et al.*, 2015) and the effects of climate change, which include increased drought frequency, reduced water availability, and amplified precipitation variability (Knox *et al.*, 2010; Archer *et al.*, 2019; IPCC, 2019). The urgent need for adequate water stress detection and mitigation strategies in South Africa is evident, as the lack of comprehensive assessment tools hinders the implementation of such measures (Bezuidenhout and Singels, 2007; Andersson *et al.*, 2009; Dunkelberg *et al.*, 2014; Olivier and Singels, 2015; Lu *et al.*, 2017).

While various factors may influence crop growth, water stress frequently emerges as the primary constraint on plant development (Haarhoff *et al.*, 2020; Zaib *et al.*, 2023). Water deficits can induce stomatal closure, reducing transpiration and increasing leaf temperature due to decreased evaporative cooling (Jackson, 1982; Saseendran *et al.*, 2015). This thermal response, quantifiable via infrared thermography, provides a non-invasive method for assessing plant water status (Brewer *et al.*, 2022a). Traditional methods for evaluating crop water stress—relying on in-situ measurements, soil moisture content, or climatic factors—are often time-consuming, expensive, and labour-intensive (González-Dugo *et al.*, 2006; Safdar *et al.*, 2023), particularly in regions like South Africa, where security concerns further compromise their efficacy (Gray *et al.*, 2022).

Remote Sensing (RS) techniques, which utilise specific regions of the electromagnetic spectrum to indirectly measure crop water content via the biochemical properties of leaves, offer a promising alternative (Brewer *et al.*, 2022a; Liu *et al.*, 2023; Safdar *et al.*, 2023). Narrow-band indices, particularly those using visible and red-edge spectral regions, have proven effective in detecting crop water stress (Zarco-Tejada *et al.*, 2013; Zhao *et al.*, 2015), and are often preferred over thermal infrared (TIR) methods due to limitations in capturing physiological changes associated with water stress, such as alterations in photosynthetic pigments and reductions in non-stomatal photosynthesis (Ihuoma *et al.*, 2021). Therefore, supplemental spectral indices sensitive to chlorophyll and other pigments are recommended to assess plant water status comprehensively (Brewer *et al.*, 2022a).

Vegetation Indices (VIs), derived from leaf reflectance in the visible and near-infrared (NIR) spectrum, are widely used to evaluate crop health and water status (Brewer *et al.*, 2022a). The Normalised Difference Vegetation Index (NDVI), while commonly employed (Zhao *et al.*, 2015; Leroux *et al.*, 2016), can be unreliable due to soil reflectance and viewing geometry

(Roujean and Breon, 1995; Haboudane *et al.*, 2002), despite its established use in estimating crop coefficients and aiding irrigation scheduling (Allen *et al.*, 1998; Baluja *et al.*, 2012; Jones, 2014). Alternative indices, such as the Green NDVI (GNDVI) and the Optimised Soil Adjusted Vegetation Index (OSAVI), improve chlorophyll detection and reduce soil brightness effects (Bajwa and Vories, 2006; Baluja *et al.*, 2012; Ihuoma and Madramootoo, 2017), providing valuable tools for monitoring plant stress.

Water indices directly assess vegetation and soil water content, offering advantages over traditional VIs for water stress detection (Virnodkar *et al.*, 2020). The NDWI, utilising NIR and shortwave infrared (SWIR) reflectance (approximately 860 nm and 1240 nm, respectively), is particularly effective (Ihuoma and Madramootoo, 2017). By including the SWIR band, the NDWI's sensitivity to vegetation water content is further enhanced; this addition reduces variability from soil brightness and non-photosynthetic materials, thereby improving the accuracy of plant water stress detection and optimising irrigation management (Ihuoma and Madramootoo, 2017). While water-absorption bands (1300-2500 nm) are highly sensitive to leaf water content, high absorption limits the precise quantification of plant canopy water content (Carter, 1991; Peñuelas and Filella, 1998). In the study by Gao (1996), the NDWI, combining the NIR and SWIR reflectance, effectively addresses this limitation by mitigating the confounding effects of leaf internal structure and dry matter content (Gao, 1996; Wang *et al.*, 2015).

RS technologies are crucial in monitoring crop conditions and water stress in precision agriculture (PA). Among these technologies, unmanned aerial vehicles (UAVs) provide a robust, cost-effective tool for high-resolution imagery acquisition, particularly for detecting crop water stress in smallholder farming (Zhang *et al.*, 2019; Nhamo *et al.*, 2020). Unlike satellite imagery, UAVs offer customisable ground sampling distances and temporal resolution, enabling continuous monitoring and mitigating atmospheric interference (Gokool *et al.*, 2023). This facilitates precise mapping and analysis of fields, empowering farmers to manage water stress proactively. Furthermore, integrating machine learning (ML) algorithms enhances remotely sensed data by identifying non-linear relationships among variables and managing complex datasets, thereby facilitating meaningful insights in diverse agricultural contexts (Yacoob *et al.*, 2024). However, while UAV-based multispectral (MS) cameras are more widely adopted than hyperspectral systems due to their cost-effectiveness, many MS cameras lack a SWIR band (Bertalan *et al.*, 2022), preventing direct NDWI calculation.

Although satellite-based RS can provide NDWI data, the spatial resolution often limits the capture of within-field variability, especially in smallholder farms. As such, accurately assessing crop water stress presents significant challenges due to limitations in traditional RS methods (which may exhibit lower spatial resolution and reduced temporal frequency) and the high cost of advanced sensor technologies (Rejeb *et al.*, 2022). Spatial trade-offs among RS platforms influence crop monitoring; satellite imagery offers broad coverage but often fails to capture fine-scale variability detectable by UAVs, which provide higher resolution at the cost of limited area coverage (Brewer *et al.*, 2022a; Gokool *et al.*, 2023). Subsequently, this study leverages ML to establish robust relationships between NDWI and various structural VIs (SVIs), inter alia, NDVI, OSAVI, and GNDVI, to overcome the limitations of using UAV-based MS sensors which lack the SWIR band. Additionally, high chlorophyll content (CC) indicates active plant growth and increased water usage, thus correlates strongly with NDWI, providing a basis for predictive modelling. Consequently, integrating Satellite Earth Observation (SEO) data with ML offers a cost-effective and comprehensive solution for monitoring crop water stress in PA.

Consequently, this study endeavours to attain the following objectives:

i. Determine the relationships between satellite-derived NDWI and other SVIs, namely NDVI, GNDVI, Red Edge NDVI (NDVIre), SAVI, Transformed Chlorophyll Absorption in Reflectance Index (TCARI), OSAVI, and TCARI/OSAVI, using ML techniques. This objective analyses the interactions and dependencies among these indices, creating a foundation for subsequent modelling efforts.
ii. Derive a predictive model for satellite-derived NDWI based on the identified UAV-acquired structural indices. By leveraging the correlations identified in the previous objective, this predictive model aims to provide an efficient framework for estimating NDWI, facilitating timely and informed decision-making for water management in agricultural practices.
iii. Correlate the predicted UAV-based NDWI estimates with in-situ derived actual evapotranspiration (ETa) measurements and the Water Deficit Index (WDI). This objective focuses on validating the accuracy of the predictive model by comparing it to traditional measures of plant water status, thereby ensuring that the estimates derived from UAV data align with established agricultural metrics.

This research aims to provide smallholder farmers in South Africa with a reliable tool for monitoring crop water stress. By integrating RS techniques and advanced ML algorithms, the study enhances the ability to more adequately account for crop water stress within smallholder farm settings, offering actionable insights into the agricultural challenges in the country. The expected outcomes include an improved understanding of crop water dynamics, enabling more effective irrigation strategies that enhance food security and livelihoods. Ultimately, this study will contribute to the sustainability of sugarcane production and strengthen the resilience of smallholder farming systems in the face of variable climatic conditions.

4.2 Methodology

4.2.1 Study site overview

The study was conducted in the uMgungundlovu District Municipality (UMDM), situated within the uMshwathi Local Municipality (LM), approximately 65 km northeast of Pietermaritzburg in KwaZulu-Natal, South Africa. The LM encompasses urban areas such as Wartburg, New Hanover, Dalton, and Cool Air, alongside significant rural residential settlements, including Swayimane, Mpolweni, Thokozani, and Ozwathini (Mahomed *et al.*, 2021). This research was specifically focused on the rural settlement of Swayimane (29°31′24″ S; 30°41′37″ E, Figure 4.1), a predominantly agricultural region covering an area of 32 km^2 (Basdew *et al.*, 2017). The region has a subtropical climate, featuring warm and wet summers and cool and dry winters. The area supports agricultural activities with annual precipitation ranging from 600 to 1200 mm (Brewer *et al.*, 2022a) and contributes as the primary source of irrigation for croplands. Notably, the KwaZulu-Natal Midlands, located within the UMDM, is recognised as a region highly vulnerable to climate change in South Africa, facing substantial environmental, social, and economic impacts due to its warmer climate and projected changes. Subsequently, the UMDM is particularly susceptible to increased rainfall and extreme events, including wildfires, flash floods, and storms (Mahomed *et al.*, 2021).

Furthermore, the region's soils, primarily loam and clay, are highly fertile, ranking among the top 2% of South Africa's highest-potential arable soils (Ndlovu *et al.*, 2021). Most households in the research study area are female-headed and encounter mild food insecurity and poverty, primarily due to high unemployment rates (Ndlovu *et al.*, 2021). Agriculture serves as the primary source of livelihood for these households, with cultivation concerning a diverse array of vegetables such as maize, taro (amadumbe), sweet potato, cabbage, spinach, carrots, and tomatoes inter alia (Brewer *et al.*, 2022a). Additionally, sugarcane is a critical cash crop in the region (Cockburn *et al.*, 2014). These crops are predominantly grown using traditional methods, with a limited reliance on chemical fertilisers and a greater emphasis on organic composting. Several governmental and non-governmental organisations actively support the agricultural sector in Swayimane (Khumalo, 2016). Their initiatives encompass training in modern agricultural techniques, the distribution of seeds and farming inputs, and facilitating market access. Local farmers predominantly utilise small-scale agrarian practices, with a subset incorporating semi-mechanised methods for planting and harvesting.

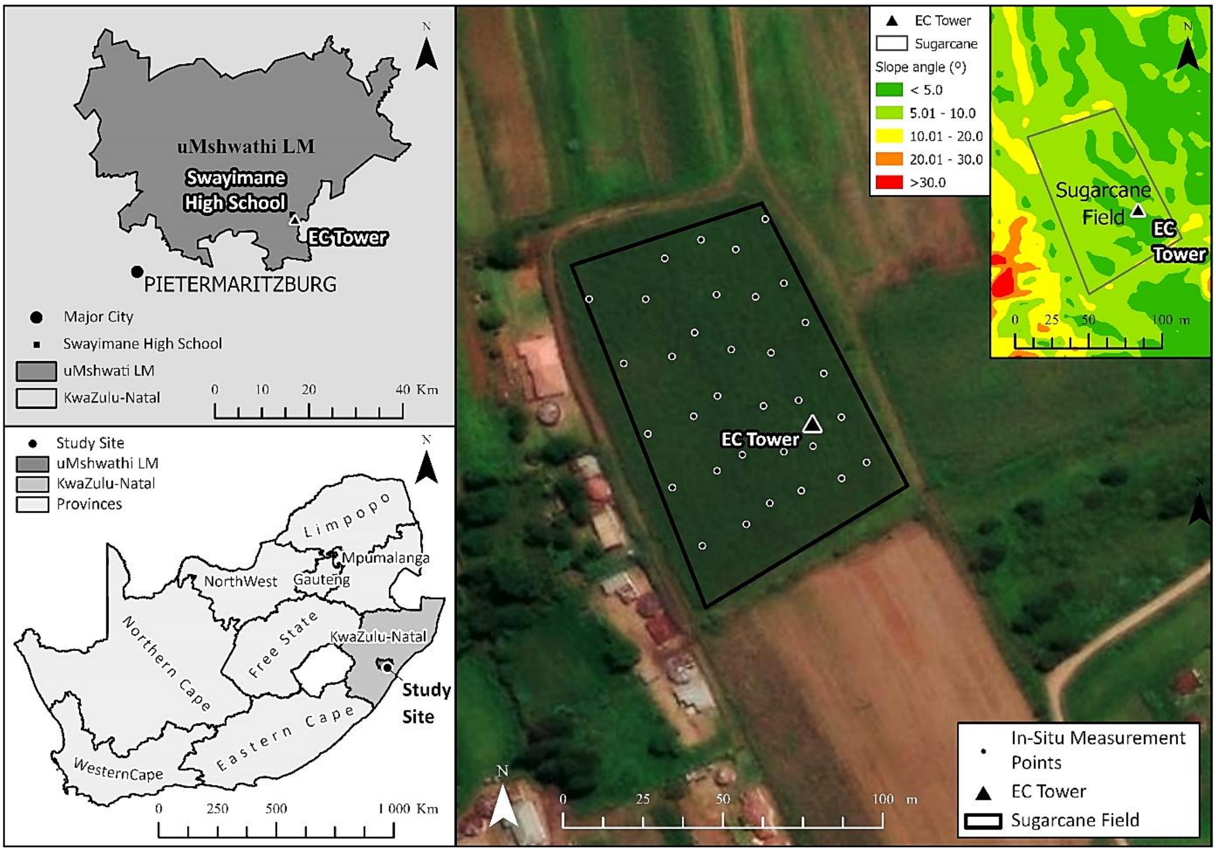

Figure 4.1 Map detailing the study area featuring a smallholder sugarcane field in Swayimane, KwaZulu-Natal, South Africa. Highlighted are the positions of the Automatic Weather Station (AWS) located at the local high school, the eddy covariance (EC) system within the sugarcane field, and an analysis of slope angles across the field.

A small-scale sugarcane field characterised by sloping terrain, covering 7253.74 m^2 with elevations ranging from 843.24 to 850.95 m, served as the research site (ESRI, 2024). Equipped with a meteorological flux tower, the site featured sensors for comprehensive measurements, including precipitation (mm), wind speed (m s^{-1}), solar irradiance (MJ m^{-2}), and air temperature (°C). During data collection (1 July 2023 to 15 May 2024), Swayimane reported a total rainfall of 1228.35 mm and an average daily air temperature of 17.93 °C, as indicated in Figure 4.2. Additionally, measurements recorded an average wind speed of 2 m s^{-1}, relative humidity of 80.71%, and solar irradiance of 13.69 MJ m^{-2} (Figure 4.3).

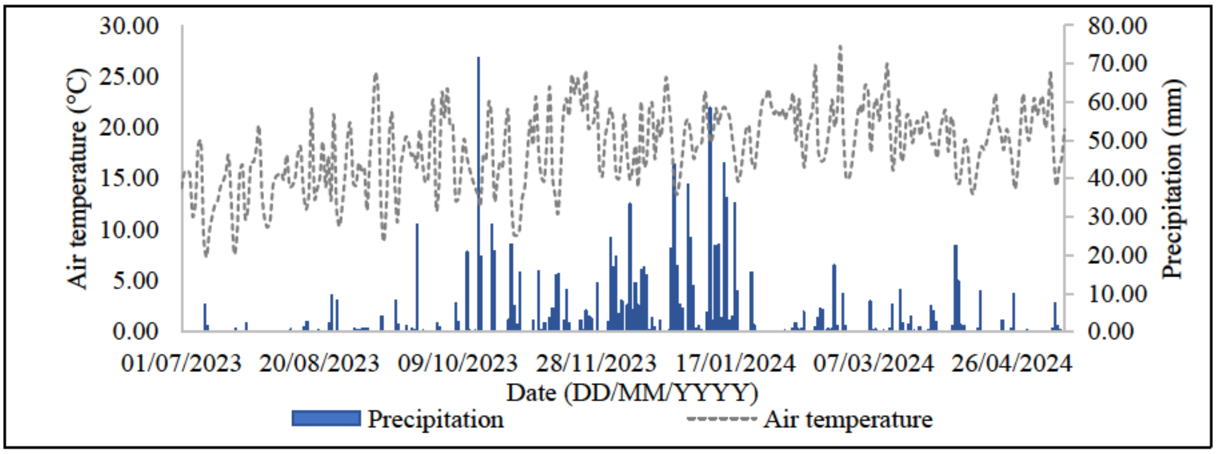

Figure 4.2 Daily recorded meteorological conditions in Swayimane over the data collection period, including precipitation (mm) and air temperature (°C) measured with site-specific instrumentation.

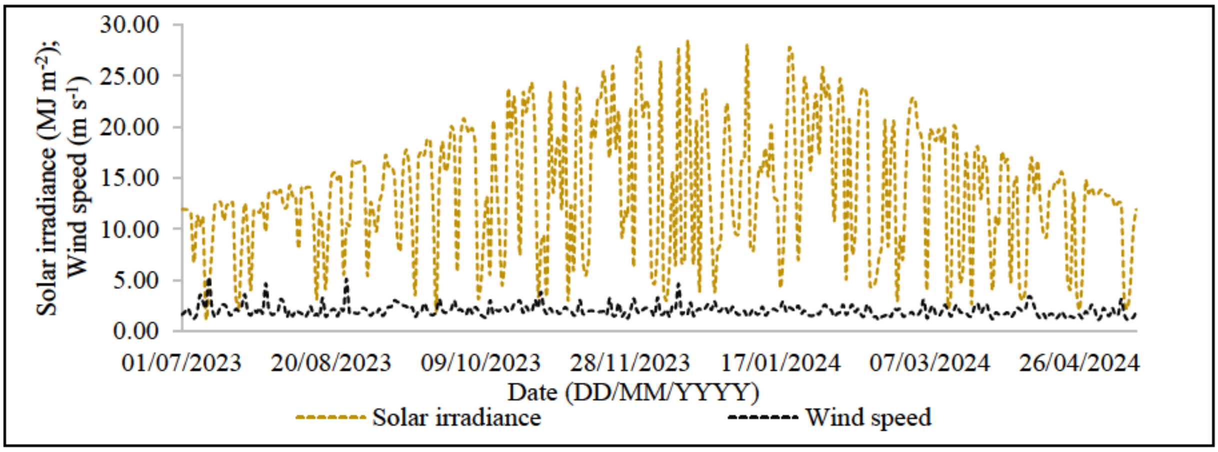

Figure 4.3 Daily meteorological conditions featuring wind speed (m s^{-1}) recorded using an on-site instrument and solar irradiance (MJ m^{-2}) data from the AWS at the high school in Swayimane.

4.2.2 Sugarcane phenotyping

The sugarcane ratoon crop completed a growth cycle of 547 days (18 months) with successive harvests from November 30, 2022, to May 30, 2024. The crop progressed through distinct developmental phases: germination (G), tillering (T), stalk elongation (SE), and maturation (M) (Figure 4.4). Data collection commenced ≈ 7.5 months into the growth cycle (July 18, 2023), revealing that the crop had already entered the SE phase. Subsequently, literature was consulted to identify typical timelines and characteristics of the G, T, SE and M phases (Table 4.1). The initial stages of M were assessed by correlating observational data with existing research despite the absence of specific cultivar details. Notably, the data collection period (July 18, 2023 – March 15, 2024) encompassed only the SE and early M phases before the scheduled harvest in May 2024.

4.2.2.1 Germination

During the ratoon stool activation phase, initiated post-harvest, dormant buds sprout into primary canes, which is crucial for the subsequent growth cycle (Stoller, 2024). Adequate soil moisture is vital; water stress can delay or inhibit sprouting, resulting in fewer, weaker shoots (Toppa *et al.*, 2011). Factors such as stool health, environmental conditions, and post-harvest practices play a critical role (Stoller, 2024). Concurrently, fibrous roots at the stool base facilitate anchorage and nutrient uptake; however, water stress detrimentally affects root proliferation and function (Moore and Berding, 2013). Simultaneously, new leaves develop, enhancing photosynthesis through stored nutrients, though reduced by water stress (Moore and Berding, 2013). Additionally, secondary shoots, or tillers, emerge from lateral buds on the primary canes, increasing stand density and yield potential (Meyer *et al.*, 2011; Xu *et al.*, 2021).

4.2.2.2 Tillering

Tillering in sugarcane involves sequential gemma budding on the primary stalk, forming secondary and tertiary stalks essential for the crown formation and final stalk population (Stoller, 2024). Each tiller develops fibrous roots, with crown roots occupying the top 30 cm of soil within 90–120 days (Stoller, 2024). Peak tillering relies on competition for light, water, and nutrients, achieving optimal yields with 10–13 tillers per metre for complete ground cover (Stoller, 2024). Water stress hinders growth, reduces tillering potential, and lowers yield by limiting leaf area and photosynthetic efficiency, affecting the crop's overall vigour and productivity (Inman-Bamber, 2004). Post-tillering, stalks increase in height and accumulate sucrose at the base internodes as older leaves desiccate and senesce (Meyer *et al.*, 2011).

4.2.2.3 Stalk elongation

During the SE phase in sugarcane, the root system undergoes dynamic lateral and deep growth (Smith *et al.*, 2005; Pierre *et al.*, 2019), forming cord roots extending over 1.5 m, primarily in the upper 0.35–0.4 m of soil (Stoller, 2024). Although the crop is inherently drought-tolerant, water stress restricts SE by limiting root development (Inman-Bamber and Smith, 2005) and nutrient uptake (Misra *et al.*, 2020) essential for height and sucrose accumulation (Meyer *et al.*, 2011). Optimal light, moisture, and temperature levels promote vertical growth, potentially adding an internode weekly (Stoller, 2024). Conversely, water stress negatively impacts flowering by reducing panicle quantity and reproductive success (Mehdi *et al.*, 2024).

4.2.2.4 Maturation

During the M phase of sugarcane, vigorous post-tillering growth facilitates the relocation of surplus photosynthates to the base internodes for storage (Stoller, 2024). By late summer to early autumn, a 2.5-metre-tall cane exhibits yellowing leaves in the middle third, indicating sucrose accumulation (Stoller, 2024). As late autumn and early winter approach, M intensifies while growth decreases, marking the completion of M (Stoller, 2024). This period sees increased sucrose transfer from leaves to mature internodes (Glassop *et al.*, 2007). Water stress compromises sugar production by hindering sett germination and impairing flowering. This leads to reduced panicle formation and fertility, thereby significantly impacting M (Mehdi *et al.*, 2024) (see Appendix C for details on sugarcane growth dynamics and management).

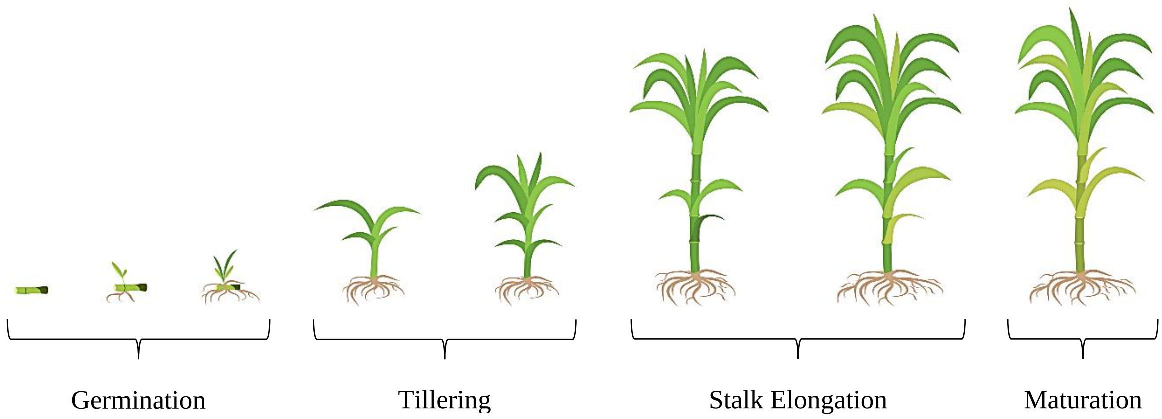

Figure 4.4 The growth phases of a sugarcane ratoon crop.

Table 4.1 Growth stages and descriptions of sugarcane.

Days after emergence	Growth stage	Description	Picture
0-30	Germination	Regrowth initiates from the residual stubble after the previous crop's harvest (Sakaigaichi *et al.*, 2013). The swelling of buds on the stubble leads to the emergence of new shoots (Edgerton, 1934).	
31-120	Tillering	Tillering, a critical yield-determining phase (Riaz *et al.*, 2023), involves the rapid development of multiple shoots from the stubble base, establishing the plant population (Matsuoka, 2012).	
121-390	Stalk Elongation	During the SE phase, sugarcane exhibits rapid stem growth, significant leaf area expansion (Som-ard *et al.*, 2021), and peak photosynthetic activity, resulting in maximal biomass accumulation (Lofton *et al.*, 2012).	
391-547	Maturation	Growth decelerates as the stalks mature, increasing sugar content due to sucrose accumulation (Lofton *et al.*, 2012). Leaf senescence commences, indicating the plant's preparation for harvest (Martins *et al.*, 2016).	

4.2.3 Methodological framework for field data collection

4.2.3.1 The Water Deficit Index calculation

The WDI quantitatively illustrates the relationship between actual ET (ETa) and potential ET (ETp) (see Equation 4.1) (Moran *et al.*, 1994; Antoniuk *et al.*, 2021). ETa was measured using an EC system that provides real-time, high-accuracy assessments of water vapour flux in the sugarcane crop (see Section 4.2.3.2 for more details). ETp was estimated by multiplying reference ET (ETo) values by crop coefficient (Kc) factors for each growth stage. The parameters were set to Kc_{mid} = 1.25 during the SE phase and Kc_{end} = 0.75 for M (Allen *et al.*, 1998) (further information regarding the calculation of ETo can be found in Section 4.2.3.3).

$$\mathrm{WDI} = 1 - \frac{\mathrm{ETa}}{\mathrm{ETp}} \tag{4.1}$$

Calculating the WDI is essential for validating UAV-derived NDWI values, providing a direct metric for assessing crop water status. While recognising the uncertainty in comparing WDI and NDWI is important due to potential impacts on the precision of water stress assessments, understanding their interaction could enhance NDWI's robustness as an indicator of vegetation water content. However, temperature-based indicators like the Crop Water Stress Index (CWSI) are often preferred for their reliability in quantifying crop water stress (Zhang *et al.*, 2019; Yacoob *et al.*, 2024). Nevertheless, these approaches can potentially support informed decision-making in agricultural water management.

4.2.3.2 Eddy covariance system implementation

ETa was quantified using an EC system to precisely measure latent heat flux (Le) in the field. A 4-metre meteorological flux tower was installed within the sugarcane field, with its instrumentation oriented to align with the prevailing wind direction (Figure 4.5a). The structure was equipped with an open-path infrared gas analyser and a sonic anemometer (IRGASON, Campbell Scientific, Logan, UT, USA), operating at a 10 Hz observation rate, enabling direct measurement of Le. A 3D sonic anemometer (CSAT3A, Campbell Scientific, Logan, UT, USA) was used to determine sensible heat flux (H). Additionally, a net radiometer (CNR4-L, Campbell Scientific, Logan, UT, USA) was incorporated to calculate net radiation (Rn) by measuring incoming and reflected longwave and shortwave radiation (Figure 4.5b).

Soil heat flux (G) was quantified in row and interrow areas utilising two heat flux plates installed at a depth of 0.06 m (HFP01-L, Hukseflux, Delft, The Netherlands). In addition, four soil averaging thermocouples were employed to monitor soil temperature at depths of 0.04 m and 0.08 m. Water content reflectometers (CS616, Campbell Scientific, Logan, UT, USA), positioned at depths of 0.30 m, 0.60 cm, and 0.90 m, provided data on soil moisture conditions. Additionally, air temperature and relative humidity were recorded via two integrated probes (H2CS3, Campbell Scientific, Logan, UT, USA) close to the IRGASON. A rain gauge (TE525MM-L, Campbell Scientific, Logan, UT, USA) accounted for precipitation events.

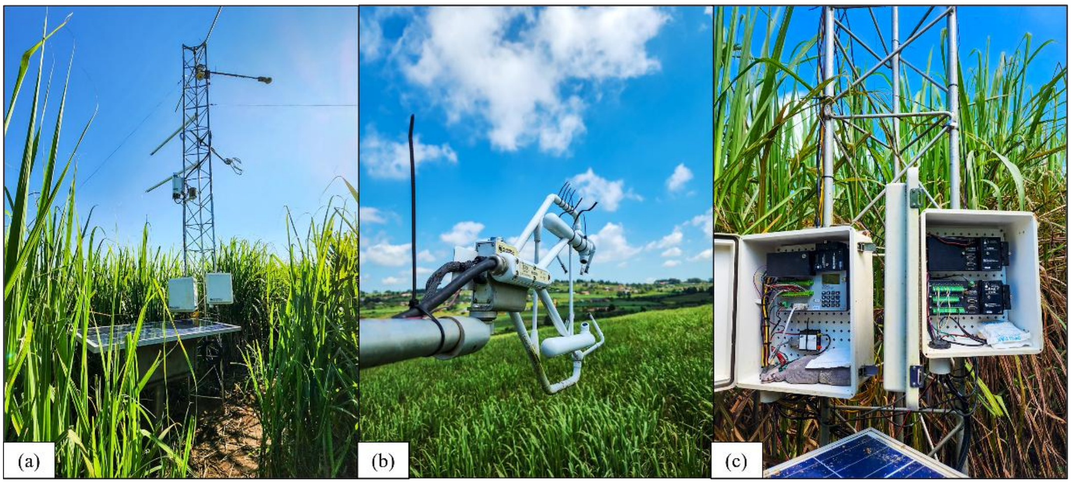

Figure 4.5 Overview of the EC system: (a) EC setup, (b) IRGASON open-path infrared gas analyser, and (c) CR3000 and CR1000 data loggers.

All instruments underwent factory calibration before deployment in the field, ensuring their accuracy and reliability. Meteorological sensors were affixed at various heights on the tower to capture a range of atmospheric conditions. Data loggers (CR3000 and CR1000, Campbell Scientific, Logan, UT, USA) were configured to record at 30-minute intervals (Figure 4.5c). Easy Flux™ DL software facilitated the acquisition of fully corrected fluxes for CO_2, Le, H, G, and momentum from the EC system. The subsequent data cleaning process involved a series of essential steps using Microsoft Excel: (1) a time-based filter was applied to include only those flux data recorded between 6:00 AM and 6:00 PM (SAST), acknowledging the significance of solar radiation in the context of energy balance; (2) negative values for Rn and G were systematically excluded, including scenarios where G exceeded Rn; (3) from September 16 to October 26, 2023, a correction factor for G was instituted due to missing data, calculated based on the mean ratio of G to Rn derived from data collected between July 1 and September 15, resulting in a correction of 6.64%; (4) any periods containing NaN (not a number) values were eliminated; and (5) rigorous quality control measures were enforced, leading to the omission of data with QA grades 6-9 (Savage *et al.*, 2017).

4.2.3.3 Reference evapotranspiration calculation using the Penman-Monteith equation

The Penman-Monteith equation (Monteith, 1965) is widely recognised as the leading approach for calculating ETo (in mm day^{-1}) (see Equation 4.2) (Chimonyo *et al.*, 2016; Roby *et al.*, 2017).

$$\mathrm{ETo} = \frac{0.408\Delta(\mathrm{R_n} - \mathrm{G}) + \gamma \frac{900}{\mathrm{T} + 273} \mathrm{u_2}(\mathrm{e_s} - \mathrm{e_a})}{\Delta + \gamma(1 + 0.34\mathrm{u_2})} \tag{4.2}$$

In this context, Δ represents the slope of the saturation vapour pressure curve in kPa°C^{-1}, Rn denotes net radiation in MJ m^{-2} day^{-1}, and G signifies soil heat flux density, also measured in MJ m^{-2} day^{-1}. The psychrometric constant (γ) is expressed in kPa°C^{-1}, T indicates air temperature in degrees Celsius, u_2 refers to wind speed in m s^{-1}, e_s represents saturation vapour pressure in kPa, and e_a indicates actual vapour pressure in kPa (for further details on ETo, see Section 3.2.3.1 in Chapter 3). ETo was calculated using Equation 4.2 over the crop analysis period from July 18, 2023, to March 15, 2024. Meteorological data required for these calculations were obtained from instruments affixed to the meteorological tower, which recorded half-hourly measurements that were subsequently aggregated into daily values. This aggregation enabled WDI calculation and subsequent validation of predicted NDWI values.

4.2.3.4 In-situ data collection techniques

Chlorophyll content in sugarcane foliage was assessed using a Konica Minolta SPAD 502 meter (Minolta Corporation, Ltd., Osaka, Japan), which provides portable, non-destructive measurements of red (650 nm) and infrared (940 nm) light transmittance through leaves. This device yields a dimensionless Soil Plant Analysis Development (SPAD) value indicative of CC (Sibanda *et al.*, 2020; Brewer *et al.*, 2022a). Measurements were conducted during optimal photosynthetic hours, specifically from 10:00 AM to 2:00 PM (SAST).

During the SE phase, SPAD readings were taken from the most recently fully expanded leaf at the leaf blade-sheath junction. In the maturity phase, the focus shifted to the uppermost flag leaf, which is vital for photosynthetic efficiency. Measurements were obtained from three specific locations on a single leaf per plant: mid-length near the primary vein, one-third from the apex, and two-thirds from the apex. The average SPAD values from these sites enhanced accuracy, with the device shielded from direct sunlight during readings (Brewer *et al.*, 2022b).

Chlorophyll measurements coincided with UAV image acquisition, facilitating a comprehensive plant health analysis. SPAD data were converted into CC using the equation from Markwell *et al.* (1995), resulting in a coefficient of determination (R^2) of 0.94 (Markwell *et al.*, 2004; Brewer *et al.*, 2022b).

$$\mathrm{Chl} = 10^{\mathrm{M}(0.264)} \quad (4.3)$$

Chl denotes the total chlorophyll concentration per unit leaf area measured in micromoles per square metre (μmol m^{-2}), while M in this context indicates the dimensionless SPAD value (Ling *et al.*, 2011).

LAI was obtained using the LAI-2200C sensor (Li-Cor, Inc., Lincoln, NE, USA)—the measurement protocol employed a sensor equipped with a 45° view cap (Castro-Nava *et al.*, 2016). To improve measurement accuracy, data collection was prioritised in the early morning and late afternoon under overcast sky conditions to minimise direct sunlight effects, reducing glare and variability in the readings (Castro-Nava *et al.*, 2016). The LAI-2200C was positioned vertically above the sugarcane canopy, aiming the sensor head downward to capture light transmission through the leaves. At each sampling point, 12 measurements were taken—four above the canopy and eight below—to account for natural variability. Above-canopy readings were performed under various conditions for reliability, including (1) diffuser caps in direct sunlight, (2) diffuser caps in shaded areas, (3) readings without a cap in shaded conditions, and (4) conducting standard readings without any modifications or caps.

The foliar temperature of the sugarcane crop was assessed using the Testo Thermal Imager 882 (Testo SE & Co. KGaA, Lenzkirch, Germany). Readings were taken between 10:00 AM and 2:00 PM (SAST) to align with UAV flight missions and optimal photosynthetic conditions (Brewer *et al.*, 2022a). The imager was aimed at the uppermost leaves, specifically, the flag leaves, from approximately 1 metre away from the canopy to ensure a clear line of sight. Multiple readings were averaged from three points on each leaf: mid-length, one-third from the apex, and two-thirds from the apex. Thermal images and numerical temperature data were documented to analyse foliar temperature distribution across the crop (see Appendix D for measurement device details). Additionally, sugarcane height was measured using a ruler positioned vertically alongside the main stem, capturing the distance from ground level to the apex (tip of the tallest leaf).

4.2.3.5 Field sampling protocols

A sampling strategy was developed to address the characteristics of sugarcane and the difficulties of traversing the field. The sugarcane field was divided into six equal sections, with sampling points strategically arranged in a grid layout along the rows approximately 10 metres apart. Six samples were extracted from each section, yielding 36 samples. However, three points were excluded from the analysis due to their proximity to the field's edge and location outside the designated sugarcane shapefile, resulting in a final sample size of 33 (Figure 4.1).

4.2.3.6 UAV: DJI Matrice 300 and MicaSense Altum camera

The DJI Matrice 300 (M300) non-RTK version drone, equipped with the MicaSense Altum multispectral sensor and a downwelling light sensor (DLS-2), was employed to capture imagery of the smallholder farm (Figures 4.6a and 4.6b). The robust quadcopter design with vertical take-off and landing (VTOL) capabilities makes the M300 ideal for operations in remote agricultural zones. The flight parameters included an 80% longitudinal image overlap at a flying height of 100 m. The platform's extended endurance of up to 42 minutes and a top speed of 27 m s^{-1} allowed extensive agricultural areas to be covered in a single flight. The DJI M300's technological features, combined with its versatile capabilities, render it an optimal choice for PA applications, as demonstrated in recent studies (Vélez *et al.*, 2023; Khormizi *et al.*, 2024).

The MicaSense Altum camera, designed for agricultural analysis, integrates a radiometric thermal camera with five narrow spectral bands, simultaneously capturing thermal, multispectral, and RGB images during one flight (Zarzar *et al.*, 2020). The spectral bands include blue (475 nm), green (560 nm), red (668 nm), red edge (717 nm), and NIR (842 nm) (as outlined in Table 4.2) (Brewer *et al.*, 2022a; Seiche *et al.*, 2024). With high spatial and radiometric resolution, this technology is ideal for plant-level ML applications such as identifying agricultural water stress. The camera was mounted on the UAV stabiliser system for automated image capture, facilitating image acquisition along predetermined flight paths and specific locations programmed into the UAV controller (Seiche *et al.*, 2024).

The Altum camera provides significant advantages through its global shutter mechanism, ensuring accurate spatial resolution and image alignment, even during high-speed UAV flights (Brewer *et al.*, 2022a). The optical sensors offer a resolution of 2064 × 1544 pixels (3.2 megapixels per spectral band) at a 120-metre altitude, resulting in a ground sample distance (GSD) of 0.052 m per pixel. This level of precision is crucial for detecting subtle variations in plant health and identifying early signs of stress or disease. The thermal infrared sensor, with a 160 × 120 pixels resolution and a GSD of 0.81 m per pixel at the same altitude, enables the detection of temperature variations in the agricultural field, providing valuable insights into plant water stress and soil moisture levels (see Appendix E for detailed specifications).

Figure 4.6 (a) MicaSense Altum camera, (b) DJI-M300 series platform.

Table 4.2 MicaSense Altum camera specifications (after Brewer *et al.*, 2022a).

Band	Spectral colour	Band centre/range (nm)	GSD at 120 m (m pixel^{-1})
1	Blue	475	0.052
2	Green	560	0.052
3	Red	668	0.052
4	Red Edge	717	0.052
5	Near-Infrared (NIR)	842	0.052
6	LWIR Thermal Infrared	8000 - 14000	0.81

4.2.3.7 UAV: image acquisition and processing

The flight area was delineated on the UAV console to define the geographical boundaries of the Swayimane study area (depicted in Figure 4.7a), facilitating semi-autonomous flight operations (refer to Table 4.3). Emphasis was placed on scheduling UAV flights during periods of minimal cloud cover to optimise data acquisition conditions. Twelve flights were conducted between 1 July 2023 and 15 March 2024, with the specific dates documented in Appendix F alongside the UAV-derived VI maps. The MicaSense Altum camera was calibrated using the Calibrated Reflectance Panel (CRP) pre- and post-flight, ensuring consistent radiometric standards (Figure 4.7b) (Brewer *et al.*, 2022a). Imaging sessions were conducted between 10:00 AM and 1:00 PM (SAST) to minimise shadows, leverage optimal sunlight angles and maintain stable air and soil temperatures (Khormizi *et al.*, 2024).

Following each UAV flight mission, aerial images were processed using Pix4Dfields photogrammetry software (Brewer *et al.*, 2022b) (version 1.8.0, Pix4D Inc., San Francisco, California, USA). The software's automated functions were employed for radiometric corrections and mosaic generation, producing an orthomosaic and digital surface model (DSM). The processed data was exported in GeoTIFF format to facilitate seamless integration into Geographic Information System (GIS) software for subsequent analytical procedures. This workflow ensured the transformation of raw aerial data into actionable geospatial information, supporting analysis and interpretation of environmental dynamics within the study area.

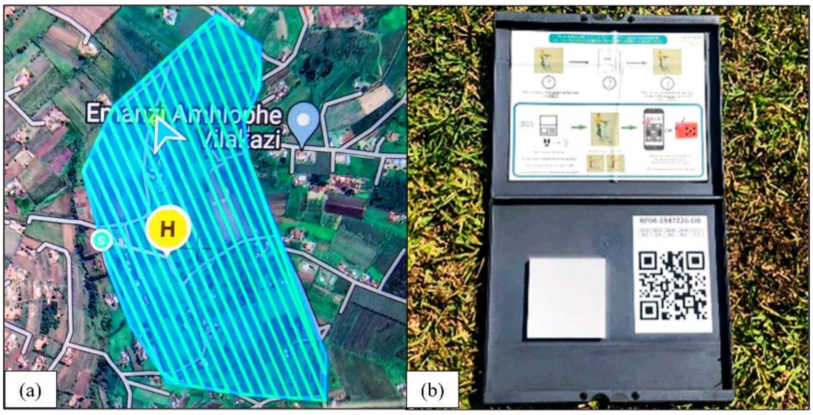

Figure 4.7 (a) Flight plan for the DJI-M300, (b) CRP for the MicaSense Altum camera.

Table 4.3 Operational details and specifications for the DJI M300 UAV.

Parameter	**Specification**
Altitude	100 m
GSD	0.07 m $pixel^{-1}$
Speed	10 m s^{-1}
Flight duration	36 minutes 32 seconds
Image overlap	80%
Camera system	MicaSense Altum

4.2.4 Remote sensing data acquisition and machine learning model development for Normalised Difference Water Index prediction

4.2.4.1 Data preparation for Sentinel-2 imagery in Google Earth Engine

In Google Earth Engine (GEE), training data acquisition points were strategically established within the sugarcane field to ensure representation. Three rows of five points were placed, avoiding proximity to field edges. Sentinel-2 data (1 July 2023–31 May 2024) were imported at 10 m (visible and near-infrared), 20 m (red-edge and shortwave infrared), and 60 m (atmospheric correction) resolutions. A 20% cloud cover threshold was applied for cloud masking to enhance data quality by removing obscured pixels. This timeframe resulted in a dataset comprising 28 images. These images generated a dataset of 420 points (28 images × 15 points) for subsequent analyses in Microsoft Excel and R Studio (Allaire, 2024). Relevant spectral bands from the Sentinel-2 data were selectively extracted to support further analysis.

Various VIs were computed for each image in the Sentinel-2 dataset to enable feature extraction using specific functions and integrated as bands within the image structure (refer to Table 4.4). Following this, the script progressed to a stage of time series analysis by implementing the VI calculation function across the image collection, thereby enhancing each image with the computed indices. Temporal information was then integrated into the image collection by incorporating date properties, enabling the retrieval of time series data for each predefined point within the feature collection. Upon completing the time series analysis, a time series of VI data for each specified point was exported to Google Drive as a Comma-Separated Values (CSV) file.

Table 4.4 Overview of VIs and corresponding equations.

Vegetation index	Abbreviation	Equation	Reference
Normalised Difference Water Index	NDWI	$\frac{(\mathrm{NIR} - \mathrm{SWIR})}{(\mathrm{NIR} + \mathrm{SWIR})}$	(Gao, 1996)
Normalised Difference Vegetation Index	NDVI	$\frac{(\mathrm{NIR} - \mathrm{RED})}{(\mathrm{NIR} + \mathrm{RED})}$	(Huang *et al.*, 2020)
Green Normalised Difference Vegetation Index	GNDVI	$\frac{(\mathrm{NIR} - \mathrm{GREEN})}{(\mathrm{NIR} + \mathrm{GREEN})}$	(Rozenstein *et al.*, 2018)
Normalised Difference Vegetation Index for Red Edge	NDVIre	$\frac{(\mathrm{NIR} - \mathrm{RED\ EDGE})}{(\mathrm{NIR} + \mathrm{RED\ EDGE})}$	(Pironato Amaro *et al.*, 2024)
Soil-Adjusted Vegetation Index	SAVI	$(1 + 0.5) \times \left(\frac{(\mathrm{NIR} - \mathrm{RED})}{(\mathrm{NIR} + \mathrm{RED} + 0.5)}\right)$	(Brewer *et al.*, 2022a)
Transformed Chlorophyll Absorption in Reflectance Index	TCARI	$3 \times ((\mathrm{RED\ EDGE} - \mathrm{RED}) - 0.2 \times (\mathrm{RED\ EDGE} - \mathrm{GREEN}) \times (\mathrm{RED\ EDGE}/\mathrm{RED}))$	(Shang *et al.*, 2015)

Table 4.5 Overview of VIs and corresponding equations – continuation of Table 4.4.

Vegetation index	Abbreviation	Equation	Reference
Optimised Soil-Adjusted Vegetation Index	OSAVI	$\frac{(\mathrm{NIR} - \mathrm{RED})}{(\mathrm{NIR} + \mathrm{RED} + 0.16)}$	(Romero Ponce *et al.*, 2018)
TCARI/OSAVI Ratio	TO	$\frac{\mathrm{TCARI}}{\mathrm{OSAVI}}$	(Haboudane *et al.*, 2002)

4.2.4.2 Predictive modelling of the Normalised Difference Water Index using UAV-derived data in R Studio

The VI time series was imported into R Studio (Allaire, 2024) to develop and assess ML algorithms (MLAs) for predicting NDWI using VIs. The methodology consisted of several stages: data preprocessing, model training, evaluation, and prediction using the trained models (Figure 4.8). Initially, the focus was on preprocessing Sentinel-2 data from the CSV file. The data was shuffled to introduce randomness, optimising the models' performance in handling unseen data, thereby increasing the reliability and accuracy of the predictions. The dataset was partitioned into training and validation sets utilising a standard 80/20 split (Gokool *et al.*, 2022), separating predictor and target variables for dedicated training and testing data frames.

A variety of MLAs, including Generalised Linear Model (GLM), k-Nearest Neighbours (kNN), Classification and Regression Trees (CART), Random Forest (RF), Gradient Tree Boosting (GTB), and Support Vector Machine (SVM) (Kibirige *et al.*, 2023), were implemented and assessed using the caret package (Kuhn, 2008; Mayer, 2014). Performance metrics such as Root Mean Squared Error (RMSE), R^2, and Mean Absolute Error (MAE) were calculated to identify the most effective models for ensemble modelling (Gokool *et al.*, 2022). The best-performing model was selected based on these metrics, and two ensemble models were then developed by combining predictions from multiple base models. The optimal ensemble model was applied to the validation dataset for predictive analysis. Performance metrics were then computed to evaluate the model's performance on unseen data.

The study extended its analysis to predict NDWI values on UAV-derived raster data. The script loaded raster data from a GeoTIFF file and transformed it into a data frame. The trained ensemble model was then used to predict NDWI values for the raster data. These predicted NDWI values were added as a new column in the raster data frame, which was converted back into a raster object and saved as a GeoTIFF file for further analysis and visualisation. In summary, this study not only detailed the process of training, evaluating, and applying ML models for estimating NDWI from VIs but also demonstrated the utility of these models in predicting NDWI values on raster data.

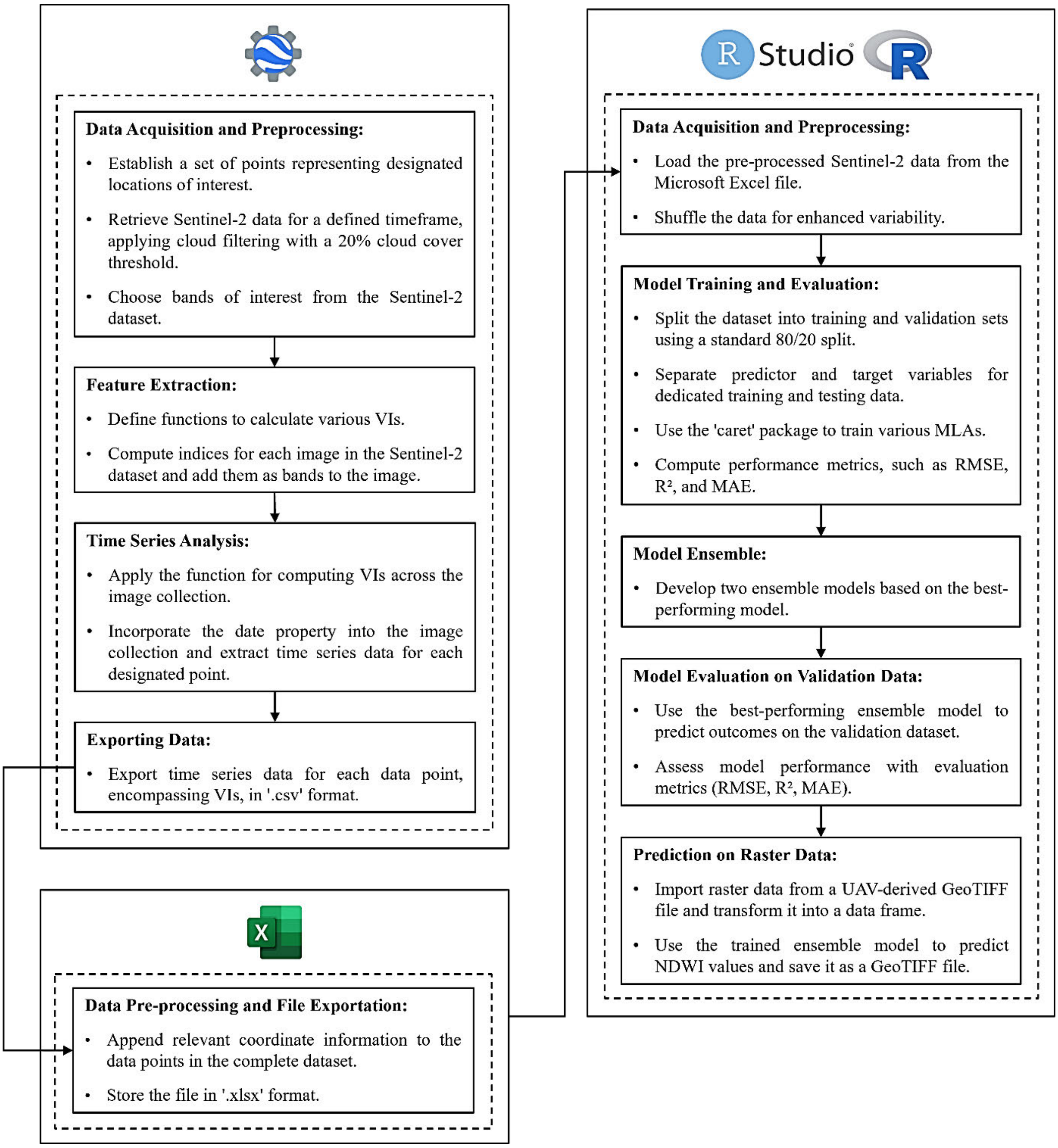

Figure 4.8 Conceptual flow diagram illustrating the methodology and framework for RS data acquisition, feature extraction, and ML model development for NDWI prediction.

4.2.5 Data processing and analytical methodology

The analysis integrated in-situ measurements, UAV-acquired multispectral data, and Sentinel-2 satellite imagery to evaluate crop water stress dynamics. This section details the methodological framework for data extraction, correlation analyses, and multivariate assessments, ensuring consistency in dataset integration and spatial alignment.

To compare Sentinel-2 satellite-derived VIs with in-situ measurements, VIs were extracted using GEE at 15 predefined sampling points across all available images between July 2023 and May 2024. Temporal trends in sugarcane's SE and early M phases were assessed using descriptive statistics, including mean, median, standard deviation, minimum, and maximum values. Corresponding in-situ measurements—CC, LAI, and crop height—were recorded at 33 sampling locations, as outlined in Section 4.2.3.5, to determine whether satellite-based indices reflected observed physiological variations.

For UAV-based analyses, multispectral data and ensemble model-predicted NDWI were spatially linked to the in-situ sampling points. The geographic coordinates of the in-situ measurement locations were imported into ArcGIS Pro to extract UAV-derived raster values, ensuring spatial consistency across datasets. This extraction process was uniformly applied to all subsequent analyses, including Pearson correlation assessments, violin plots, principal component analysis (PCA), and three-dimensional (3D) surface visualisations.

Correlation analysis quantified relationships between UAV-derived SVIs, predicted NDWI, and in-situ crop parameters. Similarly, violin plots were generated to illustrate the distribution of UAV-derived SVIs, predicted NDWI, and EC-derived ETa across sugarcane's phenological stages. PCA evaluated the interrelationships among spectral indices, predicted NDWI, and physiological parameters, offering a multivariate perspective on crop water status. Finally, 3D surface plots were developed to visualise interactions between VIs, CC, and LAI, further clarifying trends in plant water dynamics.

4.3 Results

4.3.1 Comparative analysis of vegetation indices during sugarcane growth phases: insights from Sentinel-2 imagery

Table 4.6 provides a comparative analysis of VIs for the sugarcane SE and early M phases, derived from Sentinel-2 imagery and analysed using statistical measures including mean, median, standard deviation, minimum, and maximum values.

Table 4.6 VIs derived from Sentinel-2 imagery for sugarcane SE and early M growth phases.

Statistic	Phase	NDWI	NDVI	GNDVI	NDVIre	SAVI	TCARI	OSAVI	TO
Mean	SE	0.25	0.70	0.64	0.48	0.43	0.11	0.39	0.28
	M	0.34	0.78	0.70	0.57	0.49	0.10	0.48	0.22
Median	SE	0.26	0.70	0.64	0.48	0.43	0.11	0.40	0.27
	M	0.35	0.79	0.70	0.57	0.49	0.10	0.48	0.21
Std dev	SE	0.11	0.07	0.05	0.08	0.06	0.01	0.07	0.07
	M	0.06	0.03	0.03	0.04	0.03	0.01	0.03	0.03
Min	SE	-0.09	0.51	0.51	0.23	0.29	0.07	0.18	0.18
	M	0.15	0.71	0.62	0.43	0.38	0.07	0.36	0.17
Max	SE	0.45	0.85	0.74	0.63	0.55	0.14	0.53	0.70
	M	0.43	0.84	0.75	0.65	0.55	0.13	0.55	0.33

The mean values of VIs indicate overall crop health and water status, with NDWI increasing from 0.25 in the SE phase to 0.34 in the early M phase, suggesting reduced water stress as the crop matures. Similarly, NDVI, GNDVI, and NDVIre also rise from SE to early M, reflecting improved crop health over time. These indices, sensitive to vegetation greenness and CC, imply denser and more vigorous growth during early M. The mean increases in SAVI (0.43 to 0.49) and OSAVI (0.39 to 0.48) further support this, as they account for soil brightness and provide a clearer picture of vegetation health. In contrast, TCARI shows a notable decline from 0.11 in the SE phase to 0.10 in the early M phase, indicating a slight decrease in chlorophyll absorption as the crop matures. A slight reduction in TO (TCARI/OSAVI) (from 0.28 to 0.22) suggests subtle changes in canopy structure as the crop transitions from active growth to early M.

Median values align with these trends, confirming the consistency of the VIs across growth phases. The decreasing standard deviation from SE to early M, such as the drop in NDWI from 0.11 to 0.06, indicates less variability and more uniform growth and water status during early M. This stabilisation is crucial for achieving consistent crop quality and yield. Minimum and maximum values reveal the range of crop health and water status, with higher minimum values of NDWI, NDVI, and GNDVI during the early M phase, indicating improved conditions even for the most stressed parts of the crop. While there are slight increases in maximum values, particularly in NDVIre and OSAVI, highlighting the crop's enhanced health and moisture retention, the significant drop in maximum TO from 0.70 in the SE phase to 0.33 in early M suggests a notable shift in canopy structure and potential reductions in photosynthetic efficiency.

4.3.2 In-situ analysis of sugarcane physiological parameters across growth phases: correlations with satellite-derived indices

The in-situ measurements in Table 4.7 provide a detailed analysis of sugarcane's physiological characteristics during the SE and early M phases. The parameters analysed include CC, LAI, and crop height, with statistical measures offering insights into the crop's development and health. The mean values indicate improvements in crop health as the sugarcane transitions from SE to early M. For instance, mean CC increases from 249.92 μmol m^{-2} in SE to 550.41 μmol m^{-2} in early M, suggesting enhanced chlorophyll concentration, improved photosynthetic activity, and overall plant health. Similarly, mean LAI rises from 3.92 to 5.13, reflecting more substantial leaf area development, crucial for maximising photosynthetic efficiency. Additionally, mean crop height increases significantly from 226.00 m in SE to 273.00 m in early M, signalling active vegetative growth.

The median values follow similar trends to the mean values, reinforcing the observed improvements in crop conditions from SE to early M phases. The standard deviation analysis reveals a slight reduction in variability for CC and LAI from SE to early M (CC: 54.91 to 45.23 μmol m^{-2}; LAI: 0.94 to 0.69), suggesting more uniform chlorophyll distribution and leaf area during early M. This reduction in variability is crucial for achieving consistent crop quality. The minimum values for CC and LAI show significant increases from SE to early M, indicating improved conditions even in the least developed parts of the crop. For example, the minimum CC rises from 19.67 μmol m^{-2} in SE to 249.43 μmol m^{-2} in early M, implying better CC and health even in the most stressed plants as they mature. Conversely, the maximum values remain high across both phases, with slight increases from SE to early M, highlighting the potential for optimal growth during early M.

In-situ measurements align closely with satellite-derived VIs such as NDWI, NDVI, GNDVI, NDVIre, SAVI, OSAVI, TCARI, and TO. The increase in CC from SE to early M corresponds with rises in NDVI, GNDVI, and NDVIre, which are sensitive to chlorophyll and vegetation greenness. This confirms that both in-situ and satellite data indicate healthier, more chlorophyll-rich foliage as the crop matures. Furthermore, LAI increases during the early M phase support the upward trends in NDWI, SAVI, and OSAVI. The higher NDWI indicates increased vegetation water content, suggestive of enhanced biomass and potentially reduced water stress, consistent with the observed increases in LAI. In summary, the in-situ measurements during the SE and early M phases, particularly regarding CC and LAI, strongly corroborate the trends observed in satellite-derived VIs. Both datasets show improved crop health, density, and uniformity as sugarcane matures, providing a thorough assessment of its development during these phases.

Table 4.7 Descriptive statistics of sugarcane crop parameters across the SE and early M growth phases.

Statistic	Phase	CC (μmol m^{-2})	LAI	Crop height (m)
Mean	SE	249.87	3.92	226.00
	M	550.45	5.13	273.00
Median	SE	247.52	3.67	225.00
	M	539.03	5.09	280.00
Std dev	SE	54.91	0.94	31.00
	M	45.23	0.69	55.00
Minimum	SE	19.67	2.01	121.00
	M	249.43	3.37	130.00
Maximum	SE	446.31	9.52	320.00
	M	880.52	7.72	360.00

4.3.3 Evaluating ensemble model performance for predicting the Normalised Difference Water Index: a comparative analysis

The ensemble models' performance for predicting the NDWI was evaluated using a set of performance metrics: R^2, RMSE, and MAE. Table 4.8 presents the comparative results of the two ensemble models. Ensemble Model 1 showed strong predictive capability, with an R^2 of 0.87, explaining 87% of the NDWI variance. Its RMSE and MAE values were 0.04 and 0.03, respectively, indicating reliable accuracy. Ensemble Model 2 outperformed Model 1, achieving an R^2 of 0.95, capturing 95% of the variance. It also had lower RMSE (0.03) and MAE (0.02), reflecting enhanced precision and reduced errors. These findings demonstrate that Ensemble Model 2 offers more accurate and consistent NDWI predictions, likely due to the effective integration of base models within the ensemble (refer to Appendix F for spatiotemporal NDWI maps and additional UAV-based SVI maps).

Table 4.8 Ensemble model results.

	R^2	RMSE	MAE
Ensemble model 1	0.87	0.04	0.03
Ensemble model 2	0.95	0.03	0.02

4.3.4 Correlation analysis of predicted Normalised Difference Water Index with UAV-derived structural indices and in-situ measurements

The correlation plot reveals key relationships between predicted NDWI, UAV-derived VIs, and in-situ measurements, providing significant insights into crop water status (Figure 4.9). A negative correlation between NDWI and NIR (R = −0.51) suggests that increased NIR reflectance corresponds to reduced NDWI values, indicating a possible decrease in crop water content. This relationship underlines NDWI's sensitivity to water stress, with the positive correlations observed between NDWI and indices like NDVI (R = 0.51) and GNDVI (R = 0.52), suggesting that higher vegetation vigour and CC are associated with improved water status, thus reflecting healthier crop conditions.

Further, the moderate correlation between predicted NDWI and LAI (R = 0.41) highlights the link between canopy structure and water availability, implying that a denser canopy may enhance water retention, which is critical during growth phases. The positive, albeit weaker, correlation with crop height (R = 0.31) indicates that taller crops, potentially resulting from adequate water supply, may exhibit better overall growth. This finding and the moderate correlation between predicted NDWI and CC (R = 0 .33) suggest that water status, as NDWI indicates, is integral to the crop's photosynthetic efficiency and overall vitality.

The minimal correlation between predicted NDWI and foliar temperature (R = 0.10) raises questions about the factors influencing foliar temperature independent of NDWI. This indicates that external environmental conditions or stressors may have a greater impact on foliar temperature than water status. The strong positive correlation between NDWI and OSAVI (R = 0.63) highlights the efficacy of soil-adjusted VIs in evaluating water content. OSAVI integrates vegetation structure and water status, serving as a robust indicator for crop monitoring. This analysis emphasises the importance of monitoring NDWI alongside SVIs and in-situ measurements to comprehensively assess crop water status and health during critical phenological stages.

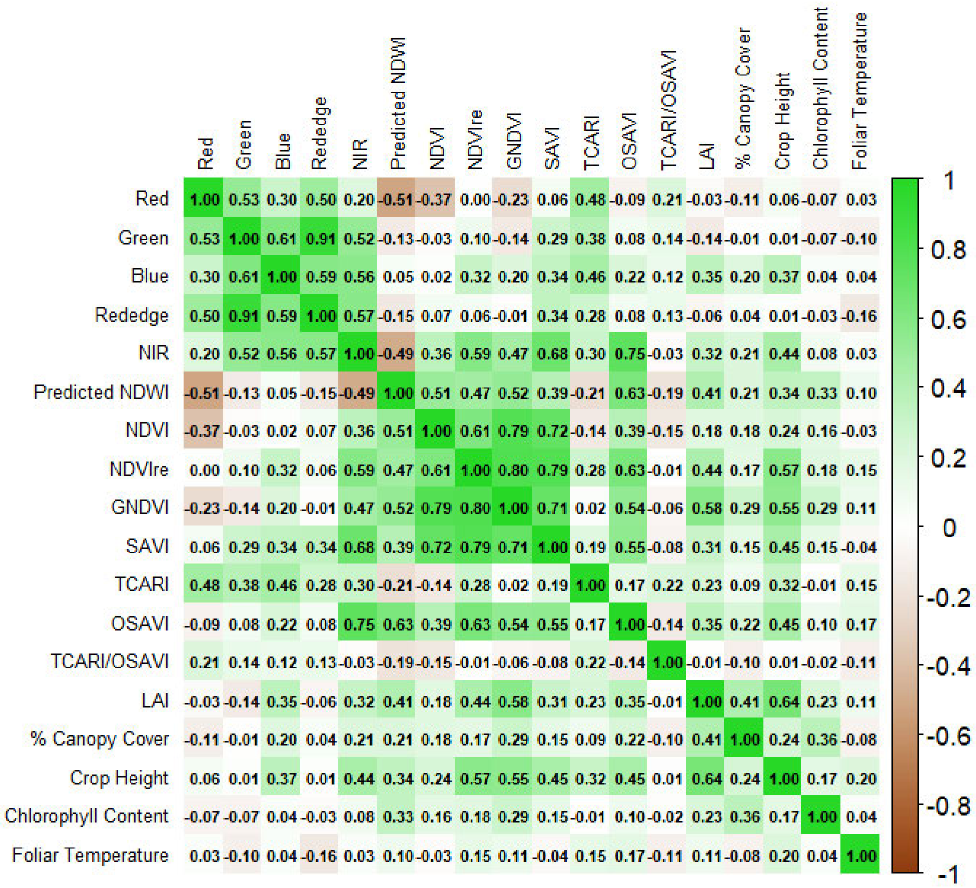

Figure 4.9 Pearson correlation (R) plot of predicted NDWI with UAV-derived SVIs and in-situ measurements across SE and early M phenological stages.

4.3.5 Comparative violin plot analysis of predicted Normalised Difference Water Index, UAV-based vegetation indices, and actual evapotranspiration during stalk elongation and early maturation phases

The ET-EC distributions demonstrate distinct patterns between growth phases. SE exhibits a broader range of ET-EC values, indicating significant variability in water loss through ETa (Figure 4.10i). Conversely, the early M phase shows a more constrained distribution, suggesting consistent ETa rates as the crop canopy fully establishes and efficiently manages water use. Predicted NDWI values reveal a marked increase during early M, reflecting enhanced vegetation water content as the crop matures (Figure 4.10a). The more consistent distribution during early M indicates stability in moisture retention across the field. In contrast, SE shows a broader range of values, possibly due to uneven plant establishment and growth rates.

NDVI, GNDVI, and NDVIre showcase higher and more consistent values during early M, denoting uniformity in canopy greenness and vigour (Figures 4.10b–d). SE displays more variability, likely due to spatial differences in growth and development. This variability highlights the heterogeneity inherent in earlier growth stages. SAVI and OSAVI patterns emphasise the impact of soil brightness and biomass accumulation on VIs (Figures 4.10e and 4.10g). The early M phase shows reduced variability in these indices, suggesting a fully developed canopy with less soil influence on spectral data. SE presents broader distributions, indicating varying degrees of canopy development.

During SE, TCARI values are more variable, possibly reflecting differences in CC as the crop is established (Figure 4.10f). In contrast, the early M phase shows higher mean TCARI values with reduced variability, indicating stabilised chlorophyll levels and a fully developed canopy. However, TCARI/OSAVI values slightly decrease during the early M phase, marking a shift in canopy health as sugarcane enters the early M phase (Figure 4.10h). This decline suggests a stabilisation of chlorophyll levels and changes in canopy structure, consistent with the crop's transition from active growth to physiological maturity. The reduced variability in the early M phase further highlights the uniformity in crop conditions as the canopy stabilises.

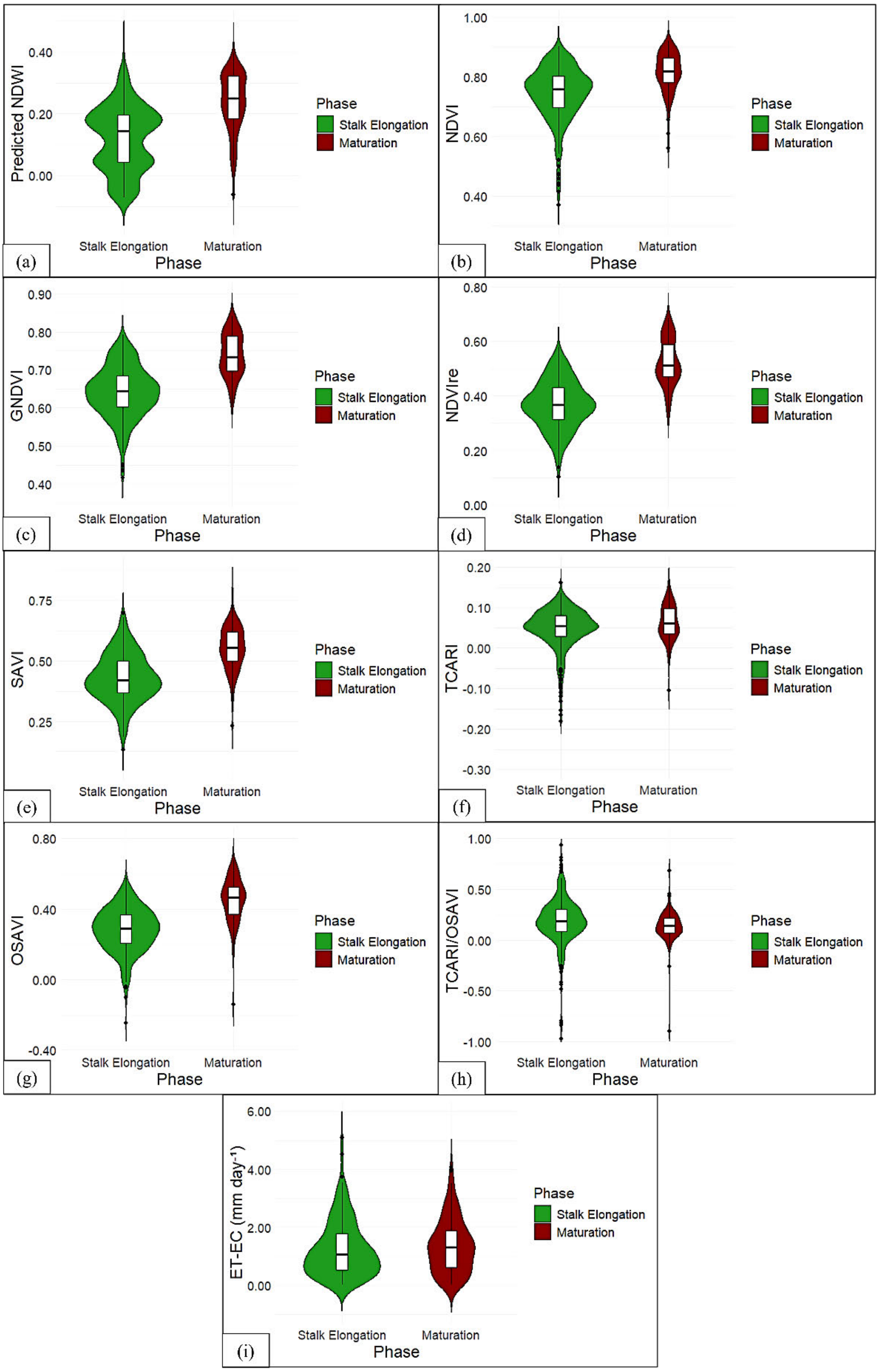

Figure 4.10 Violin plots comparing (a) Predicted NDWI, (b) NDVI, (c) GNDVI, (d) NDVIre, (e) SAVI, (f) TCARI, (g) OSAVI, (h) TCARI/OSAVI, and (i) ET-EC (mm day^{-1}) across SE and early M growth phases.

4.3.6 Validation and temporal analysis of predicted Normalised Difference Water Index against actual evapotranspiration, Water Deficit Index, precipitation, air temperature, and soil water metrics

Figure 4.11a analyses the relationship between mean predicted NDWI values obtained from 12 UAV flights conducted during the study and ETa data collected from an EC system (ET-EC) spanning July 2023 to March 2024. Higher predicted NDWI values indicate increased vegetation water content, correlating with elevated ET-EC rates and potentially lower water stress in sugarcane. Conversely, lower predicted NDWI values suggest reduced water content, which may correspond to heightened stress levels. The analysis reveals a strong positive correlation ($R^2 = 0.60$), indicating that predicted NDWI fluctuations explain 60% of ET-EC variability. This emphasises NDWI's potential as a reliable proxy for vegetation water content and intra-field water dynamics.

Low standard error values further enhance the accuracy of predicted NDWI estimates, facilitating the detection of seasonal variations and aligning trends with changes in moisture availability and crop health. Figure 4.11b presents the correlation between mean predicted NDWI values, derived from the same 12 UAV flights, and the WDI, yielding an R^2 of 0.62. This negative correlation indicates that 62% of WDI variability is explained by NDWI changes, highlighting the index's sensitivity to water stress in sugarcane. The inverse relationship suggests that as predicted NDWI decreases, water deficit increases, reflecting lower vegetation water content. These findings validate predicted NDWI's applicability in assessing crop water stress and deepen understanding of its relationship with ET-EC.

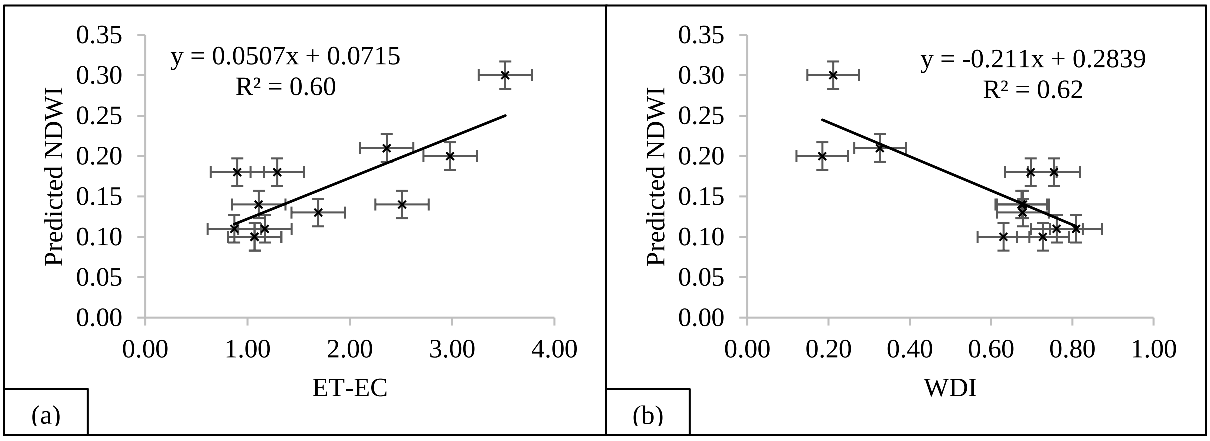

Figure 4.11 Correlation analysis between mean daily NDWI values and (a) ET-EC (mm day^{-1}) and (b) WDI for validation purposes.

Note: readers are referred to Section 3.3.1 in Chapter 3 for details on energy balance closure and the quality of in-situ data from the EC system.

Figure 4.12 illustrates the interplay between precipitation (mm), Total Soil Water Profile (TSWP) (mm^{-1}), average air temperature (°C), WDI, and mean NDWI during a segment of the sugarcane phenological cycle. Rainfall events from July 2023 to March 2024 were sporadic, with notable peaks in October, December, and January, indicating periods of substantial hydration. Conversely, July and August experienced prolonged dry spells due to seasonal climate patterns. NDWI values ranged from 0.10 to 0.30, peaking at 0.30 on February 6. This suggests a temporal relationship between NDWI and precipitation, particularly following the cumulative rainfall of 331 mm in December. This indicates that vegetation absorbs water during and after rains, albeit with a delay due to soil water infiltration and subsequent plant uptake.

TSWP generally declined from July to October 2023, with increases following rainfall events, suggesting a correlation with wet season dynamics. Notably, changes in TSWP did not directly correspond with rainfall amounts, indicating potential delays influenced by soil characteristics or ET-EC dynamics. High-stress periods, particularly from July to November, were marked by elevated WDI values (0.76 on July 18 and 0.81 on September 14), coinciding with low or zero precipitation and reduced NDWI values, signalling significant water stress. This period also shows a decline in TSWP, reflecting diminishing soil moisture. Elevated temperatures, reaching 20.74 °C on August 31 and 19.24 °C on September 14, may further exacerbate transpiration rates and stress levels.

In contrast, from February to March, water stress diminished, with WDI values decreasing (0.21 on February 6 and 0.18 on February 21) and NDWI values increasing, notably 0.30 on February 6. This improvement likely resulted from enhanced TSWP and periodic precipitation, contributing to reduced stress and a more stable crop environment. Overall, high-stress periods correlated with low NDWI and TSWP, compounded by minimal rainfall and elevated temperatures. In summary, the sugarcane crop experienced significant stress throughout the study, particularly during the dry months (July–November 2023), but improved conditions in February and March 2024 indicate periods of reduced stress. Despite some relief, the data suggests that the crop endured substantial water stress for much of the study.

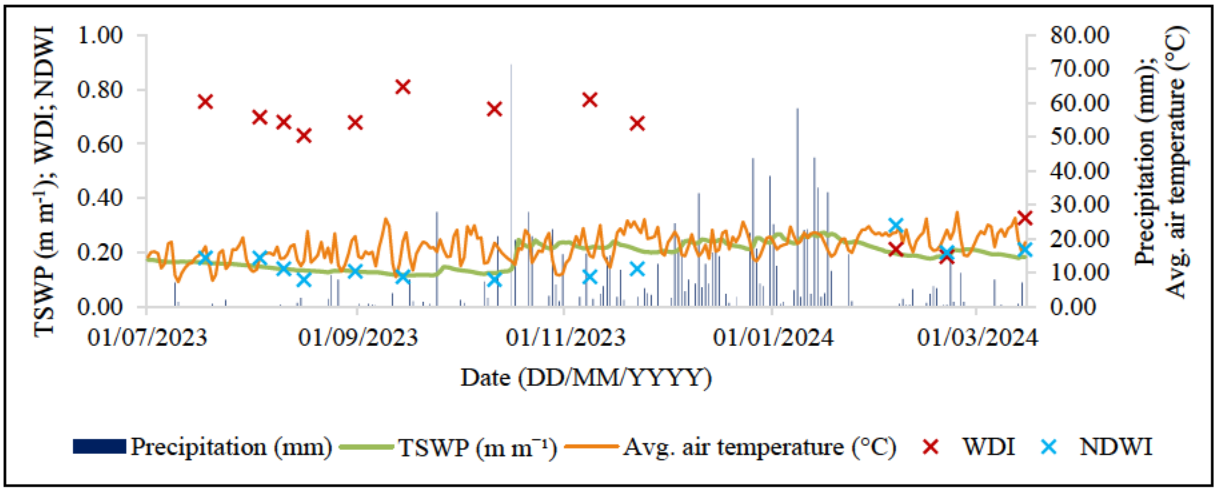

Figure 4.12 Temporal dynamics of precipitation (mm), TSWP (mm^{-1}), air temperature (°C), WDI, and NDWI during the sugarcane phenological cycle.

4.3.7 Multivariate analysis: principal component analysis of UAV-based spectral data and in-situ measurements

This PCA variables plot clarifies the multivariate relationships and contributions among spectral indices, bands, and in-situ measurements. The first two principal components (PC1 and PC2) account for 31.59% and 19.28% of the variance, respectively (Figure 4.13). Arrows indicate the direction and magnitude of each variable's contribution, highlighting dimensionality reduction and covariance. The colour gradient further demonstrates the relative influence of variables, offering nuanced insights into their contributions. This visualisation comprehensively analyses the intricate interactions between RS data and ground-based measurements, enhancing our ability to inform water management decisions.

Principal component 1 primarily captures variations associated with spectral indices such as NIR, SAVI, and NDVIre, reflecting robust correlations with overall vegetation health and density. Conversely, PC2 relates to spectral responses involving red and green wavelengths, indicating specific leaf biochemical and structural characteristics. Predicted NDWI, essential for evaluating crop water status, aligns predominantly along PC1 and slightly negatively on PC2. This suggests associations with indices indicative of water content, such as NIR, SAVI, and GNDVI, emphasising their importance in assessing canopy moisture. Variables such as red and TCARI/OSAVI, situated oppositely to predicted NDWI, highlight divergent contributions, possibly reflecting differences in leaf area and CC independent of water availability.

The analysis further reveals clusters of correlated variables, such as NDVI, OSAVI, and crop height, suggesting shared mechanisms linked to structural and photosynthetic activity. The foliar temperature and predicted NDWI, despite their differing contributions (1 versus 6), suggest potential interrelations, likely due to shared factors influencing both temperature and moisture content. Predicted NDWI's alignment with hydrosensitive indices, viz. NDVI, GNDVI, and OSAVI across PC1 highlight its effectiveness in capturing moisture variations, forming an essential construct for monitoring and predicting crop water status. Consequently, PCA demonstrates the value of integrating predicted NDWI with relevant indices for comprehensive crop hydration assessment.

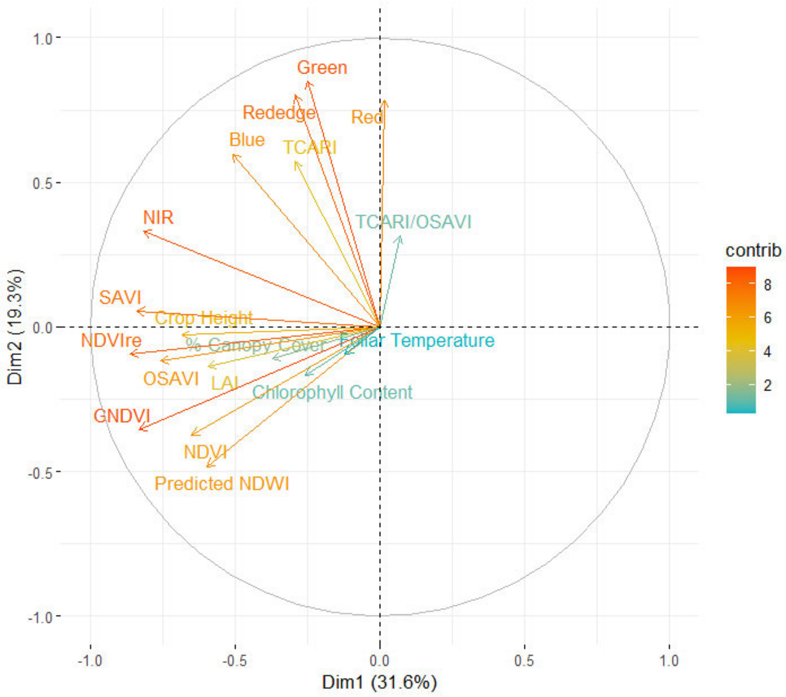

Figure 4.13 PCA variables plot illustrating contributions of UAV-based spectral data and in-situ measurements.

4.3.8 Evaluating the dynamics of vegetation indices with leaf area index and chlorophyll content

The surface plots in this study illustrate the interactions between CC on the x-axis and LAI on the y-axis, with z-values representing the corresponding VI values. Each point on the surface reflects a unique CC and LAI combination, offering a multidimensional view of how these factors influence vegetation health as measured by the VI (Figures 4.14a–h).

In Figure 4.14a, NDWI displays prominent peaks at higher CC values (approximately 500–600 µmol m^{-2}) and moderate to high LAI levels (5–6). These peaks correlate with elevated NDWI values, indicating optimal vegetation health and moisture retention. Conversely, valleys at lower CC values (approximately 100–200 µmol m^{-2}) and moderate LAI levels (3–5) correspond to significantly lower NDWI values, highlighting the necessity of adequate CC and leaf area for maintaining water content. The gradual increase in NDWI with rising LAI and CC suggests that enhanced foliage and CC significantly improve moisture retention. However, variability in water status indicates stressors typical of non-irrigated conditions.

In Figure 4.14b, the NDVI similarly exhibits substantial peaks (around 0.8) corresponding to higher CC (400–550 µmol m^{-2}) and moderate to high LAI (5–6). Figure 4.14c, representing the GNDVI, follows suit, with increased CC (400–550 µmol m^{-2}) and LAI (5–6) associated with elevated GNDVI values (around 0.75). This highlights GNDVI's sensitivity to chlorophyll variations and effectiveness in assessing sugarcane vigour. In Figure 4.14d, the NDVIre reaffirms these observations with notable increases in NDVIre values (0.5–0.55) alongside higher CC (400–600 µmol m^{-2}) and LAI (5–6). This index's sensitivity to subtle chlorophyll changes positions it as a critical indicator of sugarcane health in varying conditions.

In Figure 4.14e, the SAVI shows high values (0.6–0.65) associated with moderate LAI (4.8–5.2) and CC (300–450 µmol m^{-2}), reflecting optimal conditions, where adequate leaf area and CC enhance photosynthesis and moisture retention. In contrast, low SAVI values (0.3–0.4) correlate with reduced LAI (3.5–4.5) and lower CC (100–200 µmol m^{-2}), indicating diminished vigour and potential stress from insufficient foliage or CC. In Figure 4.14f, TCARI displays significant peaks (0.12–0.14) at high CC (400–600 µmol m^{-2}) and elevated LAI (5.5–6.5). Conversely, lower values for TCARI (0.02–0.06) align with lower to moderate LAI (3–4.5) and CC (100–250 µmol m^{-2}), reflecting reduced photosynthetic efficiency.

In Figure 4.14g, the OSAVI exhibits distinct peaks and valleys. High values (0.15–0.16) correspond to elevated LAI (5–6.5) and CC (450–650 µmol m^{-2}), indicating enhanced rainfed sugarcane health. Conversely, low OSAVI values (0.06–0.2) are linked to moderate LAI (4.0–4.5) and CC (250–300 µmol m^{-2}), suggesting impaired health. In Figure 4.14h, the TCARI/OSAVI ratio shows significant peaks, with values (0.4–0.5) associated with low to moderate LAI (3–5) and CC (100–300 µmol m^{-2}), indicating effective chlorophyll health assessment, even at lower vegetative vigour. Moderate TCARI/OSAVI values (0.15–0.3) relate to higher LAI (4.5–6.5) and CC (350–700 µmol m^{-2}).

Overall, integrating these indices offers a comprehensive assessment of sugarcane health, showing that while higher values indicate optimal growth conditions, lower values signal stress and decreased productivity. The discernible patterns across these indices affirm their utility in evaluating the physiological status of sugarcane, particularly concerning CC and leaf area, which are essential for effective crop management.

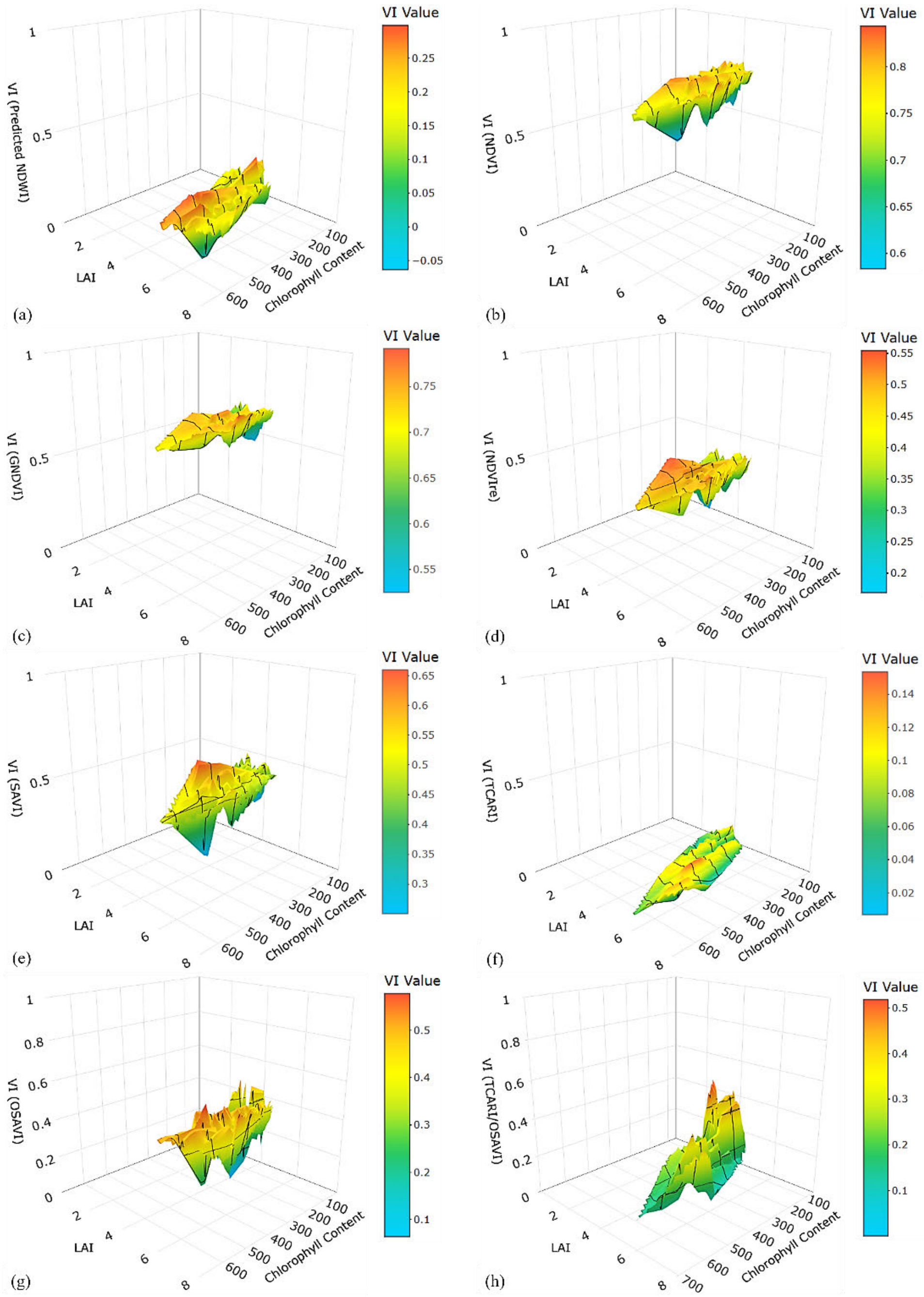

Figure 4.14 3D surface plots depicting the interaction between LAI, CC (μmol m^{-2}), and various VIs: (a) Predicted NDWI, (b) NDVI, (c) GNDVI, (d) NDVIre, (e) SAVI, (f) TCARI, (g) OSAVI, and (h) TCARI/OSAVI.

4.4 Discussion

This study addresses the pressing issue of water stress in sugarcane production across South Africa, leveraging UAV-based NDWI for monitoring and mitigation. A novel methodology integrates satellite data, in-situ measurements, and ML to develop and validate a predictive NDWI model. This is the first study to predict UAV-acquired NDWI from multispectral UAV bands using relationships with various SVIs. Findings reveal critical insights into crop water stress dynamics, demonstrating UAV-based NDWI's effectiveness for PA, with the potential to enhance agricultural practices for resource-constrained smallholder farmers in the region.

4.4.1 Analysis of predicted Normalised Difference Water Index in the study area

The validation of the NDWI predictive model employed a comprehensive approach, integrating ground-truth data and correlation analyses. Ground-truth data from in-situ measurements of CC and LAI, alongside meteorological variables, served as benchmarks for evaluating predicted NDWI values. The ensemble model achieved a high R^2 of 0.95, indicating high predictive accuracy based on UAV-derived data. Low RMSE and MAE values of 0.03 and 0.02 reflect minimal deviations between predicted and actual NDWI values. This validation adheres to best practices outlined in recent research (Dong *et al.*, 2024), assuring prediction reliability. The model also accurately captured increased vegetation water content during the early M phase, correlating with observed increases in CC and LAI.

4.4.2 Influence of climatic conditions and sugarcane phenology on Normalised Difference Water Index and structural vegetation index trends

Strong positive correlations between NDWI and SVIs (NDVI, GNDVI; $R > 0.5$) align with established literature (Gao, 1996; Strashok *et al.*, 2022). However, interpreting these trends requires careful consideration of the data collection period (July 18, 2023 – March 15, 2024), encompassing only the SE and early M phases before harvest (May 2024). Compared to the SE phase, increased NDWI and SVIs during the early M phase reflect favourable summer conditions (higher temperatures, increased rainfall) that fostered vigorous post-tillering growth, enhancing photosynthetic activity and biomass accumulation and improving water status. Increased CC and LAI further support this.

Crucially, this represents only the initial M phase; the data collection period concluded before the expected peak in sucrose accumulation and senescence of lower leaves, characteristic of the later M phase (Stoller, 2024). Conversely, unfavourable winter conditions during SE likely restricted root development and nutrient uptake, hindering SE and sucrose accumulation (Smith *et al.*, 2005; Pierre *et al.*, 2019) despite sugarcane's drought tolerance (Mehdi *et al.*, 2024). Lower NDWI and SVI values during SE may also reflect heterogeneous crop development at this earlier growth stage (Meyer *et al.*, 2011; Xu *et al.*, 2021), impacting spectral reflectance.

The SE to M transition involves a physiological shift from vegetative growth to sucrose accumulation, with the early M phase trends potentially masked by favourable environmental conditions. The absence of later-stage water stress may reflect relatively mild early M phase conditions; decreased LAI (Castro-Nava *et al.*, 2016), chlorophyll (Harakotr *et al.*, 2024), and associated index values (Pereira *et al.*, 2016) are typically expected in later M due to leaf senescence and the resource reallocation towards sugar accumulation (Mehdi *et al.*, 2024). Additionally, increased water stress during the later M phase negatively influences sugar production and flowering (Mehdi *et al.*, 2024).

4.4.3 Canopy development, water use, and photosynthetic efficiency

Canopy development impacted water status and plant health, as indicated by moderate correlations between NDWI and LAI ($R = 0.41$), crop height ($R = 0.31$), CC ($R = 0.33$), and photosynthetic indices (TCARI, TCARI/OSAVI). Improved water retention and enhanced photosynthetic activity, linked to the more developed canopy of the early M phase, contributed to higher NDWI values. Compared to the SE phase, the increased consistency in NDWI and SVI values during the early M phase reflects more uniform canopy cover, resulting in more stable water status and reduced ET-EC variability. The greater variability in ET-EC during SE may be attributed to uneven canopy development and varying solar radiation exposure.

Higher TCARI variability during SE reflects uneven chlorophyll distribution, consistent with observed SVI variability. Additionally, slightly higher and more consistent TCARI values during the early M phase suggest improved photosynthetic efficiency and plant health, directly linked to the more developed and uniform canopy structure, which enhances light interception and photosynthetic activity (Haboudane *et al.*, 2002). However, these improvements may also partly reflect favourable environmental conditions. The data does not capture the typical later-stage decline in LAI (Castro-Nava *et al.*, 2016), CC (Harakotr *et al.*, 2024), and associated indices (Pereira *et al.*, 2016) due to leaf senescence.

4.4.4 The relationship between Normalised Difference Water Index and environmental variables

The temporal analysis of NDWI, precipitation, air temperature, and TSWP reveals a dynamic interplay that significantly influences crop water status. A positive correlation between NDWI and precipitation is evident, with NDWI increasing sharply after substantial rainfall events, such as in November 2023, indicating effective water use for stress recovery. In contrast, prolonged dry periods (July-August 2023) characterised by low precipitation and reduced TSWP resulted in decreased NDWI values, underpinning the critical role of rainfall in sustaining crop health during essential growth phases.

Despite these fluctuations, the sugarcane crop exhibited persistent water stress throughout the monitoring period, especially from July to November 2023. Elevated WDI values during this timeframe reflect significant stress, with only brief recoveries following rainfall events. While February and March 2024 saw increased NDWI values coinciding with rising TSWP and resumed precipitation, the overall data emphasises the substantial water stress experienced throughout the study. This situation highlights the need for effective water management strategies to enhance resilience against variable climatic conditions during critical growth periods.

Further investigation reveals an intricate interplay between NDWI and environmental variables such as ETa and WDI that significantly influence crop water stress. A strong positive correlation with ETa ($R^2 = 0.60$) suggests NDWI's potential as a proxy for assessing sugarcane water status (Nguyen *et al.*, 2024). Yet, fluctuations in NDWI due to external factors like soil moisture, solar radiation, wind speed, and atmospheric demand significantly affect ETa rates. Thus, low ETa values can occur even when NDWI shows no stress. The negative correlation with WDI ($R^2 = 0.62$) further highlights NDWI's sensitivity to water deficits, where increased stress correlates with lower NDWI values.

For sugarcane cultivation, NDWI is a valuable indicator of crop water status; however, integrating factors such as water resource availability, climatic conditions, and overall crop health is imperative. The increase in NDWI following rainfall events, particularly in November 2023, illustrates the significant impact of immediate precipitation on water availability and recovery. This effect may be more pronounced during periods of high and moderate stress, highlighting the need for holistic approaches to understanding water stress that consider a variety of environmental variables.

4.4.5 Principal component analysis interpretation and contextualisation

The PCA revealed that PC1, strongly associated with NIR reflectance and VIs (SAVI, NDVIre) indicative of vegetation health and biomass (Zarco-Tejada *et al.*, 2013; Brewer *et al.*, 2022b), primarily influenced predicted NDWI. The predominantly positive PC1 loading, with slight negative PC2 loading (red/green wavelengths), suggests that water availability, more so than leaf biochemistry or structure, drives NDWI variations in this rainfed sugarcane system. The co-loading of NDVI, OSAVI, and crop height on PC1 indicates shared underlying mechanisms related to structural and photosynthetic activity, reinforcing the importance of integrated crop health assessment for effective water management (Ihuoma and Madramootoo, 2017).

4.4.6 Three-dimensional surface plot analysis

Three-dimensional surface plots clarify the intricate interplay between CC, LAI, and VIs. Peaks in the NDWI at CC values of 500–600 µmol m^{-2} and LAI levels (5–6) indicated optimal vegetation health and moisture retention, consistent with the established understanding of sufficient CC and leaf area in maintaining plant water content (Carter, 1991). In contrast, valleys at lower CC (100–200 µmol m^{-2}) and LAI (3–5) emphasised their significance for sugarcane health and NDWI's sensitivity to water stress. Additionally, trends across various VIs—including NDVI, GNDVI, SAVI, and TCARI—demonstrated that high index values in areas with elevated CC and LAI (Huang *et al.*, 2020) signified robust growth, while lower values reflected adverse impacts of water stress.

4.4.7 Implications for sustainable sugarcane production in South Africa

4.4.7.1 Addressing data limitations

The results of this study demonstrate the potential of UAV-based NDWI for monitoring water stress in sugarcane; however, several limitations warrant consideration. Coarse-resolution satellite imagery requires careful processing to address the mixed-pixel effect, where the high NIR reflectance of soil can artificially lower NDWI values, obscuring actual crop water content (Zhou *et al.*, 2021). Additionally, downscaling satellite data introduces uncertainty (Gokool *et al.*, 2022) due to inherent sub-pixel variability and method-dependent assumptions, necessitating cautious interpretation. Consequently, if the NDWI predictions derived from satellite data lack accuracy, they could misrepresent the severity of water stress, directly impacting water management decisions. Moreover, the limited number of training points in model development may compromise robustness (Budach *et al.*, 2022), as insufficient data might not fully capture the relationship between NDWI and various SVIs.

The reliance on a single study site restricts the generalisability of the findings (Alavi *et al.*, 2024). This limitation may not accurately reflect the diverse conditions and management practices across South Africa, potentially skewing the understanding of water dynamics. In-situ measurements may only partially capture the heterogeneity inherent in extensive sugarcane fields, introducing sampling bias (Blatchford *et al.*, 2019). Consequently, this bias could underrepresent variability in crop responses to water stress, leading to misleading conclusions about the NDWI model's overall effectiveness in broader agricultural contexts. Additionally, the study's data collection period encompassed only the SE and early M phases, precluding a comprehensive assessment of water stress dynamics throughout the growth cycle. This limitation, particularly concerning the later M stages may affect the model's reliability and generalisability.

To address these limitations, future research should prioritise (1) expanding data collection across multiple sites and diverse sugarcane cultivars and cultivation methods within South Africa; (2) employing advanced image processing techniques, such as spectral unmixing, to correct for mixed pixels and enhance NDWI accuracy; (3) extending the data collection period to encompass the complete sugarcane growth cycle; (4) increasing the size of the training dataset to improve model robustness and generalisability; and (5) exploring alternative VIs, such as GNDVI, and integrating TIR data to gain a more comprehensive understanding of the complex interplay between water stress, canopy temperature, and other environmental factors. Integrating data from multiple sources (UAV, satellite, and ground-based measurements) will further enhance the reliability and application of NDWI-based water stress assessments.

4.4.7.2 Practical applications and collaboration

The practical applications of this research highlight the value of UAV-based NDWI for early water stress detection, which is vital for proactive irrigation management and reducing yield losses. The model can empower smallholder farmers to monitor crop water status effectively, enabling timely irrigation strategies. Translating this research into real-world scenarios necessitates developing user-friendly tools that seamlessly integrate UAV technology, NDWI calculations, and data interpretation tailored to smallholder needs. Collaboration among researchers, agricultural extension services, and farmers is critical for successfully incorporating this innovative technology (Gokool *et al.*, 2023), ultimately benefiting sugarcane production in South Africa while addressing farmers' unique constraints.

4.5 Conclusion

Amid increasing water scarcity and erratic weather patterns in South Africa, effective crop water stress monitoring is crucial, particularly for smallholder sugarcane farmers. This study addresses this need by introducing a novel ML model for accurately predicting sugarcane NDWI using UAV-based multispectral imagery. The model's strong concordance with Sentinel-2 data and in-situ measurements validates UAV-derived NDWI as a robust indicator of sugarcane water status, showing significant correlations with established SVIs and vital environmental variables. This highlights NDWI's sensitivity to sugarcane health, offering substantial potential for precision water management. Accurate NDWI predictions facilitate several critical operational applications: spatially explicit, timely assessments enable optimised precision irrigation, minimising water waste and maximising resource allocation; continuous monitoring establishes an early warning system for proactive mitigation before significant yield loss; and data integration into decision support systems provides timely recommendations to farmers. This enhanced adaptive capacity is crucial in the face of climate change. However, the study's reliance on a single site, limited training dataset and data collection encompassing only the SE and early M growth phases limits generalisability. Challenges related to in-situ data (sampling bias and heterogeneity) and downscaled satellite data (sub-pixel variability) further constrain broader applicability. Future research should expand data collection across diverse sites and cultivars, incorporate advanced image processing techniques (e.g., spectral unmixing), increase the training dataset size, and extend data collection to cover the entire sugarcane growth cycle. Collaboration among researchers, extension services, and farming communities is vital for translating this research into user-friendly tools, maximising its operational value and improving water resource management and food security in vulnerable regions of South Africa.

4.6 References

Adisa, O, Botai, CM, Botai, JO, Hassen, A, Darkey, D, Tesfamariam, EH, Adisa, AF, Adeola, AM and Ncongwane, KP. 2018. Analysis of agro-climatic parameters and their influence on maize production in South Africa. *Theoretical and Applied Climatology* 134 (1): 991-1004.

Alavi, M, Albaji, M, Golabi, M, Ali Naseri, A and Homayouni, S. 2024. Estimation of sugarcane evapotranspiration from remote sensing and limited meteorological variables using machine learning models. *Journal of Hydrology* 629 (1): 130605.

Allen, R, Pereira, L, Raes, D and Smith, M. 1998. *Crop Evapotranspiration: Guidelines for Computing Crop Water Requirements.* FAO Irrigation and Drainage Paper No. 56. Food and Agriculture Organization of the United Nations, Rome, Italy.

Andersson, JCM, Zehnder, AJB, Jewitt, GPW and Yang, H. 2009. Water availability, demand and reliability of in situ water harvesting in smallholder rain-fed agriculture in the Thukela River Basin, South Africa. *Hydrology and Earth System Sciences* 13 (12): 2329-2347.

Antoniuk, V, Manevski, K, Kørup, K, Larsen, R, Sandholt, I, Zhang, X and Andersen, MN. 2021. Diurnal and seasonal mapping of water deficit index and evapotranspiration by an unmanned aerial system: a case study for winter wheat in Denmark. *Remote Sensing* 13 (15): 2998.

Archer, E, Landman, W, Malherbe, J, Tadross, M and Pretorius, S. 2019. South Africa's winter rainfall region drought: a region in transition? *Climate Risk Management* 25 (1): 100188.

Bajwa, S and Vories, E. 2006. *Spectral Response of Cotton Canopy to Water Stress*.

Baluja, J, Diago, M-P, Balda, P, Zorer, R, Meggio, F, Morales, F and Tardaguila, J. 2012. Assessment of vineyard water status variability by thermal and multispectral imagery using an unmanned aerial vehicle (UAV). *Irrigation Science* 30 (1): 511-522.

Basdew, M, Jiri, O and Mafongoya, PL. 2017. Integration of indigenous and scientific knowledge in climate adaptation in KwaZulu-Natal, South Africa. *Change and Adaptation in Socio-Ecological Systems* 3 (1): 56-67.

Bertalan, L, Holb, I, Pataki, A, Négyesi, G, Szabó, G, Kupásné Szalóki, A and Szabó, S. 2022. UAV-based multispectral and thermal cameras to predict soil water content – A machine learning approach. *Computers and Electronics in Agriculture* 200: 107262.

Bezuidenhout, CN and Singels, A. 2007. Operational forecasting of South African sugarcane production: Part 1 – System description. *Agricultural Systems* 92 (1): 23-38.

Blatchford, ML, Mannaerts, CM, Zeng, Y, Nouri, H and Karimi, P. 2019. Status of accuracy in remotely sensed and in-situ agricultural water productivity estimates: a review. *Remote Sensing of Environment* 234 (1): 111413.

Brewer, K, Clulow, A, Sibanda, M, Gokool, S, Odindi, J, Mutanga, O, Naiken, V, Chimonyo, VGP and Mabhaudhi, T. 2022a. Estimation of maize foliar temperature and stomatal conductance as indicators of water stress based on optical and thermal imagery acquired using an unmanned aerial vehicle (UAV) platform. *Drones* 6 (7): 169.

Brewer, K, Clulow, A, Sibanda, M, Gokool, S, Naiken, V and Mabhaudhi, T. 2022b. Predicting the chlorophyll content of maize over phenotyping as a proxy for crop health in smallholder farming systems. *Remote Sensing* 14 (3): 518.

Budach, L, Feuerpfeil, M, Ihde, N, Nathansen, A, Noack, N, Patzlaff, H, Harmouch, H and Naumann, F. 2022. *The effects of data quality on ML-model performance*.

Carr, M and Knox, J. 2011. The water relations and irrigation requirements of sugarcane (Saccharum officinarum): a review. *Experimental Agriculture* 47 (1): 1-25.

Carter, G. 1991. Primary and secondary effects of water content on the spectral reflectance of leaves. *American Journal of Botany* 78 (7): 916-924.

Castro-Nava, S, Huerta, AJ, Plácido-de la Cruz, JM and Mireles-Rodríguez, E. 2016. Leaf growth and canopy development of three sugarcane genotypes under high temperature rainfed conditions in Northeastern Mexico. *International Journal of Agronomy* 2016 (1): 2561026.

Chimonyo, V, Modi, A and Mabhaudhi, T. 2016. Assessment of sorghum-cowpea intercrop system under water-limited conditions using a decision support tool. *Water SA* 42 (2): 316-327.

Cockburn, J, Coetzee, H, Van den Berg, J, Conlong, D and Witthöft, J. 2014. Exploring the role of sugarcane in small-scale farmers' livelihoods in the Noodsberg Area, KwaZulu-Natal, South Africa. *The South African Journal of Agricultural Extension* 42 (1): 80-97.

Dong, H, Dong, J, Sun, S, Bai, T, Zhao, D, Yin, Y, Shen, X, Wang, Y, Zhang, Z and Wang, Y. 2024. Crop water stress detection based on UAV remote sensing systems. *Agricultural Water Management* 303 (1): 109059.

Dunkelberg, E, Finkbeiner, M and Hirschl, B. 2014. Sugarcane ethanol production in Malawi: measures to optimise the carbon footprint and to avoid indirect emissions. *Biomass and Bioenergy* 71 (1): 37-45.

Edgerton, CW. 1934. *Stubble deterioration of sugar cane.* Louisiana State University and Agricultural and Mechanical College, Agricultural Experiment Station, 256.

Ferreira, THS, Tsunada, MS, Bassi, D, Araújo, P, Mattiello, L, Guidelli, GV, Righetto, GL, Gonçalves, VR, Lakshmanan, P and Menossi, M. 2017. Sugarcane water stress tolerance mechanisms and its implications on developing biotechnology solutions. *Frontiers in Plant Science* 8 (1): 1077.

Gao, B-c. 1996. NDWI—A normalised difference water index for remote sensing of vegetation liquid water from space. *Remote Sensing of Environment* 58 (3): 257-266.

Glassop, D, Roessner, U, Bacic, A and Bonnett, GD. 2007. Changes in the sugarcane metabolome with stem development. Are they related to sucrose accumulation? *Plant and Cell Physiology* 48 (4): 573-584.

Gokool, S, Kunz, R and Warburton Toucher, M. 2022. Deriving moderate spatial resolution leaf area index estimates from coarser spatial resolution satellite products. *Remote Sensing Applications: Society and Environment* 26 (1): 100743.

Gokool, S, Mahomed, M, Kunz, R, Clulow, A, Sibanda, M, Naiken, V, Chetty, K and Mabhaudhi, T. 2023. Crop monitoring in smallholder farms using unmanned aerial vehicles to facilitate precision agriculture practices: a scoping review and bibliometric analysis. *Sustainability* 15 (4): 3557.

González-Dugo, MP, Moran, MS, Mateos, L and Bryant, RB. 2006. Canopy temperature variability as an indicator of crop water stress severity. *Irrigation Science* 24 (1): 233-240.

Gray, BA, Toucher, ML, Savage, MJ and Clulow, AD. 2022. Seasonal evapotranspiration over an invader vegetation (Pteridium aquilinum) in a degraded montane grassland using surface renewal. *Journal of Hydrology: Regional Studies* 40 (1): 101012.

Haarhoff, SJ, Kotzé, T and Swanepoel, P. 2020. A prospectus for sustainability of rainfed maize production systems in South Africa. *Crop Science* 60 (1): 14-28.

Haboudane, D, Miller, JR, Tremblay, N, Zarco-Tejada, PJ and Dextraze, L. 2002. Integrated narrow-band vegetation indices for prediction of crop chlorophyll content for application to precision agriculture. *Remote Sensing of Environment* 81 (2): 416-426.

Harakotr, P, Sornpha, W, Khonghinta, J, Gonkhamdee, S, Songsri, P and Jongrungklang, N. 2024. Correlation between rapid measurement and leaf chlorophyll content of various

sugarcane genotypes at different growth phases. *Asian Journal of Plant Sciences* 23 (1): 367-376.
Huang, S, Tang, L, Hupy, J, Wang, Y and Shao, G. 2020. A commentary review on the use of Normalised Difference Vegetation Index (NDVI) in the era of popular remote sensing. *Journal of Forestry Research* 32 (1): 1-6.
Ihuoma, SO and Madramootoo, CA. 2017. Recent advances in crop water stress detection. *Computers and Electronics in Agriculture* 141 (1): 267-275.
Ihuoma, SO, Madramootoo, CA and Kalacska, M. 2021. Integration of satellite imagery and in situ soil moisture data for estimating irrigation water requirements. *International Journal of Applied Earth Observation and Geoinformation* 102 (1): 102396.
Inman-Bamber, NG. 2004. Sugarcane water stress criteria for irrigation and drying off. *Field Crops Research* 89 (1): 107-122.
Inman-Bamber, NG and Smith, DM. 2005. Water relations in sugarcane and response to water deficits. *Field Crops Research* 92 (2): 185-202.
IPCC. 2019. *Climate Change and Land: An IPCC Special Report on Climate Change, Desertification, Land Degradation, Sustainable Land Management, Food Security, and Greenhouse Gas Fluxes in Terrestrial Ecosystems.* Cambridge University Press, Cambridge, UK and New York, USA.
Jackson, RD. 1982. Canopy temperature and crop water stress. In: ed. Hillel, D, *Advances in Irrigation*. Elsevier.
Jones, HG. 2014. Remote sensing of plant stresses and its use in irrigation management. 239-247. International Society for Horticultural Science (ISHS), Leuven, Belgium.
Jones, MR, Singels, A and Ruane, AC. 2015. Simulated impacts of climate change on water use and yield of irrigated sugarcane in South Africa. *Agricultural Systems* 139 (1): 260-270.
Khormizi, HZ, Malamiri, HRG and Ferreira, CSS. 2024. Estimation of evaporation and drought Stress of pistachio plant using UAV multispectral images and a surface energy balance approach. *Horticulturae* 10 (5): 515.
Khumalo, S. 2016. Exploring the role of women in subsistence and smallholder farming: implications for horticultural crop value chain development in Swayimane and Sweetwaters. Unpublished thesis, Agriculture and Environmental Sciences, African Centre for Food Security, University of KwaZulu-Natal, Pietermaritzburg, South Africa.
Kibirige, D, Gokool, S and Mkhize, Z. 2023. Estimation of soil moisture using environmental covariates and machine learning algorithms in Cathedral Peak Catchment, South Africa. *Vadose Zone Journal* 23 (3): e20289.
Knox, JW, Rodríguez Díaz, JA, Nixon, DJ and Mkhwanazi, M. 2010. A preliminary assessment of climate change impacts on sugarcane in Swaziland. *Agricultural Systems* 103 (2): 63-72.
Konica Minolta. 2025. SPAD-502Plus Chlorophyll Meter [Internet]. Konica Minolta Sensing Europe. Available from: https://sensing.konicaminolta.eu. [Accessed: 30 October 2024].
Kuhn, M. 2008. Building Predictive Models in R Using the caret Package. *Journal of Statistical Software* 28 (5): 1-26.
Leroux, L, Baron, C, Zoungrana, B, Traoré, SB, Seen, DL and Bégué, A. 2016. Crop monitoring using vegetation and thermal indices for yield estimates: case study of a rainfed cereal in semi-arid west africa. *IEEE Journal of Selected Topics in Applied Earth Observations and Remote Sensing* 9 (1): 347-362.
Lickley, M and Solomon, S. 2018. Drivers, timing and some impacts of global aridity change. *Environmental Research Letters* 13 (10): 104010.

LI-COR. 2025. LAI-2200C Plant Canopy Analyzer [Internet]. LI-COR Biosciences. Available from: https://www.licor.com/products/leaf-area/LAI-2200C. [Accessed: 30 October 2024].

Ling, Q, Huang, W and Jarvis, P. 2011. Use of a SPAD-502 meter to measure leaf chlorophyll concentration in Arabidopsis thaliana. *Photosynthesis Research* 107 (2): 209-214.

Liu, S, Pan, X, Yang, Y, Yuan, J, Yang, Z, Wang, Z, Xie, W, Song, H and Hao. 2023. A Crop water stress index based on remote sensing methods for monitoring drought in an arid area. *Remote Sensing Letters* 14 (1): 890-900.

Lofton, J, Tubana, B, Kanke, Y, Teboh, J, Viator, H and Dalen, M. 2012. Estimating sugarcane yield potential using an in-season determination of normalised difference vegetative index. *Sensors* 12 (1): 7529-7547.

Lu, H-d, Xue, J-q and Guo, D-w. 2017. Efficacy of planting date adjustment as a cultivation strategy to cope with drought stress and increase rainfed maize yield and water use efficiency. *Agricultural Water Management* 179 (1): 227-235.

Mahomed, M, Clulow, AD, Strydom, S, Mabhaudhi, T and Savage, MJ. 2021. Assessment of a ground-based lightning detection and near-real-time warning system in the rural community of Swayimane, Kwazulu-Natal, South Africa. *Weather, Climate, and Society* 13 (3): 605-621.

Markwell, JP, Osterman, JC and Mitchell, JL. 2004. Calibration of the Minolta SPAD-502 leaf chlorophyll meter. *Photosynthesis Research* 46 (1): 467-472.

Martins, MTB, de Souza, WR, da Cunha, BADB, Basso, MF, de Oliveira, NG, Vinecky, F, Martins, PK, de Oliveira, PA, Arenque-Musa, BC, de Souza, AP, Buckeridge, MS, Kobayashi, AK, Quirino, BF and Molinari, HBC. 2016. Characterisation of sugarcane (Saccharum spp.) leaf senescence: implications for biofuel production. *Biotechnology for Biofuels* 9 (1): 153.

Matsuoka, S. 2012. *Sugarcane tillering and ratooning: key factors for a profitable cropping.* In: Goncalves, JF and Correia, KD (eds.), *Sugarcane: Physiology, biochemistry, and functional biology.* Nova Science Publishers, Araras, Brazil.

Mehdi, F, Cao, Z, Zhang, S, Gan, Y, Cai, W, Peng, L, Wu, Y, Wang, W and Yang, B. 2024. Factors affecting the production of sugarcane yield and sucrose accumulation: suggested potential biological solutions. *Frontiers in Plant Science* 15 (1): 1374228.

Meyer, J, Rein, P, Turner, P and Mathias, K. 2011. *Good Management Practices Manual for the Cane Sugar Industry.* PGBI Sugar and Bio Energy Pty Ltd, Johannesburg, South Africa.

Misra, V, Solomon, S, Mall, AK, Prajapati, CP, Hashem, A, AbdAllah, EF and Ansari, MI. 2020. Morphological assessment of water stressed sugarcane: a comparison of waterlogged and drought affected crop. *Saudi Journal of Biological Sciences* 27 (1): 1228-1236.

Monteith, JL. 1965. Evaporation and environment. *Symposia of the Society for Experimental Biology* 19 (1): 205-234.

Moore, PH and Berding, N. 2013. Flowering. In: *Sugarcane: Physiology, biochemistry, and functional biology*.

Moran, MS, Clarke, TR, Inoue, Y and Vidal, A. 1994. Estimating crop water deficit using the relation between surface-air temperature and spectral vegetation index. *Remote Sensing of Environment* 49 (3): 246-263.

Ndlovu, PN, Thamaga-Chitja, JM and Ojo, TO. 2021. Factors influencing the level of vegetable value chain participation and implications on smallholder farmers in Swayimane KwaZulu-Natal. *Land Use Policy* 109 (1): 105611.

Ngcobo, SI. 2023. An assessment of the potential impacts of climate variability on sugarcane production across Southern Africa. Unpublished thesis, Discipline of Hydrology, University of KwaZulu-Natal, Pietermaritzburg, South Africa.

Nguyen, VL, Dao, DT, Le, MS and Nguyen, MH. 2024. Assessing the correlation between spectral indices and land surface heat fluxes by remote sensing technology: a case study in Thai Binh Province, Red River Delta, Vietnam. *Remote Sensing in Earth Systems Sciences* 7 (3): 159-171.

Nhamo, L, Magidi, J, Nyamugama, A, Clulow, AD, Sibanda, M, Chimonyo, VGP and Mabhaudhi, T. 2020. Prospects of improving agricultural and water productivity through unmanned aerial vehicles. *Agriculture* 10 (7): 256.

Olivier, FC and Singels, A. 2015. Increasing water use efficiency of irrigated sugarcane production in South Africa through better agronomic practices. *Field Crops Research* 176 (1): 87-98.

Peñuelas, J and Filella, I. 1998. Visible and near-infrared reflectance techniques for diagnosing plant physiological status. *Trends in Plant Science* 3 (1): 151-156.

Pereira, R, Casaroli, D, Vellame, L, Júnior, J and Pêgo Evangelista, A. 2016. Sugarcane leaf area estimate obtained from the corrected Normalised Difference Vegetation Index (NDVI). *Pesquisa Agropecuaria Tropical* 46 (1): 140-148.

Pierre, JS, Perroux, JM and Rae, AL. 2019. Screening for sugarcane root phenes reveals that reducing tillering does not lead to an increased root mass fraction. *Frontiers in Plant Science* 10 (1): 119.

Pironato Amaro, R, Christina, M, Todoroff, P, le Maire, G, Fiorio, P, Pereira, E and Luciano, A. 2024. Regional model to predict sugarcane yield using Sentinel-2 imagery in São Paulo State, Brazil. *Sugar Tech*.

Rejeb, A, Abdollahi, A, Rejeb, K and Treiblmaier, H. 2022. Drones in agriculture: a review and bibliometric analysis. *Computers and Electronics in Agriculture* 198 (1): 107017.

Riaz, A, Alqudah, AM, Kanwal, F, Pillen, K, Ye, L-z, Dai, F and Zhang, G-p. 2023. Advances in studies on the physiological and molecular regulation of barley tillering. *Journal of Integrative Agriculture* 22 (1): 1-13.

Roby, MC, Salas Fernandez, MG, Heaton, EA, Miguez, FE and VanLoocke, A. 2017. Biomass sorghum and maize have similar water use efficiency under non-drought conditions in the rain-fed Midwest U.S. *Agricultural and Forest Meteorology* 247 (1): 434-444.

Rockstrom, J. 2000. Water resources management in smallholder farms in Eastern and Southern Africa: an overview. *Physics and Chemistry of the Earth, Part B: Hydrology, Oceans and Atmosphere* 25 (3): 275-283.

Romero Ponce, M, Luo, Y, Su, B and Fuentes, S. 2018. Vineyard water status estimation using multispectral imagery from an UAV platform and machine learning algorithms for irrigation scheduling management. *Computers and Electronics in Agriculture* 147 (1): 109-117.

Roujean, J-L and Breon, F-M. 1995. Estimating PAR absorbed by vegetation from bidirectional reflectance measurements. *Remote Sensing of Environment* 51 (3): 375-384.

Rozenstein, O, Haymann, N, Kaplan, G and Tanny, J. 2018. Estimating cotton water consumption using a time series of Sentinel-2 imagery. *Agricultural Water Management* 207 (1): 44-52.

Ryu, J-H, Jeong, H and Cho, J. 2020. Performances of vegetation indices on paddy rice at elevated air temperature, heat stress, and herbicide damage. *Remote Sensing* 12 (16): 2654.

Safdar, M, Shahid, MA, Sarwar, A, Rasul, F, Majeed, MD and Sabir, RM. 2023. Crop water stress detection using remote sensing techniques. *Environmental Sciences Proceedings* 25 (1): 20.

Sakaigaichi, T, Terajima, Y, Terauchi, T, Hattori, T, Ishikawa, S, Hattori, I, Sugimoto, A and Matsuoka, M. 2013. Effect of stubble shaving after high-level cutting on the growth and yield of forage sugarcane, KRFo93-1, under multiple ratooning cultivation. *Plant Production Science* 16 (1): 183-190.

Saseendran, SA, Trout, TJ, Ahuja, LR, Ma, L, McMaster, GS, Nielsen, DC, Andales, AA, Chávez, JL and Ham, JM. 2015. Quantifying crop water stress factors from soil water measurements in a limited irrigation experiment. *Agricultural Systems* 137 (1): 191-205.

Savage, M, Pasi, J, Myeni, L and Clulow, A. 2017. *Open water evaporation measurement using micrometeorological methods*. TT 729/17. Water Research Commission Pretoria, South Africa.

Shang, J, Liu, J, Ma, B, Zhao, T, Jiao, X, Geng, X, Huffman, T, Kovacs, JM and Walters, D. 2015. Mapping spatial variability of crop growth conditions using RapidEye data in Northern Ontario, Canada. *Remote Sensing of Environment* 168 (1): 113-125.

Sibanda, M, Mutanga, O, Dube, T and Mafongoya, PL. 2020. Spectrometric proximally sensed data for estimating chlorophyll content of grasslands treated with complex fertiliser combinations. *Journal of Applied Remote Sensing* 14 (1): 024517-024517.

Smith, DM, Inman-Bamber, NG and Thorburn, PJ. 2005. Growth and function of the sugarcane root system. *Field Crops Research* 92 (2): 169-183.

Som-ard, J, Atzberger, C, Izquierdo-Verdiguier, E, Vuolo, F and Immitzer, M. 2021. Remote sensing applications in sugarcane cultivation: a review. *Remote Sensing* 13 (20): 4040.

Stoller. 2024. Sugarcane [Internet]. Corteva Agriscience. Available from: https://stollersouthafrica.co.za/sugarcane/. [Accessed: 14 October 2024].

Strashok, O, Ziemiańska, M and Strashok, V. 2022. Evaluation and correlation of Sentinel-2 NDVI and NDMI in Kyiv (2017–2021). *Journal of Ecological Engineering* 23 (9): 212-218.

Testo. 2025. Testo 882 Thermal Imager [Internet]. Testo SE & Co. KGaA. Available from: https://www.testo.com/en-DK/testo-882/p/0560-0882. [Accessed: 30 October 2024].

Toppa, E, Julianetti, A, Hulshof, T and Ono, E. 2011. Physiology development in the vegetative stage of sugarcane. *Applied Research & Agrotechnology* 3 (2): 177-185.

Vélez, S, Ariza-Sentís, M and Valente, J. 2023. VineLiDAR: high-resolution UAV-LiDAR vineyard dataset acquired over two years in northern Spain. *Data in Brief* 51 (1): 109686.

Virnodkar, S, Pachghare, V, Patil, VC and Jha, S. 2020. Remote sensing and machine learning for crop water stress determination in various crops: a critical review. *Precision Agriculture* 21 (13): 1121-1155.

Wang, X, Zhao, C, Guo, N, Li, Y, Jian, S and Yu, K. 2015. Determining the canopy water stress for spring wheat using canopy hyperspectral reflectance data in loess plateau semiarid regions. *Spectroscopy Letters* 48 (1): 492-498.

Xu, F, Wang, Z, Lu, G, Zeng, R and Que, Y. 2021. Sugarcane ratooning ability: research status, shortcomings, and prospects. *Biology* 10 (1): 1052.

Yacoob, A, Gokool, S, Clulow, A, Mahomed, M and Mabhaudhi, T. 2024. Leveraging unmanned aerial vehicle technologies to facilitate precision water management in smallholder farms: a scoping review and bibliometric analysis. *Drones* 8 (9): 476.

Zaib, M, Farooq, U, Adnan, M, Abbas, Z, Haider, K, Khan, N, Abbas, R, Nasir, A, Sidra, Muhay-Ul-Din, M, Farooq, T and Muhammad, A. 2023. Water stress in crop plants, implications for sustainable agriculture: current and future prospects. *Journal of Environmental and Agricultural Science* 25 (1): 37-50.

Zarco-Tejada, PJ, González-Dugo, V, Williams, LE, Suárez, L, Berni, JAJ, Goldhamer, D and Fereres, E. 2013. A PRI-based water stress index combining structural and chlorophyll effects: assessment using diurnal narrow-band airborne imagery and the CWSI thermal index. *Remote Sensing of Environment* 138 (1): 38-50.

Zarzar, CM, Dash, P, Dyer, JL, Moorhead, R and Hathcock, L. 2020. Development of a simplified radiometric calibration framework for water-based and rapid deployment unmanned aerial system (UAS) operations. *Drones* 4 (2): 17.

Zhang, L, Zhang, H, Niu, Y and Han, W. 2019a. Mapping maize water stress based on UAV multispectral remote sensing. *Remote Sensing* 11 (1): 605.

Zhao, T, Stark, B, Chen, Y, Ray, A and Doll, D. 2015. A detailed field study of direct correlations between ground truth crop water stress and normalised difference vegetation index (NDVI) from small unmanned aerial system (sUAS). *2015 International Conference on Unmanned Aircraft Systems, ICUAS 2015* 520-525.

Zhou, Y, Lao, C, Yang, Y, Zhang, Z, Chen, H, Chen, Y, Chen, J, Ning, J and Yang, N. 2021. Diagnosis of winter-wheat water stress based on UAV-borne multispectral image texture and vegetation indices. *Agricultural Water Management* 256 (1): 107076.

5. CHAPTER 5: SYNTHESIS OF AIMS AND OBJECTIVES, KEY FINDINGS, AND RECOMMENDATIONS FOR FUTURE RESEARCH

5.1 Introduction

Sugarcane production is integral to South Africa's agricultural sector, functioning as a high-value crop with the potential to alleviate poverty and improve the livelihoods of millions (German *et al.*, 2020). Despite its economic importance, sugarcane's extensive water footprint, surpassing that of crops like maize and cassava, exacerbates the strain on scarce water resources (Kayiwa *et al.*, 2021). Smallholder farmers, the backbone of sugarcane cultivation (Ngcobo, 2023), face pronounced challenges due to limited resources, hydroclimatic variability, and policy constraints that hinder sustainable production practices (Jones and Singels, 2018). Moreover, rising water demands driven by climate variability necessitate innovative solutions to optimise water use and sustain productivity (IPCC, 2019).

This thesis addresses critical water management challenges in smallholder sugarcane farming by leveraging unmanned aerial vehicles (UAVs) and precision agriculture (PA) techniques. Traditional methods for monitoring crop water dynamics, such as in-situ and satellite-based approaches, often lack the scale, resolution, and accessibility required for smallholder applications (Rejeb *et al.*, 2022; Yacoob *et al.*, 2024). UAVs equipped with multispectral and thermal sensors offer a practical alternative, enabling detailed mapping of actual evapotranspiration (ETa) and the Normalised Difference Water Index (NDWI). These tools provide site-specific insights with the potential to support sustainable irrigation management and enhance resilience to climate variability (Ngcobo, 2023).

By employing advanced methodologies, including empirical relationships and machine learning (ML) models, the thesis developed innovative approaches to estimate ETa and predict NDWI. The Enhanced Vegetation Index 2 (EVI2) model proved the most effective for ETa estimation, mitigating canopy saturation and soil reflectance effects, thus enhancing sensitivity to biophysical changes vital for monitoring sugarcane growth (Abbasi *et al.*, 2023; Woldemariam *et al.*, 2024). The Normalised Difference Water Index demonstrated robustness as a proxy for crop water stress in resource-limited smallholder contexts. These innovations emphasised the study's contribution to developing scalable, cost-efficient water management strategies tailored to resource-limited contexts.

The research highlighted that while UAV-based solutions offer transformative potential, their adoption by smallholder farmers requires targeted capacity-building and knowledge dissemination. Practical training workshops, demonstrations, and simplified tools are essential to bridge the gap between advanced technologies and field-level implementation (Yacoob *et al.*, 2024). Such efforts ensure that the methodologies developed are accessible, pragmatic, and scalable within smallholder farming systems.

In conclusion, this thesis demonstrates the potential of UAV technology and PA to revolutionise water management in smallholder sugarcane farming. By integrating advanced modelling approaches, such as ETa estimation and ML-driven NDWI prediction, the research delivers cost-effective, practical solutions to enhance agricultural sustainability and resilience. These findings advance understanding of water management practices in semi-arid regions, supporting sustainable sugarcane production and strengthening food and nutrition security efforts in South Africa (Ngcobo, 2023).

5.2 Re-evaluation of aims and objectives

The overarching aim of this thesis was to evaluate UAV-based methods for estimating ETa and monitoring crop water stress within the context of smallholder sugarcane farming. This study sought to address the practical needs of precision water management in resource-constrained settings. Three specific objectives guided this investigation:

i. Scoping Review (**Chapter 2**): to conduct a comprehensive scoping review and bibliometric analysis, identifying trends, research gaps, and practical UAV applications for ETa estimation and crop water stress monitoring.
ii. ETa Estimation (**Chapter 3**): to apply and evaluate remote sensing (RS) methodologies, including VI-based models and ML techniques, for estimating ETa using UAV-acquired data.
iii. Water Stress Monitoring (**Chapter 4**): to develop and validate a predictive model for monitoring crop water stress by integrating UAV multispectral imagery with satellite-derived indices, thereby enhancing spatiotemporal insights into sugarcane water status.

5.3 Synthesis of research aims, key findings, and outcomes

This section summarises the key findings, synthesising the re-evaluated aims and objectives with outcomes to highlight their interconnectedness within the thesis.

5.3.1 Review of UAV applications in precision water management (Chapter 2)

A comprehensive scoping review addressed the first objective (Objective i) by systematically examining the literature on UAV applications in PA. Utilising Scopus data, the Biblioshiny app via the R environment (Bibliometrix-R package), and VOSviewer (version 1.6.19), the review identified key trends and research gaps. The analysis of 49 peer-reviewed articles revealed a pressing need for practical, smallholder-focused strategies for using UAV technology to estimate ETa and monitor crop water stress. This knowledge gap informed the design of subsequent empirical chapters and laid the foundation for future research recommendations.

The review uncovered a trend towards high-resolution spatial mapping using UAVs, enhancing precision water management in agriculture. This shift moved beyond basic crop mapping to provide actionable data for irrigation decisions. Traditional crop mapping offered coarse data for general monitoring, whereas UAV advancements offered critical insights, such as ETa rates and crop coefficients (Kc), improving irrigation strategies (Zhang *et al.*, 2019). Additionally, open-source platforms like Google Earth Engine (GEE) have reduced costs and improved accessibility (Abbasi *et al.*, 2023), allowing multispectral imagery processing and integrating predictive models tailored to smallholder farmers' needs.

Methodological diversification in the literature showed a transition from complex, data-intensive energy balance models to simpler, more accessible vegetation index (VI)-based approaches. This shift emphasised the essential need for practical solutions in smallholder contexts, focusing on specific indices such as the Normalised Difference VI (NDVI), Crop Water Stress Index (CWSI), and Water Deficit Index (WDI) alongside the use of ML for Kc prediction (Gautam and Pagay, 2020). The review highlighted the comparative performance of various ML algorithms in predicting crucial parameters, enhancing ETa estimates and improving crop water status monitoring.

Furthermore, the review prioritised challenges smallholder farmers face, addressing the *heterogeneity and fragmentation* of smallholder farmlands. This nuanced approach considered resource variability, farming practices, and data availability. While broader literature often emphasised large-scale agriculture, recent reviews increasingly accounted for smallholder-specific dynamics (Gokool *et al.*, 2024; Zenda and Rudolph, 2024), reflecting a growing recognition of their importance in global food security. The adoption of RS-based ETa estimation models in smallholder settings was hindered by *complexity and data demands*, emphasising the need for models tailored to limited data and technical expertise.

Furthermore, significant gaps persisted in the literature. Research was needed on the operational complexities of UAV deployment in smallholder farming systems, including cost-effectiveness, long-term maintenance, and farmer training. Notably, there was an underrepresentation of staple crops, as much of the current research prioritised high-value crops such as pistachio (Aliabad *et al.*, 2022), olive (Messina and Modica, 2022), and pomegranate (Niu *et al.*, 2020b). Additionally, comprehensive life-cycle cost analyses were essential to evaluate the economic feasibility of UAV adoption in resource-limited environments, which is critical for sustainable implementation in smallholder agriculture.

5.3.2 Empirical investigation of UAV-based evapotranspiration estimation (Chapter 3)

The second objective of this thesis (Objective ii) was addressed by employing advanced RS methodologies to estimate ETa through UAV-acquired data. This chapter evaluated various VIs derived from UAV multispectral imagery, encompassing five distinct models: ET-NDVI, ET-NDVIscaled, ET-NDVIKc, ET-EVI, and ET-EVI2. Additionally, ML techniques correlated ground-based Kc with NDVI values and facilitated the development of a Kc prediction model. By validating these estimates against ground-based eddy covariance (EC) measurements, the research highlighted the potential of integrating UAVs into existing agricultural practices to optimise water use in farming, contributing to improved efficiency.

The study found that despite differing data requirements, the Random Forest Regression (RFR) ensemble model achieved performance levels comparable to the EVI2 model. While the EVI2 model, developed from UAV-derived and in-situ data, consistently outperformed RFR in metrics such as the coefficient of determination (R^2), Root Mean Square Error (RMSE), and Mean Absolute Error (MAE), RFR's reliance on in-situ data limited its applicability for smallholder farmers, who often lack the resources for comprehensive data collection. Thus, RFR was less feasible despite its adequate predictive capacity. In contrast, EVI2's lower dependency on in-situ data and superior robustness highlighted its practicality and scalability for effective water resource management in resource-constrained environments.

Moreover, the enhanced performance of EVI approaches compared to NDVI-based methods stemmed from their resilience against saturation effects, which is especially pertinent during later sugarcane growth stages. NDVI saturation, as previously documented (Hunsaker *et al.*, 2003), caused a deviation from linearity in the relationship between NDVI and Kc at higher NDVI values, thereby reducing accuracy. The EVI and EVI2 indices were designed to mitigate this limitation (Abbasi *et al.*, 2021). The superior performance metrics of EVI2, particularly its lower RMSE and MAE values and closer resemblance to the EC dataset, clearly demonstrated its greater reliability in ETa estimation.

The high-resolution spatial ETa maps generated using the various models were essential for precision irrigation management in smallholder farming systems. These maps facilitated the assessment of water requirements by visualising ETa dynamics across diverse landscapes. Adequate irrigation relies on understanding the balance between water availability and crop demands. Integrating ETa maps with data on these factors enables more efficient water allocation and alleviates water stress. This targeted approach supports timely irrigation adjustments, enhances crop yield, and improves agricultural productivity, while the detailed visualisation aids informed decision-making at the farm level.

5.3.3 Development of Normalised Difference Water Index predictive model for water stress assessment (Chapter 4)

The third objective (Objective iii) was to leverage UAV-acquired data to develop a predictive model for monitoring sugarcane water stress. By integrating Sentinel-2 satellite imagery with UAV-based multispectral data, the ensemble model demonstrated exceptional predictive accuracy, attaining an R^2 value of 0.95, with low RMSE and MAE values of 0.03 and 0.02, respectively. The model captured spatiotemporal variations across growth phases, such as stalk elongation (SE) and early maturation (M). The model's novelty was deriving insights from multispectral data, overcoming challenges like the limited availability of SWIR bands in UAV systems, thus providing comprehensive analysis and predictions.

Persistent water stress was revealed throughout the monitoring period, particularly during the SE phase, as evidenced by elevated WDI values and reduced NDWI from July to November

2023. Prolonged dry periods, low precipitation, and decreased soil moisture exacerbated stress, with brief recoveries following rainfall. The early M phase showed improved crop water status, coinciding with increased chlorophyll content (CC), Leaf Area Index (LAI), and NDWI, reflecting favourable summer conditions. These findings demonstrated NDWI's utility as an indicator of crop water status and stress recovery dynamics.

Additionally, the Principal Component Analysis (PCA) analysis indicated that water availability primarily drove NDWI variations, reinforced by structural and photosynthetic activity indices like NDVI and Optimised Soil-Adjusted VI (OSAVI). The transition from SE to early M provided critical insights into sugarcane phenology. During SE, lower NDWI and structural VI (SVI) values reflected restricted root development and heterogeneous crop growth due to adverse winter conditions. The early M phase, characterised by vigorous post-tillering growth (Stoller, 2024), showed increased photosynthetic activity and water retention, supported by consistent NDWI trends.

5.4 Contributions of research to new knowledge

The principal findings of this research contribute to new knowledge in the following ways:

5.4.1 Chapter 2 contributions: scoping review insights

- This study's novel bibliometric analysis provided the first quantitative assessment of UAV applications in smallholder precision water management, revealing key trends, influential works, and a foundation for future research in this understudied area.
- Analysis revealed crucial limitations in UAV implementation for smallholder irrigation, especially concerning ETa estimation and water stress detection; however, decreasing UAV costs and open-source platforms offered enhanced accessibility.
- A rigorous comparison of energy balance and empirical VI models using UAV data clarified each approach's strengths, limitations, and data requirements, which informed the selection of optimal methodologies for smallholder precision water management.
- The review provided critical, evidence-based recommendations for policymakers and technology developers to explicitly address smallholder constraints and promote effective regulatory frameworks, incentives, and technological optimisation for enhanced UAV adoption in precision irrigation.

5.4.2 Chapter 3 contributions: UAV-based evapotranspiration estimation

- This research introduced a novel application of UAV-derived multispectral imagery for ETa estimation in rainfed smallholder sugarcane, overcoming traditional methods' spatial and temporal limitations and advancing UAV technology in PA.
- A rigorous comparison of UAV-derived ETa estimates (NDVI, NDVIscaled, NDVIKc, EVI, and EVI2), validated against EC data, revealed unique insights into their relative accuracy and reliability under sugarcane growing conditions. This comparative analysis further considered integrating ML-based predictive models.
- This study presented a validated ML-based Kc predictive model, integrating ground-based Kc measurements with in-situ NDVI data. This improved Kc estimation accuracy and efficiency, potentially informing irrigation management in water-scarce contexts.
- A thorough comparison of ETa estimation methods against ground truth data identified optimal techniques for smallholder sugarcane and considered trade-offs between model complexity, accuracy, data requirements, and resource constraints. This provided practical guidance for cost-effective water management.
- This study offered actionable recommendations to improve ETa estimation and water management in resource-constrained smallholder sugarcane farming. These contributions could support the development of sustainable agricultural practices while enhancing farmers' adaptive capacity to climate variability and water scarcity.

5.4.3 Chapter 4 contributions: innovations in Normalised Difference Water Index predictive modelling

- This study introduced a novel ML-based framework that integrated UAV-acquired multispectral data with Sentinel-2 satellite imagery for predicting NDWI. By leveraging SVIs as proxies, this approach addressed the limitations of UAV systems lacking SWIR bands, expanding their applicability in monitoring crop water stress.
- The NDWI predictive model demonstrated exceptional performance metrics, emphasising its reliability in capturing spatiotemporal water stress dynamics, particularly during critical sugarcane growth phases such as SE and early M.
- The model established moderate to strong correlations between NDWI and key crop parameters, including NDVI, Green NDVI (GNDVI), OSAVI, LAI, CC, crop height,

ETa, and the WDI. These relationships highlighted the model's robustness in detecting and interpreting the impacts of water stress on crop growth and development.

- By tracking NDWI's temporal dynamics relative to precipitation, soil moisture, and other climatic variables, the research highlighted its potential for early water stress detection. This capability could equip smallholder farmers with insights to implement proactive irrigation scheduling, enhancing resilience to climate variability.
- The model capitalised on the interactions among SVIs, including NDVI, Soil-Adjusted VI (SAVI), Transformed Chlorophyll Absorption in Reflectance Index (TCARI), and OSAVI, to provide a multidimensional assessment of sugarcane health. These interactions revealed nuanced relationships between canopy structure, photosynthetic efficiency, and water content, which offered insights into crop physiology.

5.5 Research challenges

This section details methodological and practical challenges encountered during the research process, categorised by chapter for clarity.

5.5.1 Limitations of the bibliometric analysis (Chapter 2)

- Reliance on Scopus, while a robust database, may have inadvertently excluded relevant literature from less widely indexed journals or non-English language publications. This limitation could affect the overall breadth of the review and potentially bias the findings.
- The specific search terms employed, while iteratively refined, may not have captured the full spectrum of relevant research. This inherent limitation of keyword-based searches could lead to underestimating the overall body of work in this rapidly evolving field.
- While adhering to standard systematic review practices (PRISMA-SCR), excluding grey literature and unpublished works may have omitted essential insights from recent work that may not yet be comprehensively indexed in academic databases.

5.5.2 Limitations of the evapotranspiration estimation techniques (Chapter 3)

- The assumption of homogeneous canopy conditions inherent in VI-based ETa estimation methods (relying on aggregated or averaged spectral data over a given area) did not fully capture the intrinsic heterogeneity of smallholder sugarcane fields. This simplification could have resulted in biased ETa estimates.

- The EC data used for model validation encountered limitations. Sensor calibration uncertainties, atmospheric turbulence, and data loss (January 23–February 2, 2024, due to avian interference) introduced variability and potentially compromised the precision of ETa estimates derived from the EC system.
- While energy balance closure analysis indicated acceptable data quality (73–76%), discrepancies between measured and modelled energy fluxes highlighted uncertainties stemming from land surface heterogeneity, sensor footprint mismatches, advection, and large-scale turbulent eddy effects, impacting ETa estimation accuracy.
- The delayed deployment of in-situ NDVI sensors resulted in a Kc prediction period (February 3–May 15, 2024) that did not fully align with the period for other ETa estimation methods (July 1, 2023–March 31, 2024). This temporal mismatch limited robust cross-methodological comparisons.
- Processing high-frequency EC data required specialised software and expertise. The computational demands, mainly when using ML for Kc prediction, could have limited wider adoption, especially among smallholder farmers with limited computing resources.

5.5.3 Limitations of the Normalised Difference Water Index methodology (Chapter 4)

- The model was developed using data from a single study site, limiting its generalisability to diverse sugarcane cultivars, agronomic practices, and environmental conditions.
- While NDWI prediction provided valuable insights, it oversimplified the complex interactions among environmental variables such as precipitation, temperature, ETa, and soil characteristics. This reductionist approach may have obscured critical factors affecting sugarcane water stress.
- Data collection was restricted to SE and early M phases of sugarcane growth. Consequently, the model did not account for water stress dynamics during the germination, tillering, or later maturation phases, which were vital for understanding the entire crop cycle.

- The ground-truth dataset relied on a limited number of in-situ measurements, potentially underrepresenting the spatial heterogeneity inherent in smallholder sugarcane fields. This may have introduced biases, particularly in areas with variable canopy structures or soil conditions.
- Downscaling satellite imagery for integration with UAV data introduced uncertainties, particularly from mixed-pixel effects in coarse-resolution satellite images. These discrepancies may have affected NDWI accuracy and highlighted the need for advanced image processing techniques, such as spectral unmixing, to improve precision.

5.6 Recommendations for future research

This section presents suggestions for future research that can build on the findings of this study to advance knowledge in the field.

5.6.1 Future research directions

A more inclusive literature review is needed, incorporating grey literature and non-English publications for a holistic understanding of the field. Further investigation is warranted into emerging themes—integrating UAV technology with advanced techniques (e.g., AI, deep learning)—and rigorously evaluating the cost-effectiveness and practical implementation of diverse water management strategies in smallholder contexts, including exploring cost-effective sensor options (e.g., RGB). Methodological limitations (keyword bias, reliance on a single database) necessitate exploring alternative analytical approaches and multiple data sources (Rejeb *et al.*, 2022). Additionally, future research should focus on (1) quantitatively evaluating UAVs' effectiveness in improving water management, (2) identifying the most feasible operational and analytical technologies for smallholder farmers, and (3) assessing the significance of contributions to the field beyond a simple bibliometric analysis.

Chapter 3's ETa estimation models, while demonstrating high accuracy with EVI2, require further refinement to enhance robustness and generalisability (Alavi *et al.*, 2024). Incorporating additional environmental variables such as soil moisture and leaf water potential into these models could improve accuracy. Advanced ML techniques, including deep learning, may better capture complex, non-linear relationships (Jhajharia, 2022). Comparative analyses across diverse agroecological zones in South Africa, coupled with complete sugarcane growth cycles and daily UAV data acquisition, will be critical. Investigating cost-effective alternatives, such as affordable RGB sensors (Gautam *et al.*, 2021), could broaden these methods' accessibility to smallholder farmers in the region. Additionally, exploring energy balance approaches (Niu *et al.*, 2020a), especially under conditions favouring their application, could further enhance ETa estimation's practicality and scalability. Finally, methods requiring less reliance on resource-intensive EC systems for validation will increase accessibility for resource-constrained contexts (Yacoob *et al.*, 2024).

Although demonstrating exceptional accuracy, chapter 4's NDWI predictive model requires broader applicability. Future work should expand geographically to encompass diverse agroecological zones in South Africa, considering regions with varying mean annual precipitation (MAP) and soil moisture conditions to enhance robustness. The model's reliance on a limited training dataset will necessitate significant data expansion (Budach *et al.*, 2022), integrating high-quality data from diverse sources (satellite, UAV, and in-situ) through data fusion techniques. Advanced image processing methods, such as spectral unmixing, will be crucial to mitigating mixed-pixel effects and improving accuracy (Zhou *et al.*, 2021). Additionally, extending data collection to cover the complete sugarcane growth cycle will provide a more comprehensive understanding of water stress dynamics. Bridging the technology gap will require user-friendly tools for smallholder farmers, supported by collaborative training and knowledge transfer initiatives to ensure sustainable adoption (Gokool *et al.*, 2023).

5.6.2 Concluding insights

This research highlights the significant impact of innovative agronomic practices, particularly by integrating UAVs and PA, on enhancing irrigation management for sugarcane production among smallholder farmers in South Africa. The bibliometric analysis in Chapter 2 identifies critical knowledge gaps, specifically the need for accessible implementation strategies for UAV technology tailored to smallholders. Chapters 3 and 4 address these gaps by demonstrating the practical applications of UAVs in estimating ETa and monitoring crop water stress—key activities vital for improving agricultural productivity in a region facing escalating water demands exacerbated by climate variability. An evaluation of various VI models provides quantitative evidence highlighting the capability of advanced RS technologies to produce high-resolution spatial ETa maps, which are crucial for informing irrigation management decisions and optimising water use efficiency during critical growth stages of sugarcane.

Developing a novel NDWI predictive model with exceptional accuracy can provide smallholder farmers with a robust real-time water stress assessment tool. By correlating closely with crop water use, the NDWI has the potential to enhance irrigation scheduling and empower timely interventions to address the pressing challenges of water scarcity. Implementing these technologies within smallholder farming systems carries substantial implications. By improving adaptive capacity and resilience to climatic shocks, these innovations can enable farmers to maximise yields and secure their livelihoods amid fluctuating conditions. However, realising these benefits requires effective capacity-building initiatives; providing farmers with the training to utilise UAV and PA technologies is essential for successful implementation. While this study lays a strong foundation, it is important to acknowledge certain limitations. The research focuses on a specific geographical region, meaning that the applicability of the findings may vary based on local conditions like soil types, crop varieties, and socio-economic factors. Additionally, while the models developed show promising accuracy, further validation across diverse settings is needed to enhance their generalisability.

Looking ahead, future research should prioritise developing a user-friendly decision support tool tailored for smallholder farmers. This tool could integrate UAV data with predictive models, offering functionalities such as real-time water stress monitoring, irrigation scheduling recommendations, and customised alerts based on local conditions. Such a resource would empower farmers to make informed, data-driven decisions and facilitate broader adoption of precision irrigation practices, ultimately improving productivity and sustainability. In conclusion, the contributions of this research are vital for advancing sustainable agricultural practices in South Africa. The findings advocate for a collaborative, multi-faceted approach involving researchers, policymakers, and agricultural extension services to foster knowledge exchange and implement supportive policies for smallholder farmers. By adopting these strategies, stakeholders can enhance food security, improve the economic viability of small-scale operations, and ensure the resilience of sugarcane production amid ongoing climatic challenges. Ultimately, this work enriches academic discourse and establishes a foundation for actionable strategies that support food security and promote sustainability, empowering smallholder farmers to contribute effectively to resilient agricultural futures.

5.7 References

Abbasi, N, Nouri, H, Didan, K, Barreto-Muñoz, A, Chavoshi Borujeni, S, Opp, C, Nagler, P, Thenkabail, PS and Siebert, S. 2023. Mapping vegetation index-derived actual evapotranspiration across croplands using the Google Earth Engine platform. *Remote Sensing* 15 (4): 1017.

Abbasi, N, Nouri, H, Didan, K, Barreto-Muñoz, A, Chavoshi Borujeni, S, Salemi, H, Opp, C, Siebert, S and Nagler, P. 2021. Estimating actual evapotranspiration over croplands using vegetation index methods and dynamic harvested area. *Remote Sensing* 13 (24): 5167.

Alavi, M, Albaji, M, Golabi, M, Ali Naseri, A and Homayouni, S. 2024. Estimation of sugarcane evapotranspiration from remote sensing and limited meteorological variables using machine learning models. *Journal of Hydrology* 629 (1): 130605.

Aliabad, FA, Shojaei, S, Mortaz, M, Ferreira, CSS and Kalantari, Z. 2022. Use of Landsat 8 and UAV images to assess changes in temperature and evapotranspiration by economic trees following foliar spraying with light-reflecting compounds. *Remote Sensing* 14 (23): 6153.

Budach, L, Feuerpfeil, M, Ihde, N, Nathansen, A, Noack, N, Patzlaff, H, Harmouch, H and Naumann, F. 2022. *The Effects of Data Quality on ML-model Performance*.

Gautam, D, Ostendorf, B and Pagay, V. 2021. Estimation of grapevine crop coefficient using a multispectral camera on an unmanned aerial vehicle. *Remote sensing* 13 (13): 2639.

Gautam, D and Pagay, V. 2020. A review of current and potential applications of remote sensing to study the water status of horticultural crops. *Agronomy* 10 (1): 140.

German, LA, Hepinstall-Cymerman, J, Biggs, T, Parker, L and Salinas, M. 2020. The environmental effects of sugarcane expansion: a case study of changes in land and water use in southern Africa. *Applied Geography* 121 (1): 102240.

Gokool, S, Mahomed, M, Clulow, A, Sibanda, M, Kunz, R, Naiken, V and Mabhaudhi, T. 2024. Exploring the potential of remote sensing to facilitate integrated weed management in smallholder farms: a scoping review. *Drones* 8 (3): 81.

Gokool, S, Mahomed, M, Kunz, R, Clulow, A, Sibanda, M, Naiken, V, Chetty, K and Mabhaudhi, T. 2023. Crop monitoring in smallholder farms using unmanned aerial vehicles to facilitate precision agriculture practices: a scoping review and bibliometric analysis. *Sustainability* 15 (4): 3557.

Hunsaker, DJ, Pinter, P, Barnes, EM and Kimball, BA. 2003. Estimating cotton evapotranspiration crop coefficients with a multispectral vegetation index. *Irrigation Science* 22 (1): 95-104.

IPCC. 2019. *Climate Change and Land: an IPCC special report on climate change, desertification, land degradation, sustainable land management, food security, and greenhouse gas fluxes in terrestrial ecosystems*. Cambridge University Press, Cambridge, UK and New York, USA.

Jhajharia, K. 2022. A comprehensive review on machine learning in agriculture domain. *IAES International Journal of Artificial Intelligence* 11 (2): 753-763.

Jones, MR and Singels, A. 2018. Refining the Canegro model for improved simulation of climate change impacts on sugarcane. *European Journal of Agronomy* 100 (1): 76-86.

Kayiwa, R, Kasedde, H, Lubwama, M and Kirabira, JB. 2021. The potential for commercial scale production and application of activated carbon from cassava peels in Africa: a review. *Bioresource Technology Reports* 15 (1): 100772.

Messina, G and Modica, G. 2022. Twenty years of remote sensing applications targeting landscape analysis and environmental issues in olive growing: a review. *Remote Sensing* 14 (1): 5430.
Ngcobo, SI. 2023. An assessment of the potential impacts of climate variability on sugarcane production across Southern Africa. Unpublished thesis, Discipline of Hydrology, University of KwaZulu-Natal, Pietermaritzburg, South Africa.
Niu, H, Hollenbeck, D, Zhao, T, Wang, D and Chen, Y. 2020a. Evapotranspiration estimation with small UAVs in precision agriculture. *Sensors* 20 (22): 6427.
Niu, H, Wang, D and Chen, Y. 2020b. Estimating actual crop evapotranspiration using deep stochastic configuration networks model and UAV-based crop coefficients in a pomegranate orchard. *Journal of Intelligent & Robotic Systems* 104 (66).
Rejeb, A, Abdollahi, A, Rejeb, K and Treiblmaier, H. 2022. Drones in agriculture: a review and bibliometric analysis. *Computers and Electronics in Agriculture* 198 (1): 107017.
Stoller. 2024. Sugarcane [Internet]. Corteva Agriscience. Available from: https://stollersouthafrica.co.za/sugarcane/. [Accessed: 14 October 2024].
Woldemariam, GW, Awoke, BG and Maretto, RV. 2024. Remote sensing vegetation indices-driven models for sugarcane evapotranspiration estimation in the semiarid Ethiopian Rift Valley. *ISPRS Journal of Photogrammetry and Remote Sensing* 215 (1): 136-156.
Yacoob, A, Gokool, S, Clulow, A, Mahomed, M and Mabhaudhi, T. 2024. Leveraging unmanned aerial vehicle technologies to facilitate precision water management in smallholder farms: a scoping review and bibliometric analysis. *Drones* 8 (9): 476.
Zenda, M and Rudolph, M. 2024. A systematic review of agroecology strategies for adapting to climate change impacts on smallholder crop farmers' livelihoods in South Africa. *Climate* 12 (3): 33.
Zhang, L, Zhang, H, Niu, Y and Han, W. 2019. Mapping maize water stress based on UAV multispectral remote sensing. *Remote Sensing* 11 (6): 605.
Zhou, Y, Lao, C, Yang, Y, Zhang, Z, Chen, H, Chen, Y, Chen, J, Ning, J and Yang, N. 2021. Diagnosis of winter-wheat water stress based on UAV-borne multispectral image texture and vegetation indices. *Agricultural Water Management* 256 (2): 107076.

6. APPENDIX A

Table 6.1 EC instrumentation details (adapted from manufacturer descriptions).

Instrument	Description	Image	Supplier/Source
Rain Gauge: TE525MM-L, Texas Electronics, Dallas, TX, USA.	The TE525 device channels precipitation into a receptacle system, which undergoes tipping once it reaches its predetermined calibration level. The bucket's tipping mechanism is activated by a magnet affixed to it, which triggers a switch. The pulse-counting circuitry in the datalogger is responsible for tallying the switch's instantaneous closing.		(Campbell Scientific, 2024)
4-Component Net Radiometer: CNR4-L, Kipp & Zonen, Delft, The Netherlands.	The CNR4 is a net radiometer of research quality designed to quantify the energy equilibrium between incoming and outgoing radiation. The apparatus combines a pyranometer and a pyrgeometer, which measure short-wave and long-wave infrared radiation, respectively.		(Campbell Scientific, 2024)
3-D Sonic Anemometer: CSAT3A, Campbell Scientific, Logan, UT, USA.	The CSAT3A is a sonic anemometer capable of measuring three orthogonal wind components and the speed of sound. The capacity to assess the turbulent variations of horizontal and vertical wind inside EC systems enables the subsequent computation of momentum flux and friction velocity.	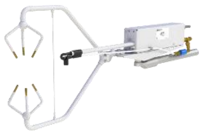	(Campbell Scientific, 2024)

Table 6.2 EC instrumentation details (adapted from manufacturer descriptions) – continuation of Table 6.1.

Instrument	Description	Image	Supplier/Source
CO_2/H_2O Open-Path Gas Analyser: EC150, Campbell Scientific, Logan, UT, USA.	As a stand-alone analyser, the device measures absolute carbon dioxide and water vapour concentrations, air temperature, and barometric pressure.		(Campbell Scientific, 2024)
Soil Heat Flux Plates: HFP01-L, Campbell Scientific, Logan, UT, USA.	The HFP01 employs a thermopile to quantify temperature differentials throughout its surface under the assumptions of stable heat flux, constant thermal conductivity of the body, and minimal impact of the sensor on the thermal flow pattern. Moreover, the signal of the HFP01 exhibits a direct relationship with the magnitude of the heat flow in the immediate vicinity.		(Campbell Scientific, 2024)
Soil Temperature Averaging Probes: TCAV-L, Campbell Scientific, Logan, UT, USA.	The TCAV-L measures the mean temperature of the uppermost 6 to 8-cm layer of soil, which is crucial for assessing energy balance in flux systems. The TCAV employs type E thermocouples, consisting of a chrome wire and a constantan wire connected at a measuring junction. Additionally, the temperature can be determined by measuring the disparities in potential generated at the junction.		(Campbell Scientific, 2024)

Table 6.3 EC instrumentation details (adapted from manufacturer descriptions) – continuation of Table 6.2.

Instrument	Description	Image	Supplier/Source
Water Content Reflectometers: CS616, Campbell Scientific, Logan, UT, USA.	The CS616-LC can quantify the volumetric water content from 0% to saturation. This technique employs time-domain measuring techniques without necessitating the use of a reflectometer. The insertion of probe rods may be conducted either from the surface or by burying the probe at any orientation relative to the surface.		(Campbell Scientific, 2024)
Infrared Radiometer (IRR): SI-111, Apogee Instruments, Logan, UT, USA.	The SI-111 is a very accurate infrared radiometer used for non-contact measurements of an object's surface temperature. The measurement encompasses the subject's surface and the sensor body's temperatures. The datalogger utilises the readings to accurately determine the body's temperature.		(Campbell Scientific, 2024)
Type E Fine-Wire Thermocouples: EXTT-E-24, Omega Inc., Stamford, CT, USA.	The FW3 is a Type E thermocouple with a diameter of 0.003 inches. It accurately measures atmospheric temperature gradients or fluctuations with research-grade precision. The FW3's compact size negates the requirement for a solar radiation shield. It comprises a connector that attaches the thermocouple to a datalogger via the FWC-L cable.		(Campbell Scientific, 2024)

Table 6.4 EC instrumentation details (adapted from manufacturer descriptions) – continuation of Table 6.3.

Instrument	Description	Image	Supplier/Source
Temperature/RH Probe: HC2S3, Rotronic AG, Bassersdorf, Switzerland.	The HC2S3 is a temperature and humidity probe that exhibits high precision and is well-suited for extended periods of use in unattended scenarios. The probe uses a sophisticated capacitive sensor to measure relative humidity. The probe is equipped with a filter that safeguards the sensor from the intrusion of dust and particles, enhancing its performance and dependability.		(Campbell Scientific, 2024)
CR3000 Datalogger: Campbell Scientific, Logan, UT, USA.	The CR3000 can effectively manage extended eddy-covariance and complete energy-balance systems. The datalogger offers three alternative power-supply choices: alkaline, rechargeable, or no battery. The Micrologger's ability to function on a battery recharged using a solar panel for lengthy periods eliminates the need for AC power, owing to its low power consumption. The device halts operation when the main power supply falls below 9.6 V, mitigating imprecise readings' potential.		(Campbell Scientific, 2024)
CR1000 Datalogger: Campbell Scientific, Logan, UT, USA.	Robust and suitable for complex configurations, the CR1000 operates with an external keyboard/display and power supply. It supports extended use with a rechargeable battery powered by a solar panel, eliminating reliance on AC power. The system automatically shuts down when power drops below 9.6 V to prevent inaccurate readings.	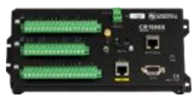	(Campbell Scientific, 2024)

7. APPENDIX B

In the context of the pre-instrumentation setup calibration procedures, the CO_2/H_2O Open-Path Gas Analyser (EC150, Campbell Scientific, Logan, UT, USA) was positioned in a controlled laboratory environment adjacent to the LI-610 device (LI-610, Licor Inc., Lincoln, NE, USA). Subsequently, the apparatus was linked to a power source, and all tubing connections were secured. The calibration of the gas analyser was verified against standard gas samples, and the resulting baseline measurements were recorded. Following this, the dew point setting on the LI-610 was established, allowing for system stabilisation (Figure 7.1a). Subsequent steps involved connecting the LI-610 output with the gas analyser, introducing zero air, and adjusting the analyser to nullify CO_2 and H_2O readings. In the calibration's span aspect, gases with predefined CO_2 and H_2O concentrations were introduced, necessitating corresponding adjustments to the analyser. Validation of calibration was conducted across various concentration levels. Lastly, the gas analyser was restored to its customary operational configuration.

Subsequently, the gas analyser and the LI-670 Flow Control Unit (LI-670, Licor Inc., Lincoln, NE, USA) were linked to a power source and subjected to warming-up (Figure 7.1b). Tubing and connections were secured to ensure operational integrity. The initial calibration status of the gas analyser was validated using established standard gas samples, and baseline measurements were documented. The output of the LI-670 was then connected with the gas analyser, followed by the introduction of zero air to facilitate the adjustment of the analyser settings to nullify CO_2 and H_2O readings. Calibration gases with predetermined CO_2 and H_2O concentrations were subsequently employed for span calibration, with due consideration given to aligning the flow rate on the LI-670 with the gas analyser's requisites. A stabilisation period was allowed before adjustments to the analyser settings were made. Calibration procedures were iterated across various concentration levels to ensure linearity and precision. Ultimately, the gas analyser was restored to its customary operational configuration.

Figure 7.1 Calibration setup for the CO_2/H_2O Open-Path Gas Analyser (EC150) using (a) the LI-610 Dew Point Generator and (b) the LI-670 Flow Control Unit, with data acquisition and analysis conducted via the EC100 Series Monitor Software.

Figure 7.2 Soil accumulation on the co-located 3-D sonic anemometer and CO_2/H_2O Open-Path Gas Analyser, attributed to avian interference, resulting in data loss from January 23, 2024, to February 2, 2024.

8. APPENDIX C

Table 8.1 Growth dynamics and management of sugarcane.

Days after emergence	Growth stage	Growth dynamics and management
0-30	Germination	Physiological changes: buds activate, and primary roots develop. Morphological changes: swelling of buds, initial root and shoot development, emergence of first leaves. Environmental factors: adequate soil moisture and warm temperatures. Challenges: pests, poor emergence. Solutions: use of healthy stubble and proper field preparation.
31-120	Tillering	Physiological changes: axillary buds activate, enhanced nutrient uptake. Morphological changes: increase in shoot number, dense leaf canopy and nodal root formation. Environmental factors: optimal moisture and nutrient availability. Challenges: competition among tillers. Solutions: proper spacing and thinning.
121-390	Stalk Elongation	Physiological changes: rapid cell division and elongation, high photosynthesis. Morphological changes: increase in stalk height and diameter, leaf development. Environmental factors: adequate sunlight and consistent water supply. Challenges: water stress, nutrient deficiency. Solutions: regular monitoring and timely interventions.
391-547	Maturation	Physiological changes: accumulation of sugars and decreased vegetative growth. Morphological changes: stalk thickening, leaf senescence. Environmental factors: cooler temperatures and reduced water requirement. Challenges: pests, diseases. Solutions: regular inspections and timely pest management.

9. APPENDIX D

Table 9.1 Details of in-situ measurement devices (adapted from manufacturer descriptions).

Device	Description	Image	Supplier/Source
SPAD502 chlorophyll meter: Minolta Corporation, Ltd., Osaka, Japan.	The SPAD-502Plus chlorophyll meter quantifies the relative chlorophyll concentration by measuring leaf absorbance in the red and near-infrared spectral bands. The device calculates a SPAD value directly correlated to the CC in the leaf.		(Konica Minolta, 2024)
LAI2200C-Plant Canopy Analyser: Li-Cor, Inc., Lincoln, NE, USA.	The LAI2200 Plant Canopy Analyser calculates LAI and other canopy structural parameters using radiation measurements obtained through a "fisheye" optical sensor. The device employs measurements taken above and below the canopy at various zenith angles to assess light interception, with LAI derived through a radiative transfer model.		(LI-COR, 2024)
Testo Thermal Imager 882: Testo SE & Co. KGaA, Lenzkirch, Germany.	The Testo 882 Thermal Imager is a robust and user-friendly thermal imaging camera designed for high-accurate non-contact measurement and display of surface temperature distribution.		(Testo, 2024)

10. APPENDIX E

Table 10.1 Additional flight specifications for DJI M300 non-RTK version with MicaSense Altum camera at 100 m altitude.

Specification	Specification detail
Max takeoff weight	9 kg
Max flight time	55 minutes (no payload)
Operating temperature	-20 °C to 50 °C
Max wind resistance	15 m s^{-1}
Max descent speed	7 m s^{-1}
Max ascent speed	6 m s^{-1}
Max transmission distance	15 km (FCC); 8 km (CE)
Positioning accuracy (GNSS)	Horizontal: ±1.5 m, vertical: ±0.5 m
Obstacle sensing range	0.5 m to 40 m (front, rear, left, right, up, down)
GNSS	GPS+GLONASS+BeiDou+Galileo
Battery type	TB60 intelligent flight battery
Battery capacity	5935 mAh
Payload capacity	Up to 2.7 kg
Max hovering time	45 minutes
Controller	DJI Smart Controller Enterprise
Operating frequency	2.400-2.4835 GHz; 5.725-5.850 GHz
Transmission system	OcuSync Enterprise

11. APPENDIX F

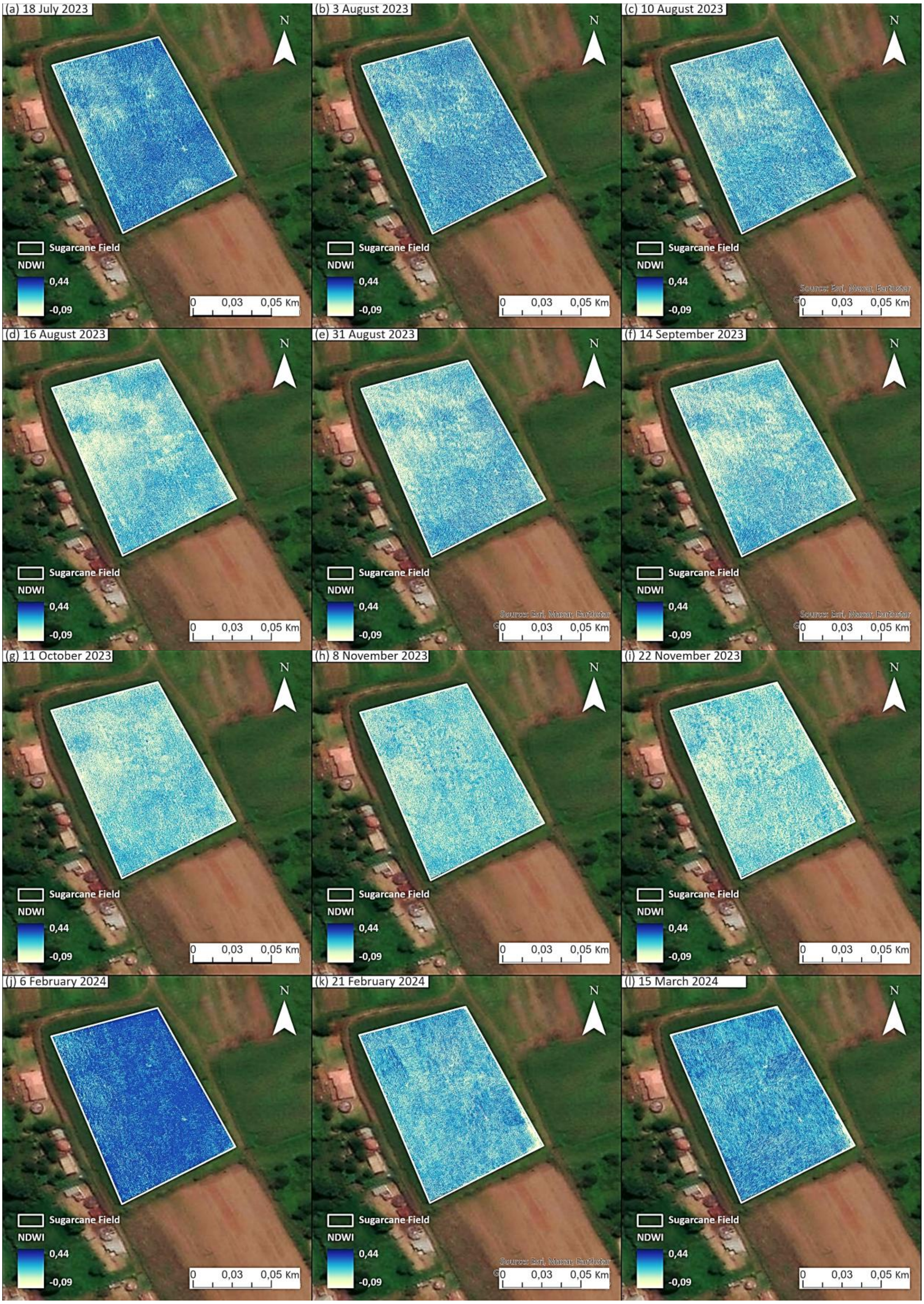

Figure 11.1 Spatiotemporal NDWI maps derived from ensemble model two.

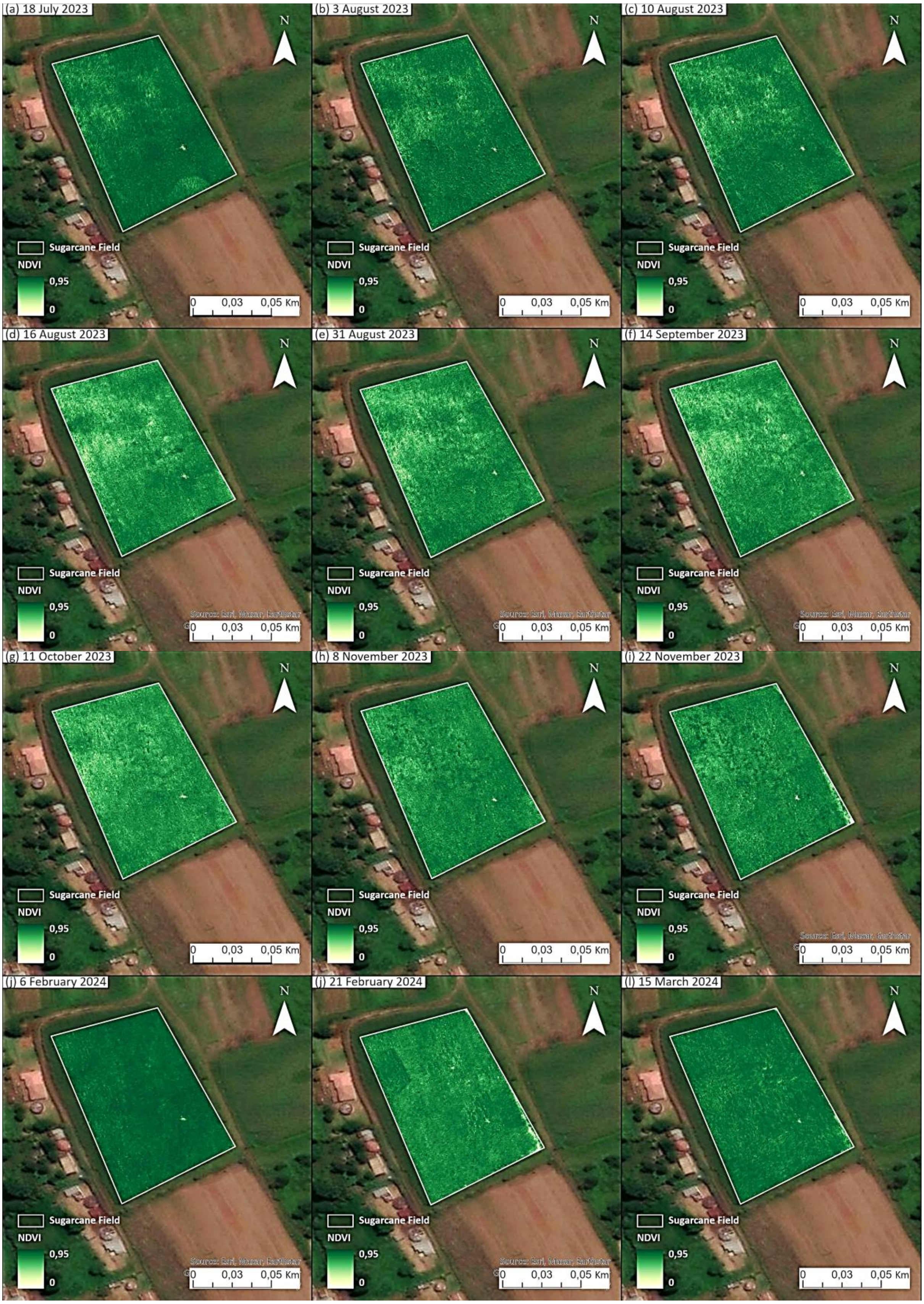

Figure 11.2 NDVI maps from twelve UAV flights over the study area.

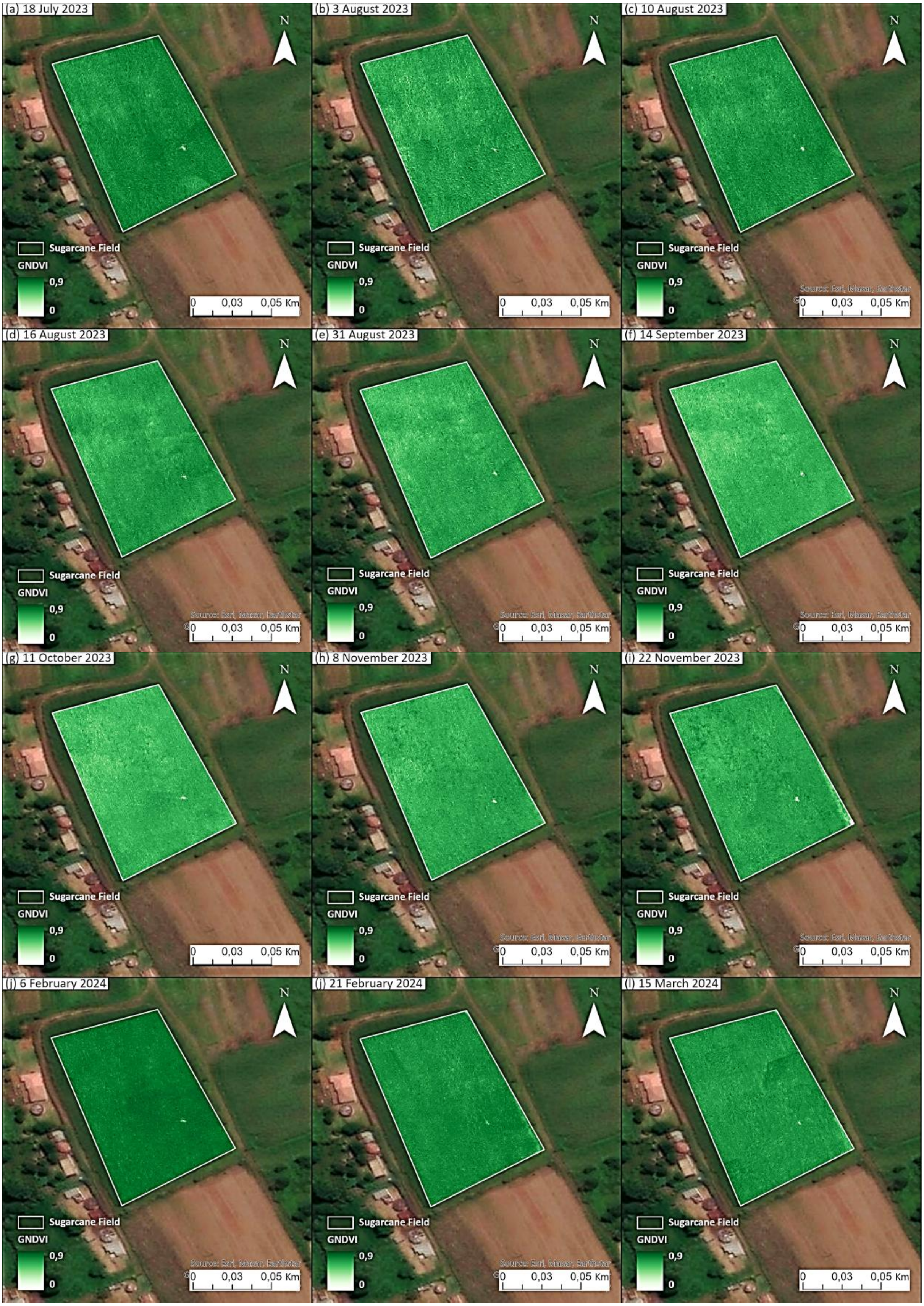

Figure 11.3 GNDVI variations captured in UAV flights showcasing temporal trends in vegetation health.

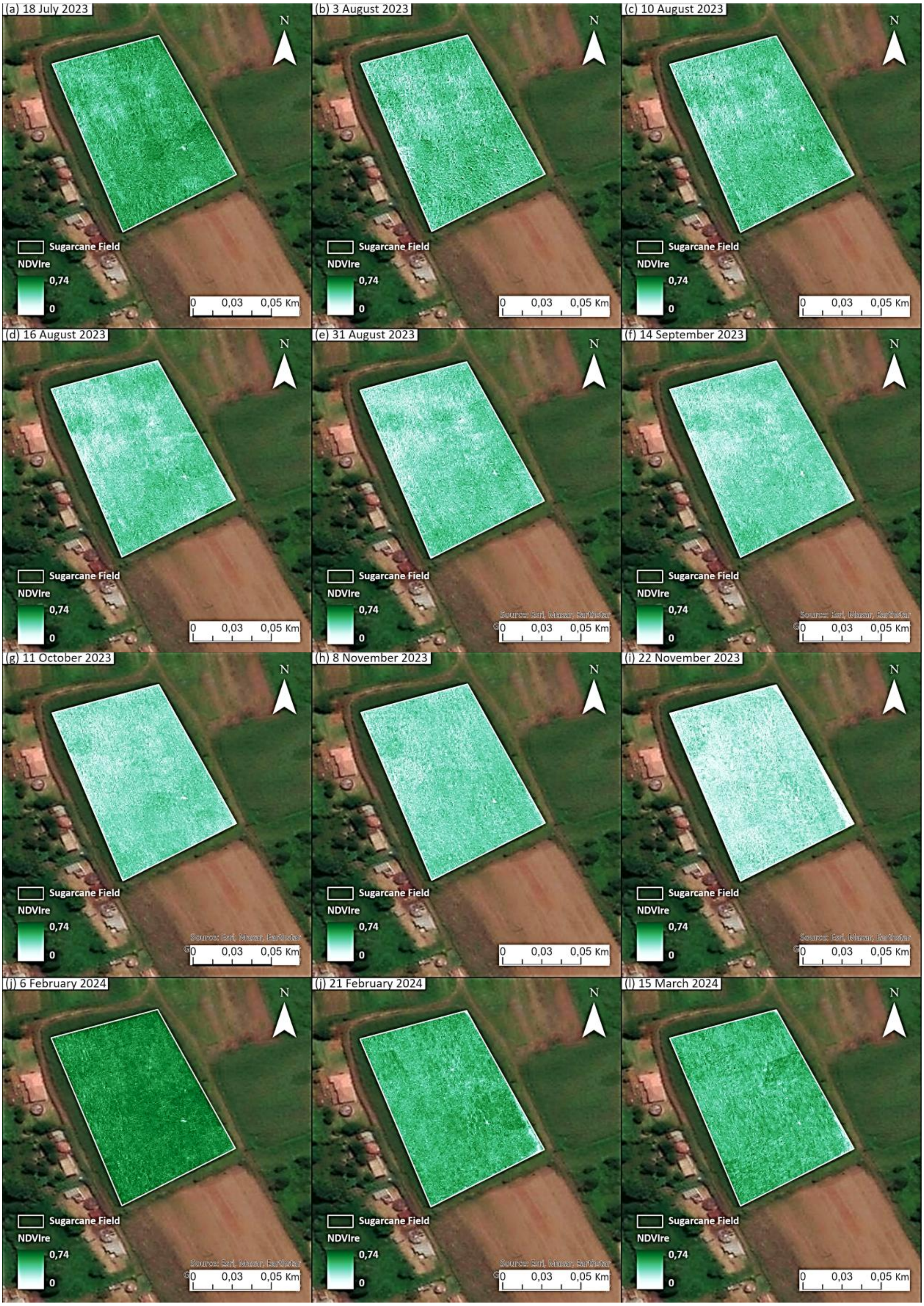

Figure 11.4 Comparative analysis of NDVIre maps from twelve UAV flights for vegetation monitoring.

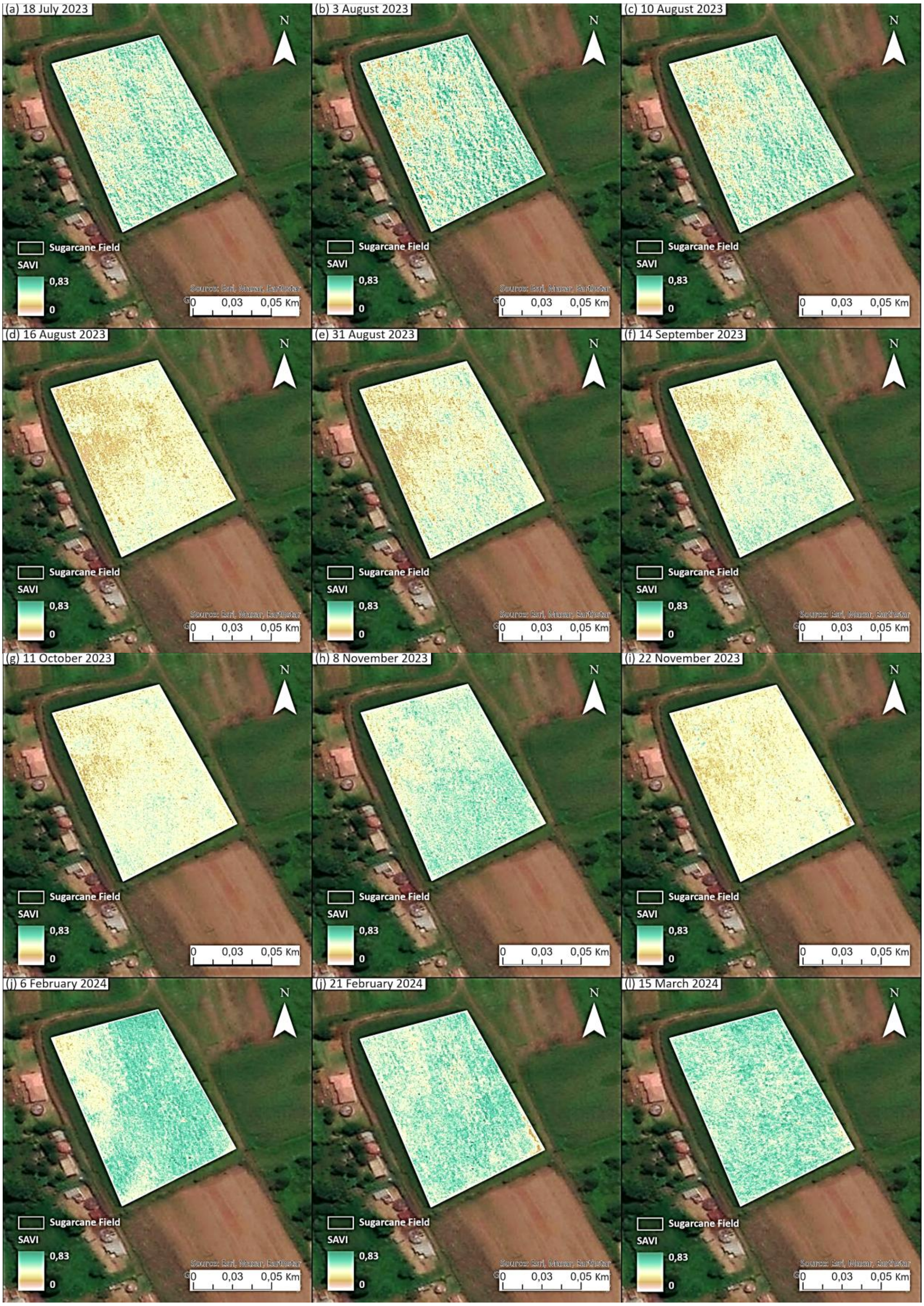

Figure 11.5 Temporal changes in SAVI values mapped across different UAV survey dates for trend analysis.

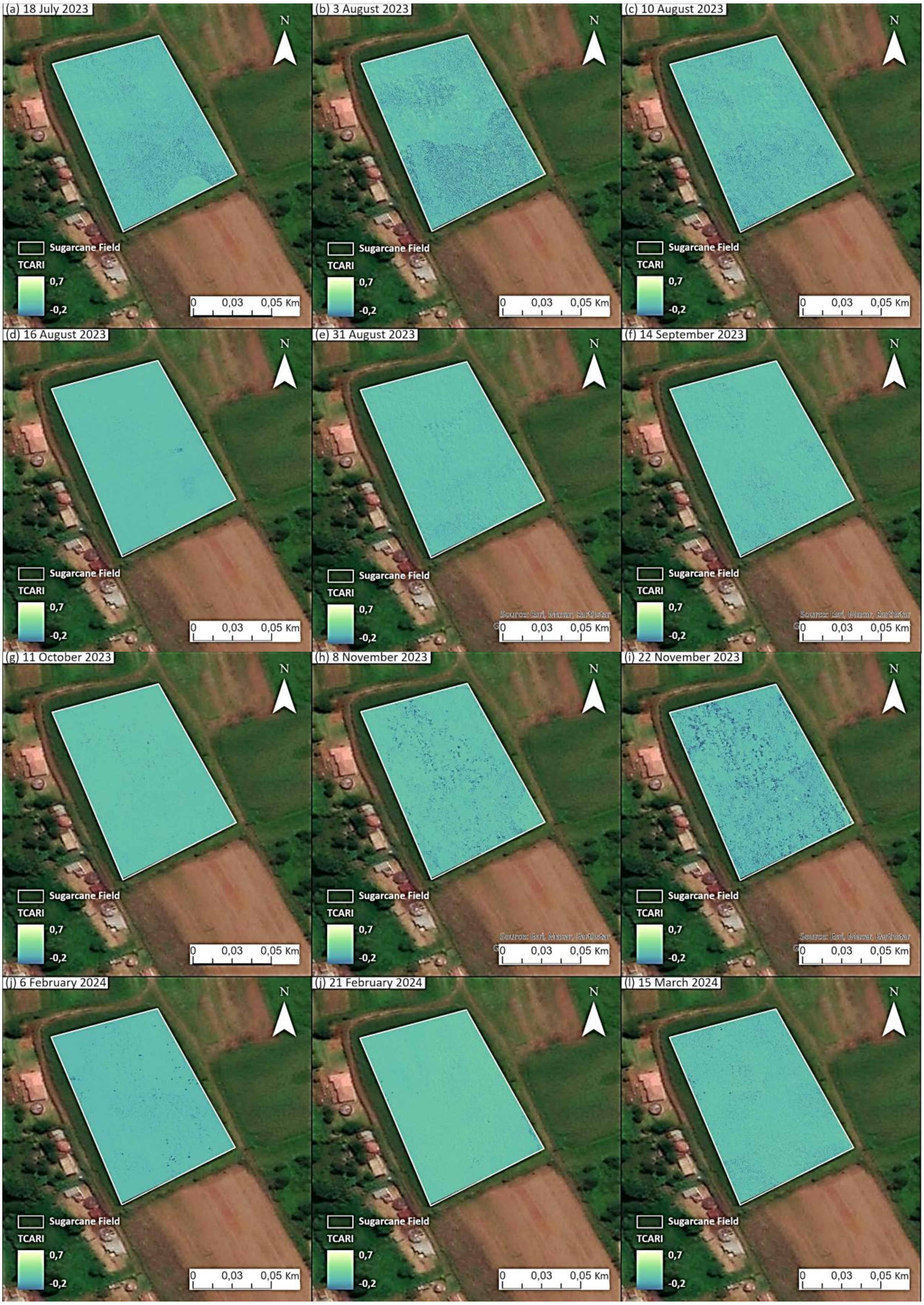

Figure 11.6 TCARI index mapping revealing CC variations across different UAV flights.

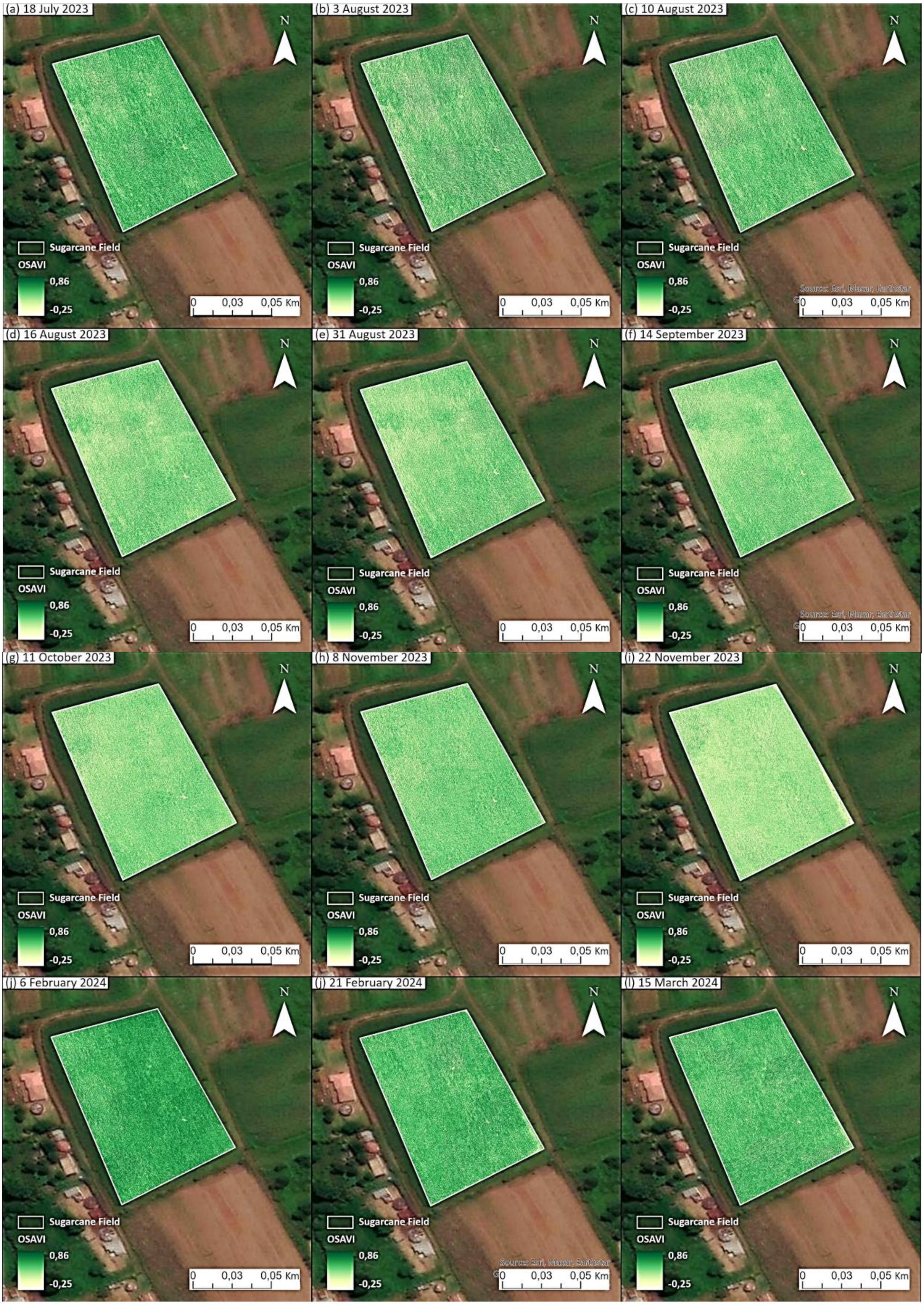

Figure 11.7 OSAVI index representations from multiple UAV flights indicating vegetation vigour dynamics.

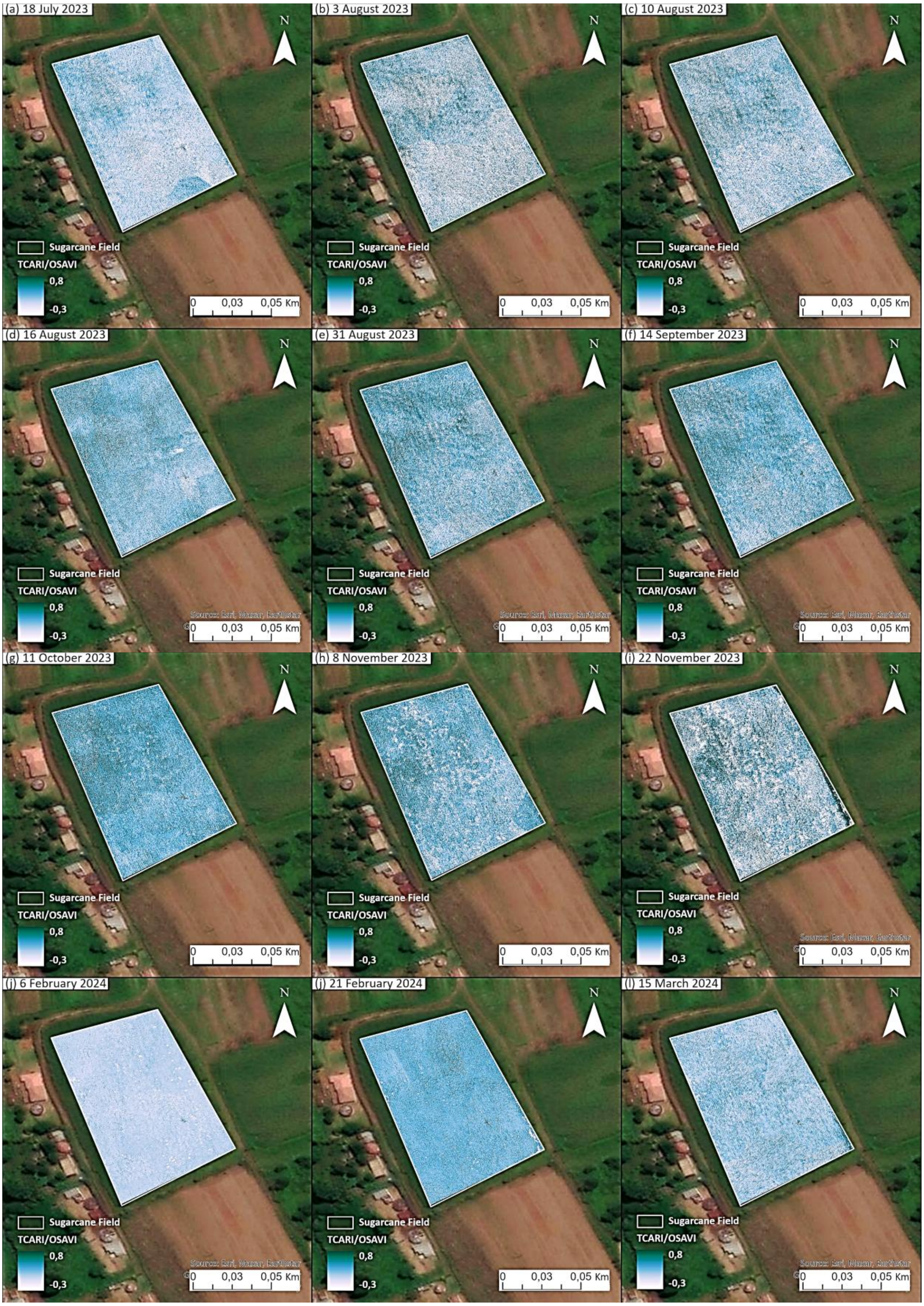

Figure 11.8 Spatial visualisation of TCARI/OSAVI ratios for assessing plant physiological status.